

**NASA
Technical
Paper
2158**

May 1983

NASA
TP
2158
c.1

LOAN COPY
AFWL TECH
KIRTLAND A

0067714



TECH LIBRARY KAFB, NM

Effects of Twin-Vertical-Tail Parameters on Twin-Engine Afterbody/Nozzle Aerodynamic Characteristics

Laurence D. Leavitt
and E. Ann Bare



NASA

25
25th Anniversary
1958-1983

**NASA
Technical
Paper
2158**

1983

TECH LIBRARY KAFB, NM



0067714

Effects of Twin-Vertical-Tail Parameters on Twin-Engine Afterbody/Nozzle Aerodynamic Characteristics

Laurence D. Leavitt
and E. Ann Bare
*Langley Research Center
Hampton, Virginia*

SUMMARY

An experimental investigation has been conducted in the Langley 16-Foot Transonic Tunnel to determine the effects of several empennage and afterbody parameters on twin-engine aft-end aerodynamic characteristics. Model variables included twin-vertical-tail cant angle, toe angle, airfoil camber, and root-chord length and afterbody/engine interfairing shape. Tests were conducted over a Mach number range from 0.6 to 1.2 and over an angle-of-attack range from -2° to 10° . Nozzle pressure ratio was varied from 1.0 (jet off) to approximately 10.0.

Results indicate that aft-end drag is sensitive to variations in twin-vertical-tail cant angle, toe angle, and camber. Significant reductions in drag can be obtained by slight outward toe of the vertical tails, outward cant of the vertical tails, or outboard placement of vertical-tail camber for most conditions tested.

INTRODUCTION

Much attention has been given in recent years to the proper integration of the propulsion system into the airframes of highly maneuverable fighter aircraft configurations. This is especially true with the requirement of multimission aircraft capable of operating over a broad range of Mach numbers, altitudes, and angles of attack. Since these multimission aircraft require variable geometry nozzles to provide high internal nozzle performance, important aft-end parameters such as closure and local boattail angles continuously change throughout the operating range of Mach number, angle of attack, and engine pressure ratio. Many studies have shown that large drag penalties can result from the installation of isolated nozzles into a realistic aft end (refs. 1 to 10). Much of this installation drag penalty results from adverse interactions originating from empennage surfaces, base areas, actuator fairings, and tail booms (refs. 11 to 19). These interactions can be especially complex on twin-engine installations, which typically have a more complicated flow field than single-engine installations.

The effects of horizontal- and vertical-tail location on twin-engine aft-end drag have been reported in reference 11. Adverse empennage interference effects on a typical twin-engine afterbody were found to be extremely significant, especially in the transonic speed range. In some cases, nearly 40 percent of the total aft-end drag could be attributed to tail interference drag. Because of the large effect of empennage surfaces on aft-end drag, an experimental investigation has been conducted in the Langley 16-Foot Transonic Tunnel to determine the effects of additional empennage and afterbody design parameters on twin-engine aft-end aerodynamic characteristics. Model variables included twin-vertical-tail cant angle, toe angle, airfoil camber, and root-chord length and afterbody/engine interfairing shape. Tests were conducted over a Mach number range from 0.6 to 1.2 and over an angle-of-attack range from -2° to 10° . Nozzle pressure ratio was varied from 1.0 (jet off) to approximately 10.0.

SYMBOLS

All forces and moments are referenced to the stability axis system. The moment reference center was located 4.45 cm above the model centerline at fuselage station 104.24.

A	local cross-sectional area, cm^2
A_{an}	total maximum cross-sectional area of internal nozzle at the nozzle exit, 42.64 cm^2 (see fig. 1(b))
A_{fus}	maximum cross-sectional area of model fuselage, 317.04 cm^2
A_{max}	maximum cross-sectional area of model fuselage/wing combination, 475.09 cm^2
A_o	total internal cross-sectional area of outer nozzle exit opening, 49.01 cm^2 (see fig. 1(b))
A_{seal}	cross-sectional area enclosed by metric-break seal, 297.21 cm^2
C_D	total aft-end drag coefficient, $D/q_\infty S$
$C_{D,a}$	afterbody drag coefficient, $D_a/q_\infty S$
$C_{D,n}$	nozzle drag coefficient, $D_n/q_\infty S$
$C_{D,tails}$	tail drag coefficient, $D_{tails}/q_\infty S$
$\Delta C_{D,ia}$	increment in empennage interference-drag coefficient on afterbody (see eq. (6))
$\Delta C_{D,in}$	increment in empennage interference-drag coefficient on nozzles (see eq. (5))
$\Delta C_{D,it}$	increment in empennage interference-drag coefficient on total aft end (see eq. (4))
C_L	total aft-end lift coefficient, $L/q_\infty S$
C_m	total aft-end pitching-moment coefficient, $m/q_\infty S\bar{c}$
$c_{r,vt}$	vertical-tail root-chord length, cm
\bar{c}	mean geometric chord of the support-system wing, 44.4 cm
D	total aft-end (afterbody + nozzles + tails) drag, N (see eq. (1))
D_a	afterbody drag, N (see eq. (3))
D_{bal}	total aft-end drag measured by balance, N
D_n	nozzle drag (pressure + skin friction), N
D_{tails}	tail drag, N

d_{\max}	maximum diameter at nozzle connect location, 9.86 cm (see fig. 1(c))
d_{th}	nozzle throat diameter, 4.71 cm (see fig. 1(c))
L	total measured afterbody lift, N
ℓ	model length from nose to nozzle exit, 174.74 cm
M	Mach number
m	total afterbody pitching moment referenced to $\bar{c}/4$ in support-system-wing chord plane, N-m
p_{an}	local pressure at nozzle annular clearance gap, Pa (see fig. 1(b))
p_{es}	local static pressure external to the metric-break seal, Pa (see fig. 1(b))
p_{in}	local internal static pressure, Pa (see fig. 1(b))
$p_{t,j}$	jet total pressure, Pa
p_{∞}	free-stream static pressure, Pa
q_{∞}	free-stream dynamic pressure, Pa
r	radius, cm
r_{\max}	maximum radius at nozzle connect station, $d_{\max}/2$, cm
S	support-system-wing reference area, 4286 cm^2
t/c	airfoil thickness ratio (ratio of local maximum thickness to local chord)
x	axial distance from model nose (positive aft), cm
y	horizontal distance from model centerline, BL 0.0 (positive to right, looking upstream), cm
z	vertical distance from model centerline, WL 0.0 (positive up), cm
α	afterbody angle of attack, deg
ϕ	meridian angle about nozzle axis (see fig. 1(c)), deg
ϕ_t	vertical-tail cant angle (positive outboard, see fig. 1(e)), deg
ψ_t	vertical-tail toe angle (positive leading edge out, see fig. 1(e)), deg

Abbreviations:

BL	butt line
Cam. In.	camber inboard
Cam. Out.	camber outboard

FS	fuselage station
fwd	forward
LH	left hand
NPR	ratio of jet total pressure to free-stream static pressure, $p_{t,j}/p_\infty$
RH	right hand
Sym.	symmetrical
WL	water line

APPARATUS AND PROCEDURE

Test Facility

This experimental investigation was conducted in the Langley 16-Foot Transonic Tunnel. The tunnel is a continuous-flow, single-return, atmospheric wind tunnel with a slotted octagonal throat and test section and continuous air exchange. The tunnel has a variable speed range from $M = 0.2$ to $M = 1.3$. Additional information regarding tunnel description and calibration is presented in reference 20.

Model and Support System

Details of the twin-engine tail interference afterbody model and wing-tip-mounted support system used in this investigation are presented in figure 1, and photographs of the model and support system installed in the Langley 16-Foot Transonic Tunnel are shown in figure 2.

The wing-tip-mounted model support system shown in figure 1(a) consisted of three major portions: the twin support booms, the forebody (nose), and the wing/centerbody. These pieces made up the nonmetric portion (that portion of the model not mounted on the force balance) of the twin-engine tail interference model. The centerbody fuselage was essentially rectangular in cross section and had a constant width and height of 25.40 cm and 12.70 cm, respectively. The four corners were rounded by a radius of 2.54 cm. Maximum cross-sectional area of the centerbody (fuselage) was 317.04 cm^2 . The support-system forebody (or nose) was typical of a powered model in that the inlets were faired over. The "wings" of the support system were mounted above the model centerline or in a "high wing" position, which is typical of many current fighter designs. The support system wing had a leading-edge sweep of 45° , a taper ratio of 0.5, an aspect ratio of 2.4, and a cranked trailing edge. The airfoil was symmetrical, and the thickness ratio near the wing fuselage junction at BL 12.70 was typical of current fighter designs ($t/c \approx 0.067$). From BL 27.94 to the support booms, wing thickness ratio increased from $t/c = 0.077$ to $t/c = 0.10$ to provide structural support for the model and to permit transfer of compressed air from the booms to the model propulsion system.

The twin-engine aft end shown in figure 1(b) was attached to the support-system wing/centerbody by mounting on a six-component strain-gage balance as shown. The combined forces and moments for the afterbody shell, empennage surfaces, and outer nozzles were measured by the balance and are termed total aft-end forces and moments

in this paper. Note that the model propulsion system (thrust) forces and moments were not measured by the balance, as the propulsion system was an integral part of the model support system. Clearance was provided between the metric and nonmetric portions of the model. The afterbody lines were chosen to be typical of current close-spaced twin-engine fighter designs and to fair the afterbody smoothly from the constant cross section of the centerbody down to the nozzles. In addition, the afterbody was required to house the afterbody balance, propulsion simulation system, and related instrumentation.

A sketch of the axisymmetric nozzle tested is shown in figure 1(c). The nozzle configuration simulates a convergent-divergent nozzle design with fully variable throat area and expansion ratio control. The nozzle throat area represented maximum nonaugmented (dry power) nozzle operation. The nozzles were sized to be consistent with advanced mixed-flow turbine engine cycles (ref. 21). As shown in the sketch, the nozzle consisted of both an inner and an outer model part. The outer nozzle attached directly to the afterbody. Note that the inner and outer nozzles were separated by a nominal 0.19-cm clearance gap to prevent fouling (or grounding) between the metric aft end and the nonmetric internal propulsion system.

The afterbody had provisions for mounting both the twin vertical tails and the horizontal tails in three axial locations as illustrated in figure 1(d). The effects of empennage location on this model have been reported in reference 11. Note that the leading edge of the root chords for both horizontal and vertical tails could be located at FS 127.00, FS 136.68, or FS 145.57. These locations will be termed fwd, mid, and aft, respectively, throughout the report. The horizontal tail was not tested at the mid position. At the fwd and mid vertical-tail locations, tail brackets provided the ability to either cant or toe the short-chord twin vertical tails. Cant angles of -10°, 0°, 10°, and 20° (outboard cant positive) and toe angles of -2°, 0°, 2°, and 4° (leading edge out positive) were tested as shown in figure 1(e). The toe-angle brackets were designed to allow the vertical tails to rotate about the midpoint of the root chord.

Sketches of the vertical and horizontal tails are shown in figures 1(f), 1(g), and 1(h). These tails were sized to be representative (as were the afterbody and nozzles) of current twin-engine fighter aircraft designs. Three different vertical-tail configurations were tested: the short-root-chord tail with a symmetrical airfoil section (fig. 1(f)), the short-root-chord tail with a cambered airfoil section (fig. 1(f)), and the long-root-chord tail with a symmetrical airfoil section (fig. 1(g)). Planform area and tail span were held constant for all the vertical-tail configurations. A sketch of the horizontal tail is found in figure 1(h). As indicated in each of the tail sketches, individual root fairings (fillers) contoured the tails to the afterbody at each tail location.

Sketches of the side view profiles and afterbody cross section contours of both the basic and alternate interfairings are shown in figures 1(i) and 1(j), respectively. As indicated in figure 1(j), contours outboard of the nozzle vertical center planes were identical for all afterbodies tested.

Normal cross-sectional area distributions for various configuration components are presented in figure 3. Note that the incremental area distributions are provided for the various individual components such as for twin-vertical-tail location in figures 3(a) and 3(b), horizontal-tail location in figure 3(c), and interfairing shape in figure 3(d). In order to determine the area distribution of a complete configuration (for example, forward twin vertical tails and aft horizontal tails used with alternate interfairing), tail area increments at their respective x/l loca-

tions for the individual tail components must be added onto the appropriate fuselage/wing area distribution (which is represented by the solid line in fig. 3).

Instrumentation

External aerodynamic forces and moments on the model aft end (afterbody, empennage surfaces, and outer nozzles) were measured with a six-component strain-gage balance. Forces and moments on the propulsion simulation system were not measured.

Eight external-seal static-pressure orifices, denoted p_{es} in figure 1(b), were located in the metric-break seal area between the centerbody and afterbody. In addition, two internal pressure orifices p_{in} located in the model cavity and eight pressure orifices p_{an} located in the annular gap between the inner and outer nozzles were used to measure internal pressures in the model. These pressures, along with corresponding areas, were used to correct the balance measurements.

Each internal nozzle was instrumented with two total-pressure probe rakes located 180° apart and staggered to prevent appreciable flow blockage. Each rake contained two total-pressure probes as shown in figure 1(c). An additional probe was located in each nozzle and contained a thermocouple, which was used for the measurement of total temperature.

Each outer nozzle had three rows of external pressure orifices (with five pressure orifices in each row) for measurement of external pressure distribution on the nozzles. A table containing the orifice locations of the 30 static taps on the nozzles can be found in figure 1(c). All orifices are shown on the left-hand nozzle for simplicity. Static-pressure measurements from these taps were used in a pressure-area integration over the nozzle surface to obtain nozzle pressure drag.

Tests

Data were obtained in the Langley 16-Foot Transonic Tunnel at Mach numbers from 0.6 to 1.2. Angle of attack was varied from -2° to 10° , and the nozzle pressure ratio (ratio of jet total pressure to free-stream static pressure) ranged from 1.0 (jet off) to approximately 10.0. Reynolds number based on the mean geometric chord of the support-system wing varied from approximately 4.4×10^6 to 6.1×10^6 .

All configurations were tested with fixed boundary-layer transition strips on the model nose and wings and on the afterbody empennage surfaces. A 0.254-cm-wide strip of No. 120 silicon carbide grit was located 5.08 cm from the nose of the forebody and in a straight line along the wing span from 5 percent of the root chord to 10 percent of the tip chord. Transition strips 0.254 cm wide of No. 120 silicon carbide grit were located 1.27 cm aft of the leading edge of the vertical and horizontal tails. The procedure used for selecting grit size and location can be found in reference 22.

Data Acquisition and Procedure

Data for both model and wind-tunnel test instrumentation were recorded on magnetic tape. At each test point, 50 samples of data were recorded over a 5-sec period. The samples were averaged, and the averaged values were used for all computations.

Total aft-end drag was measured directly from the six-component strain-gage balance but was corrected for various pressure-area terms. Total aft-end drag was computed from the following equation:

$$D = D_{bal} - \sum (p_{es} - p_{\infty})(A_{fus} - A_{seal}) - \sum (p_{in} - p_{\infty})(A_{seal} - A_o) \\ - \sum (p_{an} - p_{\infty})(A_o - A_{an}) \quad (1)$$

The first two pressure-area terms correct for forces measured by the balance. The last term in equation (1) is an external base pressure drag not actually measured by the balance but which has been charged to aft-end drag throughout this report. Use of this last term was to partially account for the additional nozzle boattail drag that would have been measured had a more realistic nozzle boattail existed where no clearance between the internal and external nozzle was required.

Nozzle drag D_n was obtained by adding nozzle pressure drag to a computed nozzle skin-friction drag. Nozzle pressure drag was determined by integration of nozzle pressure distributions over the nozzle surface area. Nozzle skin-friction drag was computed using the method of Frankl and Voishel for compressible, turbulent flow on a flat plate, as described in reference 23.

Vertical- and horizontal-tail drag D_{tails} was defined to be the sum of form drag plus skin-friction drag for $M < 0.9$, and the sum of wave drag plus skin-friction drag for $M > 1.0$. Skin-friction drag and wave drag were computed using methods of references 23 and 24. The subsonic form factors for the tails were obtained from empirical correlations of unpublished NASA data and were calculated using the equation

$$\text{Form factor} = 1 + 1.44(t/c) + 2(t/c)^2 \quad (2)$$

The individual root fairings required for each tail location were also included in the skin-friction and wave drag calculations. Using previously determined drag components, afterbody drag D_a was obtained from the following equation:

$$D_a = D - D_n - D_{tails} \quad (3)$$

The tail interference terms used in this report are consistent with those used in references 11 and 15. The increment in empennage interference-drag coefficient on the total aft end was determined from

$$\Delta C_D, it = (C_D)_{tails on} - (C_D)_{tails off} - C_{D,tails} \quad (4)$$

where $(C_D)_{tails on}$ is the measured total aft-end drag for a given configuration; $(C_D)_{tails off}$ is the measured aft-end drag for the same afterbody/nozzle configuration with the tails removed; and $C_{D,tails}$ is the computed value of tail drag as

discussed previously. Hence this total tail interference increment includes the interference effects of one empennage surface on another, of the afterbody/nozzles on the empennage surfaces, and of empennage surfaces on the afterbody/nozzles. It also includes drag increments associated with misalignment of the empennage surfaces with the afterbody flow field. The increment in empennage interference-drag coefficient on the nozzles alone was found from the following equation:

$$\Delta C_{D,in} = (C_{D,n})_{\text{tails on}} - (C_{D,n})_{\text{tails off}} \quad (5)$$

where the nozzle drag coefficients are integrated pressure distributions over the nozzle surface. This empennage interference increment, then, is the result of changes in nozzle pressure distribution resulting from adding empennage surfaces to an afterbody/nozzle configuration. The increment in empennage interference-drag coefficient on the afterbody alone was then defined to be the difference between the empennage interference increments on the total aft end and on the nozzles alone, or

$$\Delta C_{D,ia} = \Delta C_{D,it} - \Delta C_{D,in} \quad (6)$$

In an effort to avoid errors associated with computation of lift-induced drag on the horizontal-tail surfaces, afterbody, and nozzles, these interference terms were computed only at an angle of attack of 0°.

RESULTS AND DISCUSSION

Basic Data

The basic data obtained during this investigation are indexed in table I. The force and moment data listed in coefficient form are found in tables II to V. All tabulated force and moment coefficient data are presented with the corresponding Mach number M , afterbody angle of attack α , and nozzle pressure ratio NPR (ratio of averaged jet total pressure to free-stream static pressure).

Data Comparisons

In an effort to simplify the analysis, data have been cross-plotted at selected values of nozzle pressure ratio (NPR). Figure 4 presents the typical variation in turbofan-engine nozzle pressure ratio with Mach number used for this analysis. While discussion of the results is based on this particular schedule of NPR as a function of Mach number, it would also be generally true for other schedules. However, the magnitude of the differences between configuration drag coefficients might vary slightly.

Configuration comparisons are presented in figures 5 to 21. In part (a) of each figure, the total aft-end drag and lift characteristics are plotted against Mach number for two values of afterbody angle of attack, 0° and 8°. The dashed-curve fairings found for all data at $\alpha = 8^\circ$ indicate that the actual fairing would probably differ had data been acquired at intermediate Mach numbers ($0.6 < M < 0.9$). Presented in part (b) of each of these figures are the individual aft-end drag coefficient components (nozzle drag coefficient $C_{D,n}$, computed tail drag coefficient

$C_{D,tails}$, and afterbody drag coefficient $C_{D,a}$) and the tail interference-drag-coefficient increments (tail interference increment on the total aft-end $\Delta C_{D,it}$, tail interference increment on the nozzles $\Delta C_{D,in}$, and tail interference increment on the afterbody $\Delta C_{D,ia}$). The component drag coefficients and interference increments are presented only at an afterbody angle of attack of approximately 0° . Note that values of interference increments less than zero indicate favorable interference, and values greater than zero indicate unfavorable interference.

The baseline aft-end configuration consisted of the afterbody with dry power nozzles, basic engine interfairing, and short-root-chord twin vertical tails with symmetrical airfoils. Unless otherwise noted, data comparisons were made for this baseline configuration.

Twin-vertical-tail toe angle.- The effects of twin-vertical-tail toe angle on total aft-end lift and drag coefficients, individual drag-coefficient components, and tail interference-drag increments are presented in figures 5 to 7. A summary of the effects of toe-angle variation on total aft-end drag is shown in figure 22.

Examination of the drag data presented in figure 22 shows that the vertical-tail toe angle for lowest drag is a function of Mach number, angle of attack, and to a lesser extent, empennage location. At subsonic speeds and $\alpha = 0^\circ$, $\psi_t = 2^\circ$ toe out of the vertical tails provided the lowest values of aft-end drag for all configurations tested. Apparently the vertical tails with a toe-out angle of 2° are more nearly aligned with the afterbody flow field. As the toe angle is decreased (from 2°), it is believed that the flow is accelerated over the inboard surface of the tails and results in accelerated flow over much of the afterbody region between the tails (see refs. 12 and 25). As a result, afterbody pressures are reduced on the upper surface. This reduced pressure results in increased drag as well as increased lift (figs. 5 to 7). In addition, drag on the individual vertical tails is increased because the tails are effectively at an angle of incidence with respect to the afterbody flow field. Conversely, an increase of the toe angle to $\psi_t = 4^\circ$ would tend to decelerate the flow inboard of the tails. Again the vertical-tail drag would be increased (over the $\psi_t = 2^\circ$ case) because of the angle of incidence to the afterbody flow field. The net result as seen in figures 22 and 5 to 7 for the increased toe angle was an overall increase in the aft-end drag and a decrease in lift when compared with the $\psi_t = 2^\circ$ toe-out case. Data at low supersonic speeds ($M = 1.2$) and $\alpha = 0^\circ$ indicate that optimum toe angle probably occurs between 0° and 2° , depending upon empennage location.

As angle of attack is increased to 8° , the data at $M = 0.9$ (solid symbols in fig. 22) show that the $\psi_t = 4^\circ$ toe-out configuration resulted in the lowest drag. This decrease in drag due to increased toe angle is believed to result from increased angularity of the flow field relative to the model axis caused by flow from the lower to the upper surface of the afterbody.

The tail interference-drag-coefficient increments on the total aft-end $\Delta C_{D,it}$, found on part (b) of figures 5 to 7, are seen to increase with increasing subsonic Mach number and decrease with increasing supersonic Mach number. This trend was consistent for all configurations tested. The importance of this trend can be illustrated by comparisons of the tail interference on the total aft-end $\Delta C_{D,it}$ with the total aft-end drag C_D for the $\psi_t = 0^\circ$ case presented in figure 5. At $M = 0.9$, the tail interference-drag-coefficient increment on the total aft-end $\Delta C_{D,it}$ is 0.0032, and the total aft-end drag coefficient is 0.0086. Just over 37 percent of the total aft-end drag can be attributed to tail interference. Conversely, at $M = 0.6$ and $M = 1.2$, the interference increment was a small, favorable one. Tail

interference effects on drag were measured throughout the Mach number range tested and generally provided a significant percentage of total aft-end drag in the transonic speed range. A similar result has been reported in reference 15 for single-engine configurations. As would be expected from the earlier discussion of total aft-end drag, the tail interference-drag increments were relatively small for the $\psi_t = 2^\circ$ toe-out configurations.

It is obvious from the data presented that aft-end drag is extremely sensitive to vertical-tail toe angle as evidenced by the large drag penalties resulting from nonoptimized toe-angle settings (fig. 22). As is always the case with aircraft design, compromises must be made. For the afterbody configuration and test conditions presented, $\psi_t = 2^\circ$ toe out probably offers the best compromise for improved airplane performance throughout a complete mission. It must be cautioned, however, that optimum toe angle is probably highly dependent on the forebody flow field, and as a result would be a function of forebody, wing/strake/canard, and afterbody shape ahead of the tails.

Twin-vertical-tail cant angle.- The effects of twin-vertical-tail cant angle on total aft-end lift and drag coefficients, individual drag coefficient components, and tail interference-drag-coefficient increments are presented in figures 8 and 9. A summary of the effects of cant-angle variation on total aft-end drag is shown in figure 23.

As was the case for toe angle, vertical-tail cant-angle effects on aft-end drag were dependent upon Mach number, angle of attack, and empennage location. Examination of summary figure 23 indicates that, for an angle of attack of 0° , the cant position of 20° generally produced the lowest drag. At $\alpha = 8^\circ$, however, lowest drag resulted from cant angles of -10° to 0° . In general for the configurations tested, cant-angle variation did not have as large an impact on aft-end drag as toe-angle variation, but significant reductions in drag could be obtained by outward cant of the twin vertical tails at $\alpha = 0^\circ$. In fact, as seen in figures 8(b) and 9(b), a positive cant angle (10° or 20°) resulted in favorable (negative) total aft-end empennage interference-drag increments $\Delta C_{D,it}$ over much of the Mach range tested. The reasons for these drag improvements are not understood.

Effects of vertical-tail cant on lift coefficient (figs. 8(a) and 9(a)) were relatively small for $\alpha = 0^\circ$. As afterbody angle of attack increased, outward twin-vertical-tail cant resulted in significant increases in lift as might be expected, since outward cant results in a component of lift being directed normal to the afterbody axis.

Twin-vertical-tail camber.- The effects of cambering the twin vertical tails (and varying the location of that camber) on total aft-end lift and drag coefficients, individual drag-coefficient components, and tail interference-drag increments are presented in figures 10 to 15. A summary of the effects of cambering the vertical tails on total aft-end drag is shown in figure 24. Data are presented for both symmetrical and cambered twin-vertical-tail airfoils. The camber-inboard designation indicates that the mean camber line of each vertical-tail airfoil is oriented inboard of the tail chord line. Conversely, camber outboard indicates that the mean camber line is outboard of the chord line.

As shown in figure 24, the effects of camber on aft-end drag were determined for various vertical-tail cant angles at two vertical-tail axial locations. Note that vertical-tail toe angle was fixed at 0° . Symmetrical-airfoil, camber-outboard, and camber-inboard configurations were investigated at vertical-tail cant angles of 0° .

In addition, inboard camber was tested when the twin vertical tails were canted outward ($\phi_t = 10^\circ$ and 20°), and outboard camber was tested when the vertical tails were canted inward ($\phi_t = -10^\circ$). These data indicate that regardless of vertical-tail axial location or cant angle, outboard vertical-tail camber generally reduced total aft-end drag, and inboard camber generally increased total aft-end drag compared with the symmetrical airfoil. These results are not totally unexpected if it is realized that, at subsonic speeds, the effects of orientation of the vertical-tail camber are similar to those effects noted for vertical-tail toe angle. Both the symmetrical-airfoil and the camber-inboard cases probably act to accelerate the flow over the afterbody in the region between the tails as previously noted for toe angles of 0° and -2° . The camber-outboard configurations (at $\phi_t = 0^\circ$) provided aft-end drag levels nearly identical to those found previously for the $\phi_t = 2^\circ$ toe-out case (fig. 22). The outboard-camber configurations are believed to be at or near a non-lifting condition (effective tail angle of attack of approximately -2°) in the wing/forebody flow field. Hence, the outboard-camber tails have less impact on local flow velocities near the tails than would be the case of tail surfaces that are providing lift (and higher local accelerations). It is interesting to note that for $M = 1.2$, the outboard-camber configurations (at $\phi_t = 0^\circ$) resulted in lower aft-end drag levels than those obtained by outward toe of the vertical tails.

The effects of vertical-tail camber on aft-end lift (figs. 10 to 15) tended to be much more Mach number and empennage-configuration dependent than the drag results. The lift-coefficient characteristics for the afterbody configured with vertical tails in the forward location (figs. 10 to 12) indicate that, at subsonic speeds, outboard camber decreased lift, and inboard camber increased lift relative to the symmetrical airfoil. Again it is assumed that both the symmetrical-airfoil and inboard-camber configurations result in accelerated flow over the afterbody region between the tails, reduced static pressure, and increased lift in a manner similar to that noted for twin-vertical-tail toe-in angle (negative ϕ_t). At $M > 1.0$, these trends are reversed. This same reversal in trend also occurs for Mach numbers above 0.8 for the twin vertical tails located in the mid-axial position at $\phi_t = 0^\circ$ and 10° (figs. 13 and 14). These trend reversals cannot currently be explained.

It should be noted that no attempt was made during this investigation to optimize aft-end drag. (Combinations of toe angle, cant angle, and camber on the vertical tails were not tested.)

Twin-vertical-tail root-chord length.— The effects of twin-vertical-tail root-chord length on total aft-end lift and drag coefficients, individual drag-coefficient components, and tail interference-drag increments are presented in figures 16 to 18. The short-root-chord baseline tails shown in figure 1(f) had a root-chord length of 24.38 cm, while the long-root-chord tails shown in figure 1(g) had a root-chord length of 28.19 cm.

Variation in root-chord length had little effect on drag except for the empennage configuration shown in figure 16 (both horizontal and vertical tails located forward), where the long-root-chord vertical tails provided drag reductions throughout the Mach number range. The reasons for this are not understood.

Engine interfairing.— The effects of engine interfairing contour on total aft-end lift and drag coefficients and individual drag-coefficient components are presented in figures 19 to 21. Tail interference-drag increments were not obtained for the alternate interfairing configurations.

Examination of the total aft-end lift and drag characteristics indicates that the basic interfairing generally provided equal or lower drag and higher lift than did the alternate interfairing. Lower drag for the basic interfairing is opposite the trend reported in reference 17 for comparison of circular arc and elliptical interfairings installed on an isolated (no tails) twin-engine afterbody model. However, it must be noted that aft-end drag characteristics are highly dependent on such configuration variables as empennage surface locations (refs. 11 and 15), afterbody and nozzle boattail angles (ref. 17), and nozzle lateral spacing (ref. 1). The current data indicate that engine interfairing shape should be evaluated in the presence of empennage surfaces for accurate determination of its effect on aft-end drag. The magnitude of the effect of empennage location on the results from an interfairing shape study is indicated by the different drag trends ($\alpha = 0^\circ$) shown in figures 19 to 21. At subsonic speeds, as shown in part (b) of figures 19 to 21 and as previously reported in reference 17, the largest drag changes due to interfairing shape generally occur on the nozzles ($C_{D,n}$) rather than on the afterbody ($C_{D,a}$). At supersonic speeds, interfairing shape tended to affect afterbody drag slightly more than nozzle drag, with the highest afterbody drag occurring for the alternate interfairing. This trend is probably caused by increased supersonic wave drag due to the steeper aft-end slopes (see figs. 1(i) and 3(d)) of the alternate interfairing.

CONCLUSIONS

An experimental investigation has been conducted in the Langley 16-Foot Transonic Tunnel to determine the effects of several empennage and afterbody parameters on twin-engine aft-end aerodynamic characteristics. Model variables included twin-vertical-tail cant angle, toe angle, airfoil camber, and root-chord length and afterbody/engine interfairing shape. Tests were conducted over a Mach number range from 0.6 to 1.2 and over an angle-of-attack range from -2° to 10° . Nozzle pressure ratio was varied from 1.0 (jet off) to approximately 10.0. Results from this study indicate the following:

1. Tail interference effects on total aft-end drag were present throughout the Mach number range tested and provided a significant percentage of total aft-end drag in the transonic speed range.
2. Aft-end drag was sensitive to twin-vertical-tail toe angle. At subsonic speeds and an angle of attack of 0° , significant reductions in drag were obtained by a slight outward toe angle (approximately 2°) for the afterbody configuration tested. As Mach number was increased to supersonic speeds, the toe angle required for lowest drag occurred between 0° and 2° toe out, depending upon vertical- and horizontal-tail location. Generally, as angle of attack increased, lowest aft-end drag occurred at increased outboard toe angles.
3. Significant decreases in drag were achieved by outward cant of the twin vertical tails at low angles of attack. At higher angles of attack (approximately 8°), either no cant or a slight inward cant provided drag benefits.
4. Outboard placement of vertical-tail camber reduced drag for all configurations tested.

5. Twin-vertical-tail root-chord-length effects on aft-end lift and drag were generally small.

6. Engine interfairing shape effects on drag appeared to be configuration dependent and should be evaluated for a particular configuration in the presence of tails.

Langley Research Center
National Aeronautics and Space Administration
Hampton, VA 23665
March 24, 1983

REFERENCES

1. Berrier, Bobby L.: Effect of Nozzle Lateral Spacing on Afterbody Drag and Performance of Twin-Jet Afterbody Models With Cone Plug Nozzles at Mach Numbers up to 2.20. NASA TM X-2632, 1972.
2. Sams, H.: F-15 Propulsion System Design and Development. AIAA Paper No. 75-1042, Aug. 1975.
3. Martens, Richard E.: F-15 Nozzle/Afterbody Integration. AIAA Paper No. 74-1100, Oct. 1974.
4. Nichols, Mark R.: Aerodynamics of Airframe-Engine Integration of Supersonic Aircraft. NASA TN D-3390, 1966.
5. Berrier, Bobby L.; and Staff, Propulsion Integration Section: A Review of Several Propulsion Integration Features Applicable to Supersonic-Cruise Fighter Aircraft. NASA TM X-73991, 1976.
6. Bergman, Dave: Unique Characteristics of Exhaust-Plume Interference. *J. Aircr.*, vol. 10, no. 8, Aug. 1973, pp. 508-511.
7. Richey, G. K.; Suber, L. E.; and Laughrey, J. A.: Airframe/Propulsion System Flow Field Interference and the Effect on Air Intake and Exhaust Nozzle Performance. *Airframe/Propulsion Interference*, AGARD-CP-150, Mar. 1975, pp. 23-1 - 23-31.
8. Glasgow, E. R.; and Santman, D. M.: Aft-End Design Criteria and Performance Prediction Methods Applicable to Air Superiority Fighters Having Twin Buried Engines and Dual Nozzles. AIAA Paper No. 72-1111, Nov.-Dec. 1972.
9. Pendergraft, Odis C., Jr.; and Schmeer, James W.: Effect of Nozzle Lateral Spacing on Afterbody Drag and Performance of Twin-Jet Afterbody Models With Convergent-Divergent Nozzles at Mach Numbers up to 2.2. NASA TM X-2601, 1972.
10. Pendergraft, Odis C., Jr.: Fuselage and Nozzle Pressure Distributions on a 1/12-Scale F-15 Propulsion Model at Transonic Speeds. NASA TP-1521, 1979.
11. Leavitt, Laurence D.: Effect of Empennage Location on Twin-Engine Afterbody/Nozzle Aerodynamic Characteristics at Mach Numbers From 0.6 to 1.2. NASA TP-2116, 1983.
12. Pendergraft, Odis C., Jr.; and Bare, E. Ann: Effect of Nozzle and Vertical-Tail Variables on the Performance of a Three-Surface F-15 Model at Transonic Mach Numbers. NASA TP-2043, 1982.
13. Reubush, David E.; and Mercer, Charles E.: Effects of Nozzle Interfairing Modifications on Longitudinal Aerodynamic Characteristics of a Twin-Jet, Variable-Wing-Sweep Fighter Model. NASA TN D-7817, 1975.
14. Glasgow, E. R.: Integrated Airframe-Nozzle Performance For Designing Twin-Engine Fighters. AIAA Paper No. 73-1303, Nov. 1973.
15. Berrier, Bobby L.: Effect of Nonlifting Empennage Surfaces on Single-Engine Afterbody/Nozzle Drag At Mach Numbers From 0.5 to 2.2. NASA TN D-8326, 1977.

16. Maiden, Donald L.; and Berrier, Bobby L.: Effect of Airframe Modifications on Longitudinal Aerodynamic Characteristics of a Fixed-Wing, Twin-Jet Fighter Airplane Model. NASA TM X-2523, 1972.
17. Lee, Edwin E., Jr.; and Runckel, Jack F.: Performance of Closely Spaced Twin-Jet Afterbodies With Different Inboard-Outboard Fairing and Nozzle Shapes. NASA TM X-2329, 1971.
18. Exhaust System Interaction Program. Volumes I-XVII. D162-10467-11 (Contract No. F33615-70-C-1450), Boeing Co., Apr. 1973.
19. Swavely, C. E.; and Soileau, J. F.: Aircraft Aftbody/Propulsion System Integration for Low Drag. AIAA Paper No. 72-1101, Nov.-Dec. 1972.
20. Corson, Blake W., Jr.; Runckel, Jack F.; and Igoe, William B.: Calibration of the Langley 16-Foot Transonic Tunnel With Test Section Air Removal. NASA TR R-423, 1974.
21. Stevens, H. L.: F-15/Nonaxisymmetric Nozzle System Integration Study Support Program. NASA CR-135252, 1978.
22. Braslow, Albert L.; Hicks, Raymond M.; and Harris, Roy V., Jr.: Use of Grit-Type Boundary-Layer-Transition Trips on Wind-Tunnel Models. NASA TN D-3579, 1966.
23. Shapiro, Ascher H.: The Dynamics and Thermodynamics of Compressible Fluid Flow. Vol. II. The Ronald Press Co., 1954.
24. Harris, Roy V., Jr.: An Analysis and Correlation of Aircraft Wave Drag. NASA TM X-947, 1964.
25. Bare, E. Ann; Berrier, Bobby L.; and Capone, Francis J.: Effect of Simulated In-Flight Thrust Reversing on Vertical-Tail Loads of F-18 and F-15 Airplane Models. NASA TP-1890, 1981.

TABLE I.-- INDEX TO BASIC DATA

Horizontal-tail location	Vertical-tail location	Cant angle, ϕ_t , deg	Toe angle, ψ_t , deg	$c_{r,vt}$, cm	Vertical-tail airfoil	Interfairing	Table
Fwd	Fwd	0	0	24.38	Symmetrical	Basic	II(a)
		-2	-2				(b)
		2	2				(c)
		4	4				(d)
		0	0	28.19			(e)
		-2	-2				III(a)
		2	2				(b)
		4	4				(c)
		0	0	24.38			(d)
		-10	0				(e)
Aft	Aft	10					(f)
		20					(g)
		0					(h)
		0					(i)
		-10					(j)
		20					(k)
		0					(l)
		-10					(m)
		20					IV(a)
		0					(b)
Mid	Mid	0		28.19	Symmetrical	Basic	(c)
		-2					(d)
		2					(e)
		4					(f)
		0		24.38			(g)
		-10					(h)
		20					(i)
		0					(j)
		-10					(k)
		20					(l)
Aft	Aft	0					(m)
		10					IV(b)
		20					(c)
		0					(d)
		0					(e)
		10					(f)
		20					(g)
		20					(h)
		0					(i)
		-10					(j)
"	"	0		28.19	Symmetrical	Alternate	(k)
		-2					(l)
		2					(m)
		4					IV(a)
		0		24.38			(b)
		-10					(c)
		20					(d)
		0					(e)
		-10					(f)
		20					(g)

TABLE II.- BASIC FORCE AND MOMENT DATA FOR CONFIGURATION WITH
HORIZONTAL TAILS FORWARD AND VERTICAL TAILS FORWARD

(a) $c_{r,vt} = 24.38$ cm; symmetrical vertical-tail airfoil;
 $\phi_t = 0^\circ$; $\phi_v = 0^\circ$; basic interfairing

M	α , deg	NPR	C_L	C_D	C_m	M	α , deg	NPR	C_L	C_D	C_m
0.852	0.00	1.093	0.0215	0.0102	-0.0264	0.901	4.00	6.038	0.0337	0.0106	-0.0419
0.849	1.01	1.092	0.0266	0.0106	-0.0319	0.901	3.98	8.045	0.0331	0.0098	-0.0410
0.851	2.01	1.092	0.0314	0.0113	-0.0373	0.898	7.99	1.103	0.0708	0.0201	-0.0857
0.851	2.99	1.091	0.0376	0.0121	-0.0444	0.901	8.01	2.012	0.0704	0.0186	-0.0850
0.851	4.00	1.090	0.0450	0.0131	-0.0529	0.903	7.99	3.514	0.0702	0.0187	-0.0849
0.852	4.99	1.091	0.0511	0.0144	-0.0603	0.900	8.00	4.193	0.0701	0.0184	-0.0847
0.849	5.99	1.092	0.0585	0.0159	-0.0689	0.902	7.99	5.999	0.0701	0.0179	-0.0847
0.849	6.99	1.092	0.0673	0.0179	-0.0792	0.901	8.00	8.007	0.0697	0.0172	-0.0843
0.850	-0.01	1.093	0.0206	0.0100	-0.0253	0.903	-0.02	1.104	0.0192	0.0103	-0.0253
1.200	0.00	1.006	-0.0027	0.0229	-0.0006	0.852	-0.01	1.085	0.0209	0.0095	-0.0255
1.200	-2.00	1.007	-0.0334	0.0242	0.0343	0.852	0.00	2.007	0.0203	0.0078	-0.0247
1.201	-0.00	1.006	-0.0023	0.0230	-0.0011	0.850	0.00	3.505	0.0199	0.0078	-0.0243
1.202	2.00	1.003	0.0282	0.0241	-0.0363	0.849	-0.01	4.000	0.0200	0.0078	-0.0243
1.200	3.98	1.000	0.0584	0.0272	-0.0712	0.849	0.01	8.015	0.0190	0.0065	-0.0232
1.199	5.00	0.998	0.0736	0.0295	-0.0887	0.847	-0.01	1.081	0.0200	0.0091	-0.0244
1.198	6.00	0.968	0.0795	0.0324	-0.0950	0.801	-0.01	1.069	0.0178	0.0090	-0.0211
1.198	7.98	0.944	0.1023	0.0392	-0.1228	0.801	0.05	2.015	0.0172	0.0075	-0.0207
1.200	0.00	1.002	-0.0029	0.0231	-0.0005	0.802	0.02	3.930	0.0172	0.0075	-0.0205
1.202	-0.01	1.986	-0.0037	0.0219	0.0003	0.802	-0.01	5.005	0.0170	0.0072	-0.0203
1.199	-0.00	3.549	-0.0031	0.0223	-0.0002	0.799	-0.00	7.990	0.0166	0.0062	-0.0198
1.198	0.02	6.014	-0.0033	0.0217	0.0000	0.802	0.01	1.067	0.0174	0.0088	-0.0205
1.200	-0.00	10.021	-0.0036	0.0199	0.0003	1.201	3.99	0.994	0.0575	0.0265	-0.0696
1.200	3.99	0.990	0.0587	0.0271	-0.0714	1.200	3.99	1.993	0.0581	0.0257	-0.0702
1.201	3.99	1.999	0.0583	0.0261	-0.0708	1.201	4.01	3.516	0.0584	0.0263	-0.0705
1.199	4.01	3.627	0.0589	0.0266	-0.0716	1.201	3.99	6.056	0.0584	0.0256	-0.0706
1.203	3.99	3.545	0.0585	0.0264	-0.0710	1.200	4.00	9.945	0.0582	0.0238	-0.0701
0.941	-0.00	1.123	0.0136	0.0098	-0.0217	1.200	3.99	0.985	0.0584	0.0269	-0.0709
0.936	0.00	2.001	0.0140	0.0085	-0.0213	1.151	3.99	0.994	0.0576	0.0284	-0.0701
0.943	-0.00	3.532	0.0113	0.0081	-0.0186	1.150	-0.01	0.996	-0.0040	0.0242	0.0001
0.940	-0.02	4.341	0.0124	0.0081	-0.0200	1.148	-0.02	1.999	-0.0043	0.0231	0.0005
0.942	0.01	8.016	0.0112	0.0069	-0.0189	1.151	0.01	3.513	-0.0042	0.0234	0.0005
0.943	0.02	1.120	0.0119	0.0094	-0.0198	1.152	-0.00	5.619	-0.0046	0.0229	0.0010
0.898	0.00	1.105	0.0201	0.0103	-0.0259	1.152	-0.01	10.052	-0.0049	0.0204	0.0011
0.902	-2.00	1.107	0.0132	0.0096	-0.0181	1.148	-0.00	0.992	-0.0048	0.0241	0.0009
0.899	0.01	1.106	0.0204	0.0104	-0.0263	0.601	-0.01	1.032	0.0144	0.0088	-0.0167
0.900	2.01	1.105	0.0279	0.0114	-0.0343	0.602	-2.01	1.032	0.0025	0.0087	-0.0037
0.901	3.99	1.103	0.0370	0.0130	-0.0461	0.601	0.06	1.032	0.0153	0.0088	-0.0174
0.898	5.99	1.104	0.0505	0.0157	-0.0622	0.601	1.99	1.032	0.0278	0.0096	-0.0311
0.898	8.01	1.107	0.0714	0.0204	-0.0862	0.600	4.01	1.031	0.0415	0.0114	-0.0464
0.898	10.00	1.106	0.0960	0.0278	-0.1149	0.598	6.00	1.031	0.0564	0.0141	-0.0633
0.899	-0.01	1.106	0.0198	0.0105	-0.0256	0.598	7.99	1.031	0.0704	0.0178	-0.0799
0.899	-0.02	2.022	0.0178	0.0086	-0.0231	0.598	10.01	1.031	0.0879	0.0232	-0.1012
0.900	-0.00	3.510	0.0180	0.0087	-0.0234	0.600	0.05	1.031	0.0156	0.0090	-0.0175
0.899	-0.00	4.222	0.0180	0.0086	-0.0233	0.601	0.01	2.004	0.0155	0.0078	-0.0172
0.899	-0.03	6.025	0.0178	0.0081	-0.0231	0.601	-0.01	3.401	0.0147	0.0079	-0.0163
0.898	0.01	7.950	0.0172	0.0074	-0.0223	0.602	-0.01	4.019	0.0142	0.0078	-0.0158
0.903	3.99	1.100	0.0355	0.0127	-0.0446	0.602	0.00	5.992	0.0147	0.0072	-0.0163
0.899	3.95	2.000	0.0343	0.0111	-0.0422	0.601	0.00	8.038	0.0142	0.0066	-0.0157
0.899	4.02	3.512	0.0348	0.0113	-0.0426	0.600	4.00	1.029	0.0408	0.0113	-0.0451
0.902	4.01	4.218	0.0342	0.0112	-0.0423	0.600	3.99	2.009	0.0407	0.0104	-0.0447
						0.600	4.01	3.406	0.0416	0.0106	-0.0457
						0.600	4.01	4.067	0.0414	0.0105	-0.0455
						0.600	4.01	6.007	0.0415	0.0100	-0.0458
						0.600	4.00	7.987	0.0412	0.0094	-0.0454
						0.601	8.01	1.028	0.0719	0.0181	-0.0809
						0.600	7.98	2.001	0.0723	0.0172	-0.0817
						0.601	8.00	3.401	0.0722	0.0172	-0.0814
						0.600	8.01	4.066	0.0723	0.0171	-0.0813
						0.600	8.01	5.992	0.0728	0.0167	-0.0822
						0.599	8.01	7.961	0.0724	0.0160	-0.0820
						0.601	0.00	1.026	0.0165	0.0091	-0.0185

TABLE II.- Continued

(b) $c_{r,vt} = 24.38$ cm; symmetrical vertical-tail airfoil;
 $\phi_t = -2^\circ$; $\phi_t = 0^\circ$; basic interfairing

M	α , deg	NPR	C_L	C_D	C_m	M	α , deg	NPR	C_L	C_D	C_m
1.202	-0.01	0.993	-0.0024	0.0232	-0.0014	0.900	4.01	6.005	0.0360	0.0128	-0.0457
1.201	-2.00	0.999	-0.0322	0.0241	0.0325	0.900	4.00	7.985	0.0352	0.0121	-0.0446
1.202	0.01	0.991	-0.0017	0.0233	-0.0023	0.898	7.99	1.099	0.0729	0.0225	-0.0899
1.201	1.98	0.986	0.0283	0.0244	-0.0367	0.901	8.01	1.999	0.0722	0.0209	-0.0891
1.200	4.02	0.982	0.0591	0.0278	-0.0724	0.902	7.99	3.514	0.0718	0.0210	-0.0888
1.197	6.00	0.978	0.0873	0.0328	-0.1054	0.898	8.00	4.202	0.0726	0.0209	-0.0892
1.199	7.99	0.926	0.1016	0.0401	-0.1227	0.901	8.01	6.002	0.0725	0.0204	-0.0894
1.202	-0.02	0.989	-0.0029	0.0234	-0.0011	0.899	8.00	7.994	0.0724	0.0196	-0.0893
1.201	-0.00	2.011	-0.0024	0.0224	-0.0018	0.900	0.00	1.099	0.0221	0.0121	-0.0288
1.201	0.01	3.526	-0.0023	0.0227	-0.0020	0.851	-0.02	1.082	0.0250	0.0113	-0.0303
1.202	0.01	6.008	-0.0030	0.0221	-0.0011	0.850	0.00	1.989	0.0237	0.0099	-0.0284
1.200	-0.01	10.007	-0.0038	0.0203	-0.0002	0.850	0.01	3.511	0.0240	0.0101	-0.0287
1.199	4.01	0.975	0.0583	0.0278	-0.0718	0.850	-0.01	3.994	0.0233	0.0100	-0.0281
1.199	3.99	1.998	0.0567	0.0268	-0.0695	0.848	-0.01	7.988	0.0223	0.0088	-0.0270
1.199	4.01	3.503	0.0572	0.0272	-0.0702	0.849	-0.02	1.078	0.0242	0.0112	-0.0293
1.199	4.00	6.003	0.0577	0.0265	-0.0709	0.798	0.01	1.067	0.0240	0.0100	-0.0277
1.199	4.01	9.988	0.0513	0.0243	-0.0607	0.800	-0.00	2.013	0.0232	0.0086	-0.0264
1.200	0.00	0.983	-0.0039	0.0233	-0.0005	0.800	0.01	3.917	0.0234	0.0087	-0.0269
1.155	-0.01	0.994	-0.0043	0.0243	-0.0002	0.799	-0.01	5.030	0.0231	0.0085	-0.0264
1.149	0.01	2.005	-0.0040	0.0234	-0.0009	0.802	0.01	7.998	0.0220	0.0076	-0.0252
1.153	0.00	3.508	-0.0044	0.0236	-0.0005	0.796	-0.01	1.064	0.0234	0.0099	-0.0270
1.152	-0.01	5.620	-0.0041	0.0232	-0.0009	0.598	-0.02	1.033	0.0169	0.0084	-0.0190
1.151	0.00	10.019	-0.0053	0.0208	0.0012	0.603	-1.98	1.034	0.0045	0.0083	-0.0055
1.149	-0.01	0.991	-0.0041	0.0245	-0.0008	0.601	-0.03	1.033	0.0166	0.0084	-0.0188
0.939	-0.02	1.115	0.0153	0.0121	-0.0244	0.603	1.99	1.033	0.0299	0.0093	-0.0332
0.940	0.01	2.009	0.0134	0.0102	-0.0220	0.601	3.98	1.033	0.0437	0.0110	-0.0485
0.940	0.01	3.515	0.0134	0.0105	-0.0225	0.600	6.02	1.033	0.0594	0.0139	-0.0665
0.941	-0.01	4.302	0.0131	0.0103	-0.0219	0.599	8.01	1.033	0.0759	0.0179	-0.0857
0.937	-0.00	7.972	0.0133	0.0094	-0.0221	0.599	10.00	1.034	0.0917	0.0231	-0.1049
0.939	-0.00	8.026	0.0127	0.0092	-0.0214	0.600	0.00	1.034	0.0176	0.0086	-0.0196
0.939	0.00	1.112	0.0149	0.0119	-0.0243	0.600	0.02	1.993	0.0169	0.0074	-0.0189
0.900	-0.01	1.099	0.0218	0.0121	-0.0286	0.601	-0.01	3.401	0.0167	0.0074	-0.0183
0.899	-2.02	1.100	0.0156	0.0110	-0.0217	0.602	-0.04	4.005	0.0162	0.0073	-0.0180
0.899	0.01	1.100	0.0223	0.0122	-0.0293	0.601	-0.00	5.988	0.0165	0.0068	-0.0184
0.901	1.99	1.098	0.0296	0.0133	-0.0371	0.601	0.00	8.027	0.0163	0.0063	-0.0181
0.900	4.00	1.095	0.0383	0.0149	-0.0484	0.600	3.98	1.032	0.0435	0.0107	-0.0480
0.899	6.02	1.097	0.0512	0.0175	-0.0640	0.598	4.01	1.995	0.0433	0.0099	-0.0477
0.897	7.99	1.101	0.0733	0.0226	-0.0904	0.599	4.00	3.409	0.0431	0.0101	-0.0475
0.902	10.02	1.101	0.1001	0.0305	-0.1218	0.599	4.01	4.004	0.0437	0.0101	-0.0480
0.903	-0.02	1.102	0.0219	0.0124	-0.0287	0.600	4.00	6.021	0.0436	0.0096	-0.0481
0.899	-0.00	2.016	0.0210	0.0106	-0.0272	0.601	4.00	8.017	0.0430	0.0090	-0.0474
0.900	0.01	3.494	0.0210	0.0107	-0.0273	0.600	7.99	1.032	0.0757	0.0177	-0.0852
0.899	0.01	4.218	0.0207	0.0106	-0.0269	0.599	8.00	2.008	0.0763	0.0168	-0.0859
0.901	-0.02	6.002	0.0202	0.0101	-0.0265	0.598	8.01	3.405	0.0764	0.0170	-0.0857
0.901	0.00	8.030	0.0195	0.0095	-0.0258	0.601	8.02	4.012	0.0777	0.0173	-0.0875
0.896	4.01	1.092	0.0379	0.0147	-0.0477	0.599	8.01	5.998	0.0763	0.0165	-0.0858
0.901	4.02	2.024	0.0357	0.0132	-0.0448	0.599	8.01	8.002	0.0758	0.0158	-0.0853
0.898	4.01	3.522	0.0367	0.0134	-0.0460	0.598	7.98	1.032	0.0760	0.0179	-0.0858
0.899	4.00	4.211	0.0364	0.0133	-0.0456						

TABLE II.- Continued

(c) $c_{r,vt} = 24.38$ cm; symmetrical vertical-tail airfoil;
 $\psi_t = 2^\circ$; $\phi_t = 0^\circ$; basic interfairing

M	α , deg	NPR	C_L	C_D	C_m	M	α , deg	NPR	C_L	C_D	C_m
1.200	-0.02	1.012	-0.0118	0.0227	0.0103	0.901	7.99	3.521	0.0604	0.0156	-0.0749
1.200	-2.00	1.012	-0.0419	0.0247	0.0443	0.899	7.98	4.205	0.0602	0.0193	-0.0747
1.201	0.02	1.007	-0.0107	0.0228	0.0090	0.898	7.99	6.000	0.0607	0.0150	-0.0753
1.202	2.00	1.009	0.0211	0.0231	-0.0274	0.900	7.98	8.005	0.0603	0.0141	-0.0745
1.202	4.00	1.008	0.0526	0.0260	-0.0639	0.899	-0.01	1.102	0.0093	0.0084	-0.0151
1.198	6.00	0.990	0.0768	0.0308	-0.0920	0.850	-0.01	1.085	0.0087	0.0079	-0.0130
1.199	7.98	0.952	0.0968	0.0370	-0.1161	0.849	-0.02	1.974	0.0084	0.0063	-0.0127
1.202	-0.03	0.999	-0.0124	0.0231	0.0109	0.850	-0.01	3.506	0.0081	0.0064	-0.0121
1.200	-0.01	2.021	-0.0109	0.0219	0.0091	0.849	-0.00	3.997	0.0079	0.0063	-0.0121
1.199	0.00	3.512	-0.0113	0.0223	0.0097	0.852	-0.01	8.007	0.0076	0.0050	-0.0118
1.200	0.00	6.005	-0.0114	0.0217	0.0097	0.849	-0.01	1.083	0.0079	0.0076	-0.0120
1.201	-0.04	10.055	-0.0129	0.0198	0.0111	0.798	-0.03	1.068	0.0070	0.0077	-0.0104
1.200	4.01	6.005	0.0513	0.0246	-0.0627	0.800	-0.01	2.010	0.0070	0.0063	-0.0106
1.151	-0.01	0.999	-0.0133	0.0245	0.0106	0.801	-0.01	3.906	0.0068	0.0064	-0.0103
1.148	-0.01	5.666	-0.0138	0.0234	0.0113	0.801	-0.01	5.002	0.0067	0.0061	-0.0104
0.941	-0.01	1.125	0.0011	0.0079	-0.0094	0.798	-0.00	8.021	0.0066	0.0051	-0.0102
0.941	-0.01	4.304	0.0013	0.0063	-0.0091	0.798	-0.03	1.065	0.0068	0.0077	-0.0101
0.900	-0.02	1.104	0.0091	0.0084	-0.0150	0.597	-0.03	1.031	0.0053	0.0073	-0.0077
0.902	-2.03	1.105	0.0024	0.0082	-0.0077	0.600	-2.01	1.032	-0.0060	0.0075	0.0045
0.901	-0.03	1.105	0.0093	0.0085	-0.0152	0.602	-0.01	1.032	0.0063	0.0073	-0.0089
0.901	1.96	1.106	0.0171	0.0090	-0.0236	0.601	1.99	1.032	0.0184	0.0078	-0.0219
0.903	4.02	1.104	0.0271	0.0103	-0.0360	0.600	3.97	1.032	0.0312	0.0091	-0.0363
0.898	5.99	1.105	0.0405	0.0123	-0.0514	0.600	5.93	1.032	0.0463	0.0114	-0.0533
0.899	8.00	1.107	0.0615	0.0173	-0.0762	0.599	7.98	1.032	0.0619	0.0149	-0.0716
0.899	9.97	1.106	0.0860	0.0245	-0.1044	0.597	9.97	1.032	0.0780	0.0197	-0.0912
0.903	-0.01	1.107	0.0097	0.0086	-0.0155	0.603	-0.02	1.033	0.0063	0.0076	-0.0090
0.896	-0.01	2.009	0.0097	0.0067	-0.0154	0.602	-0.01	2.011	0.0058	0.0063	-0.0082
0.902	-0.04	2.017	0.0089	0.0068	-0.0147	0.601	-0.01	3.410	0.0058	0.0064	-0.0082
0.903	-0.02	3.507	0.0086	0.0069	-0.0141	0.601	-0.01	4.017	0.0055	0.0062	-0.0077
0.900	-0.01	4.193	0.0085	0.0067	-0.0140	0.600	-0.00	6.009	0.0056	0.0057	-0.0080
0.899	-0.01	6.026	0.0082	0.0062	-0.0136	0.601	-0.02	8.008	0.0048	0.0051	-0.0074
0.902	-0.02	7.989	0.0077	0.0055	-0.0133	0.600	3.97	3.391	0.0293	0.0080	-0.0341
0.898	3.98	1.100	0.0265	0.0099	-0.0347	0.599	7.98	1.032	0.0611	0.0147	-0.0707
0.900	3.97	4.007	0.0258	0.0084	-0.0337	0.599	7.99	1.993	0.0617	0.0139	-0.0714
0.899	3.98	4.183	0.0258	0.0083	-0.0336	0.599	7.98	3.413	0.0619	0.0139	-0.0715
0.899	7.98	1.105	0.0597	0.0170	-0.0742	0.600	7.98	4.025	0.0621	0.0139	-0.0719
0.899	8.00	2.013	0.0605	0.0154	-0.0749	0.600	7.99	6.037	0.0622	0.0134	-0.0722
						0.599	7.98	8.002	0.0626	0.0128	-0.0727
						0.600	-0.03	1.032	0.0056	0.0076	-0.0081

TABLE II.- Continued

(d) $c_{r,vt} = 24.38$ cm; symmetrical vertical-tail airfoil;
 $\phi_t = 4^\circ$; $\phi_v = 0^\circ$; basic interfairing

M	α , deg	NPR	C_L	C_D	C_m	M	α , deg	NPR	C_L	C_D	C_m
1.201	0.00	0.994	-0.0255	0.0258	0.0268	0.901	4.00	8.033	0.0159	0.0075	-0.0228
1.199	-1.98	0.993	-0.0559	0.0286	0.0611	0.896	7.98	1.102	0.0497	0.0161	-0.0621
1.202	-0.02	0.989	-0.0248	0.0259	0.0259	0.900	8.00	2.011	0.0498	0.0150	-0.0631
1.202	1.99	0.989	0.0076	0.0255	-0.0109	0.900	8.01	3.501	0.0498	0.0150	-0.0631
1.203	4.01	0.989	0.0410	0.0272	-0.0491	0.901	8.00	4.184	0.0498	0.0149	-0.0627
1.201	6.01	0.993	0.0723	0.0317	-0.0861	0.901	7.99	6.034	0.0503	0.0144	-0.0637
1.197	8.01	0.939	0.0901	0.0371	-0.1074	0.900	8.01	7.995	0.0503	0.0137	-0.0636
1.204	-0.00	0.982	-0.0260	0.0263	0.0273	0.902	-0.01	1.102	-0.0012	0.0100	-0.0032
1.203	-0.01	2.006	-0.0255	0.0249	0.0267	0.850	-0.02	1.083	-0.0012	0.0093	-0.0024
1.202	0.01	3.500	-0.0246	0.0252	0.0257	0.851	0.00	2.002	-0.0013	0.0077	-0.0025
1.202	0.01	5.997	-0.0252	0.0247	0.0261	0.852	-0.01	3.495	-0.0016	0.0078	-0.0020
1.201	0.01	9.983	-0.0252	0.0227	0.0260	0.852	0.00	3.995	-0.0016	0.0076	-0.0019
1.201	4.01	0.981	0.0408	0.0274	-0.0491	0.850	0.01	8.015	-0.0019	0.0064	-0.0019
1.201	4.00	2.017	0.0409	0.0262	-0.0492	0.850	-0.01	1.082	-0.0020	0.0091	-0.0015
1.201	3.99	3.508	0.0403	0.0265	-0.0486	0.801	0.00	1.068	-0.0019	0.0090	-0.0011
1.202	4.01	5.987	0.0406	0.0259	-0.0490	0.800	0.01	1.989	-0.0017	0.0075	-0.0015
1.202	3.99	9.996	0.0407	0.0240	-0.0491	0.802	-0.02	3.915	-0.0022	0.0075	-0.0009
1.202	-0.01	0.973	-0.0264	0.0262	0.0276	0.803	0.00	5.013	-0.0020	0.0073	-0.0013
1.150	-0.02	0.987	-0.0276	0.0276	0.0277	0.800	0.01	7.978	-0.0025	0.0063	-0.0009
1.148	-0.00	1.995	-0.0270	0.0265	0.0269	0.801	-0.01	1.068	-0.0019	0.0089	-0.0012
1.152	0.00	3.496	-0.0271	0.0267	0.0274	0.599	-0.00	1.031	-0.0015	0.0083	-0.0008
1.151	0.01	5.608	-0.0268	0.0262	0.0270	0.600	-2.02	1.032	-0.0133	0.0089	0.0120
1.150	0.01	9.976	-0.0273	0.0239	0.0272	0.603	0.00	1.032	-0.0013	0.0083	-0.0010
1.149	0.01	0.984	-0.0268	0.0275	0.0269	0.601	2.00	1.032	0.0110	0.0084	-0.0144
0.940	-0.00	1.123	-0.0088	0.0099	0.0009	0.600	4.01	1.032	0.0237	0.0095	-0.0286
0.943	0.01	2.011	-0.0091	0.0080	0.0010	0.599	6.02	1.033	0.0387	0.0116	-0.0457
0.940	0.01	3.498	-0.0090	0.0082	0.0011	0.600	8.01	1.033	0.0542	0.0147	-0.0637
0.940	-0.02	4.317	-0.0090	0.0081	0.0008	0.600	10.00	1.032	0.0681	0.0190	-0.0806
0.941	0.01	8.013	-0.0096	0.0069	0.0015	0.601	-0.01	1.033	-0.0015	0.0085	-0.0008
0.941	0.02	1.121	-0.0095	0.0098	0.0018	0.602	-0.00	1.985	-0.0013	0.0072	-0.0011
0.900	-0.01	1.102	-0.0014	0.0097	-0.0033	0.602	0.01	3.377	-0.0020	0.0074	-0.0003
0.899	-1.98	1.102	-0.0076	0.0100	0.0036	0.603	0.02	4.037	-0.0020	0.0072	-0.0003
0.899	0.00	1.102	-0.0010	0.0097	-0.0036	0.601	0.01	6.012	-0.0025	0.0068	0.0000
0.901	2.02	1.104	0.0071	0.0097	-0.0124	0.602	0.01	7.971	-0.0025	0.0061	-0.0001
0.898	4.01	1.102	0.0176	0.0104	-0.0251	0.600	3.99	1.031	0.0227	0.0092	-0.0272
0.898	5.99	1.104	0.0300	0.0121	-0.0396	0.599	4.00	1.972	0.0225	0.0083	-0.0269
0.897	6.00	1.105	0.0504	0.0164	-0.0635	0.600	4.01	3.388	0.0224	0.0085	-0.0267
0.898	10.01	1.105	0.0745	0.0234	-0.0914	0.599	4.02	3.988	0.0227	0.0084	-0.0272
0.899	0.01	1.103	-0.0004	0.0099	-0.0042	0.601	4.01	6.029	0.0230	0.0079	-0.0275
0.899	-0.02	2.004	-0.0009	0.0082	-0.0037	0.600	3.99	7.997	0.0229	0.0073	-0.0275
0.901	0.03	3.491	-0.0013	0.0083	-0.0036	0.599	8.01	1.032	0.0538	0.0147	-0.0629
0.902	-0.03	4.204	-0.0017	0.0081	-0.0030	0.601	8.01	1.969	0.0540	0.0137	-0.0630
0.897	0.01	5.999	-0.0016	0.0075	-0.0028	0.600	8.01	3.397	0.0537	0.0138	-0.0626
0.896	0.01	7.989	-0.0019	0.0068	-0.0027	0.600	8.01	4.004	0.0538	0.0138	-0.0633
0.902	3.98	1.102	0.0164	0.0105	-0.0234	0.599	7.99	5.983	0.0543	0.0133	-0.0635
0.900	4.00	2.010	0.0163	0.0087	-0.0232	0.601	8.00	7.990	0.0539	0.0126	-0.0633
0.901	4.00	3.507	0.0162	0.0089	-0.0231	0.601	0.00	1.032	-0.0013	0.0085	-0.0009
0.900	3.98	6.036	0.0162	0.0083	-0.0235						

TABLE II.- Concluded

(e) $c_{r,vt} = 28.19$ cm; symmetrical vertical-tail airfoil;
 $\psi_t = 0^\circ$; $\phi_t = 0^\circ$; basic interfairing

M	α , deg	NPR	C_L	C_D	C_m	M	α , deg	NPR	C_L	C_D	C_m
1.203	0.00	1.023	-0.0034	0.0215	-0.0005	0.900	0.01	6.021	0.0175	0.0072	-0.0237
1.201	-2.01	1.026	-0.0338	0.0228	0.0337	0.898	-0.01	8.012	0.0169	0.0065	-0.0229
1.202	0.01	1.021	-0.0029	0.0215	-0.0011	0.900	3.99	4.203	0.0336	0.0100	-0.0424
1.200	1.99	1.020	0.0273	0.0226	-0.0359	0.899	8.01	1.105	0.0715	0.0189	-0.0876
1.199	4.01	1.016	0.0574	0.0257	-0.0702	0.901	8.01	1.993	0.0702	0.0174	-0.0860
1.198	6.00	0.978	0.0770	0.0308	-0.0928	0.900	8.01	3.497	0.0705	0.0174	-0.0862
1.197	8.01	0.956	0.0996	0.0374	-0.1201	0.900	8.00	4.210	0.0708	0.0173	-0.0867
1.200	-0.03	1.015	-0.0043	0.0218	0.0002	0.900	8.01	6.007	0.0708	0.0169	-0.0867
1.201	-0.01	1.989	-0.0035	0.0204	-0.0008	0.899	8.01	8.003	0.0707	0.0160	-0.0863
1.199	-0.00	3.491	-0.0035	0.0210	-0.0009	0.900	0.00	1.104	0.0197	0.0093	-0.0266
1.199	0.00	5.984	-0.0039	0.0203	-0.0004	0.847	-0.02	1.086	0.0204	0.0083	-0.0255
1.199	0.01	10.021	-0.0044	0.0186	-0.0001	0.851	0.02	4.010	0.0200	0.0069	-0.0251
1.200	4.00	5.992	0.0564	0.0244	-0.0693	0.800	-0.02	1.071	0.0162	0.0078	-0.0202
1.150	-0.01	1.015	-0.0050	0.0229	0.0000	0.802	0.00	3.878	0.0163	0.0066	-0.0204
1.149	0.00	5.612	-0.0043	0.0217	-0.0009	0.598	-0.00	1.034	0.0126	0.0074	-0.0155
0.940	0.00	1.123	0.0108	0.0084	-0.0198	0.602	-2.01	1.035	0.0003	0.0074	-0.0020
0.940	0.01	4.291	0.0099	0.0069	-0.0181	0.601	0.02	1.035	0.0130	0.0074	-0.0159
0.899	0.00	1.108	0.0194	0.0092	-0.0265	0.601	2.00	1.035	0.0258	0.0081	-0.0300
0.899	-1.99	1.109	0.0132	0.0084	-0.0195	0.601	3.98	1.035	0.0390	0.0096	-0.0446
0.896	0.02	1.107	0.0204	0.0093	-0.0276	0.598	5.98	1.035	0.0543	0.0123	-0.0620
0.902	2.00	1.108	0.0262	0.0103	-0.0342	0.599	7.99	1.035	0.0698	0.0160	-0.0803
0.898	3.99	1.103	0.0361	0.0116	-0.0461	0.597	10.01	1.035	0.0864	0.0212	-0.1004
0.900	5.99	1.106	0.0481	0.0140	-0.0607	0.602	0.00	1.035	0.0137	0.0076	-0.0166
0.898	8.00	1.109	0.0705	0.0188	-0.0869	0.601	0.02	2.020	0.0141	0.0064	-0.0165
0.898	10.01	1.110	0.0960	0.0263	-0.1163	0.601	0.01	3.408	0.0135	0.0063	-0.0157
0.902	-0.01	1.111	0.0187	0.0095	-0.0261	0.601	-0.01	4.026	0.0133	0.0062	-0.0153
0.899	0.01	1.983	0.0181	0.0077	-0.0247	0.599	-0.02	5.992	0.0126	0.0058	-0.0149
0.901	-0.01	3.497	0.0178	0.0079	-0.0243	0.600	0.01	7.999	0.0128	0.0051	-0.0150
0.901	0.01	4.184	0.0178	0.0077	-0.0244	0.599	4.00	3.416	0.0388	0.0086	-0.0433
						0.600	8.00	1.033	0.0704	0.0160	-0.0801
						0.600	8.02	2.013	0.0708	0.0150	-0.0803
						0.601	8.00	3.394	0.0713	0.0152	-0.0809
						0.602	8.00	3.997	0.0713	0.0152	-0.0810
						0.601	8.01	6.015	0.0712	0.0145	-0.0810
						0.600	8.02	8.029	0.0711	0.0140	-0.0807
						0.601	0.01	1.033	0.0124	0.0075	-0.0151

TABLE III.- BASIC FORCE AND MOMENT DATA FOR CONFIGURATION WITH
HORIZONTAL TAILS AFT AND VERTICAL TAILS FORWARD

(a) $c_{r,vt} = 24.38$ cm; symmetrical vertical-tail airfoil;
 $\psi_t = 0^\circ$; $\phi_t = 0^\circ$; basic interfairing

M	α , deg	NPR	C_L	C_D	C_m	M	α , deg	NPR	C_L	C_D	C_m
0.942	-0.00	1.123	0.0089	0.0093	-0.0152	1.201	0.00	0.978	-0.0052	0.0225	0.0001
0.939	0.01	2.032	0.0083	0.0078	-0.0141	1.199	-2.02	0.988	-0.0341	0.0239	0.0382
0.939	0.00	3.501	0.0086	0.0079	-0.0146	1.199	0.00	0.975	-0.0047	0.0227	-0.0006
0.938	0.01	4.301	0.0088	0.0078	-0.0150	1.202	1.98	0.968	0.0235	0.0234	-0.0384
0.939	0.02	7.990	0.0069	0.0066	-0.0127	1.200	3.99	0.957	0.0523	0.0263	-0.0776
0.940	-0.00	1.117	0.0085	0.0090	-0.0149	1.201	6.01	0.934	0.0709	0.0303	-0.1013
0.901	-0.01	1.110	0.0147	0.0098	-0.0208	1.199	7.99	0.913	0.0884	0.0358	-0.1247
0.900	-2.00	1.111	0.0094	0.0092	-0.0140	1.199	-0.02	0.970	-0.0063	0.0229	0.0014
0.901	-0.02	1.110	0.0148	0.0097	-0.0210	1.198	-0.00	2.002	-0.0063	0.0216	0.0012
0.900	1.98	1.110	0.0221	0.0105	-0.0311	1.199	0.01	3.494	-0.0055	0.0220	0.0004
0.902	3.97	1.104	0.0290	0.0118	-0.0429	1.201	0.00	5.974	-0.0064	0.0210	0.0014
0.897	5.99	1.106	0.0405	0.0140	-0.0608	1.200	0.01	10.067	-0.0065	0.0189	0.0017
0.900	8.00	1.109	0.0579	0.0181	-0.0878	1.200	-0.02	10.019	-0.0065	0.0189	0.0015
0.899	9.96	1.108	0.0767	0.0237	-0.1145	1.201	4.01	0.947	0.0527	0.0263	-0.0789
0.900	-0.03	1.112	0.0135	0.0096	-0.0195	1.201	3.99	2.028	0.0522	0.0250	-0.0782
0.901	-0.00	2.021	0.0133	0.0080	-0.0189	1.199	4.01	3.493	0.0527	0.0255	-0.0789
0.898	-0.19	3.501	0.0128	0.0080	-0.0181	1.202	4.00	6.011	0.0524	0.0244	-0.0784
0.898	-0.03	4.182	0.0133	0.0079	-0.0188	1.199	4.00	10.084	0.0523	0.0222	-0.0777
0.901	0.01	5.980	0.0125	0.0074	-0.0178	1.200	0.00	0.961	-0.0064	0.0227	0.0012
0.899	0.00	8.015	0.0119	0.0067	-0.0170	0.598	-0.01	1.037	0.0090	0.0080	-0.0125
0.898	4.03	1.102	0.0279	0.0113	-0.0413	0.598	-1.98	1.039	-0.0036	0.0081	0.0045
0.900	3.98	2.001	0.0255	0.0098	-0.0376	0.602	-0.01	1.038	0.0086	0.0078	-0.0120
0.896	3.99	3.509	0.0267	0.0100	-0.0389	0.601	1.99	1.038	0.0222	0.0084	-0.0302
0.900	3.99	4.214	0.0262	0.0099	-0.0384	0.600	4.00	1.037	0.0361	0.0097	-0.0494
0.899	4.00	5.976	0.0258	0.0094	-0.0378	0.599	6.01	1.037	0.0523	0.0122	-0.0724
0.899	4.01	8.025	0.0250	0.0088	-0.0367	0.598	8.00	1.037	0.0665	0.0156	-0.0934
0.900	8.01	1.106	0.0563	0.0175	-0.0852	0.598	10.00	1.038	0.0829	0.0206	-0.1186
0.902	8.00	1.994	0.0550	0.0159	-0.0830	0.602	-0.01	1.039	0.0081	0.0082	-0.0109
0.899	7.98	3.487	0.0564	0.0161	-0.0847	0.600	0.01	2.018	0.0078	0.0070	-0.0105
0.899	8.01	4.192	0.0566	0.0161	-0.0852	0.600	0.02	3.394	0.0080	0.0070	-0.0106
0.900	8.01	4.216	0.0566	0.0161	-0.0850	0.602	0.00	4.006	0.0077	0.0069	-0.0102
0.897	8.00	6.014	0.0568	0.0156	-0.0851	0.600	0.01	6.000	0.0074	0.0063	-0.0097
0.902	7.99	8.017	0.0552	0.0148	-0.0832	0.602	0.01	8.002	0.0077	0.0058	-0.0100
0.902	-0.01	1.110	0.0128	0.0093	-0.0187	0.598	3.99	1.034	0.0356	0.0098	-0.0481
0.854	-0.01	1.093	0.0152	0.0088	-0.0199	0.599	4.00	1.986	0.0350	0.0089	-0.0471
0.852	0.01	1.983	0.0149	0.0073	-0.0193	0.600	4.00	3.395	0.0351	0.0091	-0.0471
0.850	0.00	3.500	0.0147	0.0074	-0.0191	0.600	4.00	3.986	0.0354	0.0090	-0.0475
0.850	0.01	4.013	0.0144	0.0072	-0.0186	0.599	3.99	5.995	0.0350	0.0086	-0.0471
0.848	0.01	8.027	0.0138	0.0060	-0.0178	0.601	4.00	8.012	0.0349	0.0079	-0.0469
0.851	-0.01	1.090	0.0151	0.0086	-0.0196	0.602	8.01	1.035	0.0671	0.0160	-0.0933
0.798	-0.01	1.076	0.0131	0.0083	-0.0168	0.601	8.01	2.009	0.0676	0.0151	-0.0938
0.799	-0.05	2.025	0.0126	0.0069	-0.0161	0.602	8.01	3.415	0.0676	0.0153	-0.0938
0.801	-0.02	3.913	0.0125	0.0069	-0.0160	0.601	7.98	4.013	0.0676	0.0152	-0.0938
0.800	-0.01	5.010	0.0124	0.0066	-0.0159	0.601	8.01	6.019	0.0682	0.0147	-0.0946
0.800	-0.00	7.993	0.0120	0.0057	-0.0154	0.601	8.00	8.014	0.0685	0.0141	-0.0950
0.801	-0.03	1.073	0.0129	0.0081	-0.0163	0.600	-0.01	1.035	0.0100	0.0083	-0.0126

TABLE III.- Continued

(b) $c_{r,vt} = 24.38$ cm; symmetrical vertical-tail airfoil;
 $\phi_t = -2^\circ$; $\phi_t = 0^\circ$; basic interfairing

M	α , deg	NPR	C_L	C_D	C_m	M	α , deg	NPR	C_L	C_D	C_m
1.199	-0.01	0.971	0.0034	0.0239	-0.0098	0.902	3.98	6.001	0.0317	0.0129	-0.0429
1.196	-2.00	0.972	-0.0245	0.0247	0.0273	0.899	4.00	7.960	0.0321	0.0123	-0.0434
1.199	-0.01	0.970	0.0036	0.0239	-0.0101	0.896	8.01	1.103	0.0669	0.0221	-0.0962
1.203	2.01	0.954	0.0319	0.0253	-0.0485	0.901	7.99	2.002	0.0654	0.0204	-0.0947
1.201	4.01	0.939	0.0593	0.0286	-0.0855	0.898	8.02	3.494	0.0669	0.0208	-0.0962
1.198	5.99	0.931	0.0807	0.0331	-0.1136	0.903	7.99	4.216	0.0656	0.0206	-0.0954
1.195	7.98	0.902	0.0939	0.0393	-0.1307	0.900	8.01	5.988	0.0665	0.0202	-0.0961
1.200	-0.00	0.966	0.0021	0.0241	-0.0084	0.902	8.01	8.014	0.0656	0.0194	-0.0948
1.199	-0.01	2.005	0.0026	0.0230	-0.0091	0.902	-0.01	1.106	0.0206	0.0120	-0.0253
1.201	-0.01	3.519	0.0023	0.0233	-0.0088	0.850	-0.01	1.090	0.0239	0.0115	-0.0274
1.202	-0.00	6.009	0.0024	0.0223	-0.0091	0.852	0.00	2.007	0.0226	0.0100	-0.0253
1.202	-0.00	10.024	0.0019	0.0201	-0.0083	0.850	-0.00	3.502	0.0225	0.0102	-0.0253
1.200	4.01	0.931	0.0592	0.0287	-0.0855	0.851	-0.01	4.020	0.0224	0.0101	-0.0253
1.201	3.49	1.953	0.0584	0.0274	-0.0850	0.849	0.01	8.006	0.0206	0.0089	-0.0228
1.200	4.00	3.492	0.0583	0.0277	-0.0849	0.849	-0.02	1.087	0.0228	0.0112	-0.0259
1.201	4.00	5.994	0.0583	0.0268	-0.0849	0.803	-0.01	1.076	0.0231	0.0102	-0.0250
1.199	4.00	10.023	0.0585	0.0247	-0.0847	0.802	0.01	2.006	0.0223	0.0089	-0.0238
1.201	-0.01	0.959	0.0017	0.0240	-0.0083	0.800	-0.01	3.916	0.0220	0.0089	-0.0233
1.150	-0.00	0.964	0.0035	0.0252	-0.0121	0.799	-0.01	5.016	0.0217	0.0086	-0.0230
1.147	-0.02	1.979	0.0031	0.0241	-0.0115	0.800	0.00	7.980	0.0207	0.0076	-0.0217
1.150	0.00	3.411	0.0038	0.0245	-0.0125	0.801	0.00	1.074	0.0226	0.0101	-0.0243
1.150	-0.00	3.492	0.0036	0.0244	-0.0121	0.601	-0.02	1.037	0.0171	0.0086	-0.0180
1.153	-0.01	5.606	0.0030	0.0237	-0.0113	0.600	1.99	1.037	0.0311	0.0095	-0.0369
1.147	-0.02	9.986	0.0026	0.0210	-0.0107	0.601	-1.98	1.038	0.0045	0.0087	-0.0010
1.150	0.01	0.963	0.0038	0.0252	-0.0124	0.599	-0.01	1.037	0.0178	0.0087	-0.0188
0.941	0.01	1.112	0.0142	0.0115	-0.0189	0.599	2.00	1.036	0.0309	0.0096	-0.0366
0.942	-0.01	2.006	0.0131	0.0099	-0.0178	0.600	4.01	1.036	0.0455	0.0113	-0.0565
0.938	0.00	2.002	0.0131	0.0100	-0.0177	0.599	5.99	1.036	0.0614	0.0142	-0.0793
0.938	0.01	3.514	0.0140	0.0103	-0.0188	0.601	7.99	1.037	0.0780	0.0183	-0.1036
0.937	0.01	4.322	0.0139	0.0102	-0.0189	0.600	10.01	1.038	0.0923	0.0234	-0.1257
0.940	0.01	8.013	0.0127	0.0090	-0.0176	0.601	-0.01	1.037	0.0176	0.0090	-0.0185
0.940	0.01	1.110	0.0140	0.0113	-0.0189	0.602	0.00	2.005	0.0170	0.0078	-0.0176
0.902	0.00	1.107	0.0218	0.0122	-0.0266	0.603	0.01	3.420	0.0170	0.0078	-0.0175
0.900	-2.00	1.109	0.0165	0.0112	-0.0191	0.602	0.00	3.994	0.0165	0.0077	-0.0168
0.902	-0.00	1.107	0.0219	0.0122	-0.0268	0.602	0.00	6.016	0.0163	0.0072	-0.0167
0.902	2.02	1.101	0.0285	0.0133	-0.0358	0.601	0.00	8.015	0.0153	0.0065	-0.0155
0.898	4.03	1.092	0.0352	0.0150	-0.0466	0.598	4.00	1.035	0.0439	0.0110	-0.0544
0.899	6.01	1.097	0.0457	0.0175	-0.0639	0.600	4.01	1.998	0.0438	0.0102	-0.0541
0.898	8.01	1.106	0.0683	0.0225	-0.0981	0.602	4.02	3.409	0.0445	0.0105	-0.0547
0.898	9.99	1.108	0.0854	0.0282	-0.1232	0.600	3.99	4.011	0.0435	0.0104	-0.0537
0.901	0.00	1.108	0.0216	0.0122	-0.0263	0.600	4.00	6.013	0.0434	0.0098	-0.0537
0.902	-0.00	2.010	0.0198	0.0106	-0.0238	0.599	4.01	7.997	0.0436	0.0093	-0.0538
0.899	0.01	3.501	0.0201	0.0108	-0.0242	0.598	7.98	1.035	0.0767	0.0181	-0.1016
0.901	-0.00	4.204	0.0197	0.0106	-0.0238	0.599	8.02	2.015	0.0775	0.0173	-0.1026
0.900	-0.00	5.997	0.0190	0.0102	-0.0226	0.600	8.02	3.399	0.0774	0.0175	-0.1026
0.901	0.00	8.018	0.0179	0.0095	-0.0214	0.600	7.99	4.020	0.0773	0.0174	-0.1027
0.903	3.94	1.091	0.0320	0.0145	-0.0430	0.599	7.99	6.008	0.0773	0.0169	-0.1024
0.902	3.99	1.990	0.0314	0.0132	-0.0423	0.601	8.01	8.018	0.0773	0.0162	-0.1025
0.901	4.01	3.491	0.0321	0.0135	-0.0432	0.601	-0.00	1.036	0.0174	0.0089	-0.0182
0.900	4.01	4.201	0.0325	0.0134	-0.0438						

TABLE III.- Continued

(c) $c_{r,vt} = 24.38$ cm; symmetrical vertical-tail airfoil;
 $\phi_t = 2^\circ$; $\phi_t = 0^\circ$; basic interfairing

M	α , deg	NPR	C_L	C_D	C_m	M	α , deg	NPR	C_L	C_D	C_m
0.939	0.01	1.129	-0.0010	0.0076	-0.0068	1.199	3.98	3.504	0.0479	0.0253	-0.0730
0.939	0.00	1.999	-0.0012	0.0058	-0.0067	1.201	4.00	6.011	0.0483	0.0244	-0.0734
0.938	-0.00	3.513	-0.0011	0.0060	-0.0069	1.199	3.99	10.002	0.0484	0.0221	-0.0732
0.937	-0.01	4.314	-0.0011	0.0059	-0.0070	1.198	-0.01	0.954	-0.0155	0.0235	0.0127
0.938	0.02	7.995	-0.0018	0.0047	-0.0064	1.147	-0.00	0.967	-0.0165	0.0249	0.0129
0.939	-0.02	1.125	-0.0019	0.0073	-0.0063	1.149	0.01	2.017	-0.0165	0.0239	0.0129
0.901	-0.01	1.109	0.0053	0.0080	-0.0129	1.149	0.00	3.498	-0.0165	0.0243	0.0128
0.899	-2.00	1.111	-0.0009	0.0080	-0.0093	1.149	-0.00	5.605	-0.0169	0.0235	0.0134
0.900	-0.02	1.109	0.0057	0.0080	-0.0134	1.150	0.02	9.955	-0.0165	0.0207	0.0126
0.900	1.98	1.109	0.0129	0.0083	-0.0229	1.149	0.01	0.966	-0.0165	0.0248	0.0131
0.899	4.02	1.105	0.0213	0.0093	-0.0366	0.849	-0.00	1.093	0.0046	0.0074	-0.0103
0.899	6.01	1.110	0.0314	0.0111	-0.0527	0.852	-0.00	2.001	0.0042	0.0059	-0.0100
0.897	8.00	1.110	0.0510	0.0149	-0.0817	0.850	0.01	3.507	0.0039	0.0060	-0.0095
0.899	10.01	1.111	0.0668	0.0199	-0.1043	0.850	-0.01	4.015	0.0039	0.0059	-0.0095
0.901	0.01	1.111	0.0045	0.0080	-0.0120	0.851	0.01	8.008	0.0034	0.0047	-0.0091
0.899	-0.01	2.011	0.0048	0.0062	-0.0120	0.852	0.01	1.091	0.0039	0.0072	-0.0095
0.901	0.00	3.507	0.0037	0.0063	-0.0107	0.801	0.01	1.077	0.0033	0.0073	-0.0083
0.899	0.00	4.213	0.0038	0.0061	-0.0109	0.802	0.00	1.996	0.0035	0.0059	-0.0086
0.899	0.03	6.005	0.0033	0.0057	-0.0104	0.800	0.01	3.903	0.0031	0.0060	-0.0082
0.899	0.00	8.026	0.0031	0.0049	-0.0099	0.801	0.02	5.021	0.0033	0.0057	-0.0083
0.899	4.00	1.104	0.0191	0.0089	-0.0332	0.802	-0.01	7.974	0.0030	0.0048	-0.0080
0.898	4.01	2.021	0.0192	0.0074	-0.0333	0.801	-0.00	1.075	0.0031	0.0073	-0.0080
0.899	4.01	3.509	0.0190	0.0075	-0.0330	0.598	-0.01	1.036	0.0030	0.0070	-0.0071
0.901	4.01	4.210	0.0182	0.0074	-0.0324	0.601	-1.99	1.038	-0.0087	0.0075	0.0090
0.901	3.99	6.034	0.0183	0.0069	-0.0323	0.601	0.01	1.037	0.0038	0.0070	-0.0080
0.901	4.00	7.993	0.0180	0.0062	-0.0312	0.602	2.01	1.037	0.0172	0.0073	-0.0261
0.896	7.98	1.109	0.0505	0.0146	-0.0807	0.599	3.99	1.036	0.0312	0.0085	-0.0454
0.899	8.01	2.002	0.0500	0.0130	-0.0796	0.599	5.98	1.037	0.0471	0.0108	-0.0600
0.899	8.01	3.514	0.0505	0.0132	-0.0803	0.601	8.01	1.038	0.0625	0.0141	-0.0911
0.901	8.00	4.211	0.0498	0.0131	-0.0795	0.598	9.98	1.039	0.0766	0.0185	-0.1125
0.900	7.99	5.993	0.0502	0.0126	-0.0800	0.599	0.00	1.037	0.0043	0.0074	-0.0086
0.899	7.99	7.996	0.0499	0.0119	-0.0794	0.600	0.01	1.997	0.0037	0.0061	-0.0077
0.901	-0.02	1.109	0.0040	0.0077	-0.0113	0.600	-0.00	3.393	0.0032	0.0062	-0.0069
1.201	-0.01	0.963	-0.0139	0.0233	0.0109	0.603	0.00	3.998	0.0032	0.0061	-0.0069
1.201	-1.99	0.969	-0.0443	0.0255	0.0514	0.600	0.01	5.994	0.0032	0.0056	-0.0071
1.201	-0.02	0.961	-0.0132	0.0235	0.0100	0.600	0.01	7.978	0.0027	0.0049	-0.0066
1.203	2.01	0.953	0.0191	0.0238	-0.0332	0.600	4.01	1.035	0.0303	0.0083	-0.0441
1.201	3.99	0.940	0.0490	0.0264	-0.0741	0.600	4.00	1.999	0.0295	0.0075	-0.0431
1.199	5.98	0.937	0.0727	0.0305	-0.1050	0.600	4.01	3.014	0.0297	0.0077	-0.0433
1.197	7.99	0.922	0.0875	0.0350	-0.1237	0.600	3.99	3.995	0.0295	0.0076	-0.0431
1.201	0.00	0.959	-0.0141	0.0235	0.0111	0.598	4.00	5.998	0.0300	0.0071	-0.0438
1.198	0.01	1.997	-0.0141	0.0226	0.0110	0.599	4.01	8.000	0.0299	0.0065	-0.0437
1.200	0.00	3.539	-0.0141	0.0229	0.0110	0.601	7.98	1.036	0.0619	0.0139	-0.0900
1.200	0.01	3.529	-0.0139	0.0229	0.0107	0.601	8.02	2.004	0.0629	0.0132	-0.0915
1.199	0.02	6.017	-0.0138	0.0218	0.0105	0.601	8.01	3.406	0.0626	0.0133	-0.0909
1.199	0.02	10.022	-0.0145	0.0196	0.0113	0.600	8.01	4.017	0.0627	0.0133	-0.0913
1.199	3.99	0.936	0.0485	0.0264	-0.0738	0.601	7.98	6.013	0.0628	0.0127	-0.0915
1.197	4.00	1.992	0.0482	0.0251	-0.0732	0.601	7.99	7.991	0.0630	0.0122	-0.0917
						0.603	-0.02	1.036	0.0040	0.0074	-0.0080

TABLE III.- Continued

(d) $c_{r,vt} = 24.38$ cm; symmetrical vertical-tail airfoil;
 $\psi_t = 4^\circ$; $\phi_t = 0^\circ$; basic interfairing

M	α , deg	NPR	C_L	C_D	C_m	M	α , deg	NPR	C_L	C_D	C_m
1.206	-0.01	0.964	-0.0248	0.0266	0.0240	0.901	3.99	8.012	0.0088	0.0066	-0.0239
1.199	-2.01	0.971	-0.0555	0.0298	0.0647	0.900	8.02	1.114	0.0389	0.0140	-0.0692
1.201	-0.00	0.961	-0.0249	0.0269	0.0240	0.896	8.00	2.005	0.0402	0.0123	-0.0699
1.199	1.99	0.955	0.0072	0.0265	-0.0193	0.903	7.99	3.506	0.0386	0.0126	-0.0686
1.200	3.98	0.953	0.0392	0.0280	-0.0621	0.901	8.00	4.205	0.0387	0.0125	-0.0686
1.194	6.02	0.956	0.0634	0.0312	-0.0942	0.901	7.99	5.998	0.0391	0.0120	-0.0692
1.200	7.98	0.929	0.0817	0.0351	-0.1176	0.900	8.01	7.984	0.0417	0.0116	-0.0727
1.201	-0.00	0.957	-0.0257	0.0271	0.0248	0.900	0.01	1.111	-0.0057	0.0093	-0.0025
1.202	-0.01	2.016	-0.0254	0.0259	0.0242	0.853	0.01	1.097	-0.0040	0.0090	-0.0035
1.200	0.01	3.483	-0.0255	0.0263	0.0243	0.852	0.02	2.018	-0.0039	0.0077	-0.0037
1.201	-0.00	6.020	-0.0257	0.0253	0.0244	0.851	-0.01	3.504	-0.0044	0.0079	-0.0030
1.200	-0.00	10.024	-0.0258	0.0230	0.0243	0.848	-0.01	3.985	-0.0043	0.0077	-0.0031
1.200	3.98	0.946	0.0391	0.0279	-0.0628	0.850	0.01	8.044	-0.0046	0.0065	-0.0029
1.199	4.00	2.008	0.0387	0.0267	-0.0622	0.850	0.01	8.014	-0.0046	0.0065	-0.0029
1.199	4.01	3.493	0.0387	0.0270	-0.0623	0.848	0.02	1.095	-0.0043	0.0091	-0.0028
1.200	3.99	5.978	0.0388	0.0261	-0.0625	0.797	-0.01	1.080	-0.0037	0.0091	-0.0031
1.199	4.00	6.015	0.0387	0.0260	-0.0623	0.799	0.01	2.021	-0.0036	0.0076	-0.0034
1.200	4.00	10.004	0.0388	0.0238	-0.0620	0.800	-0.00	3.918	-0.0040	0.0077	-0.0029
1.201	-0.03	0.952	-0.0274	0.0270	0.0265	0.801	-0.02	5.022	-0.0041	0.0074	-0.0027
1.153	0.00	0.970	-0.0289	0.0280	0.0277	0.800	-0.01	8.014	-0.0041	0.0064	-0.0030
1.149	-0.00	1.988	-0.0284	0.0270	0.0269	0.799	-0.00	1.080	-0.0040	0.0090	-0.0027
1.151	0.01	3.502	-0.0284	0.0274	0.0270	0.598	-0.01	1.040	-0.0018	0.0087	-0.0044
1.150	-0.01	5.613	-0.0288	0.0267	0.0275	0.599	-2.01	1.041	-0.0140	0.0094	0.0121
1.151	0.00	10.022	-0.0290	0.0239	0.0275	0.602	-0.00	1.041	-0.0017	0.0086	-0.0045
1.151	-0.02	0.968	-0.0290	0.0280	0.0280	0.603	2.01	1.041	0.0114	0.0087	-0.0224
0.943	0.01	1.136	-0.0157	0.0089	0.0066	0.602	4.02	1.040	0.0252	0.0097	-0.0416
0.940	0.01	2.020	-0.0143	0.0070	0.0054	0.601	5.99	1.041	0.0404	0.0117	-0.0636
0.941	-0.00	3.483	-0.0155	0.0073	0.0067	0.599	8.01	1.041	0.0559	0.0147	-0.0868
0.939	-0.00	4.306	-0.0150	0.0072	0.0062	0.600	10.00	1.042	0.0696	0.0189	-0.1080
0.941	-0.00	8.020	-0.0153	0.0060	0.0064	0.601	-0.01	1.041	-0.0020	0.0090	-0.0040
0.940	0.01	1.133	-0.0157	0.0088	0.0069	0.601	-0.00	2.011	-0.0020	0.0078	-0.0039
0.900	-0.00	1.112	-0.0055	0.0092	-0.0026	0.601	-0.00	3.394	-0.0023	0.0079	-0.0035
0.900	-1.99	1.115	-0.0122	0.0099	0.0052	0.602	0.01	4.000	-0.0023	0.0078	-0.0036
0.903	0.01	1.114	-0.0061	0.0093	-0.0023	0.601	0.01	5.993	-0.0025	0.0073	-0.0035
0.901	2.01	1.113	0.0020	0.0089	-0.0126	0.602	0.01	7.977	-0.0028	0.0067	-0.0031
0.900	3.96	1.109	0.0104	0.0094	-0.0262	0.602	0.00	8.019	-0.0030	0.0067	-0.0029
0.899	5.98	1.113	0.0217	0.0107	-0.0433	0.600	3.99	1.038	0.0239	0.0095	-0.0397
0.893	8.00	1.112	0.0418	0.0144	-0.0726	0.599	4.00	1.999	0.0240	0.0087	-0.0397
0.900	9.98	1.118	0.0559	0.0190	-0.0938	0.600	4.01	3.405	0.0239	0.0089	-0.0397
0.901	-0.00	1.114	-0.0057	0.0094	-0.0027	0.600	4.02	4.008	0.0242	0.0089	-0.0401
0.902	-0.02	2.030	-0.0058	0.0077	-0.0026	0.601	4.00	6.004	0.0237	0.0083	-0.0395
0.901	0.00	3.504	-0.0059	0.0078	-0.0023	0.600	4.01	8.009	0.0238	0.0077	-0.0397
0.901	-0.01	4.194	-0.0065	0.0077	-0.0016	0.601	8.00	1.039	0.0554	0.0148	-0.0860
0.901	-0.02	6.001	-0.0069	0.0072	-0.0012	0.602	8.01	1.995	0.0558	0.0137	-0.0862
0.900	0.01	8.030	-0.0064	0.0065	-0.0017	0.600	8.01	3.414	0.0559	0.0139	-0.0865
0.903	4.00	1.109	0.0092	0.0093	-0.0248	0.600	8.01	4.004	0.0561	0.0139	-0.0869
0.900	4.00	2.005	0.0092	0.0076	-0.0243	0.599	7.99	5.987	0.0565	0.0134	-0.0874
0.903	3.99	3.515	0.0084	0.0078	-0.0234	0.600	8.00	8.007	0.0564	0.0128	-0.0871
0.901	4.00	4.211	0.0086	0.0078	-0.0237	0.600	8.00	8.001	0.0566	0.0128	-0.0875
0.902	3.98	6.020	0.0086	0.0072	-0.0236	0.000	0.14	1.000	-0.0000	0.0004	-0.0001

TABLE III.- Continued

(e) $c_{r,vt} = 24.38$ cm; symmetrical vertical-tail airfoil;
 $\psi_t = 0^\circ$; $\phi_t = -10^\circ$; basic interfairing

M	α , deg	NPR	C_L	C_D	C_m	M	α , deg	NPR	C_L	C_D	C_m
1.202	-0.00	0.958	0.0004	0.0228	-0.0067	0.901	8.01	2.011	0.0515	0.0158	-0.0798
1.203	-2.02	0.969	-0.0274	0.0239	0.0299	0.900	8.01	3.489	0.0524	0.0161	-0.0809
1.203	-0.01	0.954	0.0004	0.0229	-0.0069	0.901	7.99	4.215	0.0518	0.0159	-0.0801
1.201	2.01	0.942	0.0282	0.0241	-0.0448	0.900	8.00	5.976	0.0522	0.0155	-0.0806
1.200	3.97	0.934	0.0540	0.0269	-0.0795	0.900	8.01	7.994	0.0519	0.0148	-0.0800
1.199	6.02	0.936	0.0757	0.0311	-0.1079	0.903	-0.00	1.107	0.0106	0.0098	-0.0164
1.200	7.99	0.918	0.0870	0.0358	-0.1230	0.598	0.01	1.035	0.0114	0.0082	-0.0150
1.201	-0.00	0.951	-0.0003	0.0232	-0.0062	0.602	-1.98	1.036	-0.0006	0.0083	0.0017
1.201	-0.01	2.005	0.0000	0.0219	-0.0069	0.602	-0.02	1.036	0.0110	0.0082	-0.0146
1.199	0.01	3.503	-0.0002	0.0224	-0.0066	0.600	2.01	1.035	0.0238	0.0088	-0.0322
1.201	0.02	5.975	-0.0001	0.0214	-0.0068	0.599	3.99	1.035	0.0371	0.0101	-0.0510
1.202	-0.01	10.069	-0.0007	0.0192	-0.0059	0.599	5.99	1.035	0.0519	0.0126	-0.0729
1.201	-0.03	0.944	-0.0008	0.0233	-0.0057	0.597	7.99	1.035	0.0668	0.0160	-0.0950
0.900	-0.01	1.105	0.0108	0.0099	-0.0168	0.600	10.01	1.036	0.0816	0.0207	-0.1180
0.900	-1.99	1.108	0.0058	0.0097	-0.0102	0.598	-0.00	1.036	0.0106	0.0083	-0.0139
0.900	-0.03	1.107	0.0108	0.0099	-0.0170	0.598	0.01	2.006	0.0103	0.0071	-0.0134
0.900	2.01	1.104	0.0170	0.0105	-0.0254	0.600	-0.00	3.339	0.0100	0.0073	-0.0129
0.897	4.00	1.097	0.0241	0.0116	-0.0376	0.601	0.00	3.396	0.0094	0.0072	-0.0122
0.898	6.00	1.101	0.0343	0.0136	-0.0541	0.601	0.00	3.999	0.0094	0.0071	-0.0122
0.898	8.01	1.105	0.0529	0.0176	-0.0824	0.601	-0.01	6.000	0.0089	0.0066	-0.0117
0.898	10.00	1.105	0.0718	0.0231	-0.1089	0.602	0.01	7.998	0.0084	0.0060	-0.0112
0.902	0.00	1.108	0.0105	0.0100	-0.0163	0.600	4.00	1.034	0.0352	0.0097	-0.0484
0.899	0.01	2.023	0.0098	0.0084	-0.0149	0.600	4.01	1.975	0.0349	0.0089	-0.0478
0.898	0.01	3.507	0.0101	0.0085	-0.0154	0.600	4.00	3.399	0.0349	0.0091	-0.0478
0.899	-0.01	4.218	0.0093	0.0084	-0.0145	0.602	4.00	4.018	0.0350	0.0091	-0.0479
0.902	-0.00	6.009	0.0086	0.0079	-0.0137	0.600	4.01	6.007	0.0350	0.0085	-0.0481
0.902	-0.01	7.983	0.0073	0.0072	-0.0119	0.600	4.00	8.011	0.0353	0.0079	-0.0482
0.899	4.00	2.008	0.0209	0.0100	-0.0326	0.598	8.01	1.992	0.0666	0.0149	-0.0944
0.901	3.99	3.493	0.0210	0.0102	-0.0330	0.600	8.01	3.404	0.0664	0.0151	-0.0943
0.899	3.99	4.198	0.0214	0.0101	-0.0334	0.602	7.99	4.005	0.0659	0.0149	-0.0942
0.899	4.01	6.000	0.0211	0.0097	-0.0332	0.601	7.99	5.983	0.0667	0.0145	-0.0947
0.901	4.00	8.007	0.0199	0.0090	-0.0318	0.600	7.98	7.986	0.0668	0.0139	-0.0947
0.899	7.99	1.104	0.0527	0.0175	-0.0817						

TABLE III.- Continued

(f) $c_{r,vt} = 24.38$ cm; symmetrical vertical-tail airfoil;
 $\psi_t = 0^\circ$; $\phi_t = 10^\circ$; basic interfairing

M	α , deg	NPR	C_L	C_D	C_m	M	α , deg	NPR	C_L	C_D	C_m
1.198	-0.01	0.969	-0.0038	0.0226	-0.0020	0.900	8.00	4.198	0.0631	0.0165	-0.0921
1.201	-2.01	0.976	-0.0359	0.0236	0.0402	0.899	8.01	6.004	0.0630	0.0160	-0.0921
1.201	-0.00	0.964	-0.0032	0.0224	-0.0031	0.900	8.00	8.022	0.0624	0.0153	-0.0915
1.201	1.99	0.965	0.0276	0.0234	-0.0449	0.901	-0.00	1.112	0.0152	0.0085	-0.0211
1.200	4.00	0.952	0.0564	0.0266	-0.0832	0.847	-0.01	1.093	0.0162	0.0079	-0.0205
1.201	6.00	0.942	0.0781	0.0309	-0.1114	0.851	0.01	1.999	0.0157	0.0064	-0.0200
1.198	7.99	0.913	0.0936	0.0368	-0.1307	0.851	0.00	3.480	0.0157	0.0066	-0.0198
1.199	-0.02	0.966	-0.0058	0.0227	-0.0001	0.852	0.01	4.011	0.0157	0.0065	-0.0197
1.200	-0.01	2.009	-0.0049	0.0213	-0.0010	0.845	0.00	7.992	0.0142	0.0051	-0.0178
1.199	-0.00	3.485	-0.0048	0.0218	-0.0013	0.850	-0.01	1.091	0.0156	0.0077	-0.0198
1.199	-0.00	6.002	-0.0050	0.0208	-0.0010	0.798	-0.00	1.077	0.0133	0.0078	-0.0172
1.199	0.00	10.064	-0.0048	0.0186	-0.0012	0.800	0.01	1.996	0.0133	0.0063	-0.0170
0.942	-0.00	1.113	0.0068	0.0074	-0.0130	0.801	-0.01	3.892	0.0132	0.0064	-0.0167
0.939	0.00	1.998	0.0066	0.0062	-0.0121	0.799	0.01	5.001	0.0132	0.0061	-0.0168
0.941	0.01	3.533	0.0066	0.0063	-0.0125	0.800	0.01	7.984	0.0127	0.0052	-0.0161
0.940	-0.00	4.296	0.0067	0.0062	-0.0127	0.800	-0.01	1.074	0.0137	0.0076	-0.0173
0.941	-0.01	8.028	0.0047	0.0051	-0.0104	0.598	-0.01	1.037	0.0113	0.0072	-0.0141
0.942	-0.02	1.114	0.0066	0.0075	-0.0128	0.598	-2.01	1.038	-0.0028	0.0074	0.0044
0.900	-0.01	1.115	0.0154	0.0086	-0.0215	0.600	-0.02	1.038	0.0115	0.0073	-0.0145
0.898	-2.02	1.116	0.0078	0.0080	-0.0125	0.602	1.98	1.038	0.0259	0.0079	-0.0336
0.902	-0.03	1.116	0.0152	0.0086	-0.0215	0.602	3.99	1.037	0.0408	0.0095	-0.0541
0.901	-0.02	1.115	0.0158	0.0086	-0.0220	0.600	5.98	1.038	0.0588	0.0123	-0.0788
0.902	2.02	1.114	0.0244	0.0095	-0.0330	0.602	7.99	1.038	0.0755	0.0161	-0.1031
0.899	3.98	1.107	0.0333	0.0111	-0.0471	0.600	10.00	1.039	0.0907	0.0211	-0.1263
0.900	5.99	1.111	0.0445	0.0136	-0.0648	0.602	-0.00	1.038	0.0117	0.0077	-0.0147
0.896	8.00	1.110	0.0652	0.0183	-0.0951	0.601	0.04	2.010	0.0117	0.0063	-0.0144
0.899	10.01	1.111	0.0823	0.0241	-0.1198	0.602	0.00	3.421	0.0111	0.0064	-0.0136
0.900	-0.02	1.116	0.0149	0.0087	-0.0210	0.599	0.01	4.005	0.0107	0.0064	-0.0132
0.901	-0.00	2.012	0.0149	0.0070	-0.0205	0.601	-0.00	6.004	0.0100	0.0058	-0.0127
0.900	0.01	3.499	0.0147	0.0071	-0.0201	0.602	-0.01	8.023	0.0097	0.0051	-0.0123
0.899	0.01	4.209	0.0146	0.0070	-0.0203	0.600	4.00	1.036	0.0404	0.0093	-0.0531
0.901	-0.02	6.012	0.0139	0.0065	-0.0190	0.598	4.00	1.036	0.0406	0.0093	-0.0531
0.901	0.00	7.996	0.0136	0.0058	-0.0188	0.600	4.01	2.007	0.0404	0.0085	-0.0528
0.901	3.98	1.106	0.0315	0.0109	-0.0448	0.599	4.01	3.430	0.0407	0.0087	-0.0531
0.899	3.97	2.005	0.0303	0.0094	-0.0422	0.600	3.99	4.008	0.0407	0.0086	-0.0531
0.900	4.00	3.521	0.0308	0.0096	-0.0435	0.600	4.00	6.008	0.0405	0.0081	-0.0529
0.902	4.01	4.208	0.0302	0.0095	-0.0426	0.600	4.01	8.031	0.0402	0.0075	-0.0525
0.898	4.00	5.992	0.0306	0.0091	-0.0429	0.601	8.01	1.036	0.0748	0.0160	-0.1020
0.901	3.99	8.005	0.0291	0.0084	-0.0410	0.602	8.00	2.000	0.0745	0.0150	-0.1020
0.897	8.01	1.108	0.0637	0.0180	-0.0932	0.601	7.99	3.410	0.0743	0.0152	-0.1017
0.899	8.00	1.988	0.0631	0.0164	-0.0919	0.602	7.99	4.022	0.0747	0.0151	-0.1021
0.899	8.01	3.197	0.0636	0.0167	-0.0927	0.600	8.00	5.992	0.0757	0.0148	-0.1033
0.900	7.99	3.511	0.0627	0.0166	-0.0916	0.601	7.98	8.010	0.0757	0.0141	-0.1032
						0.600	-0.01	1.037	0.0117	0.0075	-0.0144

TABLE III.- Continued

(g) $C_{r,vt} = 24.38$ cm; symmetrical vertical-tail airfoil;
 $\psi_t = 0^\circ$; $\phi_t = 20^\circ$; basic interfairing

M	α , deg	NPR	C_L	C_D	C_m	M	α , deg	NPR	C_L	C_D	C_m
1.201	-0.01	0.975	-0.0057	0.0223	0.0005	0.901	4.02	7.997	0.0342	0.0087	-0.0469
1.201	-2.01	0.983	-0.0399	0.0237	0.0455	0.899	8.01	1.107	0.0703	0.0190	-0.1009
1.202	-0.01	0.972	-0.0051	0.0223	-0.0003	0.900	8.00	1.986	0.0692	0.0174	-0.0991
1.202	2.03	0.974	0.0290	0.0235	-0.0458	0.899	8.00	3.518	0.0696	0.0176	-0.0998
1.199	4.01	0.962	0.0589	0.0270	-0.0853	0.901	8.01	4.189	0.0694	0.0175	-0.0995
1.197	6.01	0.950	0.0817	0.0314	-0.1144	0.900	8.00	6.019	0.0695	0.0170	-0.0994
1.197	8.00	0.912	0.1005	0.0380	-0.1370	0.899	8.01	8.014	0.0693	0.0163	-0.0991
1.201	0.00	0.971	-0.0060	0.0226	0.0006	0.903	-0.00	1.112	0.0161	0.0084	-0.0223
1.202	0.01	2.007	-0.0056	0.0213	-0.0001	0.849	-0.01	1.093	0.0150	0.0081	-0.0196
1.202	0.01	3.509	-0.0061	0.0217	0.0005	0.850	-0.00	1.805	0.0147	0.0066	-0.0190
1.201	0.02	6.010	-0.0064	0.0208	0.0008	0.851	-0.01	3.509	0.0146	0.0068	-0.0189
1.202	0.01	10.016	-0.0057	0.0185	-0.0000	0.852	-0.00	4.009	0.0148	0.0067	-0.0190
1.199	3.99	0.961	0.0584	0.0268	-0.0852	0.850	0.01	8.037	0.0143	0.0055	-0.0186
1.198	3.99	2.005	0.0581	0.0256	-0.0849	0.850	0.00	1.091	0.0148	0.0080	-0.0193
1.199	4.01	3.498	0.0578	0.0259	-0.0845	0.797	0.00	1.076	0.0136	0.0082	-0.0177
1.198	3.99	6.020	0.0578	0.0250	-0.0845	0.800	0.02	1.989	0.0132	0.0067	-0.0173
1.199	4.01	9.966	0.0583	0.0229	-0.0848	0.800	-0.00	3.926	0.0131	0.0068	-0.0170
1.201	-0.01	0.966	-0.0067	0.0224	0.0009	0.801	0.01	8.019	0.0120	0.0056	-0.0161
1.153	-0.01	0.974	-0.0096	0.0235	0.0042	0.802	0.01	1.076	0.0129	0.0081	-0.0172
1.152	0.01	1.987	-0.0088	0.0225	0.0031	0.599	0.00	1.037	0.0106	0.0080	-0.0147
1.151	0.01	3.507	-0.0086	0.0229	0.0031	0.600	-1.98	1.038	-0.0038	0.0082	0.0044
1.149	-0.01	5.592	-0.0092	0.0223	0.0036	0.601	0.00	1.037	0.0115	0.0080	-0.0152
1.151	-0.03	10.004	-0.0105	0.0195	0.0051	0.602	1.99	1.037	0.0272	0.0086	-0.0354
1.149	-0.00	0.971	-0.0092	0.0236	0.0038	0.599	4.01	1.037	0.0442	0.0105	-0.0574
0.942	-0.01	1.118	0.0091	0.0071	-0.0156	0.600	6.01	1.037	0.0623	0.0133	-0.0828
0.939	0.00	2.022	0.0089	0.0060	-0.0150	0.599	8.02	1.037	0.0800	0.0174	-0.1085
0.942	-0.01	3.512	0.0086	0.0061	-0.0148	0.599	9.99	1.038	0.0946	0.0226	-0.1318
0.940	0.00	4.304	0.0092	0.0061	-0.0158	0.600	-0.02	1.037	0.0112	0.0082	-0.0147
0.941	0.01	7.980	0.0077	0.0050	-0.0138	0.602	0.01	1.996	0.0111	0.0071	-0.0144
0.941	-0.01	1.120	0.0088	0.0071	-0.0154	0.600	0.00	3.395	0.0109	0.0072	-0.0140
0.900	-0.00	1.114	0.0161	0.0083	-0.0223	0.600	-0.02	4.016	0.0103	0.0071	-0.0132
0.900	-1.99	1.116	0.0070	0.0078	-0.0118	0.601	0.01	5.989	0.0103	0.0065	-0.0134
0.900	0.00	1.115	0.0167	0.0084	-0.0231	0.600	0.00	8.007	0.0106	0.0059	-0.0138
0.897	2.00	1.113	0.0273	0.0094	-0.0361	0.598	4.01	1.035	0.0440	0.0104	-0.0573
0.903	3.98	1.109	0.0367	0.0112	-0.0512	0.599	4.02	2.034	0.0439	0.0095	-0.0570
0.896	6.01	1.110	0.0521	0.0142	-0.0731	0.600	4.02	3.446	0.0438	0.0097	-0.0569
0.899	8.03	1.110	0.0706	0.0190	-0.1015	0.599	3.99	3.998	0.0437	0.0096	-0.0567
0.901	10.01	1.111	0.0883	0.0253	-0.1263	0.599	4.00	6.034	0.0432	0.0091	-0.0562
0.897	0.01	1.114	0.0166	0.0085	-0.0226	0.598	4.01	8.002	0.0436	0.0085	-0.0566
0.900	0.02	2.028	0.0162	0.0069	-0.0218	0.601	8.02	1.035	0.0800	0.0175	-0.1081
0.899	0.00	3.535	0.0157	0.0070	-0.0213	0.600	8.01	1.966	0.0801	0.0166	-0.1081
0.900	-0.00	4.187	0.0157	0.0069	-0.0213	0.599	8.01	3.400	0.0805	0.0168	-0.1088
0.901	-0.01	6.019	0.0151	0.0064	-0.0208	0.599	8.00	3.942	0.0799	0.0166	-0.1078
0.899	-0.01	7.942	0.0145	0.0057	-0.0198	0.599	8.00	6.026	0.0801	0.0161	-0.1081
0.897	4.00	1.105	0.0375	0.0112	-0.0516	0.598	8.00	8.037	0.0806	0.0155	-0.1089
0.901	4.02	2.007	0.0353	0.0097	-0.0482	0.600	0.04	1.035	0.0122	0.0082	-0.0157
0.902	4.01	3.509	0.0352	0.0099	-0.0484						
0.900	3.99	4.226	0.0356	0.0098	-0.0488						
0.903	4.00	5.993	0.0350	0.0093	-0.0479						

TABLE III.- Continued

(h) $c_{r,vt} = 24.38$ cm; vertical-tail airfoil cambered outboard;
 $\psi_t = 0^\circ$; $\phi_t = 0^\circ$; basic interfairing

M	α , deg	NPR	C_L	C_D	C_m	M	α , deg	NPR	C_L	C_D	C_m
1.200	0.00	0.985	0.0019	0.0218	-0.0085	0.901	3.98	6.046	0.0225	0.0079	-0.0343
1.202	-2.01	1.000	-0.0281	0.0226	0.0317	0.901	3.99	8.004	0.0228	0.0072	-0.0340
1.202	-0.03	0.983	0.0022	0.0218	-0.0089	0.901	7.99	1.109	0.0564	0.0164	-0.0852
1.201	1.99	0.978	0.0315	0.0232	-0.0488	0.900	8.00	2.019	0.0568	0.0149	-0.0849
1.200	3.98	0.970	0.0588	0.0264	-0.0856	0.901	7.98	3.513	0.0569	0.0150	-0.0851
1.198	5.99	0.944	0.0747	0.0306	-0.1064	0.898	7.98	4.205	0.0578	0.0150	-0.0862
1.197	8.00	0.925	0.0911	0.0362	-0.1287	0.898	7.98	5.999	0.0570	0.0144	-0.0850
1.201	-0.02	0.978	0.0001	0.0219	-0.0061	0.900	7.98	8.006	0.0562	0.0137	-0.0840
1.199	-0.02	2.026	0.0009	0.0207	-0.0074	0.899	-0.02	1.109	0.0102	0.0078	-0.0150
1.199	-0.02	3.482	0.0007	0.0211	-0.0069	0.851	-0.01	1.092	0.0100	0.0075	-0.0140
1.200	-0.00	6.021	0.0008	0.0201	-0.0073	0.852	-0.03	2.015	0.0090	0.0059	-0.0128
1.200	-0.03	10.029	-0.0002	0.0180	-0.0064	0.850	0.00	3.506	0.0090	0.0059	-0.0127
1.200	3.99	0.963	0.0572	0.0262	-0.0842	0.849	0.00	4.017	0.0089	0.0059	-0.0126
1.199	3.99	2.009	0.0574	0.0249	-0.0844	0.850	-0.01	8.012	0.0079	0.0046	-0.0113
1.201	3.98	3.494	0.0578	0.0253	-0.0847	0.850	-0.02	1.089	0.0087	0.0072	-0.0124
1.204	4.00	6.016	0.0583	0.0244	-0.0852	0.800	-0.02	1.075	0.0081	0.0073	-0.0115
1.200	3.97	6.029	0.0583	0.0244	-0.0852	0.800	-0.02	2.013	0.0079	0.0060	-0.0114
1.200	4.00	10.004	0.0593	0.0223	-0.0860	0.801	0.00	3.894	0.0079	0.0060	-0.0112
1.201	-0.03	0.968	-0.0001	0.0220	-0.0060	0.803	-0.03	5.043	0.0075	0.0057	-0.0108
1.150	-0.01	0.974	-0.0004	0.0234	-0.0064	0.798	0.00	8.035	0.0072	0.0047	-0.0105
1.147	-0.01	2.006	-0.0000	0.0223	-0.0071	0.798	-0.02	1.074	0.0077	0.0073	-0.0111
1.149	0.00	3.513	0.0004	0.0227	-0.0073	0.599	-0.01	1.036	0.0071	0.0068	-0.0103
1.149	0.01	5.594	0.0004	0.0220	-0.0075	0.600	-2.03	1.037	-0.0054	0.0071	0.0066
1.150	-0.02	10.053	-0.0010	0.0192	-0.0056	0.601	-0.02	1.036	0.0071	0.0069	-0.0103
1.149	-0.02	0.971	-0.0006	0.0233	-0.0059	0.602	2.00	1.035	0.0193	0.0074	-0.0272
0.940	-0.03	1.123	0.0047	0.0071	-0.0102	0.602	3.98	1.035	0.0331	0.0087	-0.0464
0.939	-0.02	2.002	0.0046	0.0055	-0.0096	0.600	5.97	1.034	0.0481	0.0110	-0.0682
0.941	-0.01	3.515	0.0046	0.0057	-0.0096	0.599	8.00	1.035	0.0636	0.0144	-0.0911
0.940	-0.04	4.325	0.0044	0.0056	-0.0095	0.601	9.99	1.036	0.0798	0.0191	-0.1152
0.937	-0.01	8.005	0.0037	0.0046	-0.0085	0.600	-0.01	1.035	0.0066	0.0072	-0.0097
0.940	-0.03	1.121	0.0049	0.0070	-0.0101	0.600	-0.01	2.022	0.0064	0.0060	-0.0094
0.902	-0.01	1.113	0.0104	0.0079	-0.0155	0.600	-0.04	3.412	0.0061	0.0061	-0.0086
0.900	-2.03	1.115	0.0035	0.0076	-0.0069	0.600	-0.03	4.015	0.0061	0.0060	-0.0059
0.897	-0.04	1.112	0.0112	0.0080	-0.0161	0.601	-0.01	6.002	0.0058	0.0054	-0.0087
0.901	2.00	1.112	0.0189	0.0087	-0.0265	0.602	-0.01	8.035	0.0058	0.0048	-0.0086
0.899	3.99	1.107	0.0275	0.0102	-0.0403	0.598	3.99	1.032	0.0333	0.0085	-0.0458
0.896	6.00	1.109	0.0388	0.0124	-0.0576	0.602	4.00	2.007	0.0333	0.0077	-0.0457
0.900	7.99	1.112	0.0581	0.0167	-0.0870	0.601	3.98	3.417	0.0328	0.0078	-0.0451
0.897	9.97	1.109	0.0770	0.0223	-0.1137	0.601	3.98	3.996	0.0328	0.0078	-0.0452
0.903	-0.02	1.115	0.0098	0.0081	-0.0147	0.602	3.99	6.007	0.0331	0.0073	-0.0455
0.901	0.00	2.010	0.0097	0.0064	-0.0140	0.602	4.00	7.988	0.0329	0.0067	-0.0452
0.902	0.00	3.509	0.0091	0.0064	-0.0133	0.599	7.98	1.032	0.0652	0.0144	-0.0921
0.899	-0.02	4.238	0.0089	0.0062	-0.0129	0.598	7.99	2.054	0.0656	0.0136	-0.0927
0.898	-0.03	5.999	0.0085	0.0057	-0.0124	0.601	8.01	3.414	0.0658	0.0138	-0.0933
0.900	-0.01	8.002	0.0079	0.0051	-0.0117	0.601	7.99	4.008	0.0656	0.0136	-0.0929
0.901	4.02	1.105	0.0259	0.0100	-0.0384	0.599	7.98	6.017	0.0658	0.0131	-0.0931
0.899	3.98	2.009	0.0248	0.0084	-0.0364	0.600	7.97	8.031	0.0658	0.0124	-0.0931
0.899	4.00	3.511	0.0246	0.0086	-0.0363	0.601	-0.03	1.032	0.0076	0.0072	-0.0107
0.899	3.98	4.219	0.0244	0.0085	-0.0362						

TABLE III.- Continued

(i) $c_{r,vt} = 24.38$ cm; vertical-tail airfoil cambered inboard;
 $\phi_t = 0^\circ$; $\phi_t = 0^\circ$; basic interfairing

M	α , deg	NPR	C_L	C_D	C_m	M	α , deg	NPR	C_L	C_D	C_m
1.200	-0.04	0.971	-0.0052	0.0228	-0.0001	0.900	0.01	3.486	0.0156	0.0095	-0.0218
1.199	-2.02	0.989	-0.0330	0.0241	0.0362	0.898	-0.03	4.203	0.0155	0.0094	-0.0215
1.201	-0.03	0.970	-0.0049	0.0228	-0.0006	0.899	-0.03	5.999	0.0145	0.0089	-0.0204
1.200	1.99	0.969	0.0238	0.0235	-0.0390	0.901	-0.00	6.004	0.0144	0.0089	-0.0203
1.200	3.98	0.963	0.0517	0.0262	-0.0767	0.901	4.01	1.094	0.0280	0.0130	-0.0415
1.200	6.00	0.947	0.0728	0.0302	-0.1044	0.901	3.98	4.195	0.0273	0.0117	-0.0405
1.201	8.00	0.917	0.0879	0.0356	-0.1245	0.896	7.99	1.105	0.0625	0.0200	-0.0940
1.198	-0.02	0.967	-0.0068	0.0230	0.0016	0.899	8.00	2.015	0.0610	0.0185	-0.0922
1.201	-0.01	2.015	-0.0057	0.0214	0.0001	0.899	7.99	4.200	0.0613	0.0185	-0.0923
1.199	-0.02	3.530	-0.0063	0.0219	0.0009	0.903	7.98	8.004	0.0608	0.0174	-0.0924
1.200	-0.01	6.023	-0.0068	0.0210	0.0013	0.903	-0.01	1.109	0.0166	0.0107	-0.0234
1.200	-0.02	9.965	-0.0071	0.0188	0.0016	0.848	-0.01	1.090	0.0207	0.0101	-0.0264
1.200	3.99	0.956	0.0517	0.0261	-0.0774	0.851	-0.01	4.006	0.0193	0.0089	-0.0244
1.201	3.99	6.002	0.0519	0.0243	-0.0776	0.797	-0.01	1.073	0.0202	0.0087	-0.0244
1.150	-0.01	0.973	-0.0067	0.0242	-0.0002	0.801	-0.00	3.900	0.0197	0.0075	-0.0235
1.151	-0.01	0.968	-0.0064	0.0244	-0.0004	0.600	0.00	1.035	0.0155	0.0076	-0.0185
1.150	-0.02	5.595	-0.0071	0.0230	0.0005	0.599	-1.99	1.036	0.0026	0.0075	-0.0012
0.939	-0.01	4.364	0.0062	0.0087	-0.0128	0.600	0.00	1.036	0.0160	0.0076	-0.0191
0.941	-0.02	4.309	0.0064	0.0086	-0.0129	0.601	2.00	1.035	0.0290	0.0083	-0.0366
0.900	-0.01	1.109	0.0169	0.0107	-0.0242	0.601	3.99	1.035	0.0430	0.0099	-0.0558
0.899	-2.01	1.112	0.0115	0.0102	-0.0174	0.599	5.98	1.035	0.0591	0.0126	-0.0790
0.901	-0.02	1.110	0.0174	0.0108	-0.0247	0.602	7.99	1.035	0.0752	0.0165	-0.1027
0.901	2.00	1.106	0.0234	0.0116	-0.0329	0.600	9.98	1.036	0.0898	0.0213	-0.1252
0.904	3.98	1.095	0.0282	0.0131	-0.0423	0.597	-0.00	1.035	0.0161	0.0078	-0.0191
0.899	6.00	1.100	0.0410	0.0155	-0.0619	0.597	0.01	2.032	0.0158	0.0067	-0.0187
0.897	7.98	1.108	0.0619	0.0201	-0.0939	0.599	0.00	3.410	0.0152	0.0069	-0.0178
0.901	10.00	1.110	0.0788	0.0256	-0.1177	0.600	-0.04	4.026	0.0149	0.0068	-0.0176
0.903	-0.01	1.111	0.0164	0.0109	-0.0234	0.600	0.01	5.991	0.0147	0.0061	-0.0173
0.901	0.00	2.001	0.0154	0.0094	-0.0214	0.600	-0.01	8.009	0.0141	0.0056	-0.0166
						0.600	3.99	1.033	0.0420	0.0097	-0.0546
						0.599	4.01	3.382	0.0418	0.0091	-0.0541
						0.602	7.97	1.033	0.0740	0.0163	-0.1009
						0.602	8.00	2.006	0.0744	0.0154	-0.1014
						0.601	7.98	3.409	0.0745	0.0155	-0.1017
						0.603	7.99	8.037	0.0744	0.0144	-0.1017
						0.601	0.02	1.033	0.0154	0.0077	-0.0183

TABLE III.- Continued

(j) $c_{r,vt} = 24.38$ cm; vertical-tail airfoil cambered outboard;
 $\phi_t = 0^\circ$; $\phi_t = -10^\circ$; basic interfairing

M	α , deg	NPR	C_L	C_D	C_m	M	α , deg	NPR	C_L	C_D	C_m
1.199	0.01	0.978	0.0015	0.0219	-0.0074	0.899	4.00	4.224	0.0202	0.0090	-0.0312
1.200	-2.00	0.999	-0.0260	0.0228	0.0287	0.894	8.00	1.105	0.0533	0.0164	-0.0812
1.202	0.02	0.975	0.0018	0.0221	-0.0081	0.897	8.01	1.106	0.0523	0.0163	-0.0802
1.199	2.02	0.973	0.0293	0.0233	-0.0455	0.899	8.00	2.035	0.0518	0.0148	-0.0794
1.199	4.00	0.966	0.0556	0.0262	-0.0815	0.899	8.00	4.203	0.0523	0.0149	-0.0799
1.200	5.99	0.952	0.0733	0.0302	-0.1054	0.900	8.00	8.027	0.0511	0.0136	-0.0783
1.198	8.00	0.932	0.0873	0.0355	-0.1249	0.904	-0.03	1.110	0.0085	0.0089	-0.0133
1.201	-0.00	2.007	0.0007	0.0209	-0.0070	0.849	-0.02	1.091	0.0095	0.0082	-0.0132
1.198	0.01	0.967	0.0005	0.0223	-0.0067	0.851	0.01	3.998	0.0093	0.0069	-0.0129
1.202	-0.01	2.011	0.0003	0.0209	-0.0066	0.798	0.00	3.576	0.0073	0.0065	-0.0105
1.200	-0.00	3.506	0.0002	0.0214	-0.0064	0.798	-0.00	1.075	0.0079	0.0078	-0.0111
1.199	-0.01	6.009	0.0003	0.0205	-0.0066	0.799	-0.00	3.910	0.0075	0.0065	-0.0108
1.199	0.00	10.058	0.0001	0.0183	-0.0064	0.598	0.02	1.036	0.0065	0.0074	-0.0095
1.201	4.00	0.959	0.0552	0.0261	-0.0814	0.597	-1.99	1.037	-0.0049	0.0077	0.0063
1.200	4.00	6.008	0.0549	0.0243	-0.0811	0.601	-0.01	1.037	0.0070	0.0074	-0.0100
1.150	-0.01	0.968	-0.0004	0.0237	-0.0068	0.600	2.02	1.036	0.0194	0.0078	-0.0272
1.149	0.00	5.618	0.0005	0.0223	-0.0078	0.601	4.02	1.036	0.0325	0.0090	-0.0455
0.941	-0.00	1.109	0.0036	0.0080	-0.0085	0.598	5.99	1.036	0.0476	0.0113	-0.0674
0.943	0.02	4.307	0.0026	0.0066	-0.0072	0.601	7.98	1.036	0.0623	0.0145	-0.0893
0.900	-0.02	1.111	0.0094	0.0089	-0.0145	0.599	9.99	1.038	0.0763	0.0189	-0.1111
0.901	-2.03	1.114	0.0039	0.0085	-0.0072	0.599	-0.00	1.037	0.0070	0.0076	-0.0100
0.900	-0.00	1.111	0.0095	0.0089	-0.0144	0.601	0.00	1.996	0.0070	0.0064	-0.0099
0.900	2.00	1.109	0.0161	0.0095	-0.0235	0.602	-0.01	3.407	0.0061	0.0065	-0.0086
0.900	4.04	1.102	0.0228	0.0106	-0.0393	0.601	0.01	3.991	0.0062	0.0064	-0.0088
0.900	6.00	1.106	0.0328	0.0125	-0.0512	0.603	-0.01	6.003	0.0056	0.0058	-0.0082
0.897	8.01	1.109	0.0531	0.0165	-0.0815	0.602	0.01	8.009	0.0054	0.0051	-0.0080
0.903	9.99	1.109	0.0724	0.0222	-0.1089	0.601	3.99	1.035	0.0317	0.0088	-0.0441
0.899	-0.02	1.111	0.0093	0.0090	-0.0140	0.601	4.01	3.402	0.0312	0.0081	-0.0435
0.900	-0.00	2.011	0.0089	0.0074	-0.0133	0.597	8.01	1.035	0.0620	0.0144	-0.0890
0.899	0.02	3.502	0.0086	0.0075	-0.0129	0.600	8.01	1.989	0.0614	0.0134	-0.0881
0.898	0.00	4.208	0.0084	0.0074	-0.0125	0.601	8.00	3.420	0.0620	0.0136	-0.0888
0.901	-0.04	6.004	0.0072	0.0068	-0.0112	0.601	7.99	8.012	0.0626	0.0125	-0.0899
0.901	-0.01	8.002	0.0066	0.0062	-0.0104	0.601	0.04	1.036	0.0069	0.0075	-0.0096
0.903	4.01	1.101	0.0212	0.0103	-0.0330						

TABLE III.- Continued

(k) $c_{r,vt} = 24.38$ cm; vertical-tail airfoil cambered inboard;
 $\phi_t = 0^\circ$; $\phi_t = 20^\circ$; basic interfairing

M	α , deg	NPR	C_L	C_D	C_m	M	α , deg	NPR	C_L	C_D	C_m
1.202	-0.00	0.978	-0.0096	0.0223	0.0051	0.905	-0.00	1.112	0.0230	0.0101	-0.0316
1.200	-2.00	0.996	-0.0422	0.0241	0.0472	0.597	0.01	1.037	0.0179	0.0083	-0.0216
1.203	-0.01	0.975	-0.0094	0.0224	0.0048	0.599	-2.00	1.038	0.0022	0.0083	-0.0019
1.202	2.00	0.977	0.0239	0.0232	-0.0393	0.602	-0.01	1.038	0.0179	0.0082	-0.0217
1.204	3.97	0.971	0.0548	0.0262	-0.0803	0.602	2.00	1.037	0.0340	0.0091	-0.0425
1.202	5.99	0.963	0.0784	0.0308	-0.1108	0.599	3.98	1.036	0.0506	0.0110	-0.0642
1.201	7.99	0.924	0.0983	0.0372	-0.1349	0.598	5.94	1.036	0.0687	0.0141	-0.0893
1.199	0.03	0.971	-0.0104	0.0227	0.0059	0.599	8.01	1.036	0.0864	0.0185	-0.1149
1.201	0.01	2.007	-0.0103	0.0214	0.0059	0.601	10.01	1.037	0.1022	0.0239	-0.1388
1.200	0.00	3.497	-0.0105	0.0218	0.0062	0.599	0.02	1.037	0.0180	0.0084	-0.0216
1.199	0.02	6.000	-0.0102	0.0209	0.0057	0.600	-0.00	1.992	0.0173	0.0072	-0.0206
1.197	0.02	9.965	-0.0103	0.0186	0.0055	0.601	0.01	3.413	0.0168	0.0073	-0.0200
1.199	-0.01	0.964	-0.0110	0.0226	0.0068	0.602	0.00	4.005	0.0170	0.0072	-0.0203
0.902	0.03	1.117	0.0252	0.0102	-0.0341	0.601	0.02	5.972	0.0168	0.0067	-0.0202
0.898	-2.04	1.118	0.0162	0.0092	-0.0232	0.603	0.00	8.010	0.0165	0.0061	-0.0198
0.900	-0.02	1.116	0.0252	0.0101	-0.0339	0.600	4.01	3.406	0.0486	0.0100	-0.0614
0.902	2.01	1.115	0.0347	0.0114	-0.0460	0.602	7.97	3.438	0.0846	0.0173	-0.1122
0.899	3.98	1.106	0.0439	0.0135	-0.0603	0.601	-0.02	1.035	0.0171	0.0082	-0.0205
0.895	6.00	1.108	0.0582	0.0168	-0.0819						
0.896	8.01	1.112	0.0787	0.0220	-0.1129						
0.901	9.99	1.115	0.0925	0.0278	-0.1333						
0.899	0.01	1.114	0.0251	0.0102	-0.0335						
0.900	-0.01	2.040	0.0237	0.0085	-0.0314						
0.899	0.00	3.507	0.0242	0.0088	-0.0322						
0.898	0.01	4.207	0.0240	0.0086	-0.0319						
0.899	-0.02	6.028	0.0233	0.0081	-0.0309						
0.900	0.00	8.035	0.0224	0.0075	-0.0299						
0.900	3.98	4.194	0.0405	0.0120	-0.0556						
0.896	7.99	4.203	0.0778	0.0204	-0.1112						

TABLE III.- Continued

(1) $c_{r,vt} = 28.19$ cm; symmetrical vertical-tail airfoil;
 $\phi_t = 0^\circ$; $\phi_t = 0^\circ$; basic interfairing

M	α , deg	NPR	C_L	C_D	C_m	M	α , deg	NPR	C_L	C_D	C_m
1.200	-0.01	0.984	0.0005	0.0218	-0.0076	0.900	7.99	3.522	0.0610	0.0168	-0.0913
1.199	-2.00	0.994	-0.0269	0.0228	0.0283	0.898	8.00	4.214	0.0619	0.0168	-0.0923
1.200	-0.03	0.982	0.0004	0.0219	-0.0076	0.898	8.01	6.032	0.0619	0.0163	-0.0921
1.201	2.00	0.965	0.0286	0.0231	-0.0453	0.901	8.00	8.002	0.0613	0.0156	-0.0915
1.199	4.00	0.953	0.0593	0.0260	-0.0811	0.901	-0.01	1.106	0.0161	0.0093	-0.0227
1.196	6.01	0.938	0.0724	0.0301	-0.1029	0.851	0.00	1.089	0.0181	0.0087	-0.0236
1.194	7.99	0.927	0.0897	0.0357	-0.1262	0.850	-0.01	3.990	0.0170	0.0073	-0.0219
1.202	7.97	0.925	0.0893	0.0353	-0.1258	0.798	-0.01	1.073	0.0157	0.0081	-0.0200
1.201	-0.03	0.976	-0.0002	0.0222	-0.0071	0.800	-0.03	3.899	0.0146	0.0068	-0.0185
1.202	0.00	2.003	0.0006	0.0208	-0.0083	0.600	0.01	1.035	0.0131	0.0076	-0.0166
1.201	0.01	3.545	0.0007	0.0213	-0.0084	0.600	-2.03	1.037	-0.0002	0.0077	0.0011
1.201	-0.01	6.013	0.0008	0.0204	-0.0087	0.601	-0.02	1.036	0.0131	0.0076	-0.0166
1.201	-0.01	10.062	-0.0000	0.0181	-0.0077	0.600	2.01	1.035	0.0268	0.0083	-0.0352
0.905	0.00	1.109	0.0153	0.0094	-0.0222	0.598	3.97	1.035	0.0407	0.0097	-0.0542
0.901	-2.04	1.110	0.0101	0.0089	-0.0151	0.599	5.97	1.035	0.0571	0.0125	-0.0780
0.900	0.01	1.107	0.0166	0.0094	-0.0235	0.603	7.98	1.037	0.0721	0.0161	-0.1006
0.900	1.97	1.104	0.0231	0.0101	-0.0324	0.598	9.99	1.037	0.0875	0.0210	-0.1241
0.898	4.00	1.097	0.0305	0.0116	-0.0448	0.599	0.01	1.036	0.0131	0.0078	-0.0166
0.900	6.01	1.102	0.0423	0.0139	-0.0633	0.601	-0.02	2.004	0.0120	0.0066	-0.0149
0.896	7.98	1.104	0.0625	0.0183	-0.0938	0.602	-0.03	3.401	0.0117	0.0066	-0.0145
0.902	9.98	1.106	0.0806	0.0242	-0.1189	0.602	-0.01	4.012	0.0119	0.0066	-0.0148
0.898	-0.01	1.107	0.0164	0.0094	-0.0230	0.602	-0.01	6.027	0.0114	0.0060	-0.0143
0.900	0.01	2.021	0.0146	0.0077	-0.0204	0.602	-0.02	7.997	0.0109	0.0054	-0.0138
0.903	-0.00	3.515	0.0143	0.0078	-0.0202	0.600	4.00	3.407	0.0399	0.0090	-0.0530
0.900	0.00	4.204	0.0144	0.0078	-0.0203	0.600	7.98	1.035	0.0725	0.0161	-0.1006
0.899	-0.01	6.007	0.0140	0.0073	-0.0197	0.598	8.00	2.014	0.0732	0.0152	-0.1014
0.898	-0.02	7.995	0.0132	0.0066	-0.0186	0.599	7.98	3.422	0.0724	0.0154	-0.1004
0.899	7.99	1.103	0.0616	0.0182	-0.0923	0.599	7.98	4.006	0.0725	0.0152	-0.1007
0.901	7.99	2.014	0.0610	0.0166	-0.0912	0.599	7.98	6.042	0.0726	0.0148	-0.1008
						0.599	7.98	7.967	0.0729	0.0142	-0.1012
						0.600	-0.02	1.036	0.0133	0.0078	-0.0166

TABLE III.- Concluded

(m) $c_{r,vt} = 24.38$ cm; symmetrical vertical-tail airfoil;
 $\psi_t = 0^\circ$; $\phi_t = 0^\circ$; alternate interfairing

M	α , deg	NPR	C_L	C_D	C_m	M	α , deg	NPR	C_L	C_D	C_m
1.200	-0.02	0.952	-0.0039	0.0234	-0.0015	0.902	-0.01	3.509	0.0094	0.0076	-0.0148
1.201	-2.03	0.967	-0.0326	0.0246	0.0364	0.901	-0.01	4.199	0.0094	0.0075	-0.0147
1.199	0.01	0.951	-0.0024	0.0236	-0.0034	0.897	-0.00	6.004	0.0096	0.0069	-0.0150
1.201	2.01	0.941	0.0263	0.0246	-0.0420	0.902	0.00	7.998	0.0087	0.0063	-0.0141
1.197	3.99	0.929	0.0535	0.0275	-0.0783	0.899	4.01	1.095	0.0232	0.0107	-0.0353
1.202	6.00	0.920	0.0761	0.0316	-0.1079	0.900	3.98	4.185	0.0230	0.0093	-0.0352
1.200	7.96	0.879	0.0885	0.0371	-0.1239	0.898	8.00	1.104	0.0544	0.0168	-0.0826
1.199	-0.02	0.950	-0.0048	0.0239	-0.0004	0.901	7.99	1.999	0.0535	0.0152	-0.0815
1.202	-0.02	1.997	-0.0047	0.0221	-0.0003	0.900	7.98	4.190	0.0532	0.0153	-0.0812
1.199	-0.02	3.522	-0.0042	0.0228	-0.0014	0.900	7.98	7.994	0.0537	0.0142	-0.0816
1.200	-0.00	6.017	-0.0058	0.0214	0.0014	0.900	-0.03	1.108	0.0103	0.0092	-0.0159
1.201	-0.01	9.972	-0.0072	0.0190	0.0036	0.849	-0.02	1.092	0.0129	0.0086	-0.0174
1.199	3.97	0.925	0.0533	0.0275	-0.0786	0.850	-0.01	4.001	0.0122	0.0072	-0.0166
1.200	4.00	5.984	0.0502	0.0251	-0.0735	0.800	-0.01	1.077	0.0111	0.0083	-0.0148
1.201	-0.01	0.946	-0.0050	0.0237	-0.0004	0.801	-0.01	3.881	0.0106	0.0070	-0.0140
1.153	-0.01	0.958	-0.0059	0.0247	-0.0004	0.602	-0.02	1.040	0.0093	0.0077	-0.0124
1.150	0.00	5.600	-0.0064	0.0234	0.0003	0.602	-2.02	1.040	-0.0032	0.0079	0.0044
0.941	-0.02	1.122	0.0034	0.0082	-0.0094	0.600	-0.03	1.039	0.0091	0.0077	-0.0121
0.939	0.00	4.269	0.0038	0.0068	-0.0102	0.601	2.00	1.039	0.0217	0.0083	-0.0290
0.899	-0.01	1.110	0.0110	0.0092	-0.0170	0.600	3.98	1.039	0.0352	0.0097	-0.0477
0.899	-2.04	1.111	0.0051	0.0088	-0.0094	0.599	5.99	1.038	0.0513	0.0122	-0.0709
0.899	-0.01	1.110	0.0113	0.0092	-0.0173	0.601	7.98	1.039	0.0668	0.0157	-0.0936
0.899	1.98	1.108	0.0175	0.0098	-0.0259	0.599	9.99	1.039	0.0805	0.0202	-0.1148
0.901	3.98	1.097	0.0239	0.0109	-0.0367	0.601	8.10	1.039	0.0656	0.0158	-0.0921
0.897	5.99	1.104	0.0362	0.0130	-0.0593	0.601	-0.00	2.019	0.0085	0.0067	-0.0112
0.897	7.98	1.105	0.0543	0.0168	-0.0826	0.600	-0.01	3.397	0.0080	0.0068	-0.0105
0.902	10.00	1.104	0.0709	0.0221	-0.1065	0.601	-0.01	3.996	0.0080	0.0067	-0.0104
0.901	-0.03	1.112	0.0100	0.0093	-0.0157	0.601	-0.01	6.021	0.0080	0.0062	-0.0104
0.902	-0.00	2.010	0.0099	0.0074	-0.0155	0.601	-0.02	7.992	0.0075	0.0057	-0.0099
						0.600	3.98	1.037	0.0343	0.0095	-0.0463
						0.599	4.00	3.400	0.0345	0.0088	-0.0464
						0.602	7.97	1.038	0.0660	0.0157	-0.0923
						0.599	8.00	1.993	0.0667	0.0147	-0.0932
						0.600	7.98	3.417	0.0665	0.0149	-0.0930
						0.601	7.99	7.994	0.0673	0.0138	-0.0941
						0.601	-0.01	1.038	0.0091	0.0080	-0.0118

TABLE IV.- BASIC FORCE AND MOMENT DATA FOR CONFIGURATION WITH
HORIZONTAL TAILS AFT AND VERTICAL TAILS MID

(a) $c_{r,vt} = 24.38$ cm; symmetrical vertical-tail airfoil;
 $\phi_t = 0^\circ$; $\phi_t = 0^\circ$; basic interfairing

M	α , deg	NPR	C_L	C_D	C_m	M	α , deg	NPR	C_L	C_D	C_m
1.200	0.01	0.957	-0.0055	0.0220	0.0035	0.901	8.01	3.496	0.0512	0.0163	-0.0801
1.200	-2.00	0.966	-0.0319	0.0233	0.0392	0.900	7.98	4.207	0.0515	0.0162	-0.0804
1.198	0.02	0.953	-0.0052	0.0223	0.0033	0.900	8.00	6.007	0.0517	0.0158	-0.0806
1.192	2.01	0.944	0.0217	0.0232	-0.0333	0.900	7.99	7.998	0.0517	0.0150	-0.0804
1.199	4.00	0.942	0.0482	0.0255	-0.0695	0.901	-0.01	1.101	0.0161	0.0100	-0.0253
1.205	6.01	0.926	0.0668	0.0299	-0.0941	0.851	-0.01	1.086	0.0193	0.0094	-0.0283
1.174	8.01	0.909	0.0830	0.0359	-0.1176	0.853	0.00	2.008	0.0170	0.0079	-0.0249
1.207	0.00	0.949	-0.0068	0.0222	0.0051	0.849	0.01	3.503	0.0174	0.0080	-0.0253
1.201	0.01	2.021	-0.0065	0.0216	0.0047	0.852	0.05	3.993	0.0172	0.0080	-0.0253
1.203	0.02	3.481	-0.0065	0.0220	0.0047	0.850	0.00	8.000	0.0151	0.0067	-0.0223
1.194	0.03	5.954	-0.0069	0.0214	0.0052	0.852	-0.01	1.084	0.0185	0.0093	-0.0274
1.202	0.00	10.091	-0.0068	0.0191	0.0049	0.800	-0.01	1.073	0.0178	0.0085	-0.0251
1.197	4.02	0.934	0.0477	0.0257	-0.0695	0.802	0.01	2.002	0.0166	0.0072	-0.0233
1.203	4.03	1.998	0.0477	0.0247	-0.0698	0.801	-0.03	3.903	0.0163	0.0073	-0.0229
1.203	4.03	3.536	0.0480	0.0251	-0.0702	0.802	-0.01	4.978	0.0161	0.0070	-0.0227
1.202	4.02	6.004	0.0480	0.0243	-0.0702	0.801	0.00	7.998	0.0149	0.0061	-0.0211
1.201	4.01	9.954	0.0476	0.0225	-0.0692	0.801	0.00	8.009	0.0143	0.0061	-0.0204
1.201	0.00	0.941	-0.0075	0.0223	0.0057	0.801	-0.01	1.071	0.0173	0.0085	-0.0245
0.000	-0.01	1.000	-0.0003	-0.0000	0.0003	0.597	0.02	1.035	0.0150	0.0079	-0.0202
0.938	0.07	1.101	0.0100	0.0104	-0.0175	0.601	-2.01	1.037	0.0025	0.0080	-0.0032
0.939	0.15	2.001	0.0074	0.0089	-0.0137	0.601	0.06	1.036	0.0154	0.0079	-0.0208
0.938	0.00	2.008	0.0078	0.0088	-0.0145	0.602	-0.00	1.036	0.0151	0.0079	-0.0203
0.935	0.00	3.496	0.0093	0.0090	-0.0167	0.599	1.99	1.035	0.0281	0.0087	-0.0384
0.943	0.02	4.303	0.0068	0.0091	-0.0132	0.600	4.01	1.035	0.0418	0.0101	-0.0578
0.943	-0.01	8.042	0.0058	0.0079	-0.0119	0.602	6.00	1.036	0.0576	0.0128	-0.0807
0.940	-0.01	1.098	0.0090	0.0104	-0.0165	0.601	8.01	1.036	0.0723	0.0164	-0.1027
0.900	0.00	1.101	0.0165	0.0102	-0.0256	0.599	10.01	1.037	0.0885	0.0213	-0.1274
0.897	-2.01	1.103	0.0120	0.0096	-0.0189	0.600	-0.01	1.037	0.0151	0.0082	-0.0202
0.901	0.00	1.101	0.0168	0.0102	-0.0261	0.600	0.00	2.007	0.0143	0.0070	-0.0190
0.901	2.01	1.095	0.0227	0.0110	-0.0349	0.601	0.00	3.395	0.0140	0.0071	-0.0187
0.901	4.01	1.082	0.0248	0.0123	-0.0395	0.601	0.01	3.987	0.0140	0.0070	-0.0186
0.899	5.99	1.084	0.0355	0.0143	-0.0563	0.600	0.01	5.998	0.0132	0.0065	-0.0177
0.899	8.01	1.087	0.0544	0.0181	-0.0843	0.599	0.00	7.993	0.0122	0.0058	-0.0166
0.898	9.98	1.090	0.0749	0.0239	-0.1124	0.601	4.00	1.034	0.0402	0.0099	-0.0556
0.898	0.01	1.102	0.0170	0.0102	-0.0263	0.600	4.02	2.003	0.0403	0.0090	-0.0555
0.902	0.01	2.003	0.0133	0.0086	-0.0207	0.601	4.00	3.399	0.0399	0.0092	-0.0549
0.899	0.00	3.498	0.0142	0.0088	-0.0221	0.602	4.00	3.999	0.0399	0.0091	-0.0550
0.900	0.02	4.170	0.0138	0.0087	-0.0217	0.602	4.02	6.000	0.0399	0.0087	-0.0551
0.900	0.01	5.999	0.0124	0.0082	-0.0200	0.599	4.00	8.010	0.0387	0.0080	-0.0533
0.901	-0.00	8.013	0.0108	0.0075	-0.0177	0.601	8.01	1.035	0.0712	0.0162	-0.1011
0.901	4.05	1.081	0.0233	0.0120	-0.0375	0.601	7.99	2.000	0.0712	0.0152	-0.1011
0.899	4.02	2.024	0.0217	0.0104	-0.0349	0.601	8.01	3.410	0.0714	0.0155	-0.1012
0.900	4.01	3.492	0.0224	0.0107	-0.0361	0.600	8.00	3.999	0.0711	0.0153	-0.1009
0.899	4.01	4.202	0.0225	0.0106	-0.0363	0.602	7.99	5.994	0.0711	0.0148	-0.1009
0.898	4.00	6.031	0.0226	0.0102	-0.0362	0.600	7.99	8.007	0.0710	0.0142	-0.1007
0.900	3.99	8.004	0.0217	0.0094	-0.0351	0.600	-0.02	1.035	0.0146	0.0081	-0.0195
0.901	8.01	1.088	0.0527	0.0177	-0.0819						
0.898	8.00	1.970	0.0519	0.0160	-0.0802						

TABLE IV.- Continued

(b) $c_{r,vt} = 24.38$ cm; symmetrical vertical-tail airfoil;
 $\psi_t = -2^\circ$; $\phi_t = 0^\circ$; basic interfairing

M	α , deg	NPR	C_L	C_D	C_m	M	α , deg	NPR	C_L	C_D	C_m
1.201	-0.00	0.935	-0.0057	0.0237	0.0045	0.899	4.01	5.985	0.0244	0.0149	-0.0381
1.200	-1.99	0.947	-0.0321	0.0247	0.0395	0.900	3.99	8.003	0.0236	0.0142	-0.0372
1.200	0.02	0.934	-0.0056	0.0238	0.0041	0.895	7.99	1.064	0.0551	0.0226	-0.0847
1.201	2.01	0.923	0.0209	0.0247	-0.0322	0.897	8.00	1.981	0.0533	0.0209	-0.0820
1.199	4.02	0.914	0.0474	0.0275	-0.0680	0.898	7.99	3.523	0.0539	0.0213	-0.0833
1.201	5.98	0.899	0.0681	0.0314	-0.0942	0.899	8.00	4.226	0.0541	0.0212	-0.0834
1.198	8.01	0.879	0.0834	0.0369	-0.1173	0.897	8.00	5.980	0.0551	0.0209	-0.0849
1.201	-0.01	0.931	-0.0075	0.0237	0.0064	0.899	8.00	8.004	0.0539	0.0201	-0.0833
1.200	-0.01	0.931	-0.0071	0.0237	0.0060	0.903	-0.02	1.077	0.0143	0.0143	-0.0207
1.200	0.00	2.589	-0.0078	0.0233	0.0071	0.847	-0.01	1.074	0.0216	0.0133	-0.0298
1.200	0.00	2.027	-0.0079	0.0230	0.0072	0.851	0.01	2.014	0.0174	0.0120	-0.0234
1.200	0.00	3.516	-0.0073	0.0234	0.0064	0.850	-0.01	3.507	0.0181	0.0122	-0.0247
1.200	-0.00	5.995	-0.0075	0.0226	0.0065	0.852	-0.00	4.010	0.0179	0.0122	-0.0244
1.206	0.01	10.006	-0.0076	0.0204	0.0065	0.850	-0.06	4.013	0.0176	0.0121	-0.0241
1.200	4.01	0.916	0.0473	0.0274	-0.0672	0.848	-0.03	6.019	0.0175	0.0115	-0.0238
1.200	4.01	2.043	0.0468	0.0267	-0.0661	0.848	-0.00	8.006	0.0165	0.0109	-0.0224
1.201	4.02	3.528	0.0474	0.0271	-0.0671	0.848	0.02	1.071	0.0209	0.0133	-0.0287
1.201	4.02	5.948	0.0479	0.0264	-0.0679	0.797	0.00	1.068	0.0258	0.0120	-0.0343
1.199	4.01	9.984	-0.0469	0.0248	-0.0662	0.800	-0.00	2.010	0.0228	0.0106	-0.0299
1.200	-0.01	0.930	-0.0061	0.0238	0.0055	0.799	0.01	3.909	0.0232	0.0107	-0.0305
1.147	0.01	0.925	-0.0048	0.0258	0.0030	0.800	-0.01	5.017	0.0225	0.0105	-0.0297
1.150	0.01	1.997	-0.0055	0.0250	0.0040	0.804	-0.00	8.013	0.0206	0.0096	-0.0272
1.148	0.01	3.505	-0.0054	0.0254	0.0039	0.797	-0.01	1.066	0.0253	0.0119	-0.0336
1.150	0.01	5.610	-0.0054	0.0248	0.0035	0.599	0.01	1.034	0.0206	0.0098	-0.0265
1.151	0.03	10.027	-0.0063	0.0226	0.0047	0.600	-1.99	1.036	0.0078	0.0097	-0.0089
1.149	0.02	0.922	-0.0050	0.0254	0.0032	0.600	-0.02	1.035	0.0211	0.0098	-0.0270
0.000	-0.08	1.000	-0.0005	-0.0000	0.0005	0.602	2.02	1.034	0.0338	0.0108	-0.0448
0.940	0.01	1.083	0.0123	0.0152	-0.0187	0.601	3.97	1.034	0.0474	0.0124	-0.0640
0.938	0.00	2.012	0.0115	0.0134	-0.0160	0.599	6.01	1.033	0.0632	0.0155	-0.0871
0.940	-0.02	3.540	0.0113	0.0137	-0.0181	0.598	8.00	1.034	0.0788	0.0195	-0.1105
0.940	0.02	4.250	0.0113	0.0136	-0.0183	0.597	10.01	1.035	0.0934	0.0247	-0.1331
0.937	-0.02	8.024	0.0101	0.0123	-0.0170	0.602	-0.03	1.035	0.0204	0.0100	-0.0259
0.937	0.01	1.077	0.0114	0.0150	-0.0178	0.601	-0.01	2.027	0.0193	0.0089	-0.0243
0.901	-0.03	1.078	0.0156	0.0145	-0.0234	0.603	-0.01	3.404	0.0190	0.0090	-0.0239
0.902	-2.00	1.084	0.0116	0.0138	-0.0162	0.601	-0.00	4.000	0.0190	0.0089	-0.0239
0.897	0.01	1.079	0.0164	0.0145	-0.0234	0.602	0.01	6.014	0.0187	0.0084	-0.0235
0.903	1.98	1.070	0.0203	0.0155	-0.0295	0.602	0.01	8.009	0.0180	0.0078	-0.0227
0.900	3.97	1.061	0.0248	0.0169	-0.0384	0.599	4.00	1.033	0.0462	0.0122	-0.0623
0.898	6.01	1.062	0.0355	0.0188	-0.0556	0.600	4.01	2.022	0.0452	0.0113	-0.0606
0.899	8.02	1.067	0.0554	0.0229	-0.0855	0.599	4.00	3.378	0.0455	0.0115	-0.0611
0.895	10.00	1.071	0.0756	0.0284	-0.1145	0.600	4.01	4.009	0.0457	0.0115	-0.0614
0.904	0.00	1.079	0.0148	0.0145	-0.0216	0.600	3.99	5.991	0.0447	0.0110	-0.0601
0.900	-0.00	2.001	0.0127	0.0128	-0.0182	0.601	3.99	8.033	0.0439	0.0104	-0.0590
0.901	0.00	3.521	0.0132	0.0131	-0.0193	0.602	7.99	1.033	0.0779	0.0193	-0.1090
0.898	-0.07	4.191	0.0131	0.0130	-0.0191	0.601	8.01	2.008	0.0776	0.0184	-0.1085
0.899	0.04	6.008	0.0130	0.0125	-0.0193	0.601	8.01	3.429	0.0779	0.0186	-0.1091
0.899	0.03	8.017	0.0122	0.0118	-0.0181	0.603	7.99	3.995	0.0776	0.0185	-0.1086
0.901	3.98	1.058	0.0234	0.0166	-0.0364	0.601	7.99	6.007	0.0773	0.0180	-0.1082
0.900	4.02	2.012	0.0231	0.0150	-0.0360	0.601	8.00	8.006	0.0766	0.0173	-0.1074
0.900	4.00	3.504	0.0241	0.0154	-0.0373	0.601	8.01	1.034	0.0204	0.0100	-0.0259
0.897	4.01	4.206	0.0248	0.0193	-0.0386						

TABLE IV.- Continued

(c) $c_{r,vt} = 24.38$ cm; symmetrical vertical-tail airfoil;
 $\phi_t = 2^\circ$; $\phi_t = 0^\circ$; basic interfairing

M	α , deg	NPR	C_L	C_D	C_m	M	α , deg	NPR	C_L	C_D	C_m
1.201	0.03	0.978	-0.0097	0.0221	0.0061	0.900	7.77	4.194	0.0470	0.0128	-0.0760
1.200	-1.90	0.981	-0.0367	0.0240	0.0444	0.900	7.76	6.012	0.0460	0.0122	-0.0746
1.198	0.00	0.975	-0.0111	0.0223	0.0098	0.901	7.75	6.015	0.0458	0.0114	-0.0741
1.199	1.89	0.966	0.0157	0.0225	-0.0272	0.900	-0.07	1.112	0.0086	0.0081	-0.0177
1.200	3.80	0.964	0.0429	0.0244	-0.0641	0.849	-0.04	1.098	0.0088	0.0076	-0.0160
1.198	5.71	0.958	0.0632	0.0281	-0.0914	0.848	-0.04	2.003	0.0083	0.0061	-0.0153
1.197	7.66	0.936	0.0783	0.0328	-0.1117	0.848	-0.05	3.511	0.0080	0.0063	-0.0149
1.198	0.01	0.975	-0.0118	0.0224	0.0106	0.851	-0.04	4.010	0.0079	0.0062	-0.0148
1.198	0.02	0.974	-0.0116	0.0224	0.0103	0.850	-0.04	6.014	0.0072	0.0049	-0.0140
1.201	0.01	2.051	-0.0116	0.0215	0.0104	0.848	-0.03	1.095	0.0082	0.0075	-0.0152
1.201	0.01	1.999	-0.0115	0.0215	0.0102	0.799	-0.02	1.080	0.0073	0.0077	-0.0135
1.202	0.02	3.506	-0.0113	0.0219	0.0100	0.799	-0.03	2.007	0.0070	0.0063	-0.0131
1.201	0.03	5.981	-0.0117	0.0210	0.0104	0.800	-0.04	3.900	0.0068	0.0064	-0.0130
1.201	-0.02	10.022	-0.0123	0.0188	0.0113	0.800	-0.03	4.997	0.0066	0.0061	-0.0128
1.200	3.77	0.956	0.0423	0.0244	-0.0635	0.800	-0.02	6.004	0.0063	0.0052	-0.0124
1.200	3.78	2.010	0.0417	0.0235	-0.0626	0.802	-0.02	1.076	0.0070	0.0077	-0.0131
1.200	3.78	3.909	0.0417	0.0240	-0.0629	0.600	0.04	1.037	0.0063	0.0073	-0.0114
1.199	3.79	6.018	0.0420	0.0232	-0.0632	0.600	-1.98	1.038	-0.0057	0.0077	0.0053
1.200	3.78	9.967	0.0415	0.0211	-0.0622	0.601	-0.03	1.037	0.0061	0.0073	-0.0111
1.202	0.00	0.967	-0.0125	0.0223	0.0115	0.602	1.94	1.037	0.0191	0.0077	-0.0291
0.940	-0.08	1.128	0.0080	0.0088	-0.0179	0.602	3.93	1.036	0.0330	0.0089	-0.0488
0.938	-0.06	2.009	0.0060	0.0069	-0.0150	0.600	5.86	1.036	0.0478	0.0110	-0.0703
0.942	-0.07	3.502	0.0059	0.0071	-0.0147	0.599	7.83	1.037	0.0614	0.0140	-0.0903
0.939	-0.06	4.286	0.0064	0.0070	-0.0156	0.598	9.81	1.038	0.0763	0.0184	-0.1132
0.937	-0.04	7.986	0.0044	0.0058	-0.0130	0.599	-0.01	1.037	0.0064	0.0075	-0.0116
0.938	-0.06	1.125	0.0069	0.0085	-0.0168	0.602	-0.03	1.997	0.0055	0.0063	-0.0104
0.901	-0.08	1.110	0.0090	0.0084	-0.0182	0.602	-0.02	3.414	0.0052	0.0064	-0.0099
0.897	-2.04	1.111	0.0034	0.0081	-0.0104	0.599	-0.01	4.005	0.0055	0.0043	-0.0103
0.899	-0.05	1.110	0.0094	0.0084	-0.0187	0.599	-0.03	6.002	0.0050	0.0057	-0.0097
0.901	1.92	1.110	0.0163	0.0088	-0.0285	0.600	-0.03	7.999	0.0048	0.0051	-0.0094
0.899	3.87	1.106	0.0235	0.0098	-0.0402	0.599	3.92	1.035	0.0320	0.0085	-0.0473
0.898	5.82	1.107	0.0331	0.0114	-0.0558	0.599	3.93	1.996	0.0313	0.0077	-0.0463
0.895	7.74	1.107	0.0511	0.0148	-0.0822	0.599	3.92	3.405	0.0315	0.0078	-0.0466
0.901	9.65	1.107	0.0703	0.0201	-0.1075	0.598	3.93	4.013	0.0311	0.0078	-0.0462
0.899	-0.07	1.114	0.0091	0.0083	-0.0182	0.598	3.94	5.988	0.0311	0.0073	-0.0462
0.899	-0.06	2.021	0.0086	0.0066	-0.0174	0.599	3.91	6.035	0.0306	0.0066	-0.0455
0.899	-0.05	3.494	0.0082	0.0067	-0.0169	0.600	7.85	1.036	0.0616	0.0139	-0.0907
0.899	-0.07	4.205	0.0076	0.0065	-0.0162	0.600	7.86	1.996	0.0620	0.0130	-0.0909
0.900	-0.03	6.004	0.0073	0.0060	-0.0159	0.600	7.84	3.409	0.0617	0.0132	-0.0909
0.898	-0.06	8.012	0.0066	0.0052	-0.0148	0.600	7.85	3.994	0.0616	0.0131	-0.0907
0.900	3.87	1.108	0.0222	0.0094	-0.0392	0.599	7.83	6.009	0.0617	0.0125	-0.0908
0.902	3.87	2.009	0.0190	0.0077	-0.0339	0.599	7.83	8.005	0.0621	0.0120	-0.0913
0.901	3.88	3.495	0.0201	0.0079	-0.0355	0.600	-0.03	1.037	0.0058	0.0074	-0.0107
0.899	3.89	4.205	0.0206	0.0079	-0.0360						
0.900	3.89	5.990	0.0194	0.0073	-0.0344						
0.899	3.88	7.995	0.0179	0.0066	-0.0323						
0.896	7.73	1.109	0.0495	0.0145	-0.0798						
0.898	7.77	2.001	0.0468	0.0126	-0.0751						
0.900	7.76	3.514	0.0467	0.0128	-0.0753						

TABLE IV.- Continued

(d) $c_{r,vt} = 24.38$ cm; symmetrical vertical-tail airfoil;
 $\psi_t = 4^\circ$; $\phi_t = 0^\circ$; basic interfairing

M	α , deg	NPR	C_L	C_D	C_m	M	α , deg	NPR	C_L	C_D	C_m
1.200	0.02	0.979	-0.0186	0.0248	0.0204	0.899	4.01	4.220	0.0135	0.0076	-0.0285
1.202	-2.01	0.984	-0.0476	0.0277	0.0592	0.899	3.99	6.021	0.0133	0.0071	-0.0284
1.199	-0.00	0.976	-0.0185	0.0250	0.0202	0.900	4.01	8.003	0.0133	0.0064	-0.0283
1.202	1.99	0.960	0.0128	0.0247	-0.0232	0.899	8.01	1.117	0.0428	0.0138	-0.0725
1.201	3.98	0.961	0.0425	0.0264	-0.0637	0.900	8.01	2.003	0.0432	0.0122	-0.0726
1.200	5.99	0.957	0.0617	0.0300	-0.0886	0.898	8.01	3.504	0.0438	0.0124	-0.0734
1.200	8.00	0.938	0.0801	0.0347	-0.1143	0.902	7.99	4.202	0.0429	0.0123	-0.0725
1.200	-0.01	0.973	-0.0196	0.0252	0.0215	0.898	8.00	6.029	0.0441	0.0118	-0.0735
1.200	0.00	2.028	-0.0188	0.0241	0.0204	0.902	8.00	8.010	0.0432	0.0111	-0.0727
1.202	0.00	3.530	-0.0191	0.0244	0.0207	0.851	0.00	1.097	-0.0009	0.0089	-0.0053
1.201	-0.01	6.042	-0.0193	0.0235	0.0209	0.851	0.00	2.002	-0.0006	0.0073	-0.0060
1.200	-0.00	10.028	-0.0195	0.0213	0.0210	0.848	-0.00	3.510	-0.0011	0.0075	-0.0052
1.200	3.99	0.954	0.0420	0.0264	-0.0635	0.849	0.00	4.001	-0.0011	0.0076	-0.0053
1.203	4.01	2.019	0.0423	0.0293	-0.0638	0.851	-0.01	8.004	-0.0012	0.0063	-0.0052
1.202	4.01	3.546	0.0417	0.0257	-0.0631	0.849	-0.00	1.095	-0.0014	0.0089	-0.0046
1.202	3.99	4.025	0.0418	0.0256	-0.0634	0.799	-0.01	1.081	-0.0014	0.0089	-0.0042
1.201	4.02	6.000	0.0418	0.0248	-0.0633	0.799	0.03	2.028	-0.0010	0.0074	-0.0051
1.202	3.99	9.986	0.0410	0.0225	-0.0620	0.801	0.01	3.899	-0.0010	0.0075	-0.0046
1.201	-0.01	0.969	-0.0203	0.0250	0.0221	0.799	-0.01	5.028	-0.0013	0.0071	-0.0044
1.154	0.00	0.976	-0.0214	0.0257	0.0230	0.798	-0.01	5.002	-0.0015	0.0071	-0.0042
1.150	0.01	2.006	-0.0208	0.0247	0.0221	0.799	-0.00	7.997	-0.0015	0.0062	-0.0044
1.150	0.01	3.505	-0.0202	0.0252	0.0214	0.798	-0.02	1.078	-0.0016	0.0087	-0.0040
1.147	0.02	0.969	-0.0209	0.0260	0.0221	0.599	-0.00	1.039	-0.0010	0.0084	-0.0039
1.149	-0.01	1.997	-0.0208	0.0250	0.0221	0.598	-1.98	1.040	-0.0127	0.0090	0.0123
1.151	0.01	3.502	-0.0204	0.0254	0.0216	0.601	0.00	1.039	-0.0002	0.0086	-0.0050
0.941	0.00	1.137	-0.0025	0.0089	-0.0062	0.601	1.98	1.039	0.0125	0.0086	-0.0227
0.941	-0.01	2.021	-0.0023	0.0072	-0.0066	0.600	3.99	1.039	0.0262	0.0095	-0.0421
0.941	0.01	3.502	-0.0025	0.0074	-0.0063	0.600	5.99	1.039	0.0416	0.0115	-0.0643
0.943	-0.01	4.308	-0.0032	0.0072	-0.0052	0.601	7.98	1.039	0.0559	0.0145	-0.0856
0.940	-0.01	8.033	-0.0027	0.0060	-0.0061	0.602	9.98	1.041	0.0705	0.0186	-0.1082
0.939	0.01	1.135	-0.0025	0.0089	-0.0062	0.602	-0.01	1.040	0.0005	0.0087	-0.0055
0.902	-0.01	1.117	-0.0016	0.0087	-0.0058	0.602	0.02	2.020	-0.0002	0.0077	-0.0048
0.902	-1.99	1.118	-0.0070	0.0093	0.0021	0.600	-0.01	3.392	-0.0005	0.0077	-0.0043
0.900	0.00	1.116	-0.0012	0.0088	-0.0061	0.601	0.00	4.015	-0.0010	0.0074	-0.0037
0.898	2.01	1.116	-0.0070	0.0087	-0.0176	0.602	0.00	6.004	-0.0010	0.0069	-0.0040
0.898	3.99	1.113	0.0151	0.0092	-0.0312	0.602	0.00	8.035	-0.0013	0.0063	-0.0036
0.898	6.02	1.116	0.0252	0.0105	-0.0468	0.600	4.00	1.039	0.0252	0.0094	-0.0406
0.897	8.01	1.118	0.0436	0.0140	-0.0735	0.600	4.01	2.007	0.0253	0.0084	-0.0407
0.900	10.01	1.119	0.0655	0.0198	-0.1028	0.600	3.99	3.414	0.0249	0.0086	-0.0401
0.901	-0.03	1.118	-0.0010	0.0090	-0.0062	0.601	3.99	4.005	0.0249	0.0085	-0.0401
0.902	-0.00	2.007	-0.0010	0.0072	-0.0064	0.599	4.00	5.992	0.0251	0.0080	-0.0404
0.898	0.01	3.517	-0.0012	0.0073	-0.0059	0.600	4.01	8.019	0.0251	0.0074	-0.0405
0.900	-0.04	4.195	-0.0015	0.0072	-0.0055	0.598	8.01	1.038	0.0552	0.0144	-0.0845
0.899	0.05	4.194	-0.0014	0.0071	-0.0058	0.600	7.99	2.017	0.0557	0.0135	-0.0853
0.901	-0.01	6.016	-0.0018	0.0067	-0.0053	0.601	8.01	3.407	0.0558	0.0138	-0.0854
0.900	-0.00	8.006	-0.0018	0.0060	-0.0055	0.601	8.01	4.011	0.0558	0.0136	-0.0855
0.903	3.99	1.113	0.0137	0.0091	-0.0295	0.602	8.00	6.000	0.0560	0.0131	-0.0857
0.901	4.01	2.015	0.0137	0.0075	-0.0289	0.601	8.04	7.990	0.0563	0.0127	-0.0863
0.900	4.00	3.519	0.0134	0.0076	-0.0287	0.599	-0.00	1.039	0.0003	0.0088	-0.0054

TABLE IV.- Continued

(e) $c_{r,vt} = 24.38$ cm; symmetrical vertical-tail airfoil;
 $\phi_t = 0^\circ$; $\phi_t = 10^\circ$; basic interfairing

M	α , deg	NPR	C_L	C_D	C_m	M	α , deg	NPR	C_L	C_D	C_m
1.200	-0.02	0.965	-0.0040	0.0211	0.0009	0.900	-0.01	2.010	0.0183	0.0079	-0.0279
1.200	-2.01	0.973	-0.0320	0.0223	0.0362	0.899	-0.00	3.500	0.0178	0.0081	-0.0276
1.201	-0.02	0.961	-0.0040	0.0212	0.0007	0.899	-0.02	4.203	0.0175	0.0079	-0.0272
1.201	1.97	0.952	0.0235	0.0221	-0.0364	0.899	-0.01	5.980	0.0166	0.0075	-0.0261
1.200	4.01	0.944	0.0507	0.0249	-0.0732	0.902	-0.01	8.005	0.0148	0.0068	-0.0238
1.195	5.97	0.940	0.0732	0.0290	-0.1034	0.901	3.99	4.555	0.0279	0.0105	-0.0441
1.191	7.99	0.910	0.0862	0.0348	-0.1203	0.898	7.99	4.214	0.0602	0.0170	-0.0920
1.201	-0.00	0.958	-0.0049	0.0214	0.0016	0.850	-0.01	1.090	0.0210	0.0086	-0.0306
1.202	-0.00	1.987	-0.0059	0.0207	0.0028	0.852	-0.01	2.080	0.0197	0.0071	-0.0285
1.199	-0.00	3.489	-0.0058	0.0212	0.0027	0.849	0.00	3.490	0.0197	0.0072	-0.0285
1.201	-0.00	5.975	-0.0059	0.0203	0.0026	0.851	0.00	3.937	0.0196	0.0072	-0.0285
1.202	-0.02	10.044	-0.0060	0.0183	0.0026	0.850	-0.02	8.004	0.0175	0.0059	-0.0255
1.199	4.01	5.993	0.0506	0.0238	-0.0737	0.849	-0.01	1.087	0.0211	0.0085	-0.0308
0.942	0.00	1.109	0.0115	0.0097	-0.0200	0.798	0.00	1.076	0.0189	0.0082	-0.0269
0.941	0.00	2.021	0.0097	0.0081	-0.0173	0.799	-0.01	1.933	0.0176	0.0068	-0.0250
0.939	0.00	3.490	0.0107	0.0083	-0.0189	0.799	-0.01	3.885	0.0178	0.0069	-0.0254
0.941	-0.01	4.301	0.0102	0.0082	-0.0184	0.800	-0.00	5.037	0.0175	0.0066	-0.0249
0.939	-0.02	7.998	0.0088	0.0070	-0.0167	0.800	-0.00	7.999	0.0161	0.0057	-0.0231
0.940	-0.05	1.109	0.0122	0.0096	-0.0213	0.800	-0.00	1.076	0.0185	0.0081	-0.0264
0.940	-0.02	1.107	0.0117	0.0097	-0.0202	0.597	-0.01	1.037	0.0148	0.0077	-0.0209
0.903	-0.03	1.110	0.0197	0.0094	-0.0310	0.601	-1.99	1.039	0.0014	0.0077	-0.0027
0.899	-2.03	1.112	0.0139	0.0087	-0.0225	0.601	-0.00	1.038	0.0152	0.0077	-0.0214
0.902	-0.02	1.110	0.0205	0.0095	-0.0319	0.602	1.99	1.038	0.0297	0.0084	-0.0413
0.902	1.99	1.104	0.0268	0.0105	-0.0406	0.601	3.92	1.038	0.0442	0.0099	-0.0615
0.897	3.99	1.090	0.0315	0.0121	-0.0489	0.601	5.98	1.037	0.0609	0.0129	-0.0860
0.900	5.98	1.094	0.0427	0.0145	-0.0668	0.598	7.98	1.038	0.0772	0.0167	-0.1102
0.899	8.01	1.095	0.0623	0.0188	-0.0955	0.601	9.99	1.039	0.0927	0.0218	-0.1343
0.899	9.97	1.096	0.0811	0.0246	-0.1197	0.599	-0.01	1.038	0.0150	0.0079	-0.0210
0.900	-0.00	1.109	0.0206	0.0096	-0.0318	0.600	-0.00	1.999	0.0144	0.0067	-0.0202
						0.600	0.00	3.408	0.0138	0.0068	-0.0193
						0.601	-0.02	4.007	0.0138	0.0067	-0.0193
						0.599	-0.01	6.000	0.0131	0.0062	-0.0186
						0.601	-0.01	8.016	0.0128	0.0055	-0.0181
						0.599	4.00	3.396	0.0426	0.0091	-0.0593
						0.600	7.99	3.384	0.0763	0.0157	-0.1090
						0.602	-0.02	1.038	0.0148	0.0078	-0.0208

TABLE IV.- Continued

(f) $c_{r,vt} = 24.38$ cm; symmetrical vertical-tail airfoil;
 $\psi_t = 0^\circ$; $\phi_t = 20^\circ$; basic interfairing

M	α , deg	NPR	C_L	C_D	C_m	M	α , deg	NPR	C_L	C_D	C_m
1.202	-0.02	0.976	-0.0029	0.0207	-0.0009	0.902	8.00	3.524	0.0652	0.0168	-0.0978
1.202	-2.01	0.984	-0.0334	0.0219	0.0394	0.902	7.98	4.217	0.0652	0.0168	-0.0982
1.202	0.01	0.972	-0.0031	0.0209	-0.0009	0.899	7.99	6.016	0.0663	0.0164	-0.0993
1.200	1.98	0.965	0.0260	0.0220	-0.0399	0.898	7.98	8.043	0.0666	0.0157	-0.0996
1.199	4.00	0.955	0.0543	0.0249	-0.0777	0.903	-0.02	1.113	0.0218	0.0084	-0.0330
1.201	5.99	0.947	0.0776	0.0292	-0.1087	0.849	-0.01	1.095	0.0209	0.0077	-0.0297
1.199	7.99	0.919	0.0908	0.0349	-0.1262	0.850	-0.02	1.992	0.0197	0.0063	-0.0279
1.200	-0.01	0.969	-0.0040	0.0212	0.0001	0.851	-0.00	3.519	0.0197	0.0064	-0.0278
1.201	-0.01	1.989	-0.0047	0.0204	0.0009	0.852	-0.02	4.006	0.0196	0.0063	-0.0279
1.201	-0.01	3.469	-0.0049	0.0209	0.0012	0.852	-0.01	7.993	0.0180	0.0050	-0.0257
1.201	-0.01	5.991	-0.0044	0.0201	0.0005	0.850	-0.02	1.093	0.0204	0.0075	-0.0290
1.200	0.01	9.994	-0.0042	0.0180	0.0003	0.803	-0.02	1.079	0.0185	0.0076	-0.0261
1.202	-0.01	0.963	-0.0043	0.0210	0.0004	0.801	-0.03	1.993	0.0176	0.0062	-0.0249
1.146	-0.01	0.964	-0.0020	0.0228	-0.0034	0.798	-0.01	3.915	0.0174	0.0063	-0.0245
1.151	0.00	1.982	-0.0020	0.0219	-0.0030	0.803	-0.03	5.023	0.0170	0.0060	-0.0240
1.151	-0.01	3.498	-0.0022	0.0225	-0.0028	0.798	-0.03	7.993	0.0160	0.0051	-0.0228
1.149	-0.02	5.604	-0.0026	0.0219	-0.0023	0.803	-0.03	1.078	0.0176	0.0075	-0.0251
1.150	-0.01	10.044	-0.0031	0.0194	-0.0017	0.601	-0.01	1.038	0.0144	0.0070	-0.0206
1.149	-0.03	0.960	-0.0024	0.0226	-0.0026	0.602	-2.00	1.040	0.0000	0.0071	-0.0008
0.943	-0.01	1.112	0.0137	0.0087	-0.0229	0.603	-0.02	1.039	0.0151	0.0070	-0.0210
0.942	-0.01	1.998	0.0122	0.0070	-0.0206	0.600	2.00	1.036	0.0305	0.0078	-0.0419
0.937	-0.00	3.513	0.0140	0.0071	-0.0234	0.598	3.97	1.037	0.0472	0.0095	-0.0648
0.937	-0.04	4.324	0.0135	0.0071	-0.0228	0.601	5.98	1.038	0.0648	0.0125	-0.0903
0.938	-0.04	7.995	0.0116	0.0059	-0.0204	0.599	7.99	1.038	0.0808	0.0166	-0.1147
0.938	-0.04	1.116	0.0149	0.0085	-0.0250	0.597	9.99	1.038	0.0960	0.0216	-0.1380
0.903	-0.02	1.114	0.0216	0.0084	-0.0333	0.600	-0.00	1.039	0.0151	0.0073	-0.0209
0.899	-2.04	1.116	0.0136	0.0077	-0.0220	0.601	-0.01	2.018	0.0145	0.0061	-0.0199
0.902	-0.02	1.115	0.0220	0.0085	-0.0336	0.602	-0.03	3.423	0.0140	0.0062	-0.0190
0.899	1.99	1.110	0.0311	0.0095	-0.0459	0.601	-0.02	4.019	0.0135	0.0060	-0.0185
0.898	3.98	1.099	0.0376	0.0114	-0.0568	0.601	-0.02	6.037	0.0140	0.0055	-0.0191
0.897	6.02	1.100	0.0509	0.0143	-0.0773	0.602	-0.02	6.005	0.0135	0.0055	-0.0187
0.899	7.97	1.098	0.0677	0.0185	-0.1017	0.601	-0.02	8.008	0.0130	0.0049	-0.0181
0.899	9.99	1.100	0.0861	0.0246	-0.1258	0.601	8.00	1.037	0.0810	0.0165	-0.1144
0.898	-0.02	1.114	0.0223	0.0085	-0.0336	0.602	7.98	2.008	0.0812	0.0154	-0.1143
0.901	-0.00	2.030	0.0201	0.0069	-0.0303	0.602	8.00	3.409	0.0809	0.0157	-0.1141
0.900	-0.01	3.492	0.0205	0.0070	-0.0307	0.601	7.99	4.007	0.0814	0.0156	-0.1148
0.902	-0.03	4.204	0.0195	0.0069	-0.0298	0.600	7.99	6.009	0.0813	0.0151	-0.1147
0.898	0.00	6.019	0.0191	0.0064	-0.0290	0.601	7.97	8.007	0.0814	0.0144	-0.1146
0.901	0.01	7.995	0.0174	0.0057	-0.0270	0.599	7.98	8.008	0.0818	0.0145	-0.1153
0.898	7.99	1.097	0.0673	0.0185	-0.1009	0.601	-0.02	1.037	0.0150	0.0072	-0.0205
0.902	8.00	2.016	0.0648	0.0167	-0.0973						

TABLE IV.- Continued

(g) $c_{r,vt} = 24.38$ cm; vertical-tail airfoil cambered outboard;
 $\psi_t = 0^\circ$; $\phi_t = 0^\circ$; basic interfairing

M	α , deg	NPR	C_L	C_D	C_m	M	α , deg	NPR	C_L	C_D	C_m
1.201	-0.01	0.964	0.0000	0.0216	-0.0045	0.901	-0.03	0.017	0.0104	0.0067	-0.0170
1.200	-2.01	0.985	-0.0263	0.0224	0.0311	0.901	3.98	1.085	0.0235	0.0116	-0.0376
1.202	-0.02	0.959	0.0004	0.0217	-0.0051	0.897	4.00	4.216	0.0230	0.0101	-0.0366
1.200	1.99	0.942	0.0270	0.0230	-0.0415	0.899	7.98	1.095	0.0574	0.0182	-0.0884
1.204	3.99	0.942	0.0532	0.0256	-0.0772	0.897	7.98	2.014	0.0558	0.0164	-0.0856
1.206	6.01	0.949	0.0758	0.0296	-0.1073	0.901	8.00	4.202	0.0557	0.0166	-0.0857
1.199	7.97	0.920	0.0869	0.0354	-0.1219	0.899	7.99	6.011	0.0538	0.0151	-0.0829
1.198	-0.00	0.952	-0.0006	0.0221	-0.0037	0.904	-0.02	1.103	0.0154	0.0094	-0.0239
1.201	0.00	6.023	-0.0007	0.0207	-0.0034	0.848	-0.01	1.088	0.0156	0.0085	-0.0227
1.200	-0.03	2.015	-0.0010	0.0212	-0.0030	0.850	-0.02	4.021	0.0142	0.0071	-0.0207
1.199	-0.01	3.495	-0.0010	0.0217	-0.0031	0.798	-0.02	1.074	0.0130	0.0082	-0.0188
1.202	-0.01	5.984	-0.0011	0.0207	-0.0030	0.800	-0.01	3.919	0.0117	0.0068	-0.0172
1.202	-0.01	10.046	-0.0015	0.0186	-0.0026	0.800	-0.02	1.035	0.0100	0.0076	-0.0146
1.201	-0.02	0.941	-0.0006	0.0220	-0.0039	0.599	-2.02	1.037	-0.0026	0.0078	0.0028
1.201	-0.01	0.941	-0.0007	0.0220	-0.0037	0.600	-0.02	1.036	0.0106	0.0076	-0.0153
1.201	-0.02	0.943	-0.0011	0.0220	-0.0033	0.601	2.00	1.036	0.0233	0.0082	-0.0332
1.152	-0.03	0.949	-0.0002	0.0230	-0.0051	0.601	3.97	1.035	0.0369	0.0095	-0.0521
1.150	-0.01	5.630	-0.0006	0.0222	-0.0044	0.600	5.98	1.035	0.0525	0.0120	-0.0749
0.942	-0.02	1.096	0.0087	0.0098	-0.0193	0.599	7.99	1.035	0.0683	0.0156	-0.0984
0.941	0.00	4.323	0.0074	0.0083	-0.0138	0.597	9.99	1.037	0.0822	0.0202	-0.1204
0.899	-0.03	1.096	0.0157	0.0096	-0.0246	0.599	-0.02	1.036	0.0105	0.0079	-0.0151
0.899	-2.06	1.102	0.0096	0.0089	-0.0163	0.601	-0.01	2.016	0.0097	0.0067	-0.0140
0.901	-0.00	1.098	0.0161	0.0095	-0.0250	0.601	-0.01	3.418	0.0089	0.0068	-0.0130
0.898	1.99	1.094	0.0218	0.0105	-0.0334	0.602	-0.02	4.020	0.0089	0.0067	-0.0129
0.902	3.97	1.084	0.0242	0.0118	-0.0387	0.602	-0.01	6.013	0.0084	0.0061	-0.0124
0.898	6.00	1.090	0.0370	0.0141	-0.0585	0.600	-0.01	6.003	0.0079	0.0056	-0.0119
0.898	7.98	1.094	0.0583	0.0185	-0.0900	0.599	3.98	1.034	0.0360	0.0093	-0.0509
0.899	10.01	1.093	0.0769	0.0241	-0.1144	0.601	3.99	3.434	0.0356	0.0087	-0.0501
0.902	4.01	1.086	0.0237	0.0118	-0.0380	0.603	8.00	1.035	0.0680	0.0156	-0.0979
0.900	-0.02	1.103	0.0162	0.0096	-0.0249	0.604	7.98	2.009	0.0675	0.0146	-0.0971
0.903	0.00	2.017	0.0137	0.0079	-0.0214	0.598	7.98	3.418	0.0674	0.0147	-0.0969
0.901	-0.00	3.535	0.0139	0.0081	-0.0216	0.601	7.98	7.989	0.0673	0.0135	-0.0971
0.901	-0.01	4.210	0.0136	0.0080	-0.0211	0.600	-0.02	1.036	0.0105	0.0079	-0.0150
0.900	-0.01	5.577	0.0129	0.0076	-0.0203						
0.900	-0.02	5.992	0.0119	0.0074	-0.0191						

TABLE IV.- Continued

(h) $c_{r,vt} = 24.38$ cm; vertical-tail airfoil cambered inboard;
 $\phi_t = 0^\circ$; $\phi_t = 0^\circ$; basic interfairing

M	α , deg	NPR	C_L	C_D	C_m	M	α , deg	NPR	C_L	C_D	C_m
1.203	-0.02	0.961	-0.0107	0.0220	0.0115	0.901	4.02	1.063	0.0179	0.0144	-0.0301
1.200	-2.03	0.971	-0.0367	0.0237	0.0461	0.901	3.98	4.204	0.0183	0.0131	-0.0311
1.202	-0.02	0.958	-0.0101	0.0222	0.0105	0.899	7.98	1.068	0.0499	0.0202	-0.0788
1.199	2.00	0.947	0.0175	0.0229	-0.0271	0.900	7.98	2.060	0.0487	0.0186	-0.0769
1.198	4.00	0.945	0.0447	0.0253	-0.0641	0.900	7.97	4.198	0.0497	0.0189	-0.0788
1.198	5.98	0.942	0.0696	0.0294	-0.0988	0.900	7.98	4.199	0.0504	0.0190	-0.0800
1.199	7.97	0.904	0.0823	0.0340	-0.1160	0.898	8.00	7.996	0.0504	0.0177	-0.0796
1.198	-0.04	0.955	-0.0118	0.0225	0.0126	0.902	-0.03	1.082	0.0094	0.0126	-0.0154
1.199	-0.02	2.002	-0.0118	0.0217	0.0128	0.850	-0.00	1.080	0.0174	0.0116	-0.0258
1.199	-0.01	3.514	-0.0122	0.0220	0.0133	0.851	-0.01	4.011	0.0133	0.0104	-0.0201
1.198	-0.01	6.015	-0.0113	0.0213	0.0120	0.799	-0.02	3.834	0.0182	0.0088	-0.0256
1.199	-0.03	10.058	-0.0120	0.0193	0.0125	0.800	-0.01	3.930	0.0179	0.0088	-0.0253
1.201	-0.01	0.948	-0.0112	0.0223	0.0116	0.600	-0.02	1.036	0.0165	0.0081	-0.0222
1.151	-0.02	0.946	-0.0124	0.0239	0.0125	0.599	-2.02	1.038	0.0042	0.0081	-0.0052
1.149	-0.00	5.589	-0.0120	0.0231	0.0121	0.601	-0.03	1.037	0.0175	0.0081	-0.0234
0.941	0.00	1.087	0.0046	0.0128	-0.0100	0.603	2.00	1.036	0.0303	0.0088	-0.0412
0.941	-0.03	1.086	0.0043	0.0127	-0.0096	0.600	3.97	1.036	0.0438	0.0104	-0.0603
0.941	0.00	4.310	0.0041	0.0113	-0.0098	0.600	5.98	1.036	0.0596	0.0131	-0.0832
0.902	-0.01	1.082	0.0088	0.0127	-0.0151	0.598	7.98	1.035	0.0756	0.0169	-0.1071
0.900	-2.04	1.091	0.0054	0.0122	-0.0105	0.600	9.99	1.037	0.0904	0.0220	-0.1304
0.903	-0.03	1.083	0.0093	0.0127	-0.0154	0.602	-0.01	1.037	0.0180	0.0084	-0.0241
0.899	2.00	1.073	0.0140	0.0133	-0.0223	0.602	0.01	2.000	0.0166	0.0073	-0.0220
0.900	3.97	1.065	0.0193	0.0146	-0.0322	0.601	-0.01	3.395	0.0159	0.0074	-0.0211
0.897	6.00	1.066	0.0305	0.0165	-0.0499	0.602	-0.01	4.005	0.0154	0.0073	-0.0205
0.897	7.99	1.070	0.0509	0.0205	-0.0804	0.601	-0.01	5.993	0.0146	0.0067	-0.0197
0.901	9.98	1.077	0.0722	0.0266	-0.1102	0.601	-0.01	6.929	0.0143	0.0065	-0.0193
0.901	-0.01	1.084	0.0091	0.0128	-0.0151	0.598	3.98	1.033	0.0417	0.0102	-0.0576
0.899	-0.00	2.383	0.0079	0.0114	-0.0133	0.599	3.99	3.397	0.0415	0.0096	-0.0572
0.898	-0.00	2.413	0.0079	0.0114	-0.0131	0.600	7.97	1.034	0.0741	0.0166	-0.1054
0.901	-0.00	2.016	0.0065	0.0112	-0.0113	0.600	7.99	2.002	0.0741	0.0158	-0.1051
0.900	0.00	3.507	0.0072	0.0114	-0.0124	0.600	7.98	3.392	0.0742	0.0160	-0.1055
0.899	0.00	4.580	0.0072	0.0113	-0.0126	0.601	7.98	7.987	0.0736	0.0148	-0.1047
0.900	-0.02	4.213	0.0070	0.0113	-0.0124	0.598	0.16	1.583	0.0164	0.0068	-0.0222
0.900	-0.02	5.995	0.0072	0.0108	-0.0125	0.600	-0.03	1.036	0.0173	0.0085	-0.0239
0.901	-0.03	8.003	0.0067	0.0101	-0.0118						

TABLE IV.- Continued

(i) $c_{r,vt} = 24.38$ cm; vertical-tail airfoil cambered inboard;
 $\psi_t = 0^\circ$; $\phi_t = 10^\circ$; basic interfairing

M	α , deg	NPR	C_L	C_D	C_m	M	α , deg	NPR	C_L	C_D	C_m
1.199	-0.01	0.961	-0.0088	0.0213	0.0083	0.899	4.01	4.178	0.0274	0.0127	-0.0440
1.201	-2.04	0.970	-0.0367	0.0229	0.0455	0.899	7.99	1.068	0.0599	0.0208	-0.0931
1.203	0.00	0.958	-0.0082	0.0214	0.0075	0.901	8.00	1.994	0.0584	0.0192	-0.0908
1.201	2.00	0.949	0.0198	0.0220	-0.0304	0.899	7.99	4.214	0.0601	0.0195	-0.0932
1.199	4.01	0.940	0.0478	0.0246	-0.0681	0.900	7.99	8.012	0.0602	0.0183	-0.0935
1.195	6.00	0.931	0.0720	0.0291	-0.1017	0.901	-0.03	1.090	0.0185	0.0114	-0.0292
1.198	7.98	0.901	0.0860	0.0340	-0.1204	0.600	-0.02	1.034	0.0198	0.0080	-0.0270
1.195	-0.00	0.951	-0.0096	0.0219	0.0091	0.600	-2.01	1.035	0.0058	0.0080	-0.0081
1.201	-0.02	0.952	-0.0091	0.0217	0.0084	0.602	-0.02	1.035	0.0194	0.0081	-0.0266
1.202	-0.01	2.020	-0.0101	0.0210	0.0099	0.601	2.01	1.034	0.0341	0.0089	-0.0468
1.200	0.01	3.508	-0.0095	0.0214	0.0091	0.602	4.00	1.034	0.0487	0.0106	-0.0673
1.200	0.01	6.023	-0.0096	0.0207	0.0090	0.600	5.99	1.033	0.0655	0.0136	-0.0915
1.200	0.00	9.971	-0.0095	0.0187	0.0087	0.600	7.99	1.033	0.0814	0.0175	-0.1154
1.201	-0.01	0.944	-0.0095	0.0217	0.0087	0.599	10.02	1.034	0.0974	0.0229	-0.1402
0.900	-0.03	1.090	0.0193	0.0115	-0.0305	0.598	-0.02	1.035	0.0194	0.0082	-0.0265
0.901	-2.01	1.098	0.0134	0.0108	-0.0229	0.598	0.00	2.017	0.0190	0.0072	-0.0259
0.900	-0.00	1.091	0.0194	0.0116	-0.0305	0.601	-0.00	3.404	0.0183	0.0073	-0.0249
0.899	2.00	1.078	0.0235	0.0126	-0.0362	0.600	0.01	4.006	0.0184	0.0071	-0.0250
0.896	3.97	1.067	0.0301	0.0143	-0.0474	0.601	-0.01	5.986	0.0176	0.0065	-0.0241
0.899	5.99	1.068	0.0409	0.0167	-0.0650	0.601	-0.00	8.001	0.0171	0.0059	-0.0236
0.898	7.99	1.070	0.0608	0.0210	-0.0944	0.601	3.99	1.032	0.0475	0.0102	-0.0656
0.899	10.00	1.076	0.0796	0.0268	-0.1199	0.600	4.01	3.428	0.0466	0.0096	-0.0642
0.900	0.00	1.091	0.0192	0.0116	-0.0301	0.601	7.99	1.032	0.0804	0.0172	-0.1138
0.898	-0.02	2.016	0.0158	0.0101	-0.0247	0.599	8.01	2.007	0.0803	0.0164	-0.1137
0.899	0.02	3.505	0.0165	0.0103	-0.0259	0.600	8.00	3.415	0.0806	0.0166	-0.1143
0.898	-0.02	4.194	0.0156	0.0102	-0.0248	0.599	7.99	8.023	0.0799	0.0154	-0.1134
0.898	0.00	6.004	0.0153	0.0097	-0.0244	0.603	-0.02	1.033	0.0186	0.0081	-0.0254
0.900	-0.01	8.024	0.0138	0.0090	-0.0224						
0.901	3.96	1.066	0.0268	0.0140	-0.0433						

TABLE IV.- Continued

(j) $c_{r,vt} = 24.38$ cm; vertical-tail airfoil
 cambered outboard; $\phi_t = 0^\circ$; $\phi_t = 20^\circ$;
 basic interfairing

M	α , deg	NPR	C_L	C_D	C_m
0.899	0.02	1.111	0.0161	0.0083	-0.0232
0.900	-2.01	1.114	0.0059	0.0079	-0.0100
0.897	-0.00	1.110	0.0162	0.0084	-0.0232
0.899	2.01	1.109	0.0262	0.0094	-0.0373
0.898	3.98	1.103	0.0374	0.0114	-0.0552
0.901	6.02	1.105	0.0498	0.0143	-0.0748
0.899	8.01	1.104	0.0706	0.0192	-0.1054
0.898	9.98	1.102	0.0882	0.0250	-0.1277
0.901	0.01	1.112	0.0146	0.0084	-0.0216
0.898	-0.01	2.049	0.0134	0.0066	-0.0197
0.899	-0.00	3.505	0.0128	0.0066	-0.0189
0.898	-0.03	4.169	0.0126	0.0065	-0.0187
0.903	-0.02	5.993	0.0120	0.0059	-0.0183
0.901	-0.01	8.013	0.0112	0.0051	-0.0171
0.897	4.01	1.100	0.0352	0.0107	-0.0524
0.899	4.01	4.193	0.0320	0.0092	-0.0478
0.899	7.99	1.101	0.0698	0.0186	-0.1034
0.898	7.99	1.985	0.0677	0.0167	-0.1000
0.899	7.98	4.228	0.0684	0.0169	-0.1008
0.900	8.02	7.966	0.0673	0.0158	-0.0998
0.905	6.67	1.103	0.0507	0.0147	-0.0771

TABLE IV.- Continued

(k) $c_{r,vt} = 24.38$ cm; vertical-tail airfoil cambered inboard;
 $\phi_t = 0^\circ$; $\phi_t = 20^\circ$; basic interfairing

M	α , deg	NPR	C_L	C_D	C_m	M	α , deg	NPR	C_L	C_D	C_m
1.198	0.03	0.950	-0.0068	0.0215	0.0048	0.900	-0.02	6.021	0.0225	0.0086	-0.0350
1.201	-2.02	0.961	-0.0372	0.0228	0.0452	0.900	-0.01	7.990	0.0210	0.0079	-0.0328
1.203	-0.02	0.948	-0.0073	0.0213	0.0093	0.902	3.99	1.071	0.0368	0.0137	-0.0572
1.202	2.00	0.942	0.0225	0.0220	-0.0350	0.900	3.99	4.204	0.0371	0.0123	-0.0573
1.201	4.01	0.933	0.0515	0.0247	-0.0740	0.899	8.00	1.072	0.0689	0.0212	-0.1050
1.200	6.01	0.927	0.0771	0.0292	-0.1087	0.898	7.99	2.001	0.0686	0.0196	-0.1038
1.201	7.98	0.897	0.0907	0.0346	-0.1266	0.900	8.00	4.194	0.0693	0.0197	-0.1050
1.204	0.00	0.947	-0.0091	0.0215	0.0072	0.900	7.99	8.015	0.0691	0.0186	-0.1047
1.200	-0.01	1.993	-0.0093	0.0209	0.0079	0.901	7.99	1.071	0.0684	0.0211	-0.1041
1.200	0.00	3.543	-0.0091	0.0213	0.0075	0.851	-0.02	1.084	0.0307	0.0093	-0.0441
1.201	0.03	5.997	-0.0083	0.0204	0.0063	0.850	0.00	3.995	0.0276	0.0077	-0.0398
1.202	-0.01	10.027	-0.0086	0.0184	0.0064	0.798	0.00	1.070	0.0264	0.0082	-0.0371
1.200	-0.02	0.941	-0.0085	0.0215	0.0068	0.801	0.00	3.875	0.0251	0.0069	-0.0393
0.940	-0.01	1.093	0.0162	0.0108	-0.0274	0.599	-0.02	1.033	0.0210	0.0074	-0.0291
0.942	-0.01	2.043	0.0148	0.0093	-0.0255	0.601	-2.00	1.034	0.0062	0.0073	-0.0092
0.941	-0.00	4.294	0.0159	0.0093	-0.0272	0.602	-0.02	1.033	0.0217	0.0074	-0.0299
0.941	-0.03	1.091	0.0163	0.0107	-0.0277	0.601	2.00	1.033	0.0373	0.0083	-0.0510
0.899	-0.00	1.095	0.0271	0.0105	-0.0417	0.601	3.99	1.032	0.0538	0.0102	-0.0738
0.900	-2.02	1.099	0.0195	0.0096	-0.0317	0.599	5.97	1.032	0.0707	0.0134	-0.0982
0.901	0.00	1.096	0.0270	0.0106	-0.0417	0.598	7.98	1.032	0.0876	0.0177	-0.1234
0.901	1.97	1.086	0.0332	0.0120	-0.0501	0.597	9.95	1.033	0.1038	0.0231	-0.1484
0.898	4.01	1.073	0.0394	0.0141	-0.0605	0.600	-0.01	1.033	0.0220	0.0076	-0.0301
0.899	6.01	1.074	0.0525	0.0170	-0.0809	0.599	0.01	2.003	0.0210	0.0066	-0.0287
0.899	8.00	1.073	0.0717	0.0217	-0.1085	0.601	0.01	3.415	0.0203	0.0067	-0.0279
0.898	9.99	1.079	0.0875	0.0273	-0.1296	0.603	-0.00	4.014	0.0197	0.0065	-0.0272
0.899	-0.02	1.096	0.0270	0.0106	-0.0415	0.601	-0.01	6.012	0.0198	0.0059	-0.0273
0.901	-0.03	2.000	0.0240	0.0090	-0.0365	0.602	-0.00	8.012	0.0195	0.0053	-0.0269
0.901	0.00	3.498	0.0243	0.0092	-0.0374	0.601	3.98	1.030	0.0519	0.0100	-0.0712
0.899	-0.03	4.200	0.0241	0.0090	-0.0370	0.600	3.99	3.389	0.0517	0.0094	-0.0707
						0.598	7.99	1.030	0.0876	0.0177	-0.1231
						0.601	7.99	2.017	0.0883	0.0168	-0.1237
						0.600	7.98	3.399	0.0877	0.0170	-0.1232
						0.601	7.99	8.003	0.0881	0.0158	-0.1240
						0.601	-0.02	1.035	0.0219	0.0076	-0.0300

TABLE IV.- Concluded

(1) $c_{r,vt} = 24.38$ cm; symmetrical vertical-tail airfoil;
 $\psi_t = 0^\circ$; $\phi_t = 0^\circ$; alternate interfairing

M	α , deg	NPR	C_L	C_D	C_m	M	α , deg	NPR	C_L	C_D	C_m
1.200	-0.00	0.938	-0.0087	0.0242	0.0074	0.898	4.00	1.029	0.0078	0.0117	-0.0153
1.201	-2.02	0.960	-0.0347	0.0252	0.0422	0.900	3.99	4.206	0.0094	0.0110	-0.0184
1.200	0.02	0.934	-0.0075	0.0242	0.0058	0.898	8.01	1.053	0.0401	0.0170	-0.0644
1.201	2.00	0.925	0.0189	0.0249	-0.0302	0.900	8.01	2.021	0.0391	0.0157	-0.0634
1.201	4.00	0.931	0.0451	0.0274	-0.0656	0.901	8.00	4.217	0.0404	0.0160	-0.0653
1.201	5.98	0.939	0.0693	0.0314	-0.0987	0.900	8.00	7.980	0.0407	0.0150	-0.0657
1.201	8.01	0.916	0.0821	0.0374	-0.1163	0.901	-0.01	1.044	-0.0023	0.0111	0.0014
1.204	0.02	0.928	-0.0087	0.0243	0.0071	0.848	0.01	1.052	0.0059	0.0104	-0.0094
1.197	0.00	2.019	-0.0094	0.0233	0.0082	0.849	0.01	1.460	0.0053	0.0089	-0.0084
1.201	0.01	3.523	-0.0090	0.0236	0.0075	0.847	-0.01	4.011	0.0055	0.0091	-0.0085
1.201	-0.01	6.008	-0.0099	0.0224	0.0091	0.797	-0.00	1.050	0.0111	0.0091	-0.0158
1.200	0.01	10.032	-0.0105	0.0197	0.0098	0.802	0.01	3.913	0.0101	0.0081	-0.0144
1.202	3.99	0.918	0.0449	0.0275	-0.0661	0.598	0.01	1.031	0.0115	0.0083	-0.0163
1.200	4.00	6.005	0.0431	0.0254	-0.0629	0.602	-1.99	1.032	0.0003	0.0083	-0.0008
1.201	-0.02	0.918	-0.0102	0.0244	0.0087	0.603	-0.01	1.032	0.0119	0.0082	-0.0167
1.150	-0.01	0.936	-0.0099	0.0256	0.0078	0.600	1.99	1.030	0.0234	0.0089	-0.0327
1.148	0.00	5.593	-0.0110	0.0245	0.0095	0.598	4.01	1.030	0.0374	0.0103	-0.0523
1.150	-0.00	0.935	-0.0100	0.0256	0.0081	0.598	5.99	1.030	0.0519	0.0128	-0.0735
0.000	-0.05	1.001	-0.0007	-0.0001	0.0007	0.597	7.99	1.031	0.0671	0.0163	-0.0963
0.940	-0.00	1.051	-0.0037	0.0115	0.0025	0.602	9.99	1.032	0.0808	0.0209	-0.1177
0.937	0.01	4.304	-0.0032	0.0105	0.0006	0.602	-0.02	1.033	0.0122	0.0084	-0.0169
0.901	-0.02	1.051	-0.0008	0.0115	-0.0006	0.601	-0.00	2.013	0.0106	0.0074	-0.0145
0.901	-0.03	1.052	-0.0005	0.0115	-0.0008	0.601	-0.00	3.395	0.0095	0.0075	-0.0133
0.900	0.01	1.052	-0.0002	0.0116	-0.0012	0.601	-0.01	3.987	0.0095	0.0074	-0.0133
0.897	2.00	1.050	0.0056	0.0117	-0.0096	0.602	-0.00	6.025	0.0083	0.0069	-0.0120
0.899	4.01	1.037	0.0099	0.0122	-0.0177	0.601	0.00	8.018	0.0075	0.0064	-0.0111
0.899	6.00	1.040	0.0207	0.013e	-0.0354	0.599	3.99	1.029	0.0350	0.0101	-0.0494
0.898	8.00	1.062	0.0416	0.0175	-0.0666	0.601	4.02	3.405	0.0340	0.0095	-0.0478
0.897	10.01	1.061	0.0605	0.0224	-0.0934	0.601	8.00	1.030	0.0659	0.0161	-0.0949
0.900	-0.01	1.052	-0.0008	0.0113	-0.0004	0.601	7.99	1.030	0.0661	0.0162	-0.0950
0.901	-0.00	2.011	-0.0019	0.0100	0.0002	0.599	8.01	2.008	0.0658	0.0152	-0.0942
0.899	-0.00	3.508	-0.0013	0.0103	-0.0008	0.602	8.00	3.403	0.0653	0.0153	-0.0937
0.898	0.00	4.212	-0.0011	0.0101	-0.0010	0.601	8.00	7.998	0.0647	0.0142	-0.0932
0.900	0.00	6.005	-0.0012	0.0098	-0.0012	0.600	0.04	1.031	0.0112	0.0085	-0.0159
0.897	-0.00	8.009	-0.0009	0.0090	-0.0016						

TABLE V.- BASIC FORCE AND MOMENT DATA FOR CONFIGURATION WITH
HORIZONTAL TAILS AFT AND VERTICAL TAILS AFT

(a) $c_{r,vt} = 24.38$ cm; symmetrical vertical-tail airfoil;
 $\phi_t = 0^\circ$; $\phi_t = 0^\circ$; basic interfairing

M	α , deg	NPR	C_L	C_D	C_m	M	α , deg	NPR	C_L	C_D	C_m
1.203	0.00	0.883	-0.0155	0.0239	0.0211	0.899	7.99	4.196	0.0370	0.0140	-0.0626
1.200	-2.00	0.894	-0.0391	0.0256	0.0524	0.901	8.00	6.005	0.0376	0.0136	-0.0636
1.203	-0.02	0.881	-0.0157	0.0240	0.0213	0.897	8.00	7.973	0.0398	0.0131	-0.0667
1.202	1.99	0.871	0.0098	0.0243	-0.0134	0.901	-0.01	1.061	-0.0027	0.0104	-0.0005
1.200	4.02	0.862	0.0357	0.0263	-0.0486	0.850	0.01	1.063	0.0028	0.0101	-0.0078
1.199	5.98	0.855	0.0535	0.0290	-0.0730	0.851	0.00	2.004	0.0024	0.0086	-0.0074
1.202	8.00	0.838	0.0746	0.0342	-0.1040	0.851	0.02	3.477	0.0031	0.0088	-0.0086
1.199	-0.01	0.879	-0.0168	0.0242	0.0225	0.852	0.02	3.499	0.0026	0.0088	-0.0079
1.200	-0.01	2.051	-0.0169	0.0235	0.0229	0.852	-0.00	4.006	0.0028	0.0087	-0.0080
1.200	0.01	3.500	-0.0161	0.0241	0.0217	0.854	-0.01	8.046	0.0020	0.0076	-0.0074
1.201	0.01	5.982	-0.0162	0.0227	0.0220	0.853	-0.02	8.026	0.0020	0.0075	-0.0074
1.203	-0.00	10.054	-0.0158	0.0204	0.0212	0.852	-0.02	1.061	0.0023	0.0098	-0.0073
1.200	4.01	0.855	0.0354	0.0261	-0.0483	0.800	-0.01	1.060	0.0047	0.0095	-0.0103
1.202	4.01	1.993	0.0351	0.0254	-0.0477	0.798	-0.02	1.059	0.0047	0.0096	-0.0103
1.203	4.01	3.484	0.0351	0.0260	-0.0480	0.799	0.00	1.997	0.0042	0.0084	-0.0097
1.200	4.01	6.000	0.0347	0.0248	-0.0471	0.805	-0.02	3.908	0.0045	0.0086	-0.0102
1.202	3.99	10.010	0.0341	0.0225	-0.0464	0.799	0.00	4.992	0.0046	0.0083	-0.0104
1.202	0.01	0.873	-0.0166	0.0238	0.0225	0.799	0.01	8.004	0.0040	0.0074	-0.0099
1.151	-0.01	0.889	-0.0152	0.0253	0.0202	0.799	0.01	1.056	0.0047	0.0097	-0.0104
1.152	0.01	2.083	-0.0150	0.0253	0.0200	0.600	-0.01	1.032	0.0080	0.0090	-0.0140
1.151	0.01	3.479	-0.0150	0.0258	0.0200	0.600	-2.01	1.034	-0.0033	0.0093	0.0019
1.150	-0.00	5.591	-0.0150	0.0250	0.0197	0.600	0.02	1.033	0.0083	0.0091	-0.0144
1.150	0.03	9.916	-0.0144	0.0222	0.0186	0.600	2.00	1.032	0.0199	0.0095	-0.0310
1.150	0.01	0.886	-0.0152	0.0252	0.0204	0.600	4.00	1.031	0.0316	0.0106	-0.0480
0.939	0.00	1.079	0.0051	0.0117	-0.0136	0.599	6.02	1.030	0.0461	0.0128	-0.0696
0.940	-0.00	2.008	0.0065	0.0098	-0.0160	0.600	8.00	1.029	0.0601	0.0159	-0.0906
0.937	0.01	3.510	0.0064	0.0101	-0.0159	0.600	10.00	1.030	0.0762	0.0205	-0.1153
0.938	0.01	4.313	0.0061	0.0101	-0.0156	0.602	-0.02	1.033	0.0077	0.0092	-0.0135
0.941	-0.02	7.996	0.0083	0.0087	-0.0164	0.598	-0.05	1.034	0.0144	0.0091	-0.0229
0.939	-0.01	1.078	0.0049	0.0115	-0.0137	0.598	-2.01	1.035	0.0024	0.0091	-0.0059
0.899	-0.02	1.064	-0.0010	0.0103	-0.0032	0.602	-0.02	1.035	0.0141	0.0090	-0.0225
0.900	-2.00	1.071	-0.0047	0.0104	0.0026	0.598	2.02	1.034	0.0260	0.0095	-0.0395
0.898	-0.01	1.065	-0.0007	0.0103	-0.0039	0.599	3.99	1.035	0.0387	0.0107	-0.0578
0.901	2.00	1.060	0.0041	0.0103	-0.0115	0.601	5.99	1.035	0.0525	0.0130	-0.0785
0.899	4.01	1.061	0.0112	0.0109	-0.0240	0.599	7.95	1.034	0.0666	0.0162	-0.0996
0.899	6.01	1.056	0.0196	0.0121	-0.0378	0.601	9.98	1.036	0.0817	0.0209	-0.1231
0.898	8.02	1.050	0.0367	0.0150	-0.0623	0.600	-0.01	1.035	0.0131	0.0090	-0.0215
0.900	10.00	1.054	0.0592	0.0202	-0.0930	0.601	-0.01	2.036	0.0128	0.0078	-0.0208
0.901	-0.00	1.065	-0.0019	0.0103	-0.0021	0.600	-0.02	3.414	0.0125	0.0079	-0.0204
0.899	-0.00	2.005	-0.0013	0.0088	-0.0033	0.600	-0.00	3.982	0.0118	0.0078	-0.0197
0.899	0.00	3.515	-0.0006	0.0090	-0.0043	0.601	-0.01	6.005	0.0113	0.0073	-0.0191
0.897	0.01	4.197	-0.0004	0.0089	-0.0047	0.602	-0.01	8.049	0.0107	0.0067	-0.0185
0.898	-0.03	5.991	-0.0004	0.0084	-0.0048	0.600	3.97	1.034	0.0373	0.0104	-0.0559
0.898	-0.02	6.003	-0.0005	0.0077	-0.0050	0.599	3.98	2.033	0.0363	0.0095	-0.0543
0.904	4.02	1.057	0.0086	0.0107	-0.0204	0.600	4.00	3.400	0.0368	0.0098	-0.0549
0.900	3.99	1.980	0.0105	0.0094	-0.0228	0.600	4.00	4.016	0.0370	0.0097	-0.0552
0.897	4.00	3.513	0.0113	0.0097	-0.0239	0.600	4.00	5.994	0.0368	0.0093	-0.0550
0.894	4.00	4.208	0.0123	0.0097	-0.0293	0.601	3.98	6.017	0.0360	0.0086	-0.0540
0.901	4.01	5.984	0.0113	0.0093	-0.0247	0.600	8.02	1.033	0.0664	0.0162	-0.0992
0.901	4.02	8.038	0.0115	0.0086	-0.0250	0.599	7.99	2.019	0.0661	0.0152	-0.0985
0.900	7.99	1.048	0.0354	0.0148	-0.0604	0.599	8.00	3.400	0.0664	0.0155	-0.0990
0.899	8.00	1.999	0.0371	0.0137	-0.0625	0.602	8.00	4.021	0.0666	0.0154	-0.0993
0.900	8.00	3.501	0.0360	0.0139	-0.0612	0.601	8.00	6.000	0.0665	0.0149	-0.0994
						0.601	7.99	8.027	0.0662	0.0143	-0.0991
						0.602	-0.07	1.034	0.0138	0.0089	-0.0218

TABLE V.- Continued

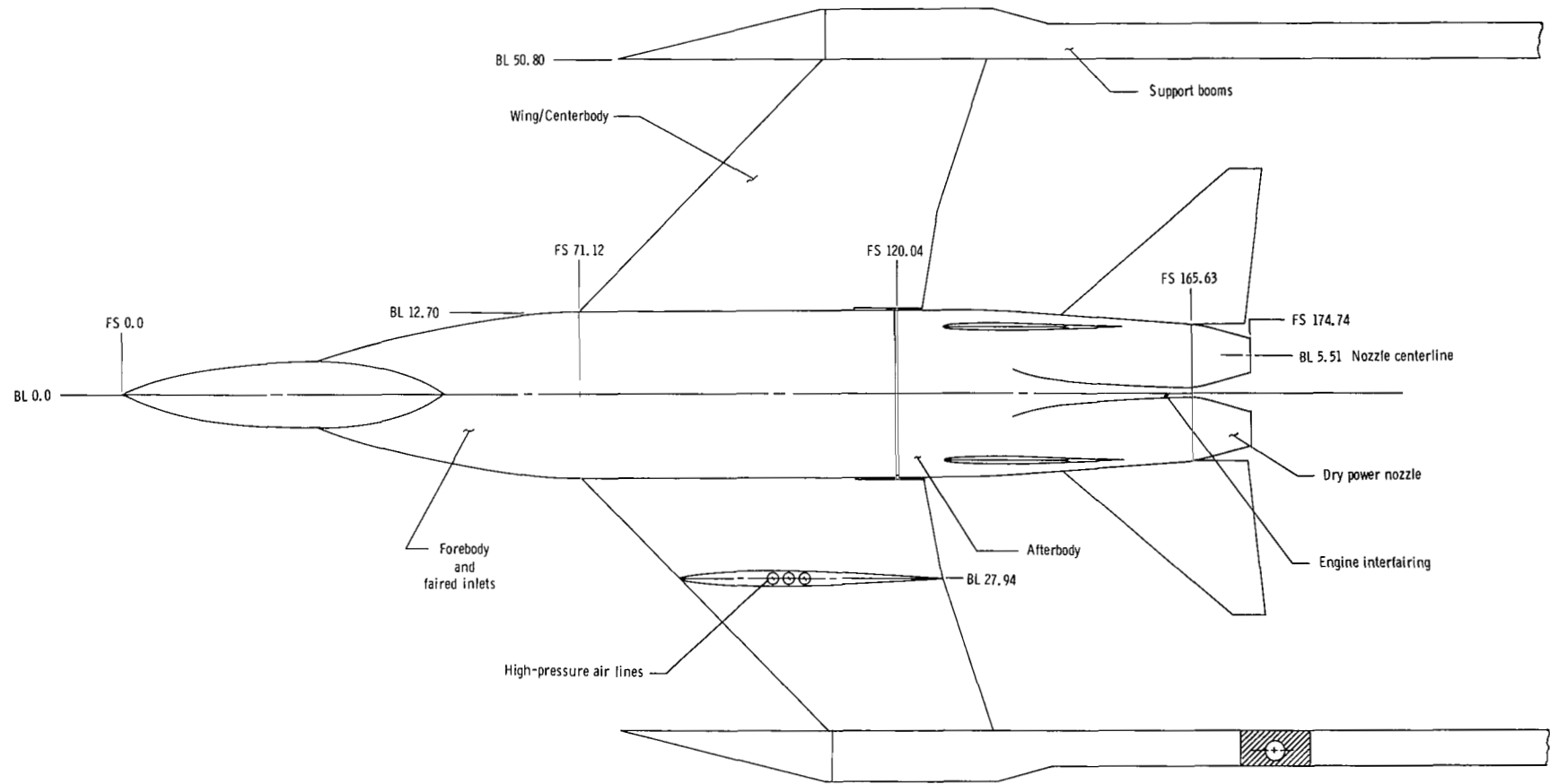
(b) $c_{r,vt} = 28.19$ cm; symmetrical vertical-tail airfoil;
 $\phi_t = 0^\circ$; $\phi_t = 0^\circ$; basic interfairing

M	α , deg	NPR	C_L	C_D	C_m	M	α , deg	NPR	C_L	C_D	C_m
1.198	-0.01	0.874	-0.0141	0.0239	0.0187	0.900	3.98	3.515	0.0173	0.0102	-0.0333
1.200	-2.03	0.883	-0.0377	0.0293	0.0501	0.900	3.99	4.226	0.0175	0.0101	-0.0337
1.202	-0.02	0.867	-0.0150	0.0238	0.0197	0.899	3.96	5.993	0.0176	0.0096	-0.0342
1.201	1.99	0.854	0.0090	0.0245	-0.0130	0.900	3.97	6.001	0.0174	0.0089	-0.0340
1.201	3.98	0.854	0.0333	0.0264	-0.0462	0.903	7.98	1.044	0.0434	0.0158	-0.0728
1.200	5.98	0.851	0.0532	0.0293	-0.0739	0.898	7.99	2.030	0.0463	0.0147	-0.0762
1.195	7.98	0.832	0.0729	0.0342	-0.1026	0.899	7.97	3.520	0.0469	0.0150	-0.0774
1.202	7.99	0.832	0.0729	0.0343	-0.1033	0.900	7.99	4.226	0.0468	0.0149	-0.0773
1.201	-0.01	0.859	-0.0160	0.0242	0.0211	0.900	7.98	6.006	0.0481	0.0145	-0.0792
1.200	-0.00	1.995	-0.0161	0.0235	0.0215	0.900	7.98	7.981	0.0493	0.0139	-0.0807
1.201	0.01	3.491	-0.0160	0.0241	0.0212	0.901	-0.04	1.061	0.0034	0.0101	-0.0102
1.202	0.01	5.975	-0.0154	0.0227	0.0205	0.850	-0.01	1.060	0.0076	0.0099	-0.0152
1.201	-0.03	9.985	-0.0154	0.0204	0.0204	0.849	0.00	2.006	0.0075	0.0084	-0.0152
1.200	3.99	0.845	0.0343	0.0266	-0.0473	0.849	-0.01	3.479	0.0076	0.0086	-0.0155
1.200	3.97	2.022	0.0336	0.0256	-0.0459	0.853	-0.01	4.007	0.0073	0.0086	-0.0153
1.200	3.97	3.552	0.0338	0.0262	-0.0465	0.850	-0.01	8.026	0.0072	0.0073	-0.0152
1.200	3.98	6.008	0.0336	0.0249	-0.0460	0.850	-0.03	1.059	0.0071	0.0096	-0.0146
1.202	3.99	10.063	0.0343	0.0225	-0.0470	0.801	-0.03	1.056	0.0092	0.0095	-0.0171
1.201	3.98	10.012	0.0339	0.0225	-0.0465	0.800	-0.04	1.999	0.0084	0.0082	-0.0159
1.200	-0.01	0.857	-0.0153	0.0240	0.0206	0.800	-0.02	3.887	0.0086	0.0084	-0.0164
1.149	-0.02	0.870	-0.0132	0.0261	0.0167	0.801	-0.02	5.018	0.0084	0.0081	-0.0163
1.152	-0.01	2.004	-0.0127	0.0255	0.0164	0.801	-0.00	8.002	0.0079	0.0071	-0.0158
1.149	-0.01	3.487	-0.0127	0.0262	0.0163	0.801	-0.02	1.054	0.0089	0.0095	-0.0167
1.152	0.00	5.632	-0.0127	0.0252	0.0163	0.598	-0.03	1.029	0.0129	0.0088	-0.0208
1.150	-0.02	9.977	-0.0123	0.0223	0.0152	0.599	-2.01	1.031	0.0018	0.0089	-0.0052
1.151	-0.02	0.869	-0.0128	0.0260	0.0166	0.602	-0.03	1.030	0.0133	0.0089	-0.0213
0.941	-0.02	1.076	0.0030	0.0113	-0.0117	0.602	2.00	1.029	0.0244	0.0095	-0.0372
0.941	-0.02	1.999	0.0034	0.0092	-0.0124	0.602	3.97	1.029	0.0368	0.0108	-0.0552
0.940	-0.01	3.482	0.0034	0.0096	-0.0125	0.601	5.99	1.028	0.0513	0.0132	-0.0770
0.943	-0.02	4.309	0.0032	0.0096	-0.0123	0.600	7.98	1.027	0.0658	0.0164	-0.0992
0.940	-0.01	7.982	0.0036	0.0081	-0.0131	0.599	16.01	1.028	0.0819	0.0213	-0.1243
0.939	-0.01	1.074	0.0027	0.0109	-0.0112	0.601	-0.01	1.031	0.0133	0.0091	-0.0212
0.902	-0.01	1.071	0.0061	0.0104	-0.0148	0.601	-0.00	2.018	0.0125	0.0080	-0.0202
0.901	-2.03	1.077	0.0019	0.0104	-0.0082	0.600	-0.00	3.408	0.0125	0.0082	-0.0204
0.901	-0.02	1.071	0.0064	0.0104	-0.0151	0.601	-0.01	4.015	0.0117	0.0081	-0.0194
0.899	2.00	1.064	0.0117	0.0106	-0.0231	0.600	-0.01	6.045	0.0110	0.0075	-0.0187
0.901	3.97	1.063	0.0185	0.0116	-0.0356	0.601	-0.01	7.985	0.0108	0.0069	-0.0185
0.899	6.00	1.060	0.0295	0.0133	-0.0529	0.600	3.98	1.028	0.0358	0.0105	-0.0539
0.898	7.98	1.046	0.0477	0.0165	-0.0785	0.599	3.99	1.996	0.0351	0.0097	-0.0528
0.898	9.98	1.052	0.0680	0.0216	-0.1049	0.600	3.99	3.403	0.0355	0.0099	-0.0534
0.900	-0.01	1.063	0.0050	0.0105	-0.0126	0.599	3.99	4.008	0.0351	0.0099	-0.0531
0.900	-0.03	2.024	0.0053	0.0088	-0.0132	0.598	3.98	6.003	0.0355	0.0095	-0.0537
0.901	-0.01	3.500	0.0050	0.0091	-0.0131	0.599	3.98	7.989	0.0347	0.0088	-0.0528
0.903	-0.03	4.218	0.0052	0.0089	-0.0133	0.598	7.99	1.025	0.0658	0.0164	-0.0993
0.903	-0.03	6.015	0.0054	0.0084	-0.0137	0.599	7.99	1.985	0.0660	0.0154	-0.0993
0.900	-0.03	7.972	0.0052	0.0076	-0.0137	0.598	7.99	3.383	0.0665	0.0158	-0.1001
0.897	3.96	1.052	0.0167	0.0113	-0.0321	0.600	8.00	3.975	0.0670	0.0158	-0.1010
0.902	3.98	2.008	0.0165	0.0098	-0.0320	0.600	7.97	6.001	0.0666	0.0152	-0.1004
						0.600	7.99	8.031	0.0667	0.0146	-0.1009
						0.602	-0.00	1.029	0.0138	0.0092	-0.0217

TABLE V.- Concluded

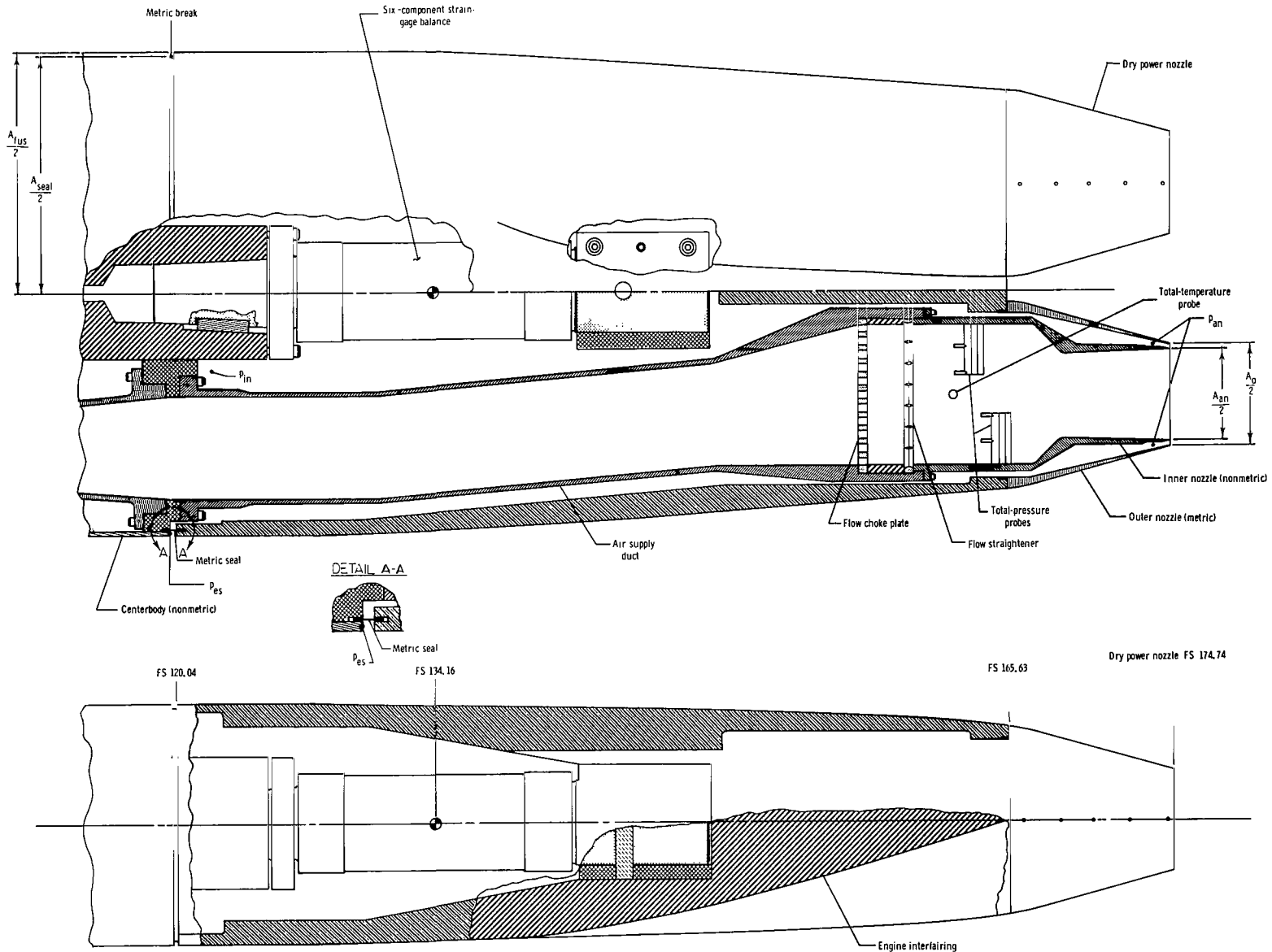
(c) $c_{r,vt} = 24.38$ cm; symmetrical vertical-tail airfoil;
 $\psi_t = 0^\circ$; $\phi_t = 0^\circ$; alternate interfairing

M	α , deg	NPR	C_L	C_D	C_m	M	α , deg	NPR	C_L	C_D	C_m
1.198	-0.01	0.871	-0.0165	0.0258	0.0226	0.897	4.00	1.047	0.0066	0.0111	-0.0171
1.201	-2.01	0.881	-0.0390	0.0272	0.0524	0.896	4.01	4.180	0.0071	0.0102	-0.0174
1.199	-0.01	0.869	-0.0165	0.0259	0.0224	0.898	7.98	1.052	0.0336	0.0154	-0.0574
1.199	2.00	0.862	0.0077	0.0262	-0.0104	0.899	8.00	2.002	0.0344	0.0139	-0.0585
1.199	3.99	0.858	0.0313	0.0281	-0.0424	0.899	8.01	4.169	0.0350	0.0143	-0.0598
1.201	6.01	0.851	0.0565	0.0315	-0.0776	0.899	7.98	7.999	0.0358	0.0132	-0.0609
1.204	8.00	0.840	0.0714	0.0358	-0.0995	0.903	-0.03	1.054	-0.0050	0.0105	0.0022
1.200	0.01	0.871	-0.0175	0.0261	0.0235	0.850	-0.00	1.054	0.0001	0.0102	-0.0044
1.200	-0.00	2.002	-0.0173	0.0251	0.0232	0.852	-0.00	3.954	-0.0001	0.0092	-0.0041
1.200	-0.01	3.523	-0.0173	0.0256	0.0231	0.801	-0.02	1.052	0.0032	0.0100	-0.0083
1.201	0.00	6.008	-0.0169	0.0243	0.0226	0.801	0.01	3.885	0.0026	0.0090	-0.0074
1.199	0.03	9.944	-0.0170	0.0220	0.0229	0.599	0.01	1.030	0.0068	0.0092	-0.0124
1.201	4.02	0.854	0.0324	0.0281	-0.0444	0.601	-1.98	1.031	-0.0038	0.0093	0.0026
1.201	3.96	5.978	0.0313	0.0262	-0.0429	0.602	0.00	1.031	0.0068	0.0091	-0.0125
1.200	0.00	0.865	-0.0174	0.0258	0.0235	0.600	2.00	1.029	0.0179	0.0095	-0.0281
1.150	-0.00	0.881	-0.0165	0.0277	0.0218	0.600	4.01	1.030	0.0296	0.0107	-0.0453
1.151	0.01	5.609	-0.0162	0.0266	0.0213	0.599	6.01	1.030	0.0438	0.0127	-0.0663
1.148	-0.00	0.879	-0.0163	0.0277	0.0218	0.600	8.01	1.030	0.0575	0.0158	-0.0873
0.940	-0.00	1.066	-0.0073	0.0114	0.0044	0.599	9.99	1.031	0.0708	0.0197	-0.1080
0.942	-0.00	4.301	-0.0071	0.0102	0.0038	0.600	8.70	1.030	0.0614	0.0170	-0.0931
0.900	-0.02	1.054	-0.0036	0.0104	0.0001	0.598	-0.02	1.031	0.0073	0.0094	-0.0127
0.898	-1.99	1.041	-0.0071	0.0107	0.0060	0.602	0.01	2.009	0.0067	0.0083	-0.0118
0.900	0.00	1.050	-0.0034	0.0105	-0.0001	0.602	0.02	3.406	0.0069	0.0086	-0.0120
0.900	2.00	1.057	0.0011	0.0107	-0.0071	0.602	-0.00	4.009	0.0064	0.0084	-0.0114
0.903	4.03	1.049	0.0065	0.0113	-0.0177	0.602	0.01	6.011	0.0062	0.0079	-0.0113
0.899	5.99	1.054	0.0166	0.0125	-0.0332	0.600	0.01	7.996	0.0057	0.0073	-0.0107
0.898	8.00	1.054	0.0354	0.0156	-0.0603	0.599	3.99	1.028	0.0297	0.0105	-0.0450
0.898	9.99	1.059	0.0568	0.0203	-0.0896	0.599	4.01	3.394	0.0281	0.0098	-0.0430
0.902	-0.02	1.049	-0.0039	0.0106	0.0010	0.601	7.98	1.029	0.0567	0.0155	-0.0862
0.901	-0.00	1.998	-0.0039	0.0093	0.0009	0.601	8.00	2.027	0.0561	0.0146	-0.0852
0.901	-0.00	3.491	-0.0039	0.0097	0.0010	0.598	8.00	3.405	0.0563	0.0150	-0.0858
0.902	0.01	4.177	-0.0041	0.0097	0.0011	0.602	8.00	8.000	0.0581	0.0141	-0.0878
0.899	0.01	6.015	-0.0038	0.0092	0.0006	0.601	0.00	1.030	0.0075	0.0093	-0.0132
0.900	0.00	8.004	-0.0040	0.0084	0.0007						



(a) Twin-tail interference model and wing-tip support system.

Figure 1.- Model sketches. All dimensions are in centimeters unless otherwise noted.



(b) Afterbody.

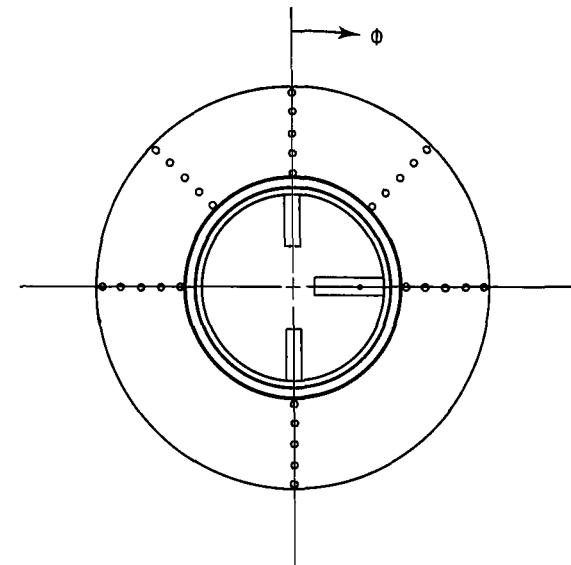
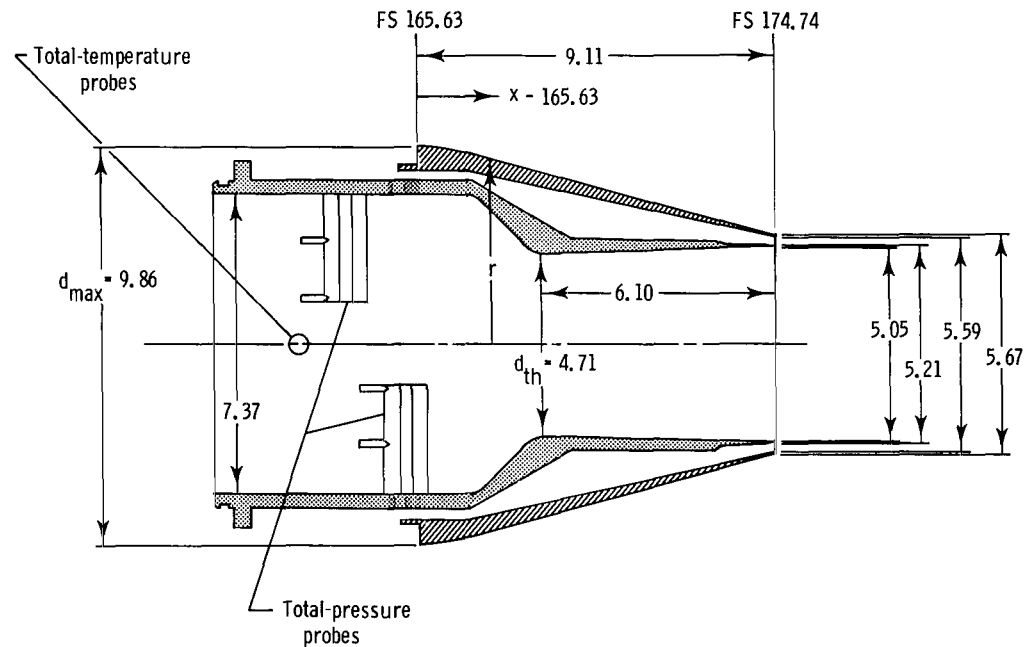
Figure 1.- Continued.

Nozzle External Geometry

x/l	r/r_{\max}
.948	1.000
.949	.996
.951	.991
.952	.984
.954	.975
.955	.963
1.000	.575

External Nozzle Static-Pressure Orifice Locations

ϕ , deg		x/l		Nozzle
0	.	.951	.963	RH
45	↓			LH
90				RH
180				RH
270	↑			LH
315	↓	↓	↓	LH

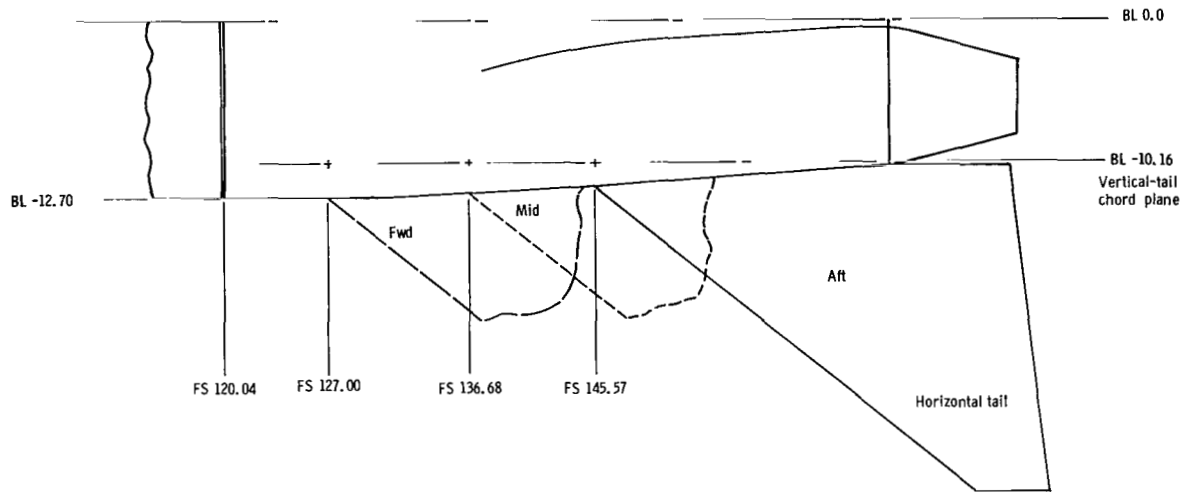


NOTE: All orifices are shown on the left-hand nozzle for simplicity.

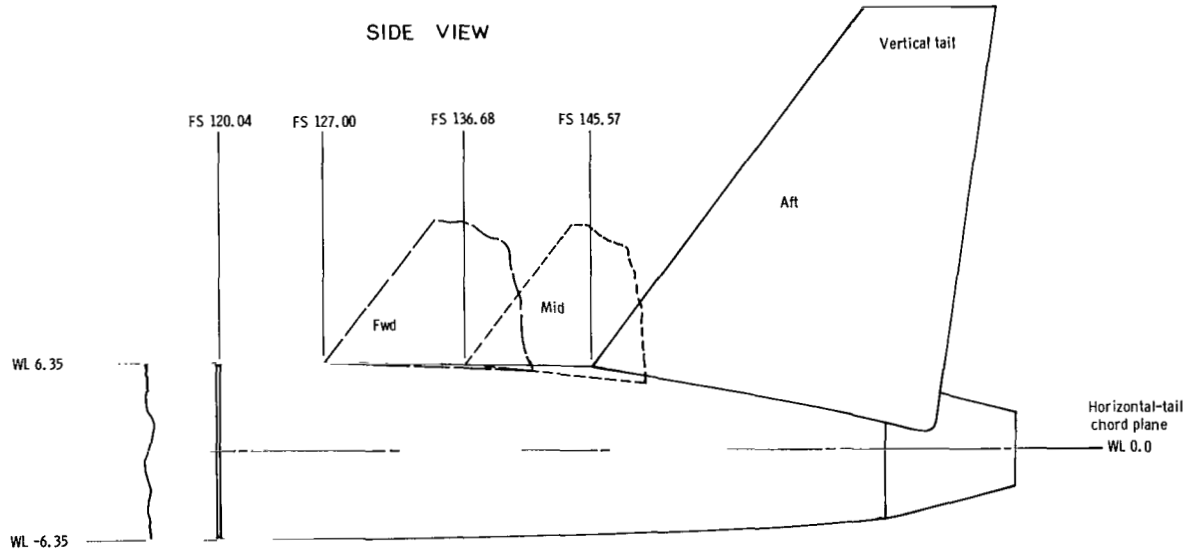
(c) Dry power nozzle.

Figure 1.- Continued.

TOP VIEW

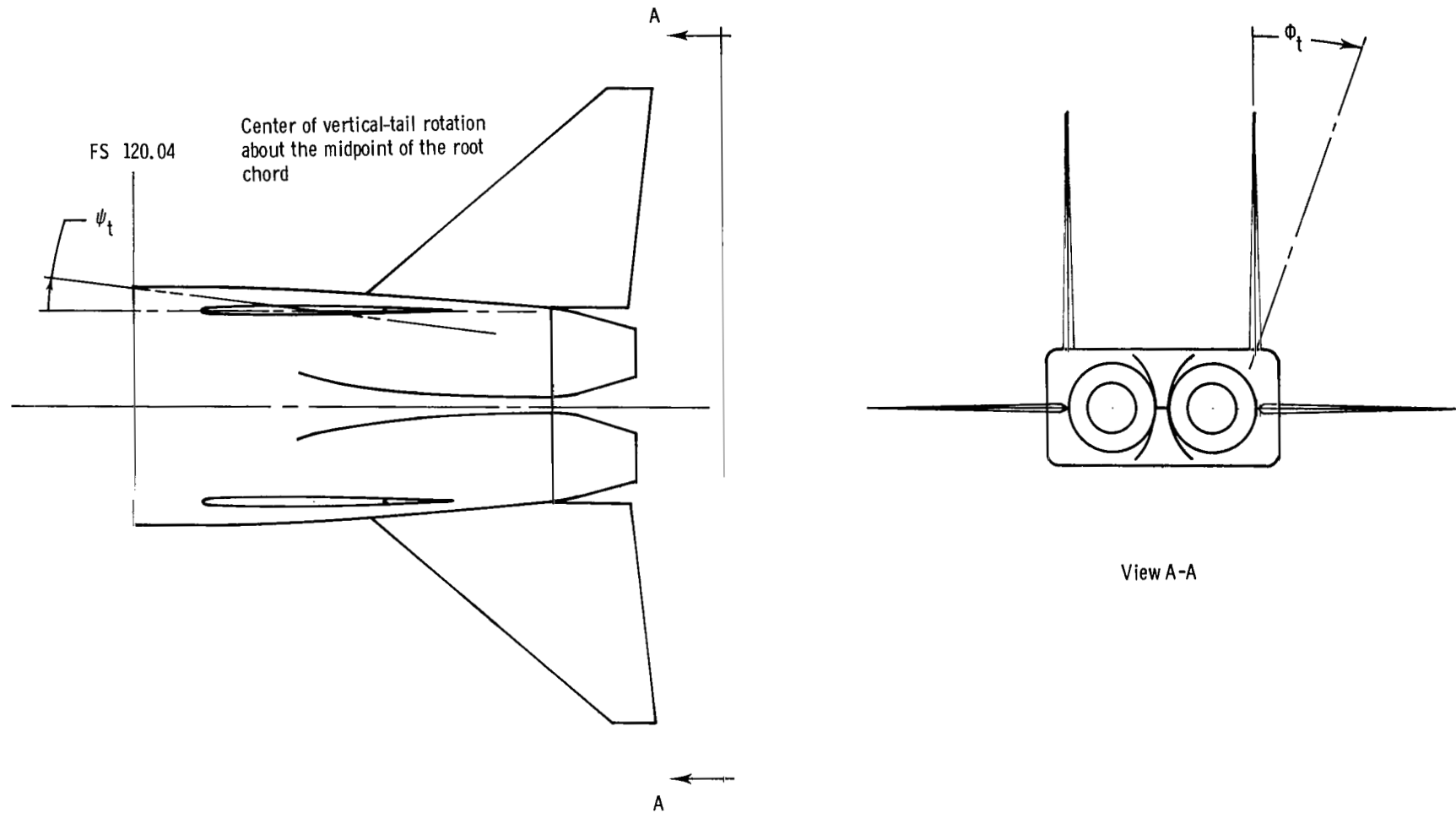


SIDE VIEW



(d) Empennage locations.

Figure 1.- Continued.

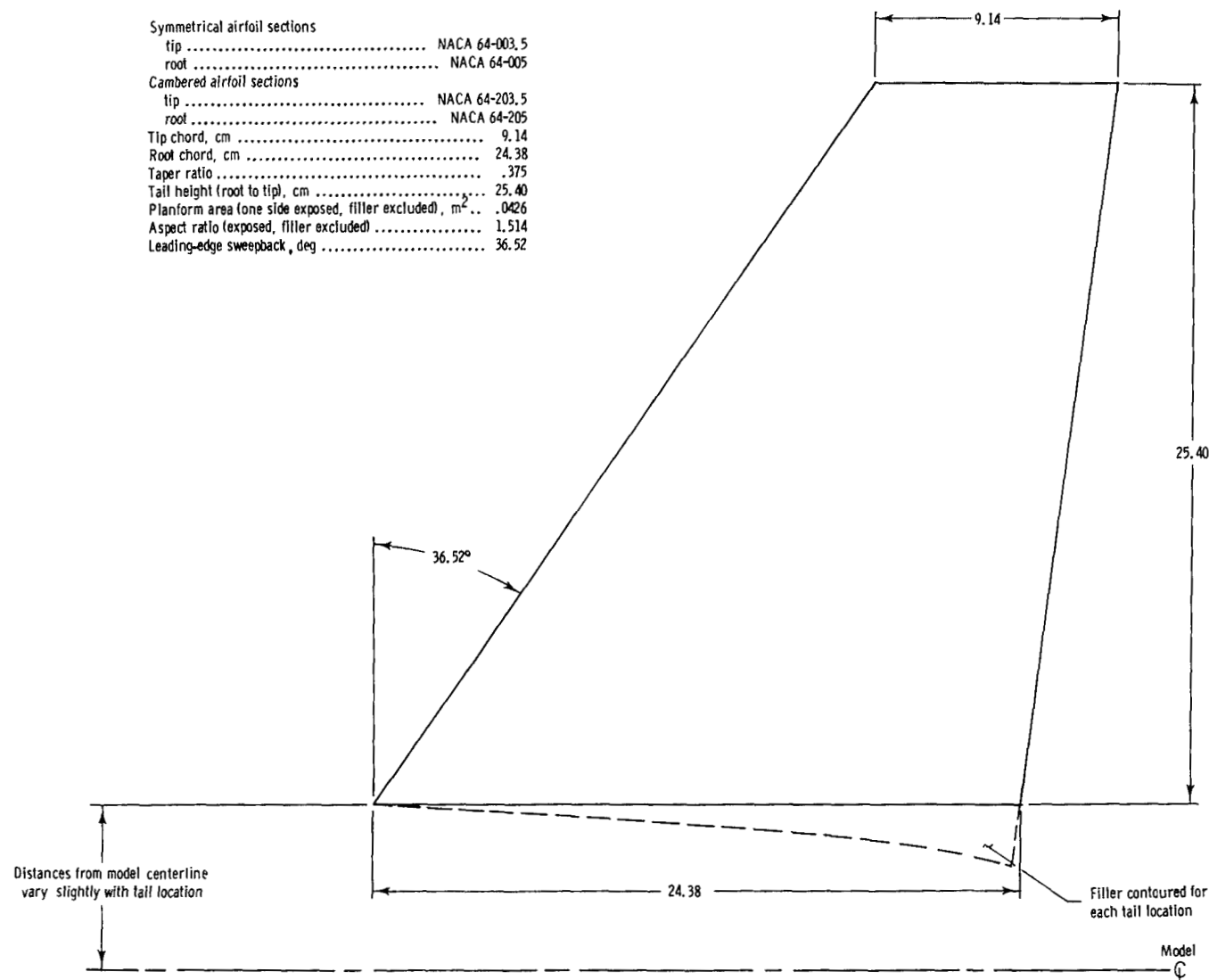


(e) Vertical-tail toe angle and cant angle definition and sign convention.

Figure 1.- Continued.

Symmetrical and Cambered
Vertical-Tail Geometry

Symmetrical airfoil sections	
tip	NACA 64-003.5
root	NACA 64-005
Cambered airfoil sections	
tip	NACA 64-203.5
root	NACA 64-205
Tip chord, cm	9.14
Root chord, cm	24.38
Taper ratio375
Tail height (root to tip), cm	25.40
Planform area (one side exposed, filler excluded), m ² ..	.0426
Aspect ratio (exposed, filler excluded)	1.514
Leading-edge sweepback, deg	36.52



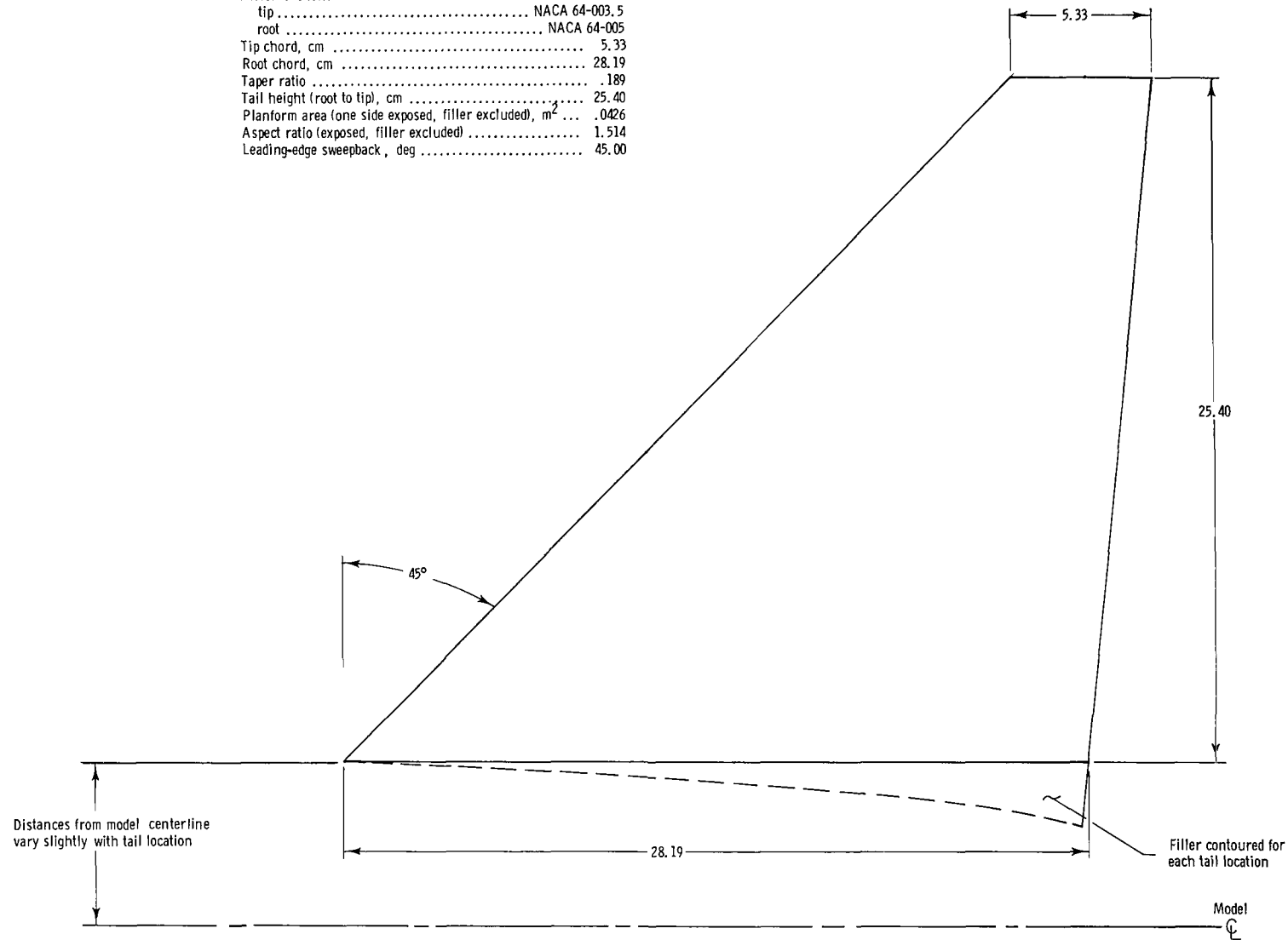
(f) Symmetrical and cambered short-root-chord twin-vertical-tail geometry.

Figure 1.- Continued.

Vertical-Tail Geometry

Airfoil sections

tip	NACA 64-003.5
root	NACA 64-005
Tip chord, cm	5.33
Root chord, cm	28.19
Taper ratio189
Tail height (root to tip), cm	25.40
Planform area (one side exposed, filler excluded), m ²0426
Aspect ratio (exposed, filler excluded)	1.514
Leading-edge sweepback, deg	45.00



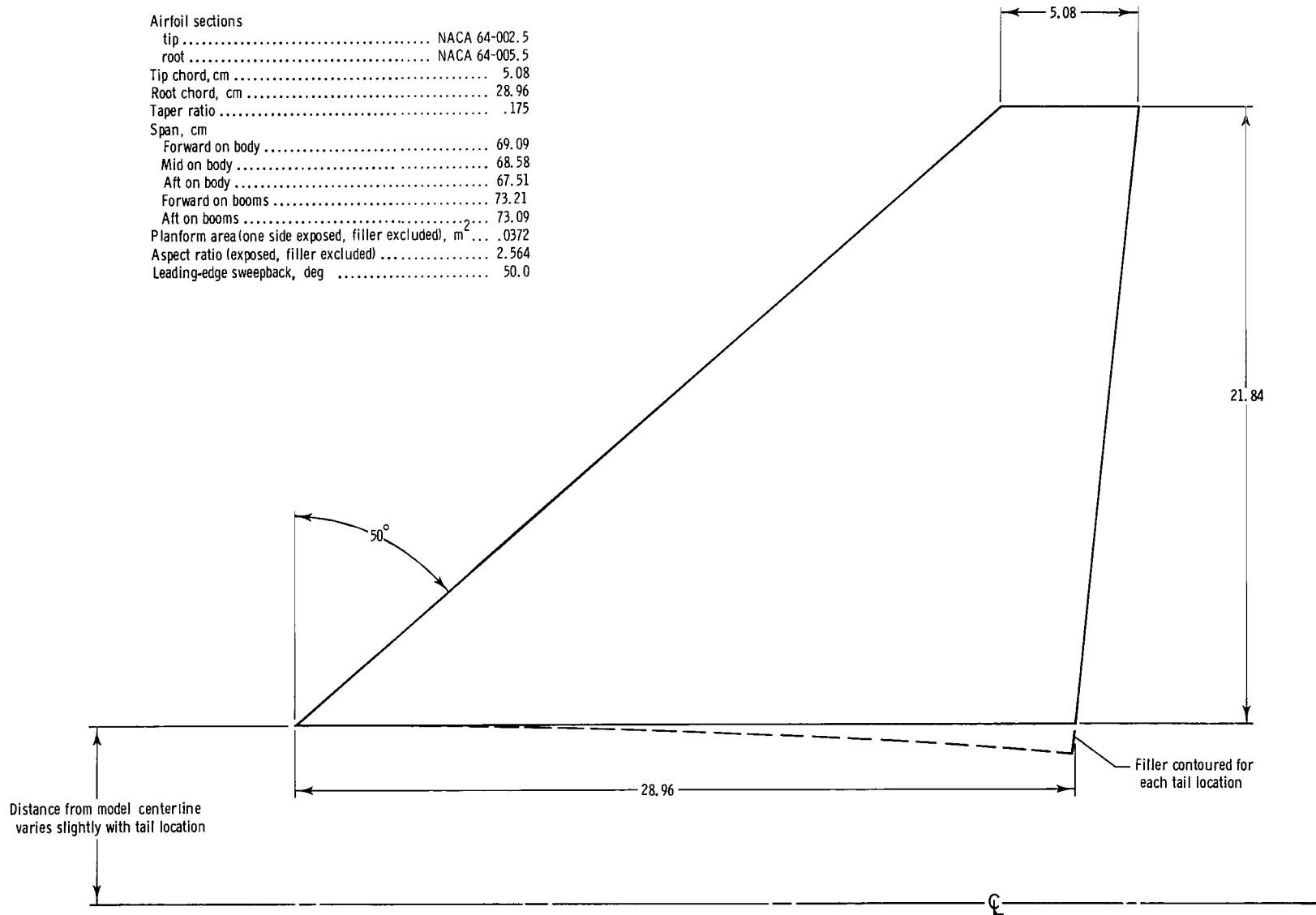
(g) Symmetrical long-root-chord twin-vertical-tail geometry.

Figure 1.- Continued.

Horizontal-Tail Geometry

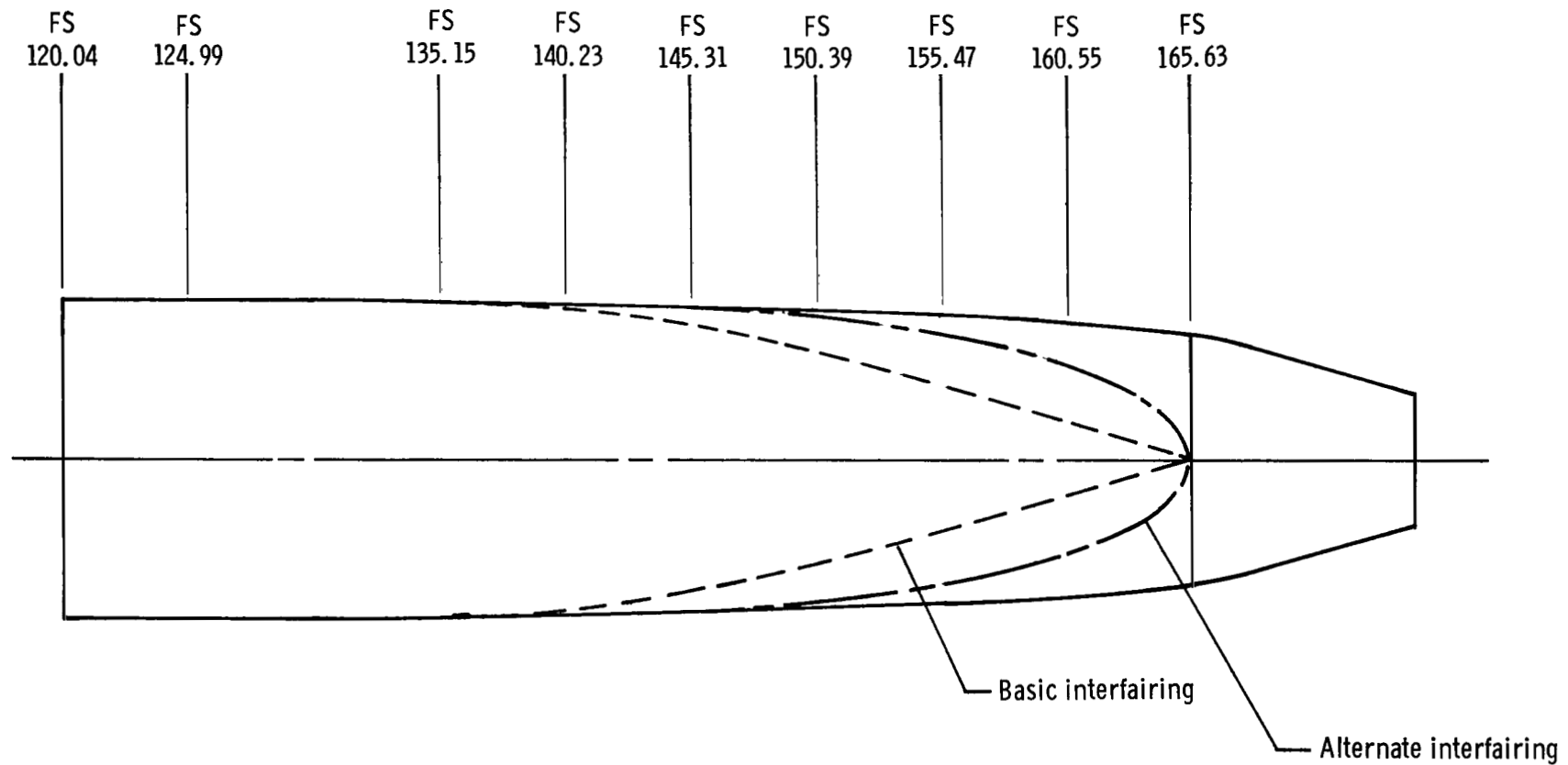
Airfoil sections

tip	NACA 64-002.5
root	NACA 64-005.5
Tip chord, cm	5.08
Root chord, cm	28.96
Taper ratio175
Span, cm	
Forward on body	69.09
Mid on body	68.58
Aft on body	67.51
Forward on booms	73.21
Aft on booms	73.09
Planform area (one side exposed, filler excluded), m ²0372
Aspect ratio (exposed, filler excluded)	2.564
Leading-edge sweepback, deg	50.0



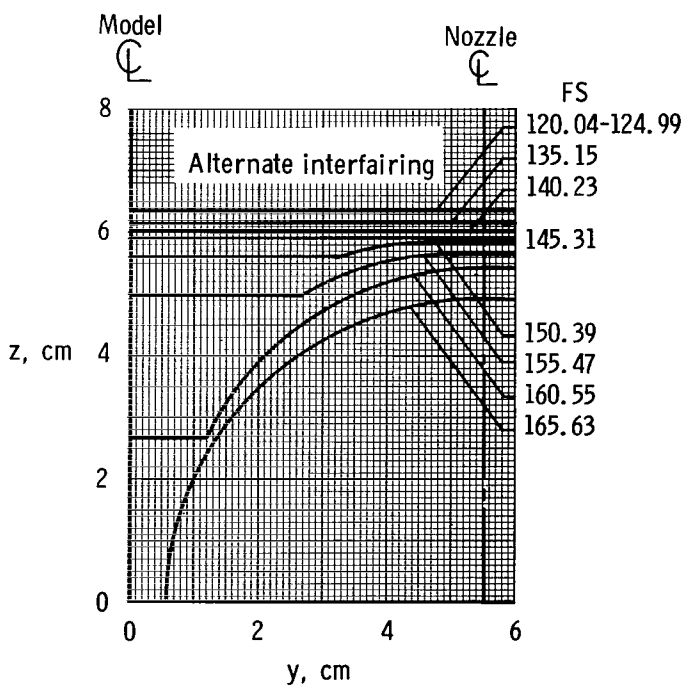
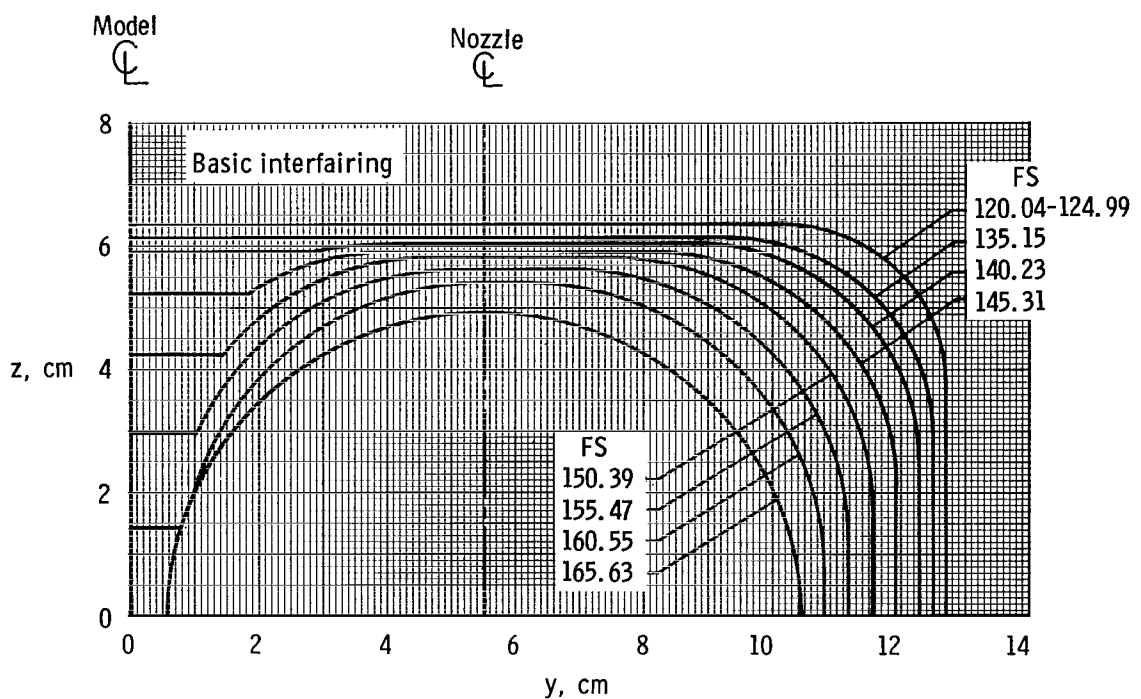
(h) Horizontal-tail geometry.

Figure 1.- Continued.



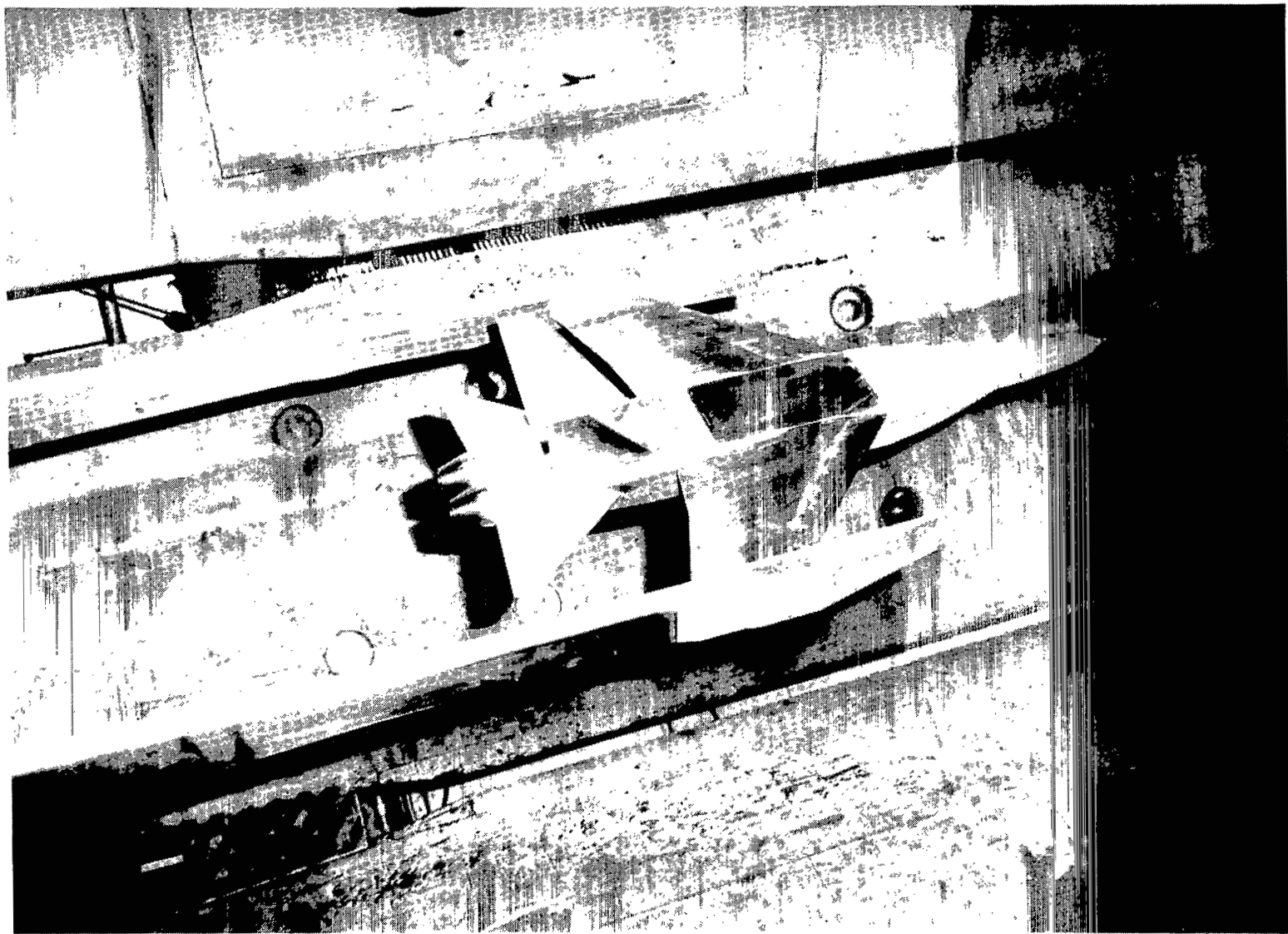
(i) Basic and alternate engine interfairing contours.

Figure 1.- Continued.



(j) Afterbody cross sections. (Note that all cross sections outboard of the nozzle centerline are identical.)

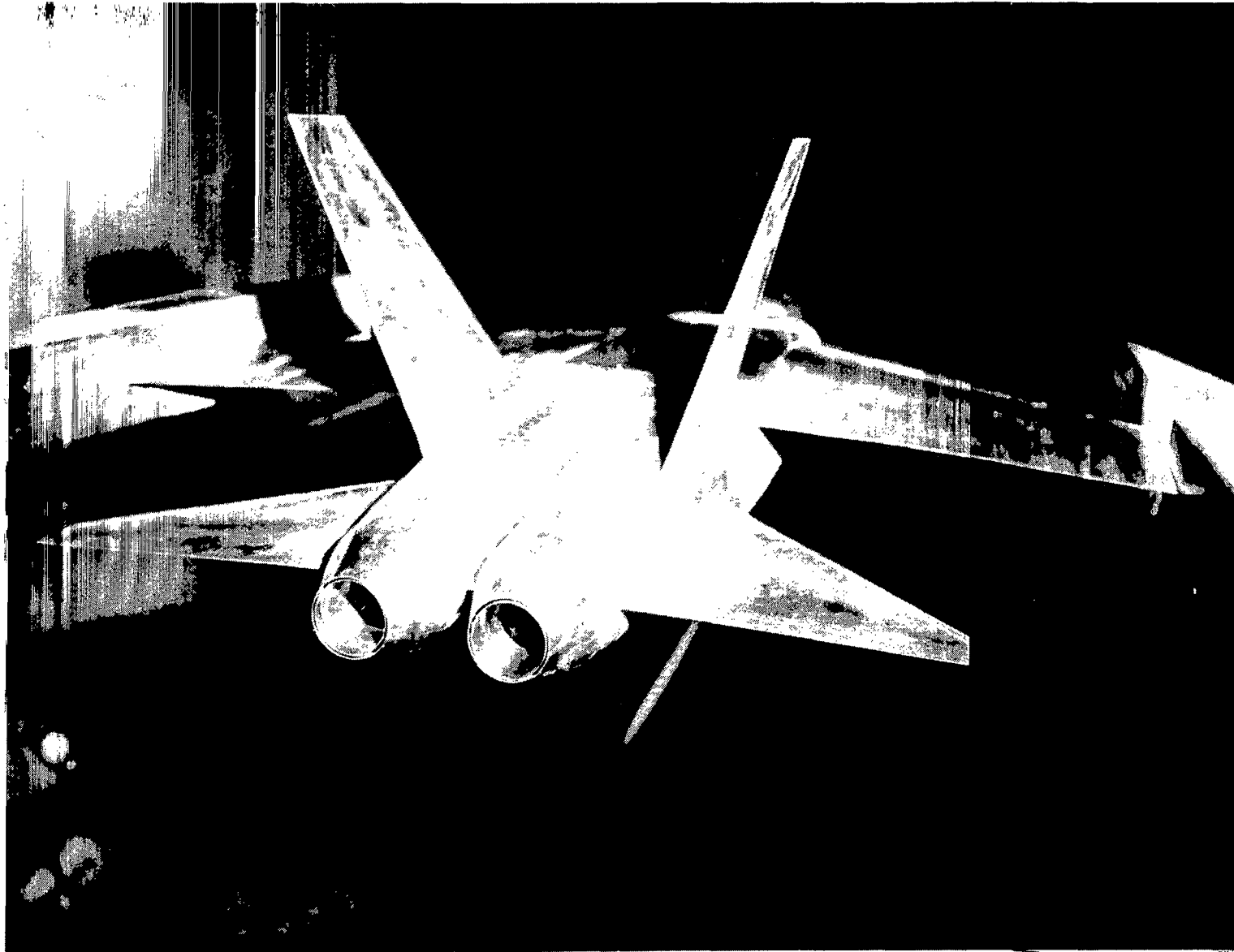
Figure 1.- Concluded.



L-81-6971

(a) Model and wing-tip support system.

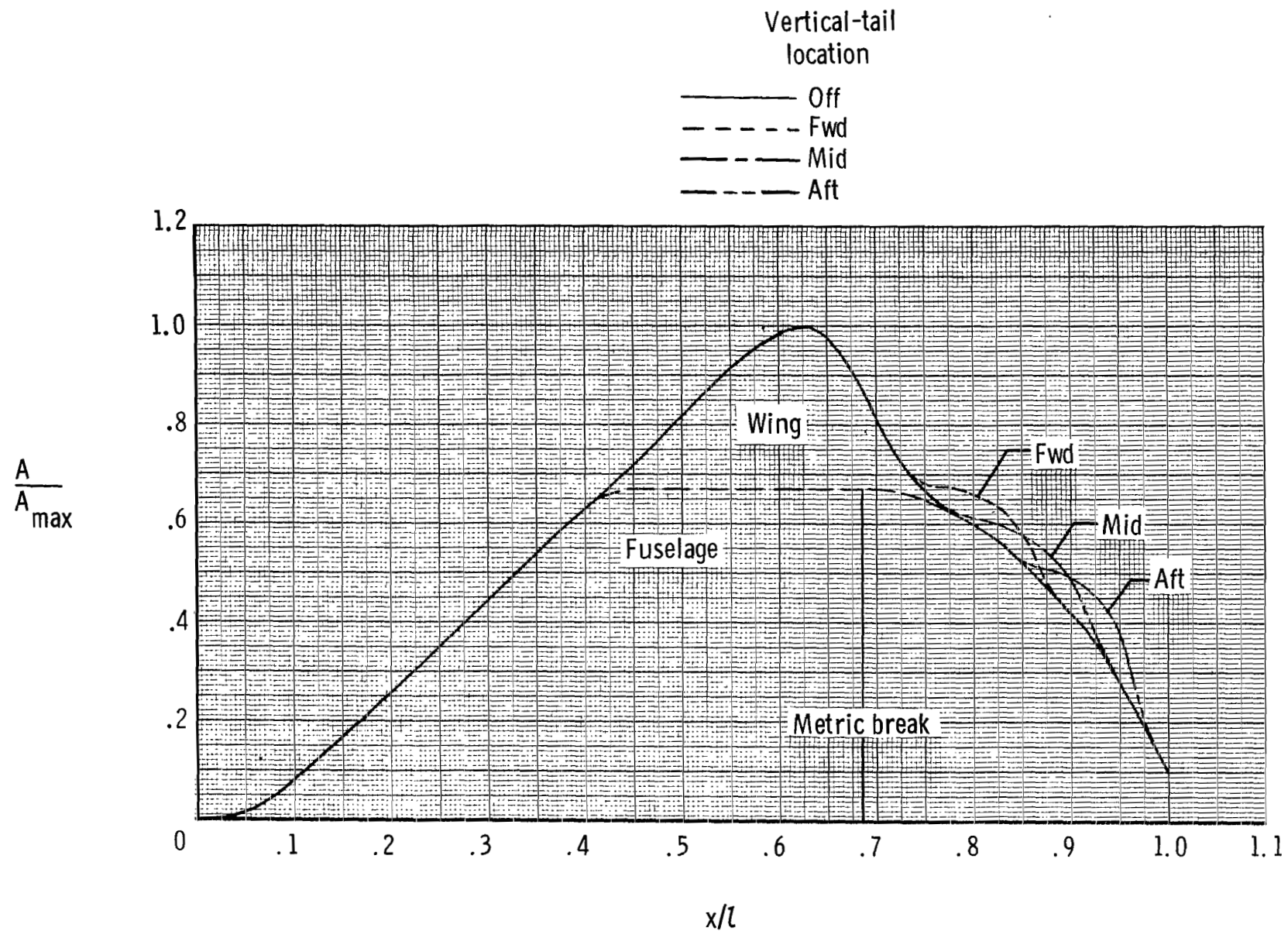
Figure 2.- Photographs of twin-engine tail interference model installed
in the Langley 16-Foot Transonic Tunnel.



L-81-6973

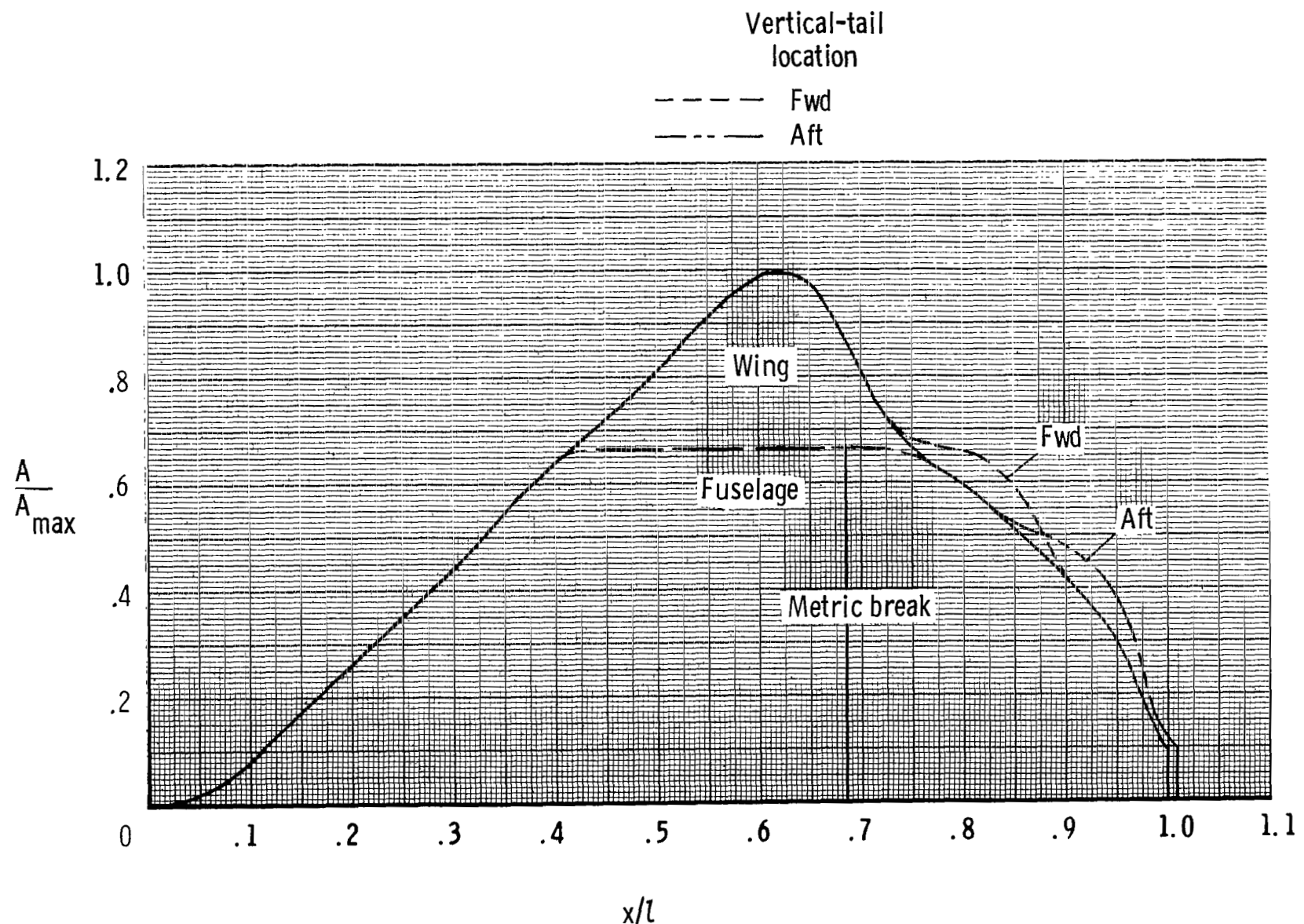
(b) Afterbody.

Figure 2.- Concluded.



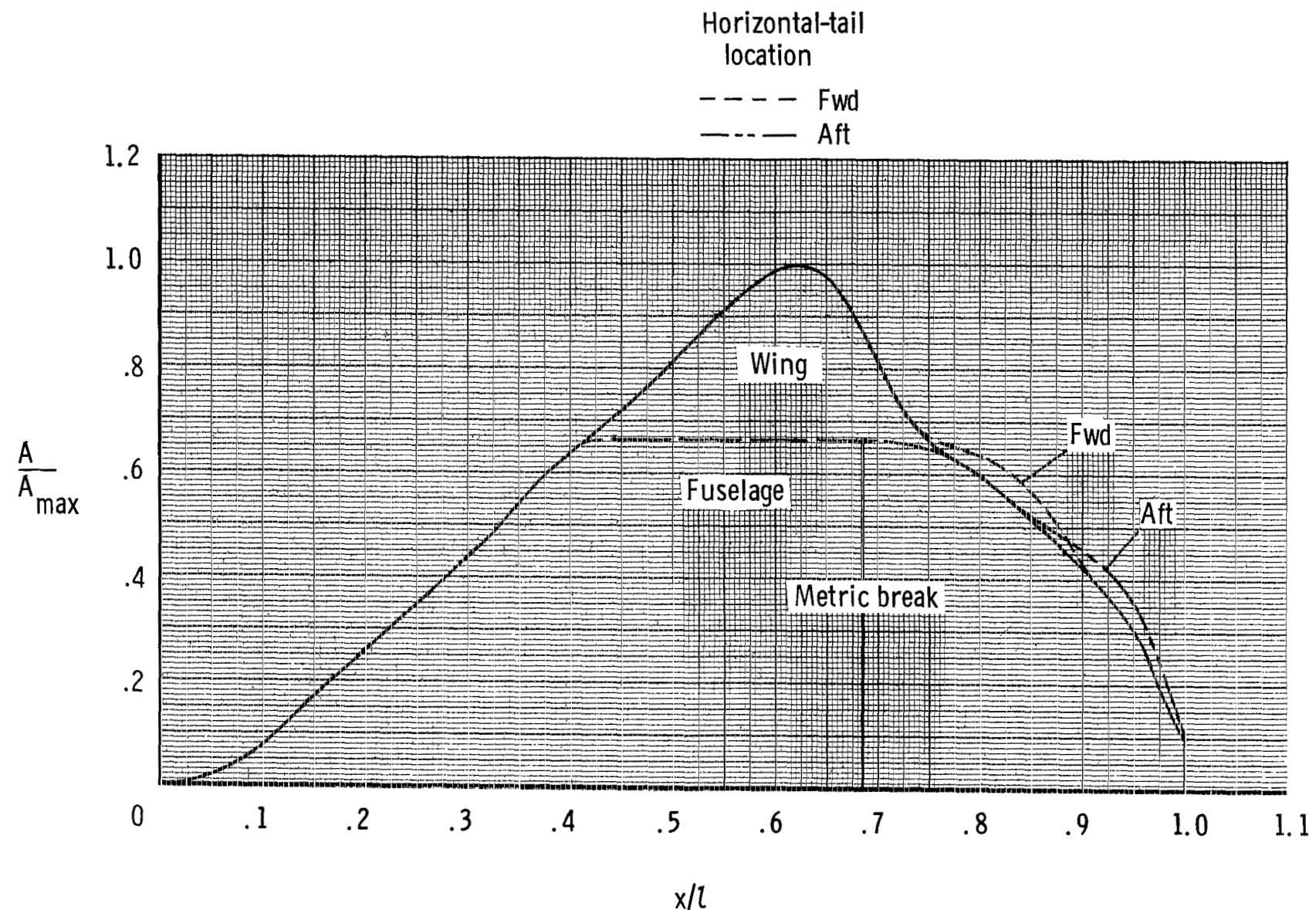
(a) Symmetrical and cambered twin vertical tails; short root chord; basic interfairing.

Figure 3.- Normal area distribution for various model components. $A_{\max} = 475.09 \text{ cm}^2$;
 $\tau = 174.74 \text{ cm}$.



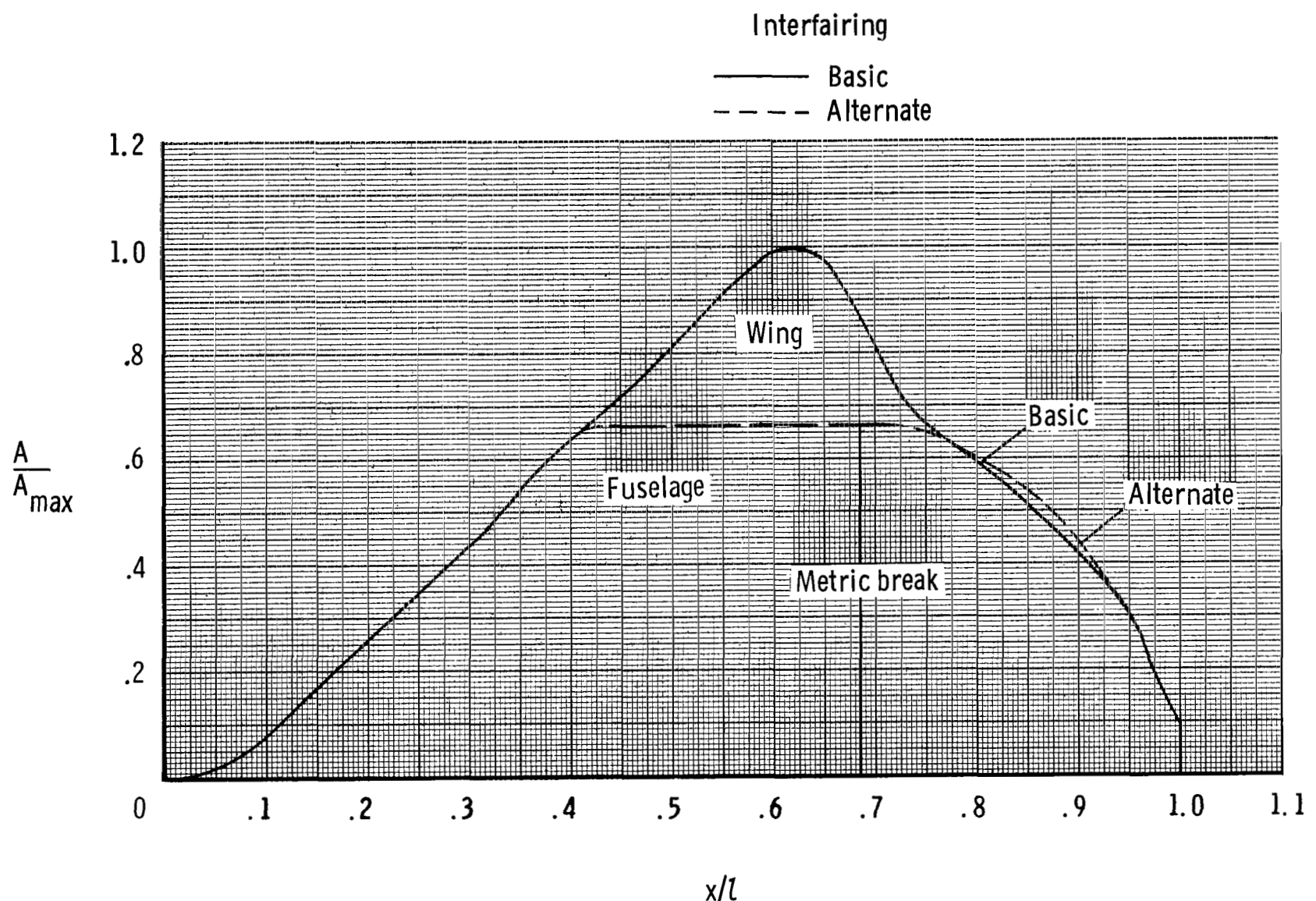
(b) Symmetrical twin vertical tails; long root chord; basic interfairing.

Figure 3.- Continued.



(c) Horizontal tails; basic interfairing.

Figure 3.- Continued.



(d) Engine interfairing.

Figure 3.- Concluded.

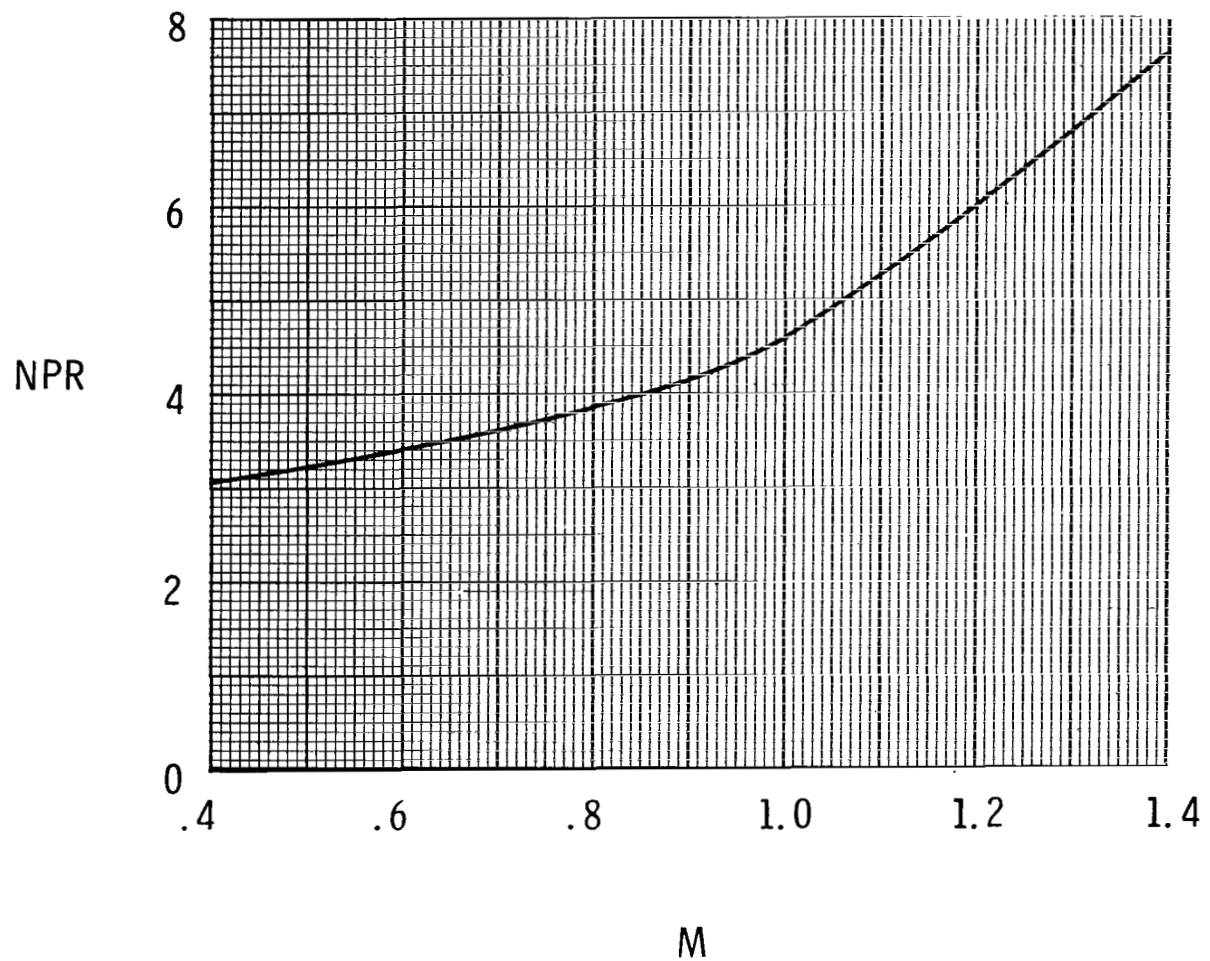
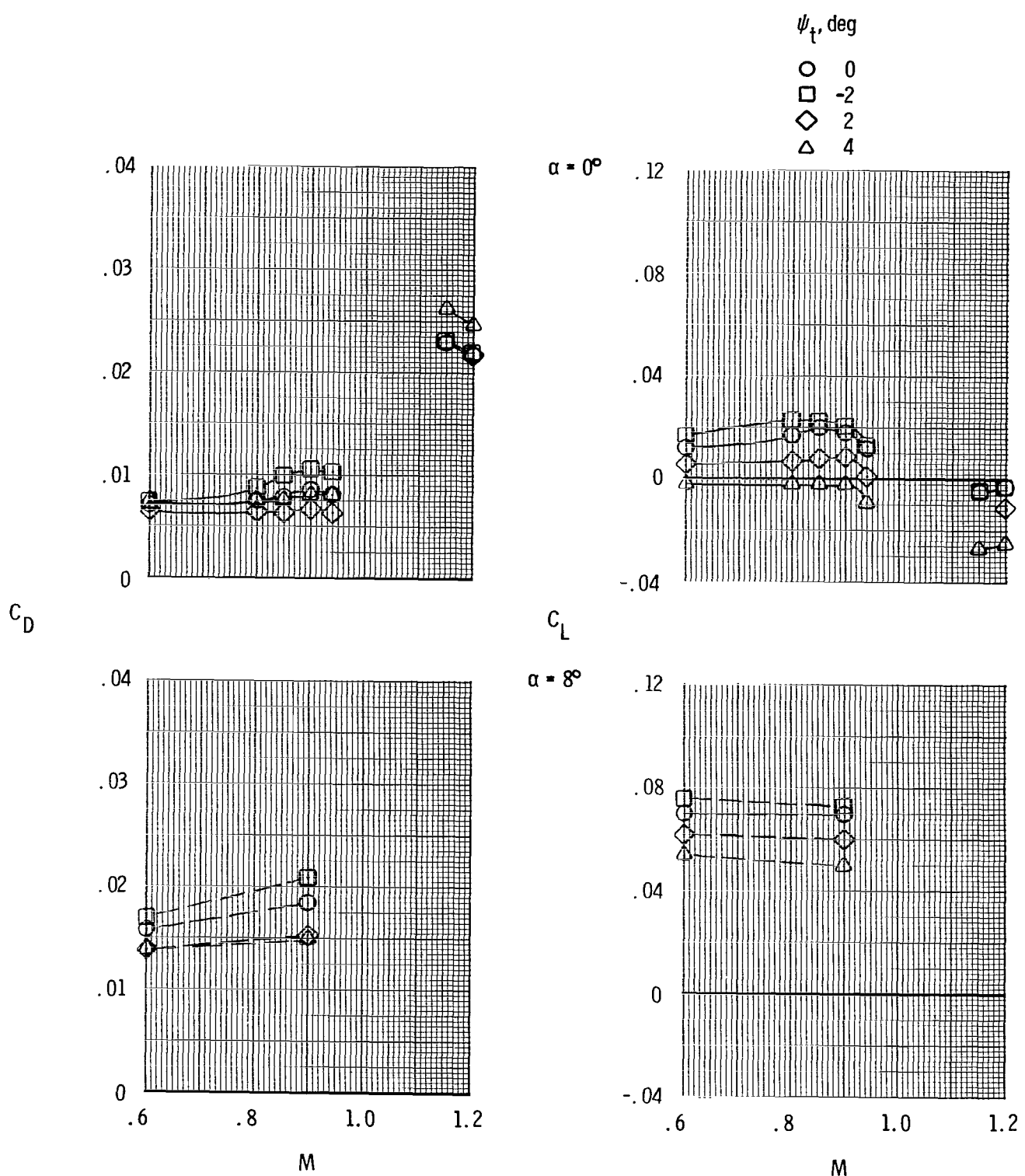
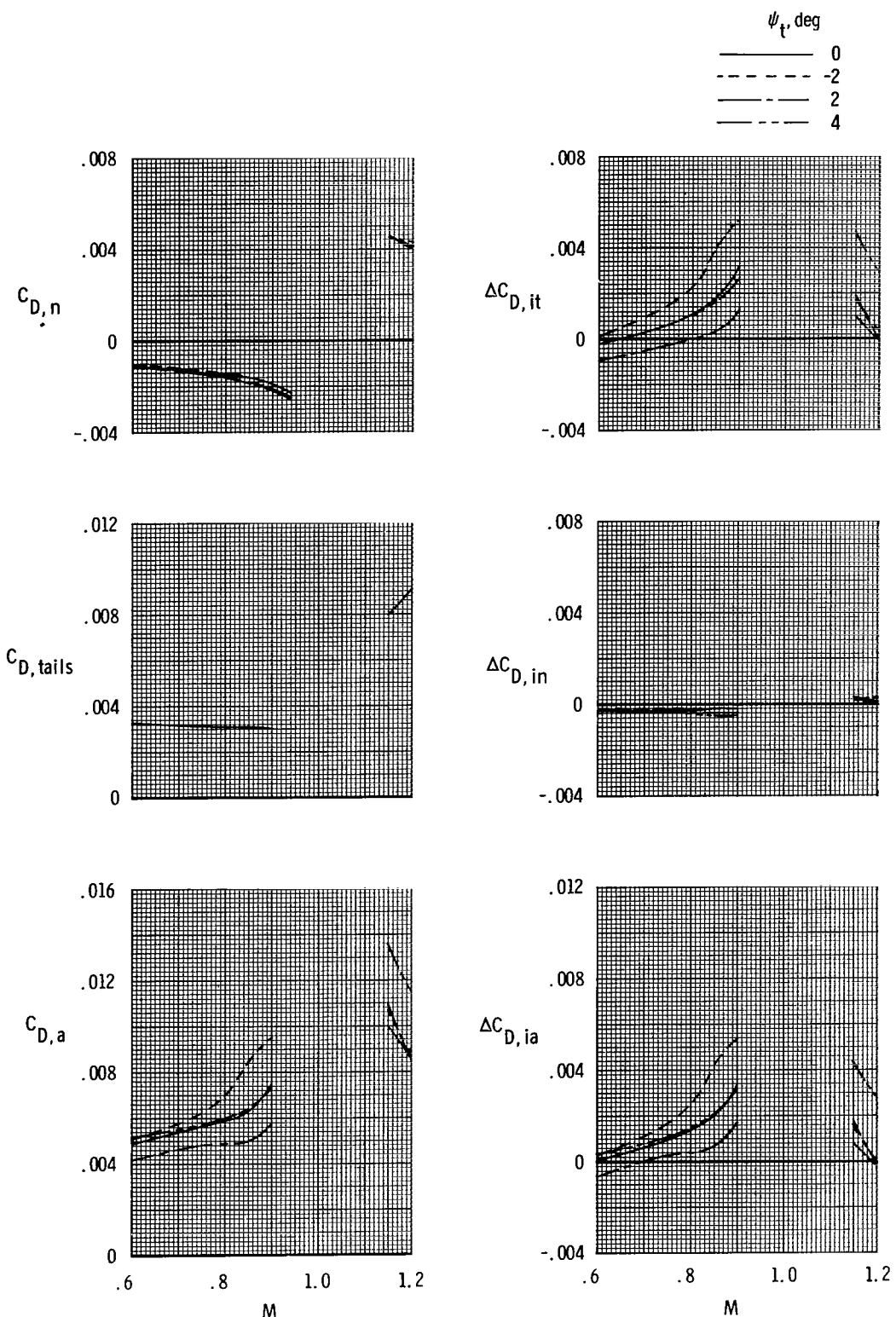


Figure 4.- Typical variation of nozzle pressure ratio with Mach number for a turbofan engine.



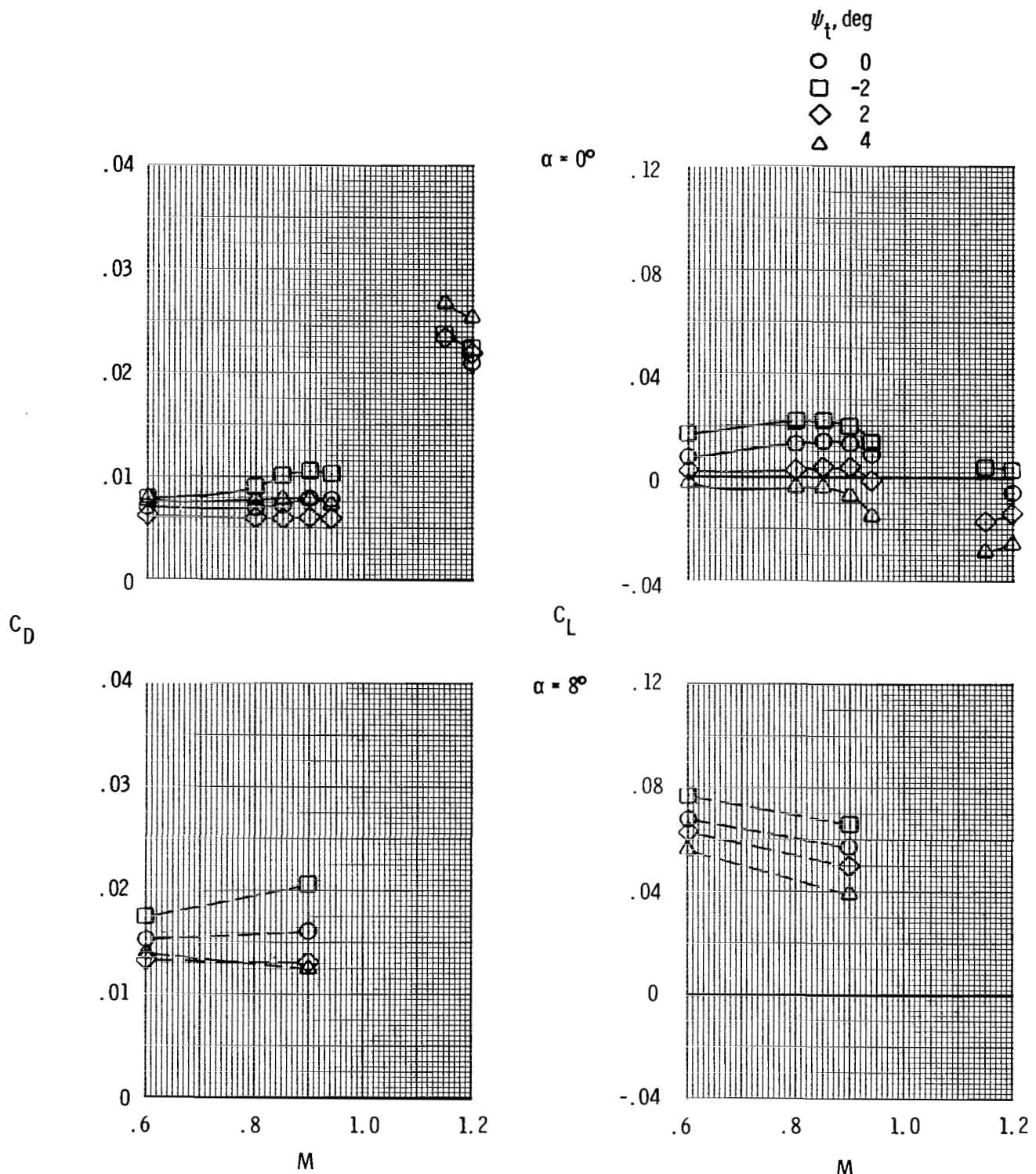
(a) Total aft-end lift and drag coefficients.

Figure 5.- Effect of twin-vertical-tail toe angle on aft-end characteristics for scheduled NPR. Horizontal tails fwd; short-root-chord vertical tails fwd; symmetrical vertical-tail airfoil; $\phi_t = 0^\circ$; basic interfairing.



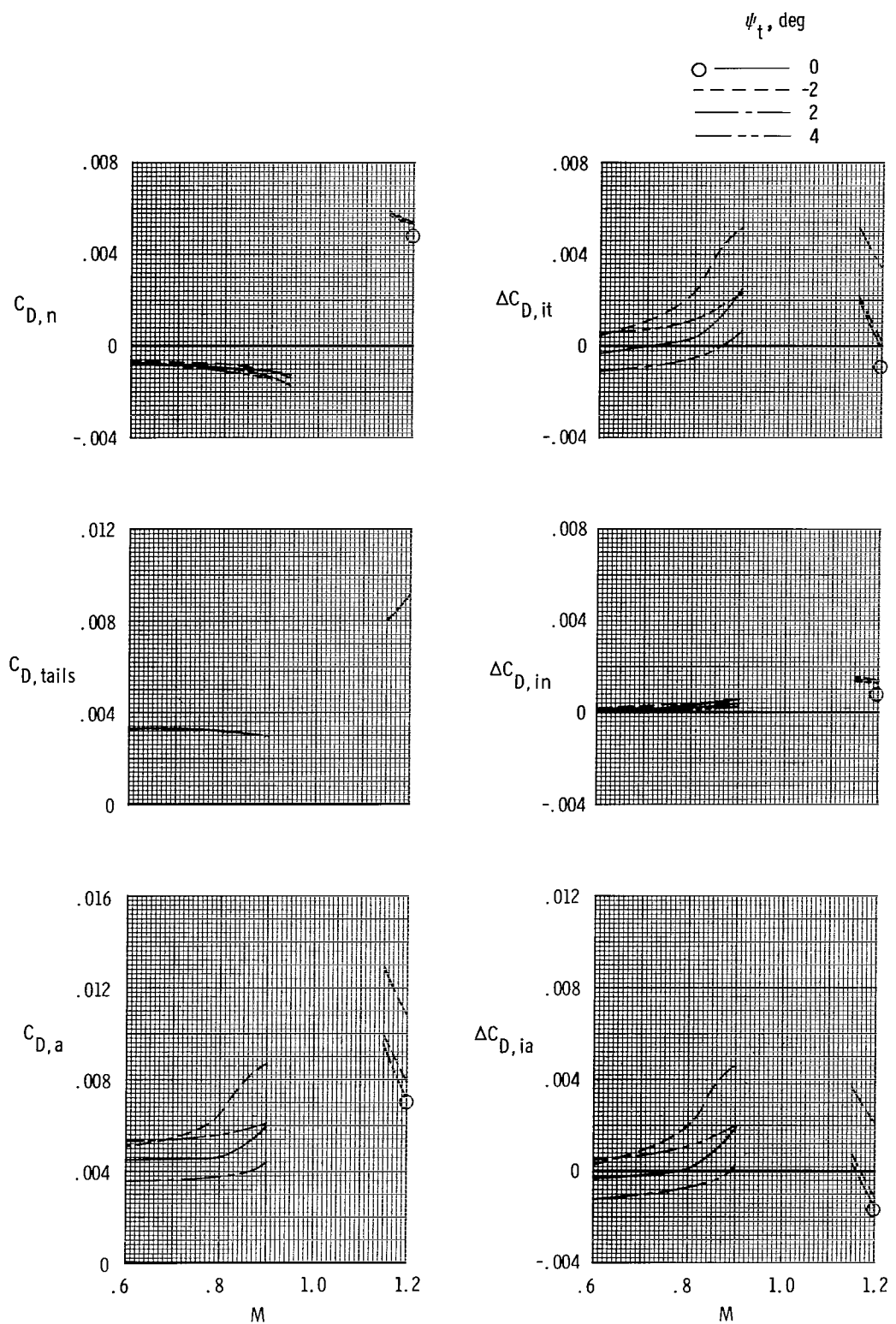
(b) Aft-end drag-coefficient components and tail interference-drag-coefficient increments; $\alpha = 0^\circ$.

Figure 5.- Concluded.



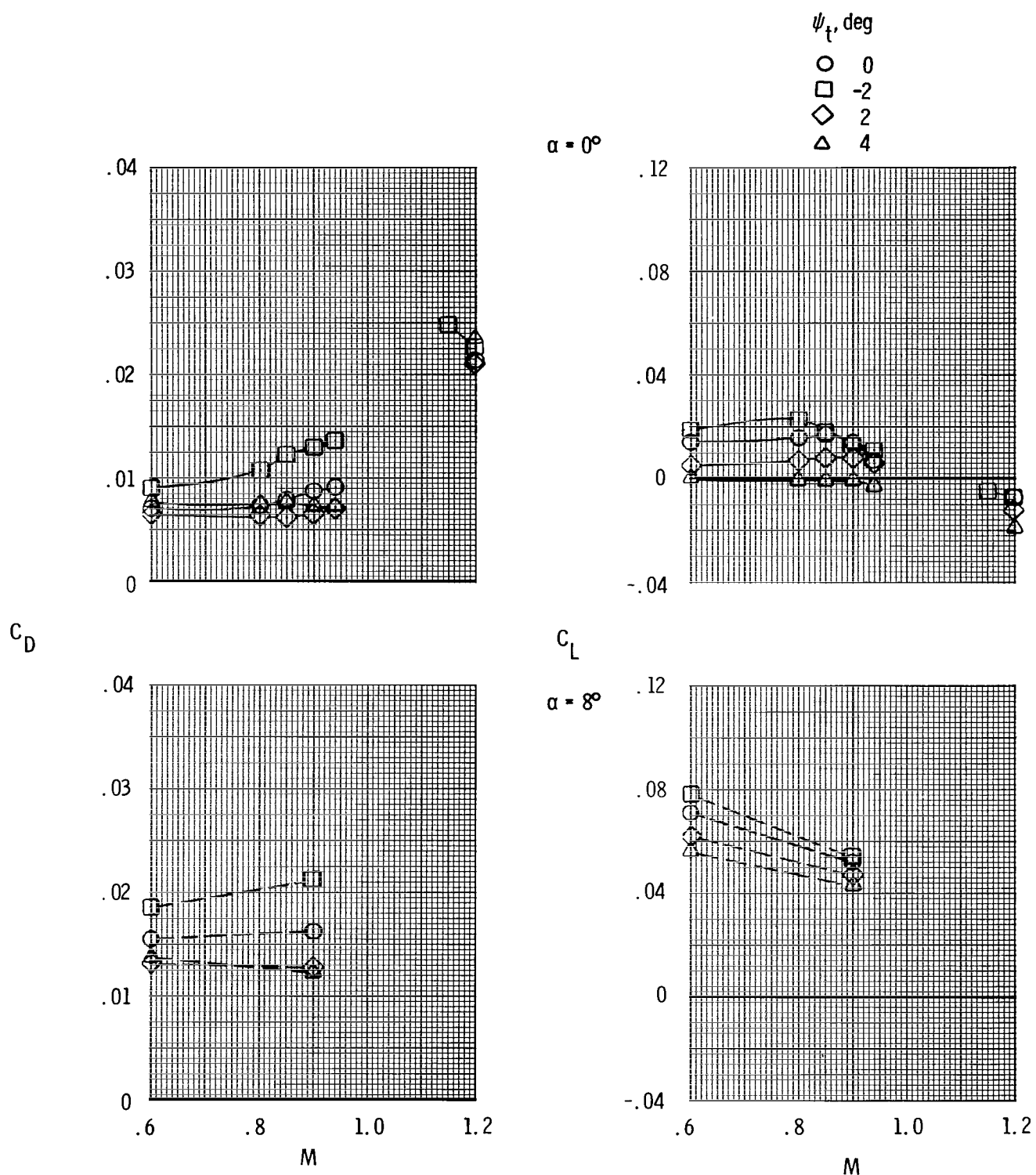
(a) Total aft-end lift and drag coefficients.

Figure 6.- Effect of twin-vertical-tail toe angle on aft-end characteristics for scheduled NPR. Horizontal tails aft; short-root-chord vertical tails fwd; symmetrical vertical-tail airfoil; $\phi_t = 0^\circ$; basic interfairing.



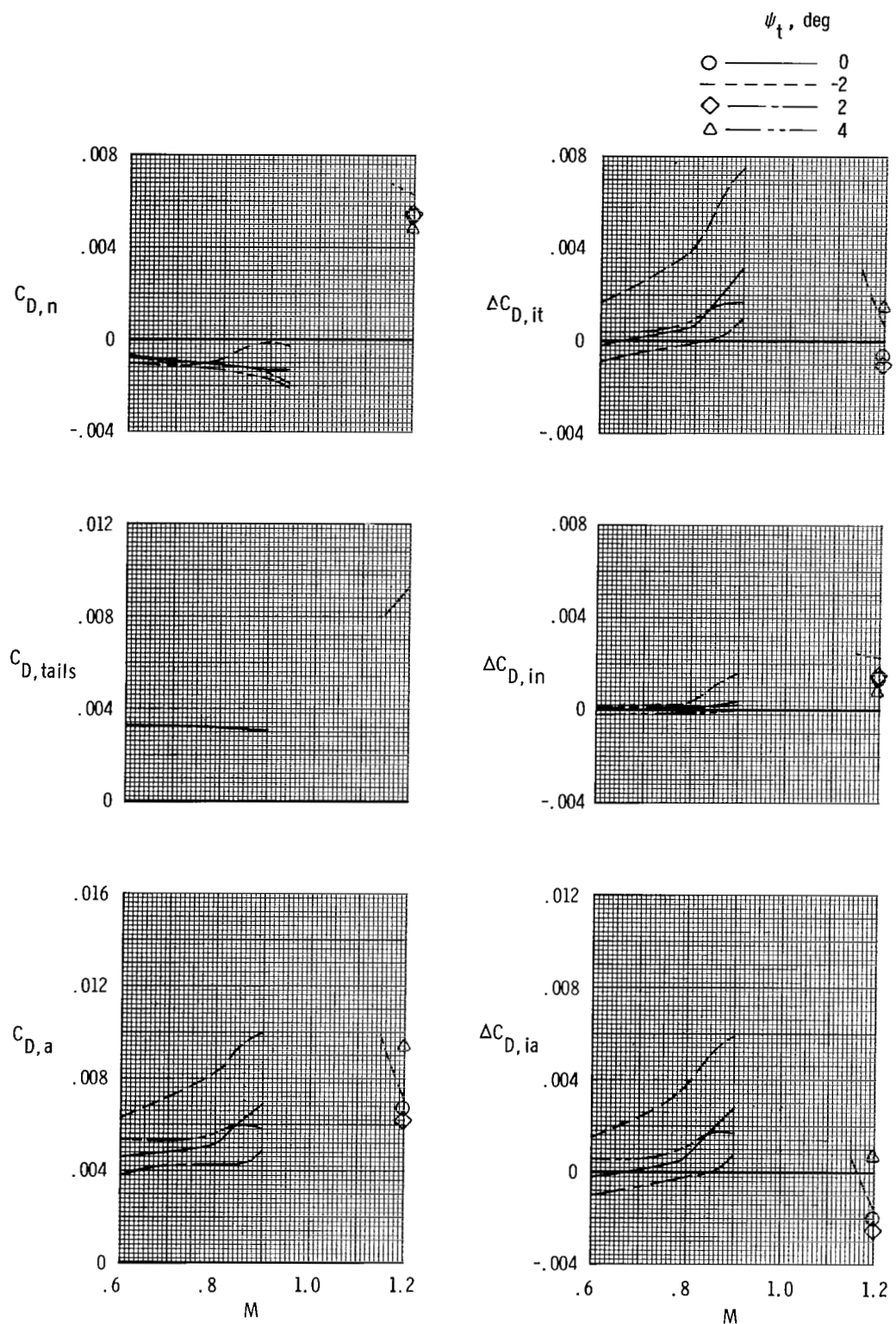
(b) Aft-end drag-coefficient components and tail interference-drag-coefficient increments; $\alpha = 0^\circ$.

Figure 6.- Concluded.



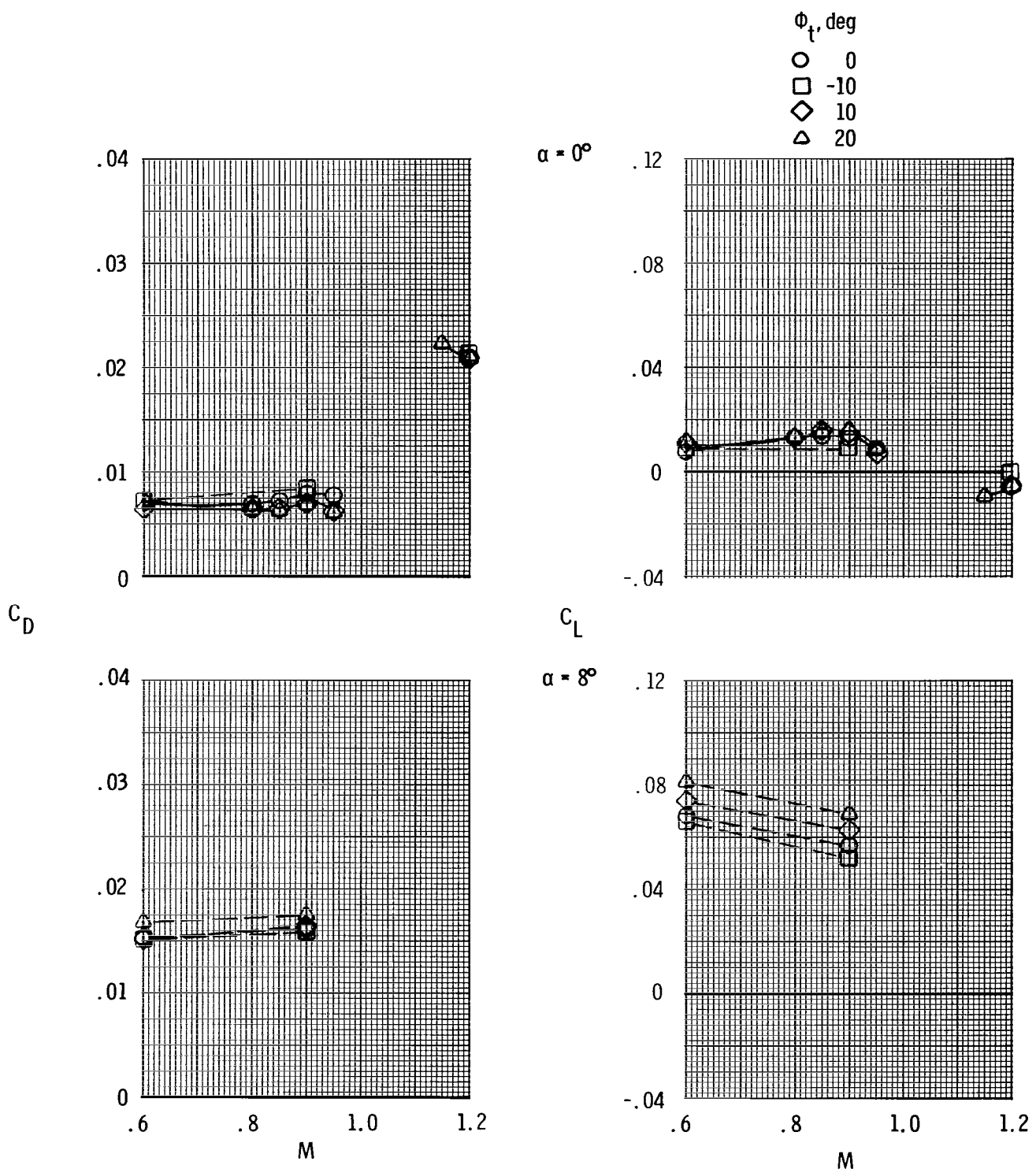
(a) Total aft-end lift and drag coefficients.

Figure 7.- Effect of twin-vertical-tail toe angle on aft-end characteristics for scheduled NPR. Horizontal tails aft; short-root-chord vertical tails mid; symmetrical vertical-tail airfoil; $\phi_t = 0^\circ$; basic interfairing.



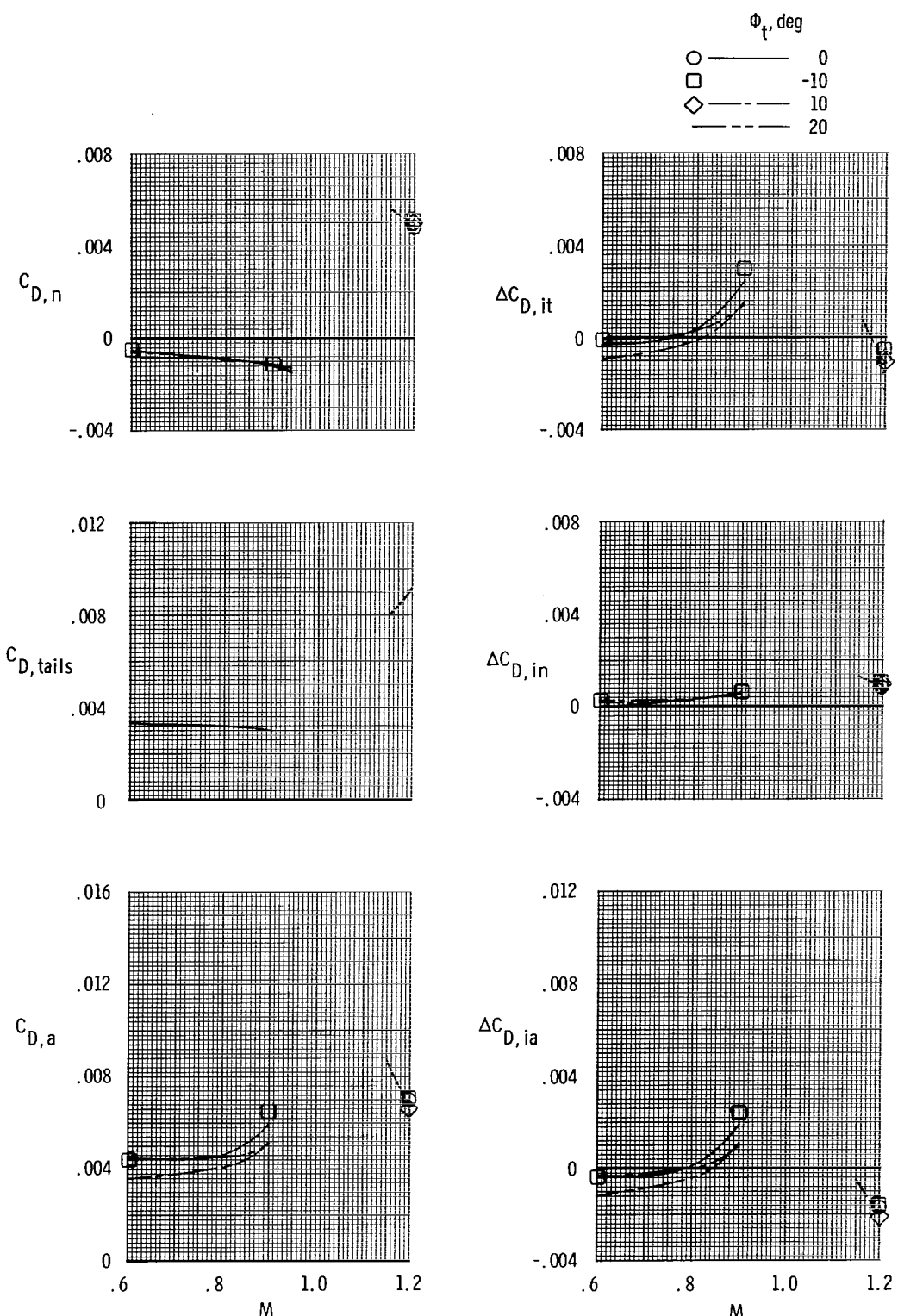
(b) Aft-end drag-coefficient components and tail interference-drag-coefficient increments; $\alpha = 0^\circ$.

Figure 7.- Concluded.



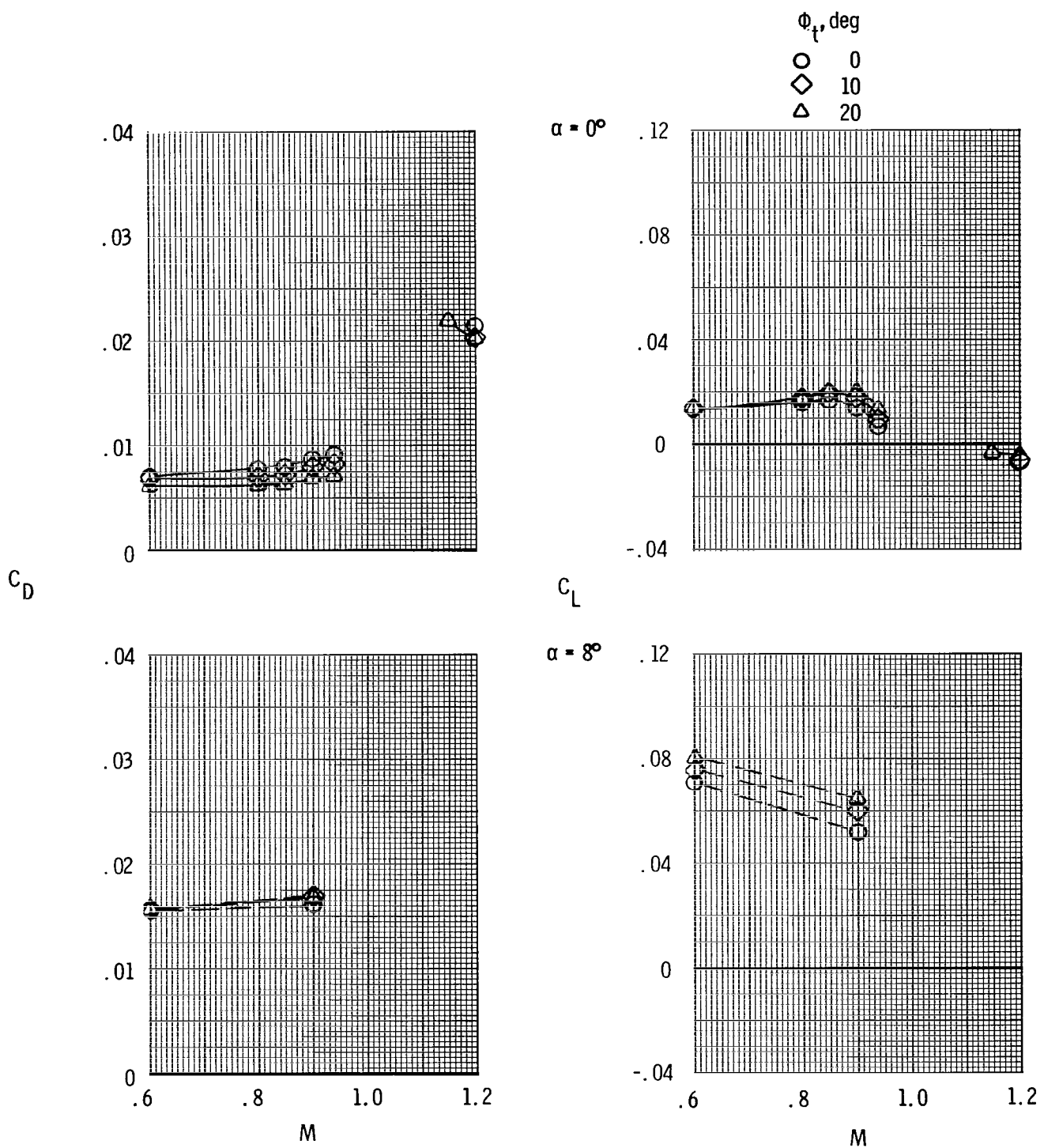
(a) Total aft-end lift and drag coefficients.

Figure 8.- Effect of twin-vertical-tail cant angle on aft-end characteristics for scheduled NPR. Horizontal tails aft; short-root-chord vertical tails fwd; symmetrical vertical-tail airfoil; $\phi_t = 0^\circ$; basic interfairing.



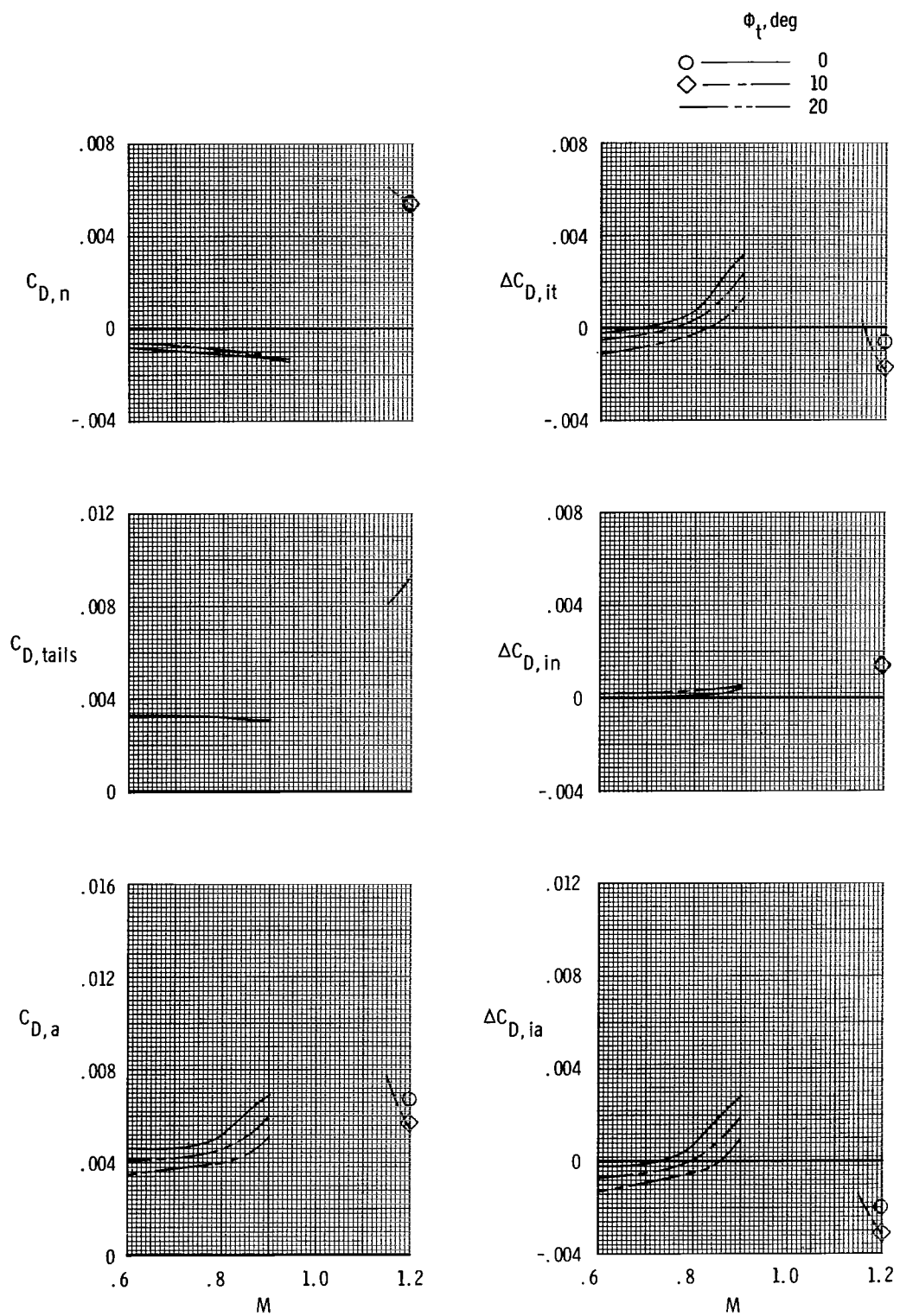
(b) Aft-end drag-coefficient components and tail interference-drag-coefficient increments; $\alpha = 0^\circ$.

Figure 8.- Concluded.



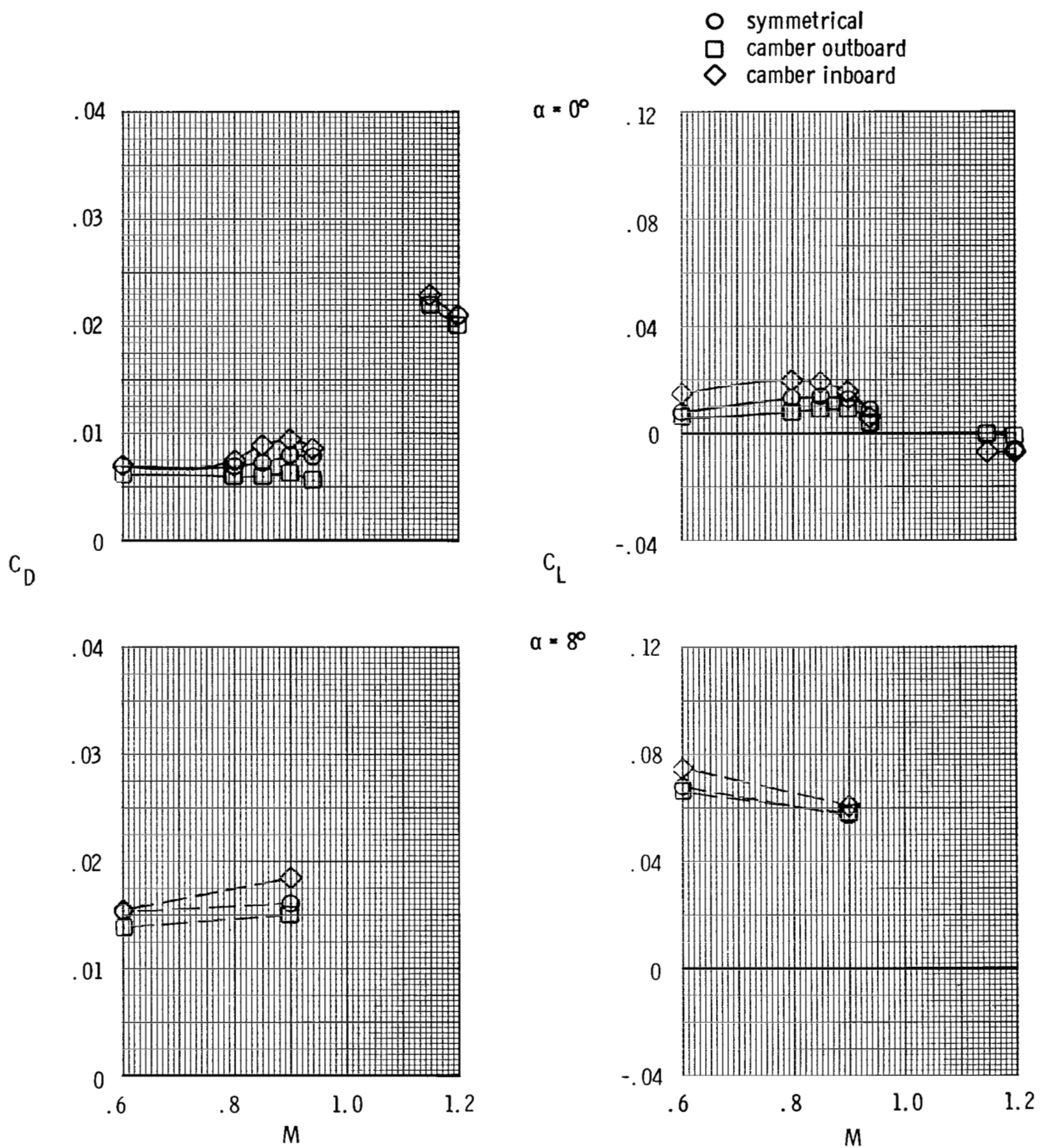
(a) Total aft-end lift and drag coefficients.

Figure 9.- Effect of twin-vertical-tail cant angle on aft-end characteristics for scheduled NPR. Horizontal tails aft; short-root-chord vertical tails mid; symmetrical vertical-tail airfoil; $\phi_t = 0^\circ$; basic interfairing.



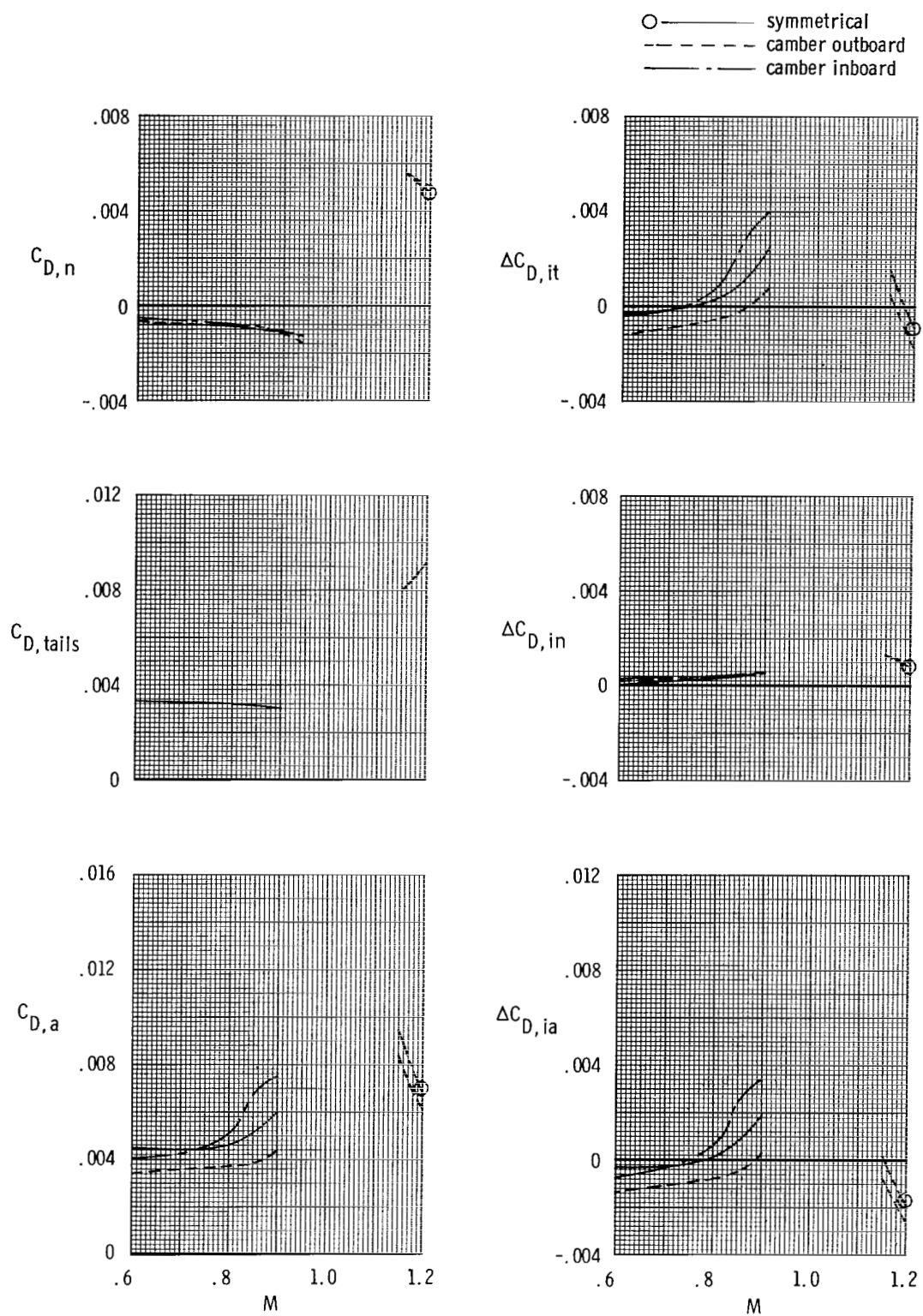
(b) Aft-end drag-coefficient components and tail interference-drag-coefficient increments; $\alpha = 0^\circ$.

Figure 9.- Concluded.



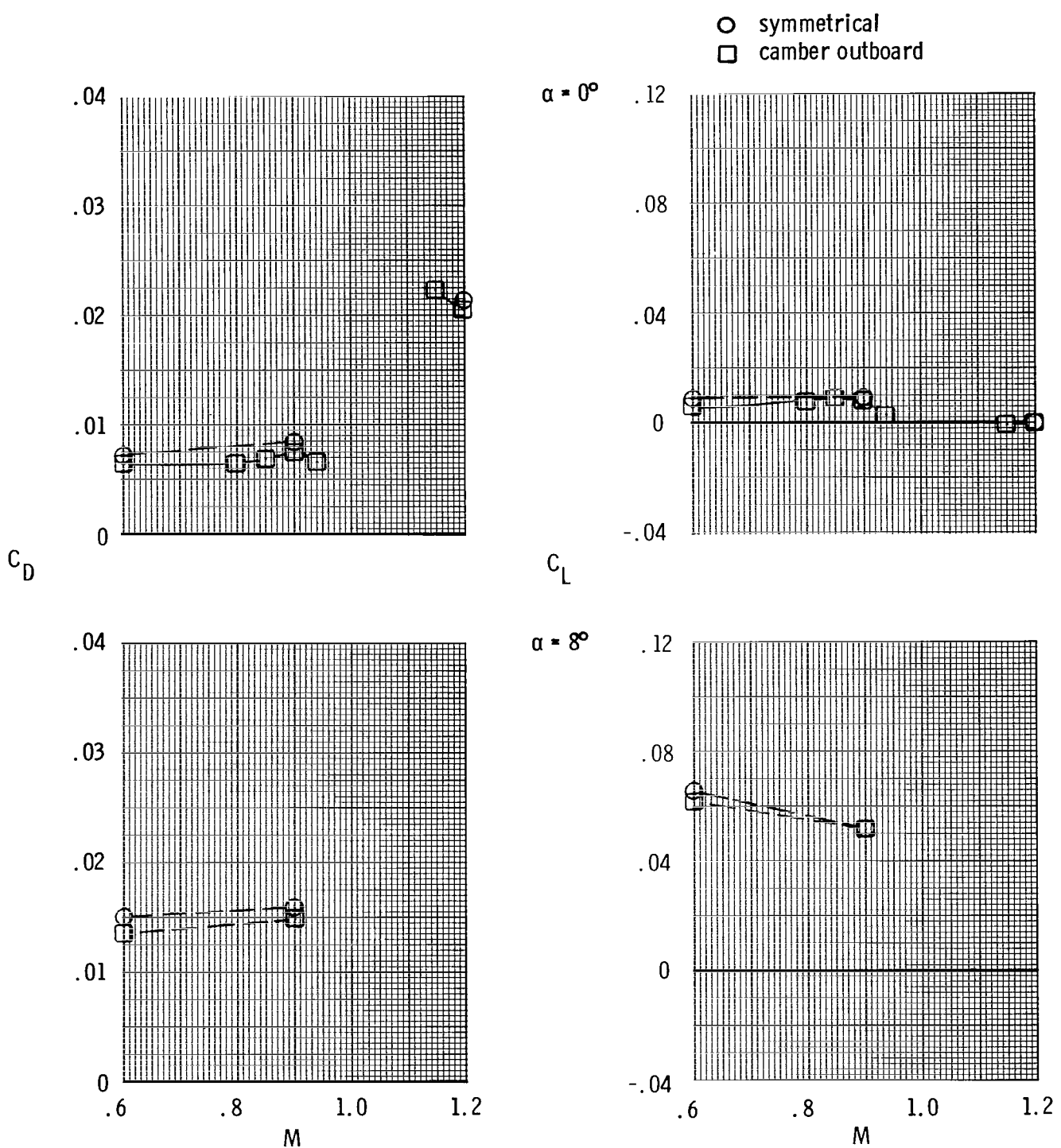
(a) Total aft-end lift and drag coefficients.

Figure 10.- Effect of twin-vertical-tail camber on aft-end characteristics for scheduled NPR. Horizontal tails aft; short-root-chord vertical tails fwd; $\phi_t = 0^\circ$; $\psi_t = 0^\circ$; basic interfairing.



(b) Aft-end drag-coefficient components and tail interference-drag-coefficient increments; $\alpha = 0^\circ$.

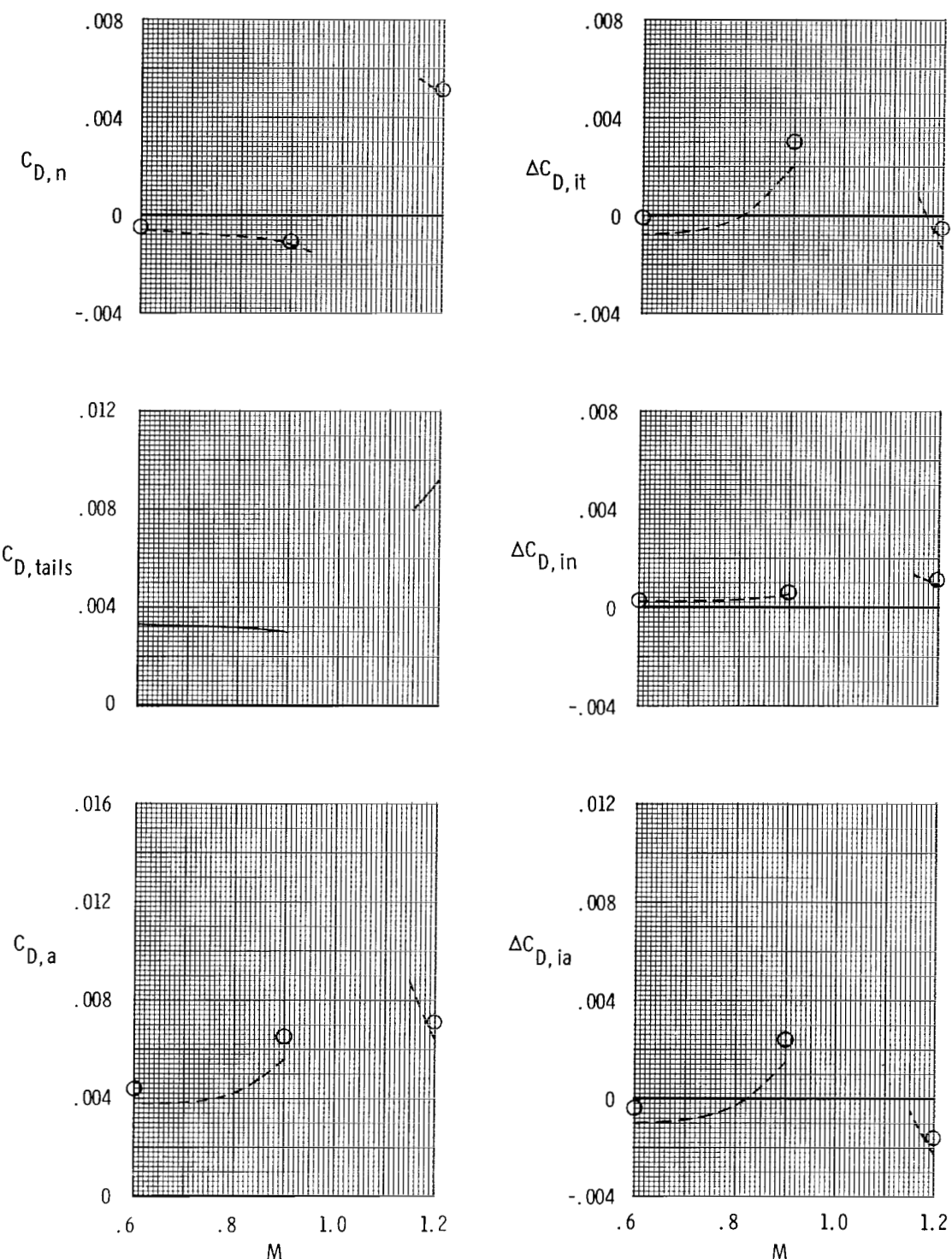
Figure 10.- Concluded.



(a) Total aft-end lift and drag coefficients.

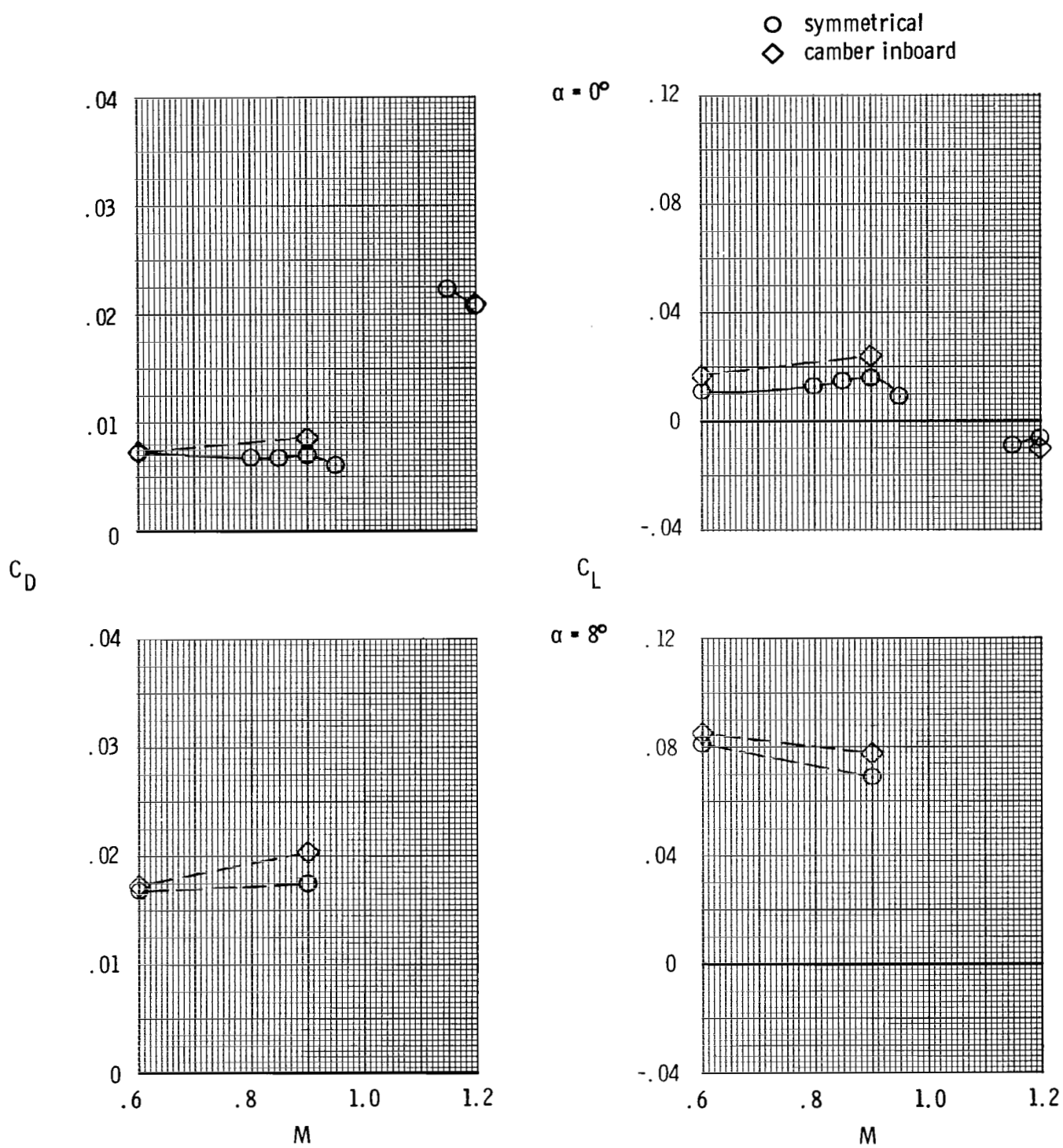
Figure 11.- Effect of twin-vertical-tail camber on aft-end characteristics for scheduled NPR. Horizontal tails aft; short-root-chord vertical tails fwd; $\psi_t = 0^\circ$; $\phi_t = -10^\circ$; basic interfairing.

○ —— symmetrical
 - - - camber outboard



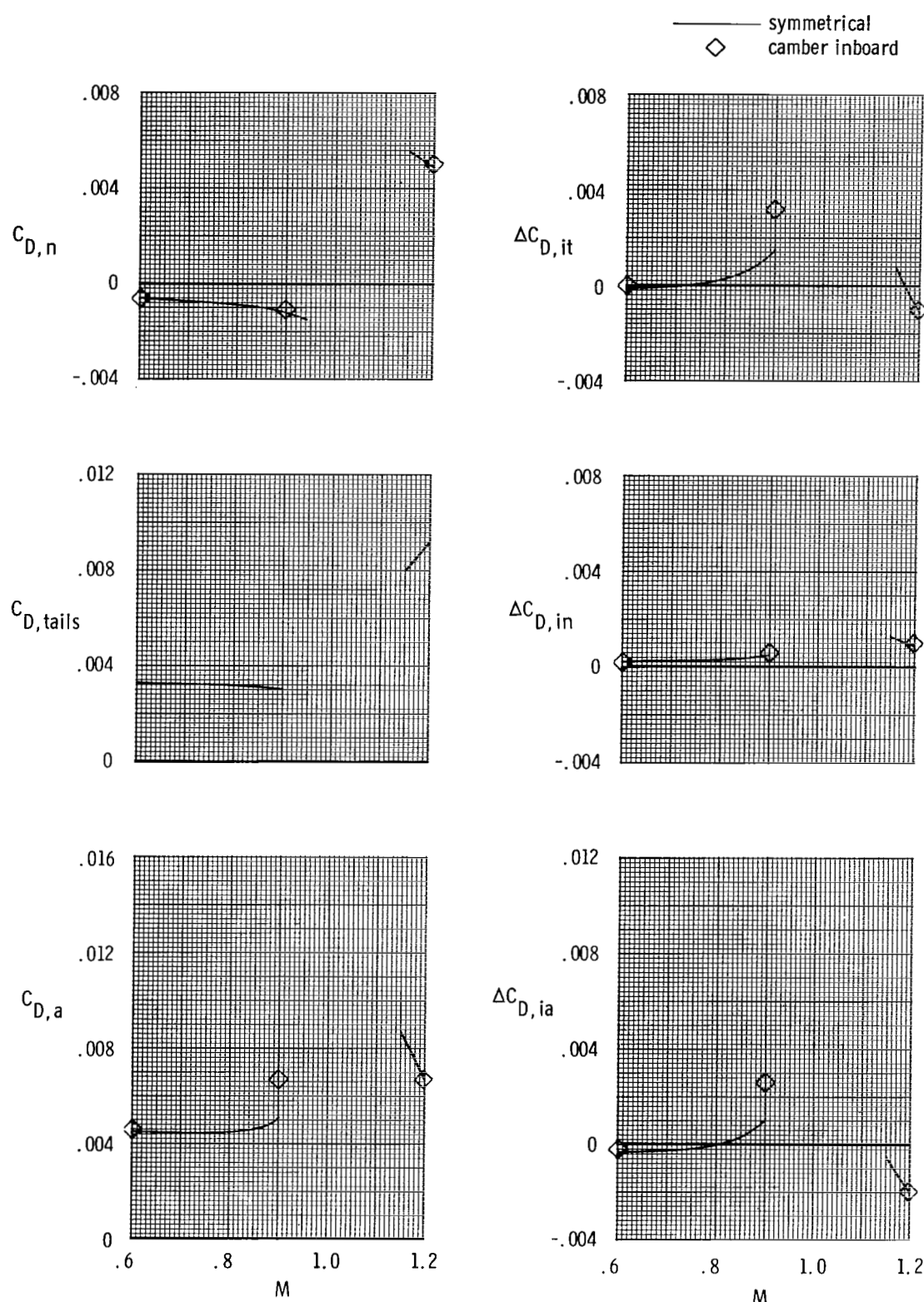
(b) Aft-end drag-coefficieint components and tail interference-drag-coefficient increments; $\alpha = 0^\circ$.

Figure 11.- Concluded.



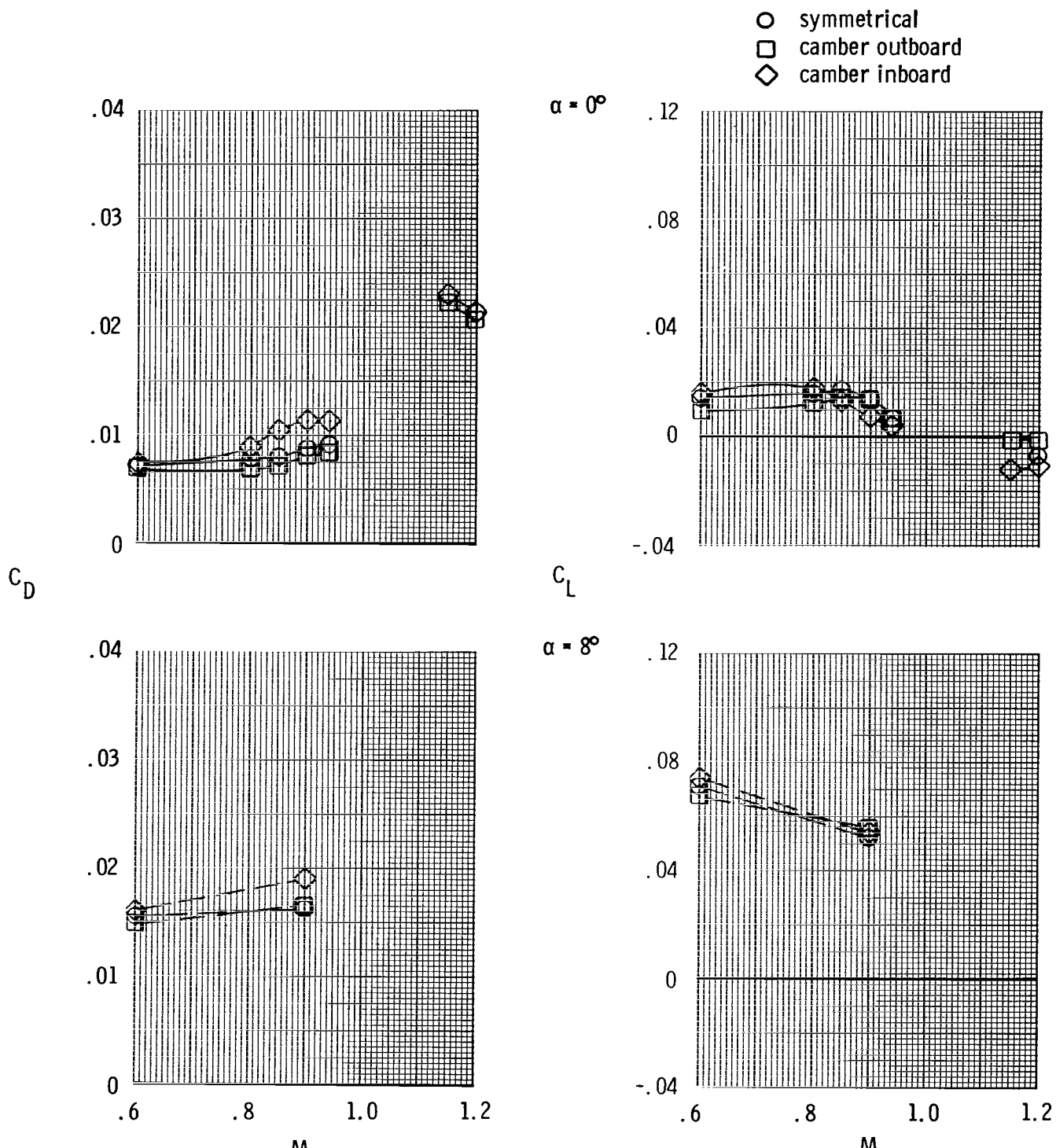
(a) Total aft-end lift and drag coefficients.

Figure 12.- Effect of twin-vertical-tail camber on aft-end characteristics for scheduled NPR. Horizontal tails aft; short-root-chord vertical tails fwd; $\psi_t = 0^\circ$; $\phi_t = 20^\circ$; basic interfairing.



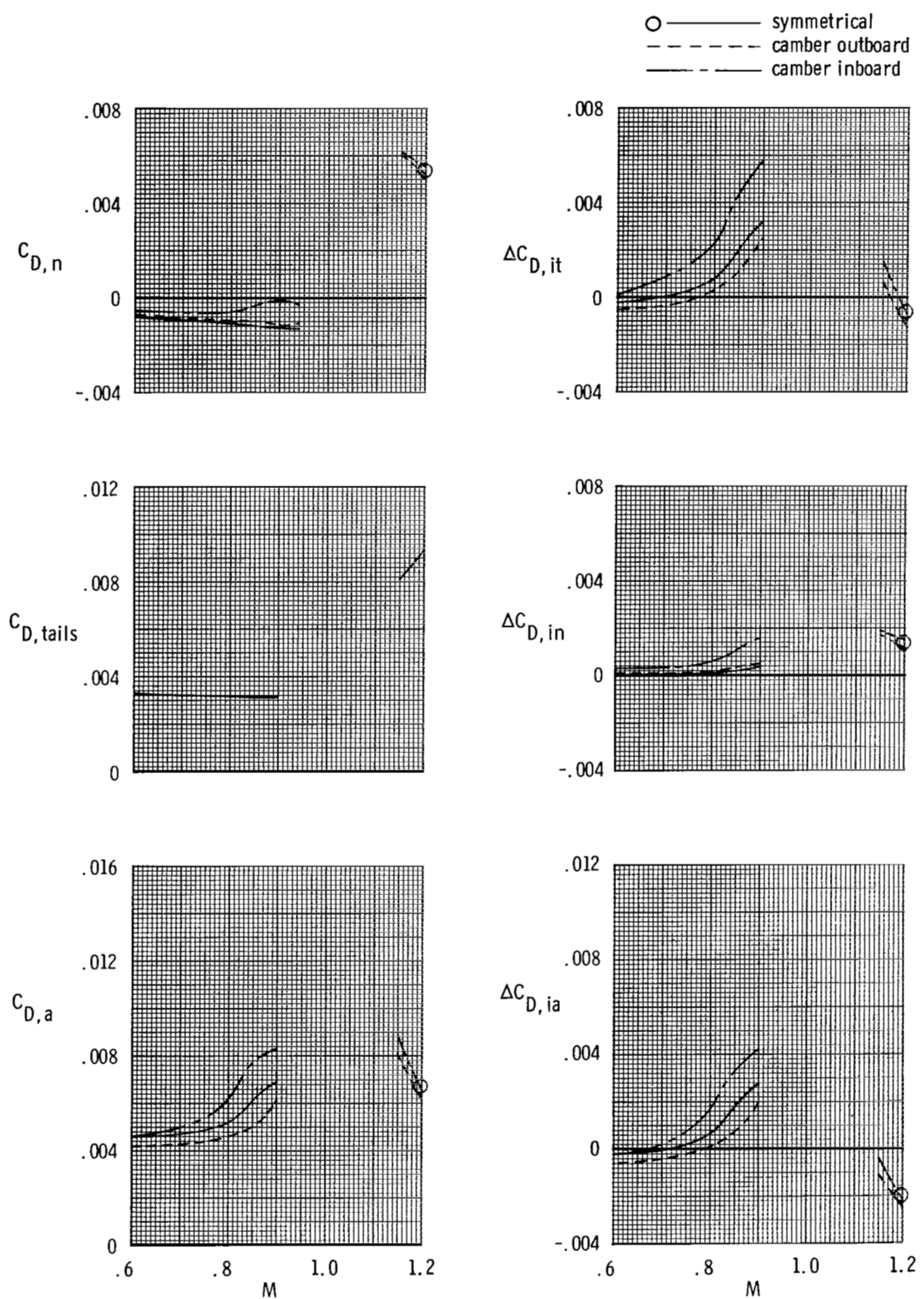
(b) Aft-end drag-coefficient components and tail interference-drag-coefficient increments; $\alpha = 0^\circ$.

Figure 12.- Concluded.



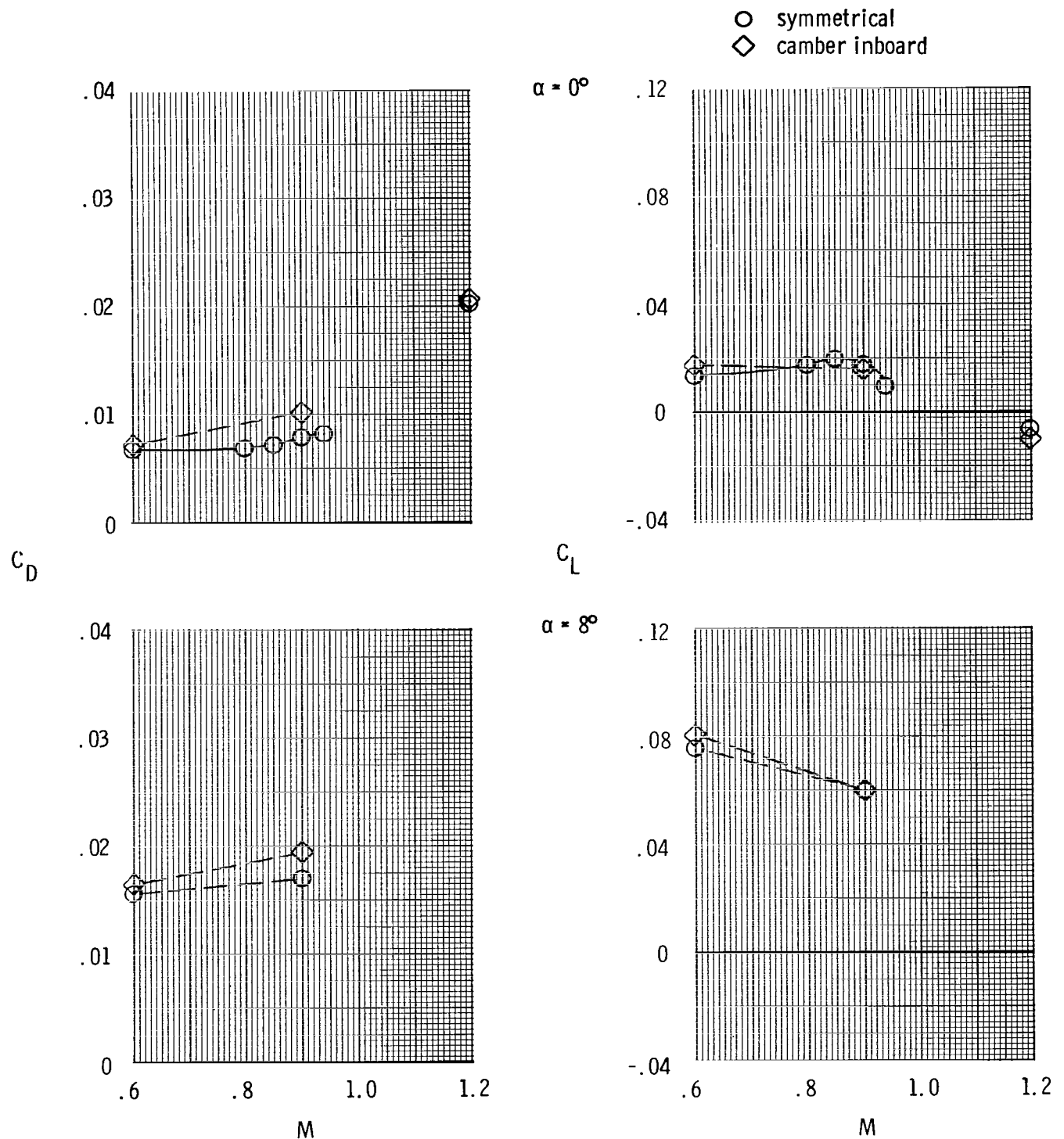
(a) Total aft-end lift and drag coefficients.

Figure 13.- Effect of twin-vertical-tail camber on aft-end characteristics for scheduled NPR. Horizontal tails aft; short-root-chord vertical tails mid; $\phi_t = 0^\circ$; $\psi_t = 0^\circ$; basic interfairing.



(b) Aft-end drag-coefficient components and tail interference-drag-coefficient increments; $\alpha = 0^\circ$.

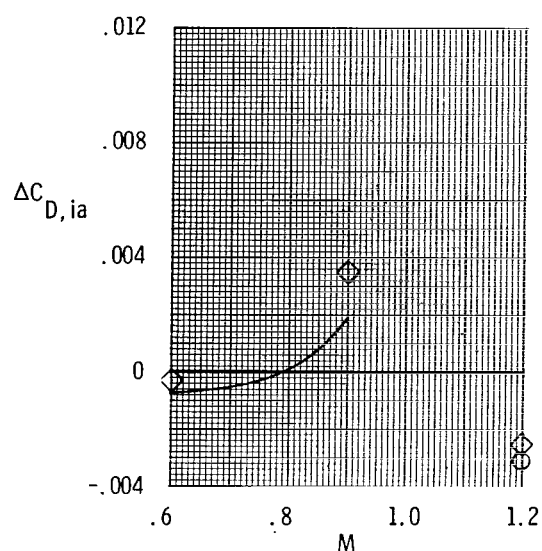
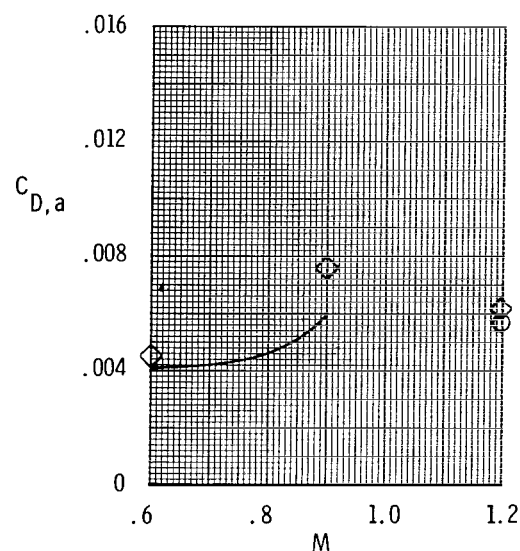
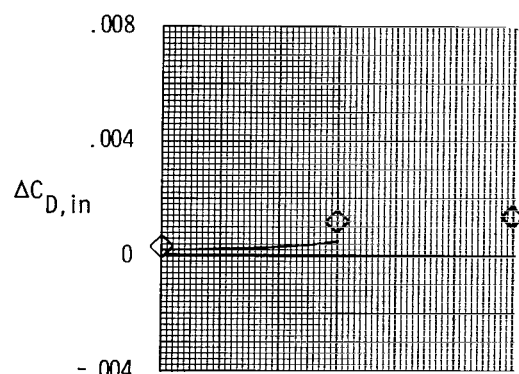
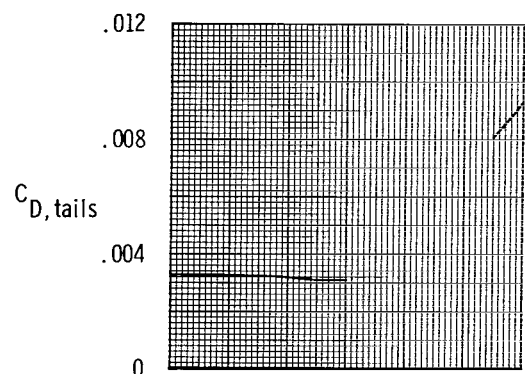
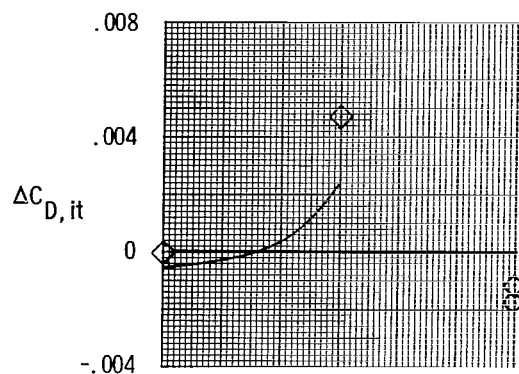
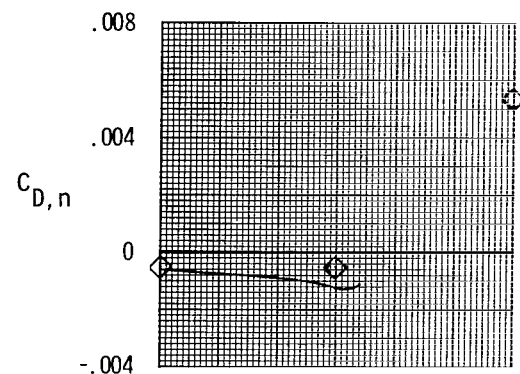
Figure 13.- Concluded.



(a) Total aft-end lift and drag coefficients.

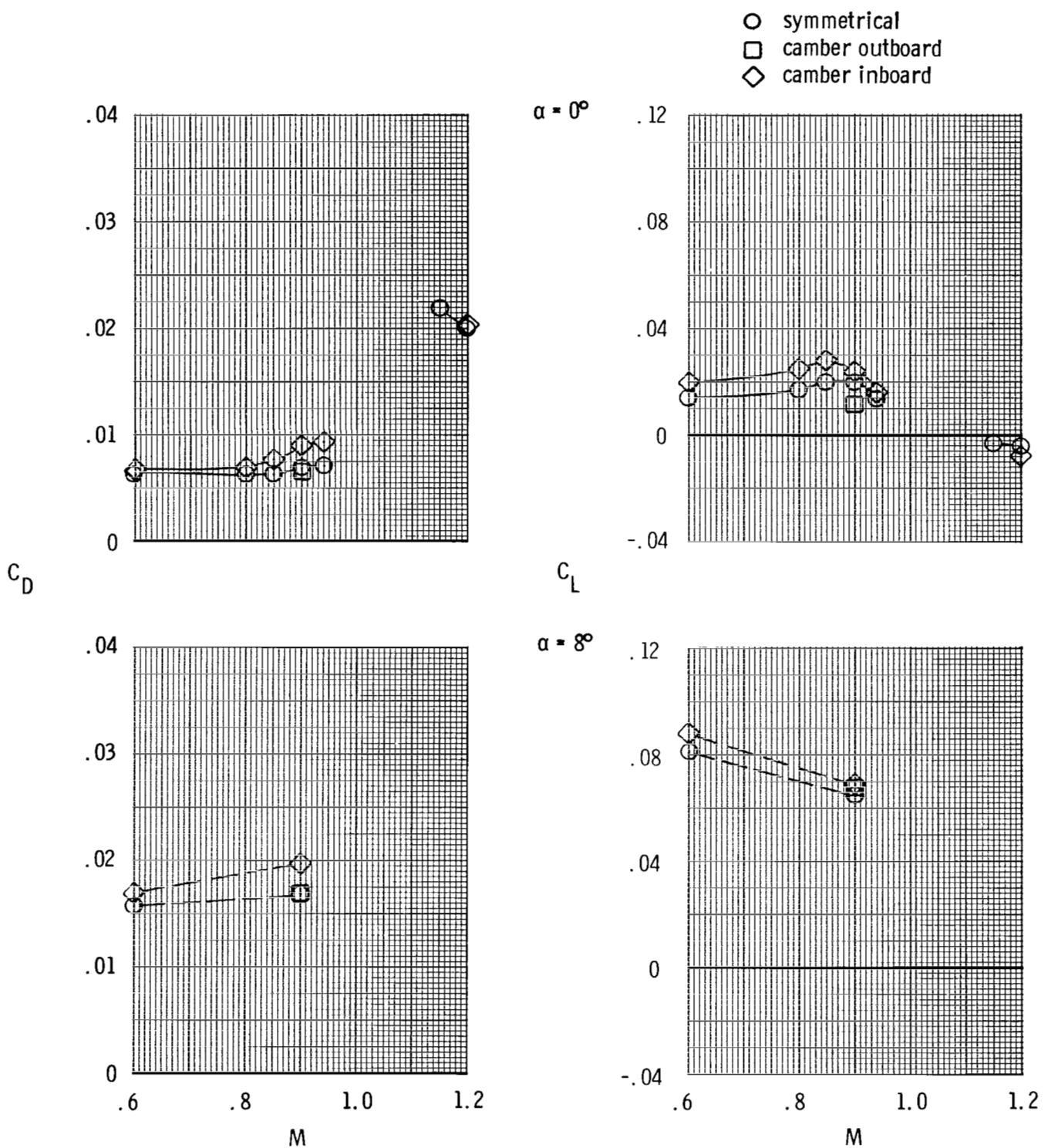
Figure 14.- Effect of twin-vertical-tail camber on aft-end characteristics for scheduled NPR. Horizontal tails aft; short-root-chord vertical tails mid; $\psi_t = 0^\circ$; $\phi_t = 10^\circ$; basic interfairing.

— symmetrical camber inboard



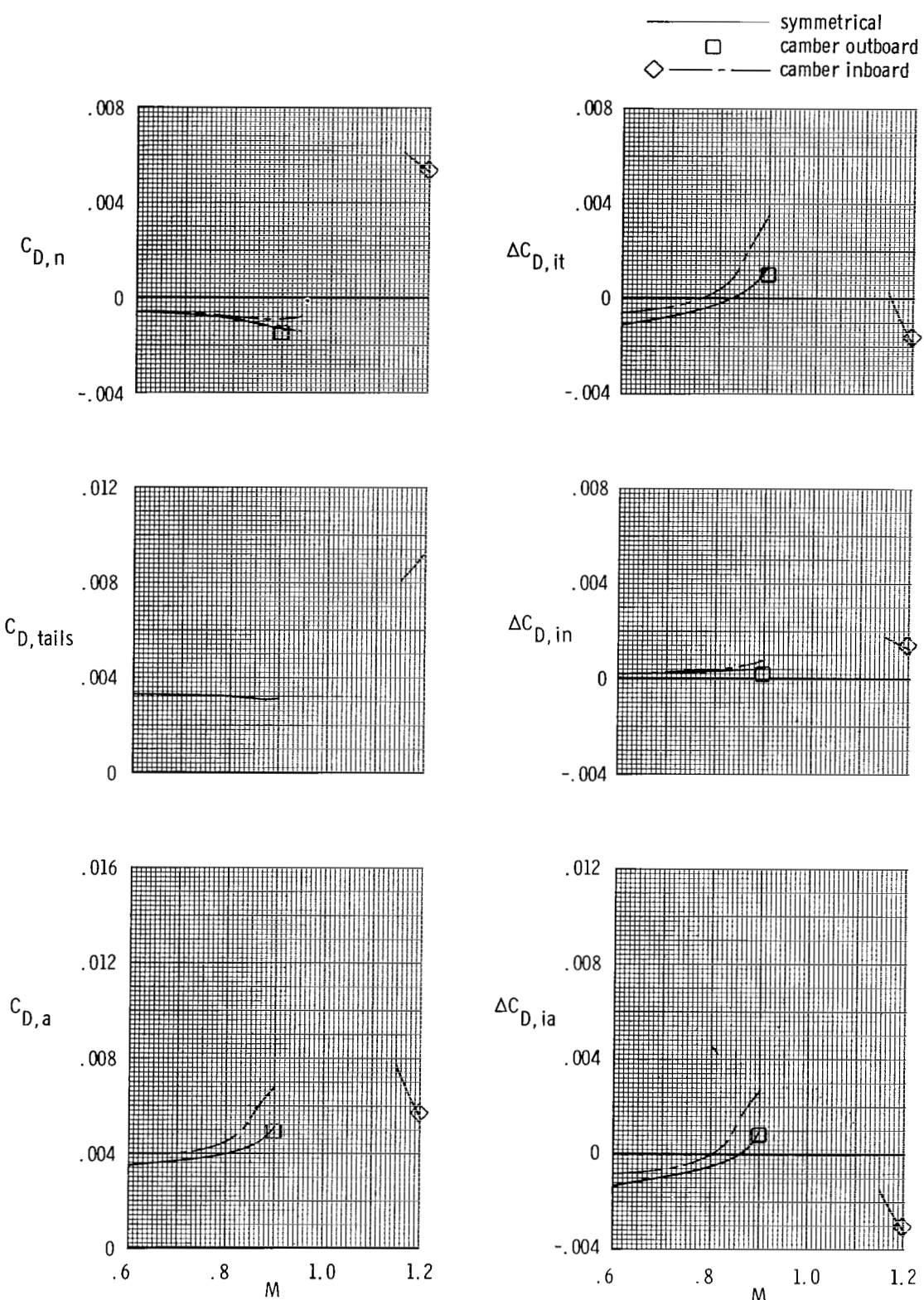
(b) Aft-end drag-coefficient components and tail interference-drag-coefficient increments; $\alpha = 0^\circ$.

Figure 14.- Concluded.



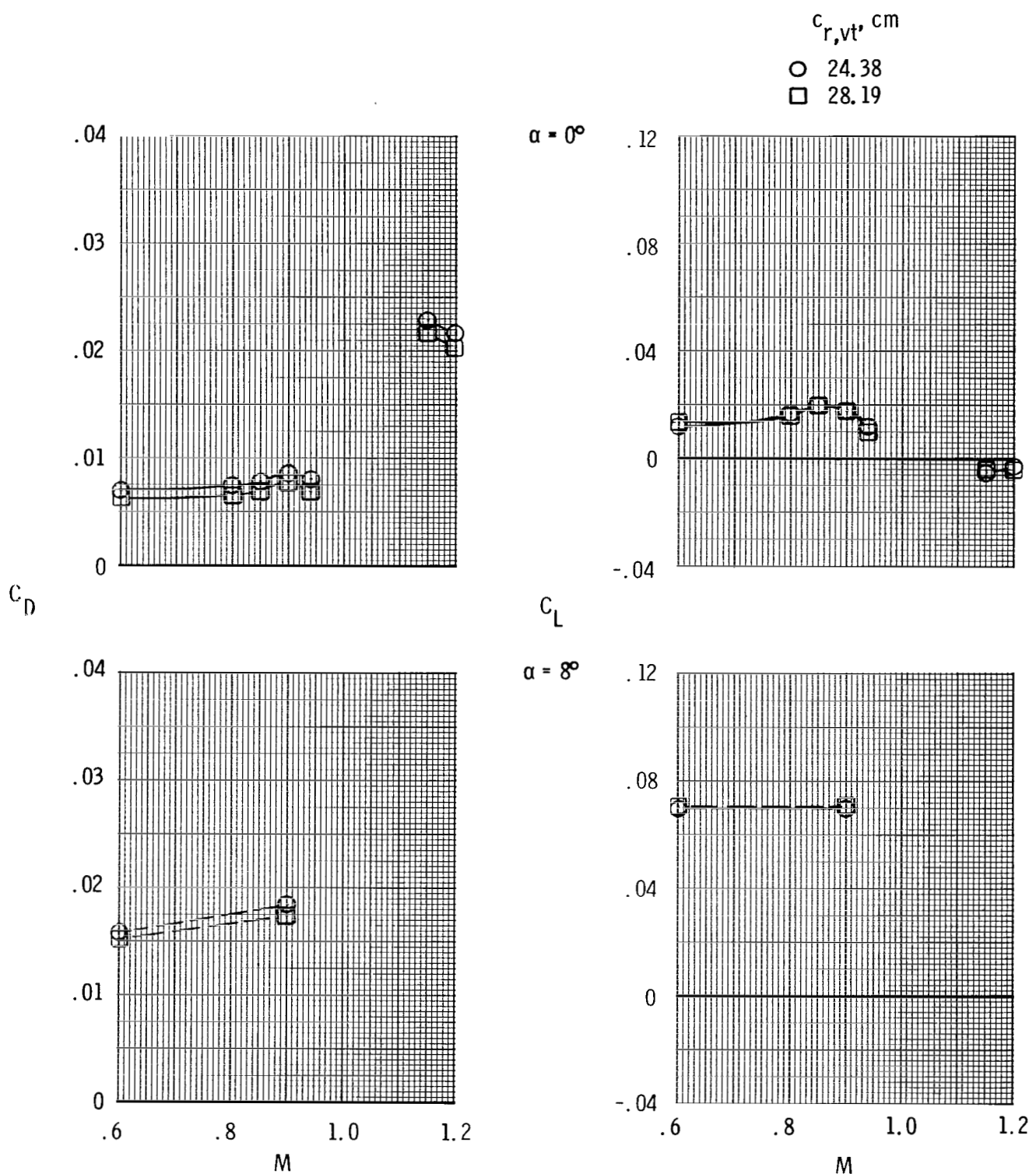
(a) Total aft-end lift and drag coefficients.

Figure 15.- Effect of twin-vertical-tail camber on aft-end characteristics for scheduled NPR. Horizontal tails aft; short-root-chord vertical tails mid; $\phi_t = 0^\circ$; $\psi_t = 20^\circ$; basic interfairing.



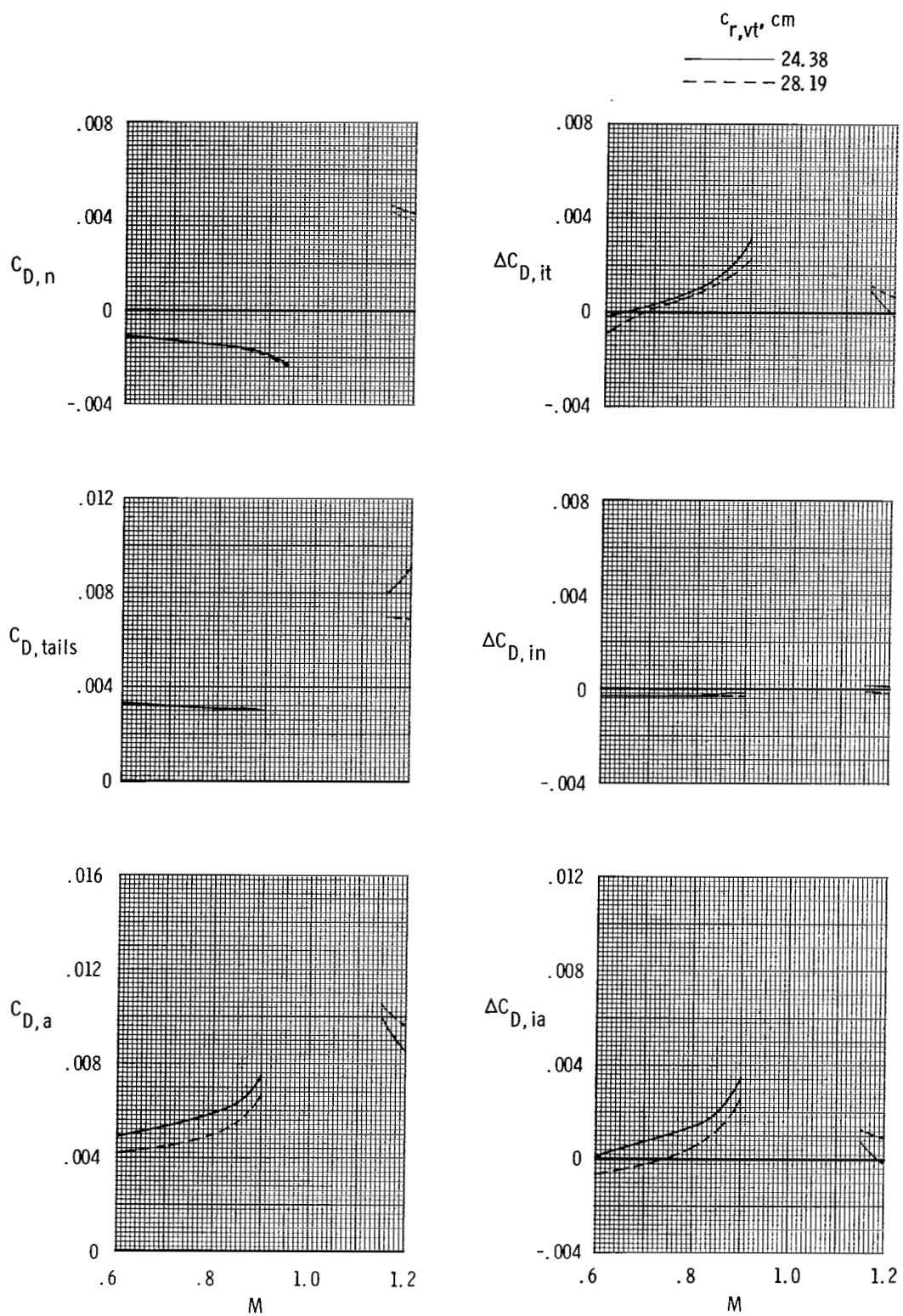
(b) Aft-end drag-coefficient components and tail interference-drag-coefficient increments; $\alpha = 0^\circ$.

Figure 15.- Concluded.



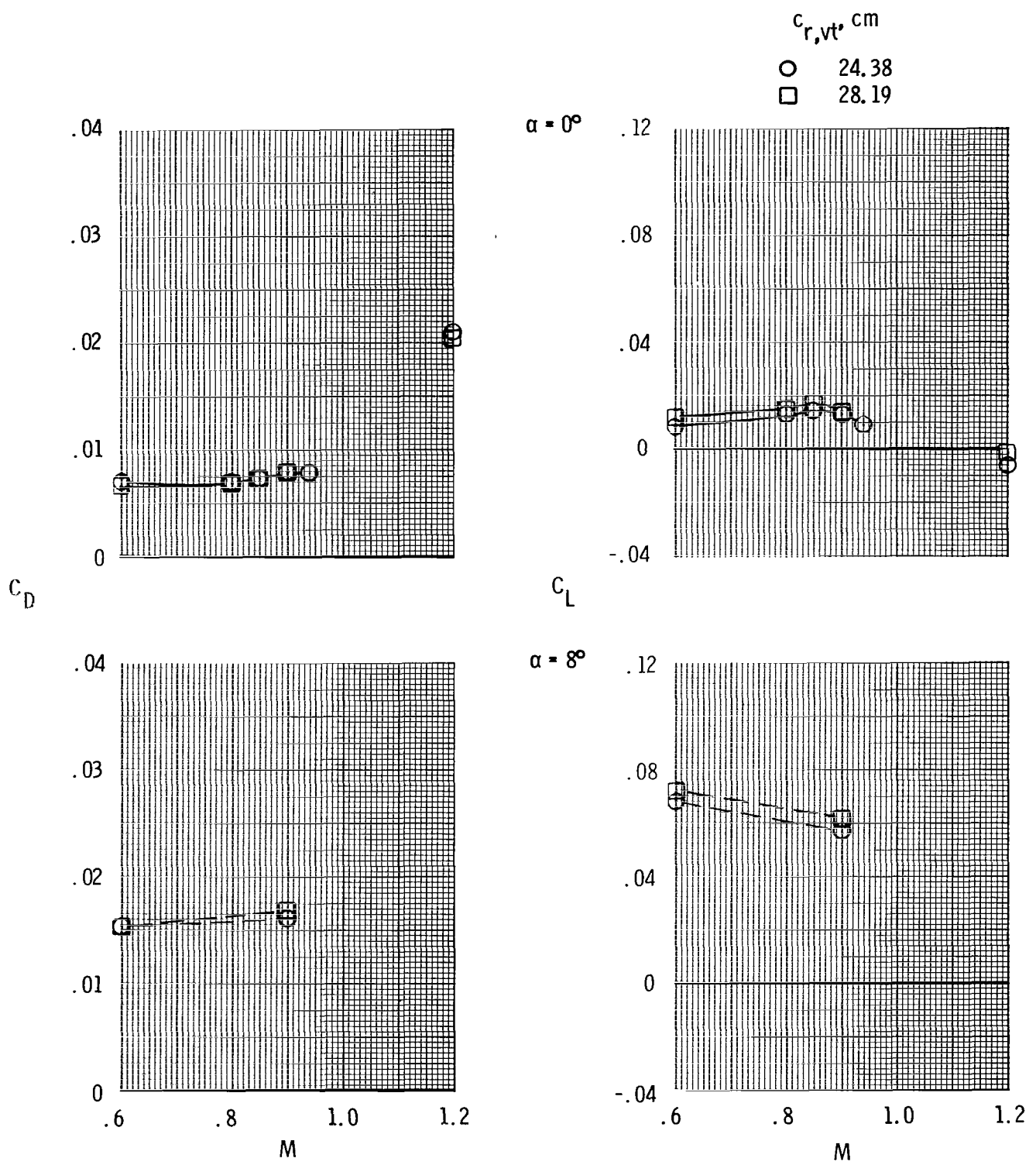
(a) Total aft-end lift and drag coefficients.

Figure 16.- Effect of twin-vertical-tail root-chord length on aft-end characteristics for scheduled NPR. Horizontal tails fwd; vertical tails fwd; symmetrical vertical-tail airfoil; $\phi_t = 0^\circ$; $\phi_{vt} = 0^\circ$; basic interfairing.



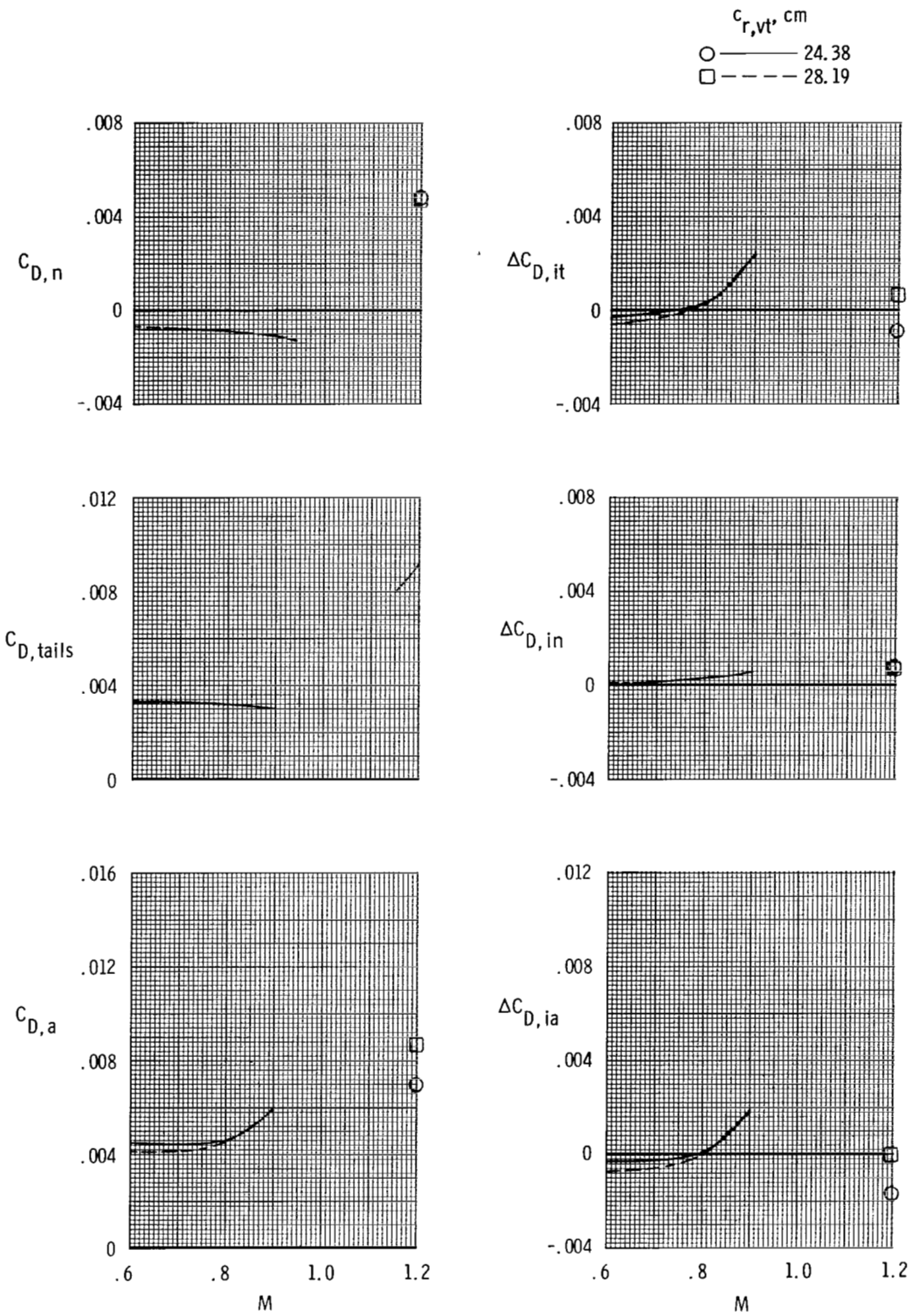
(b) Aft-end drag-coefficient components and tail interference-drag-coefficient increments; $\alpha = 0^\circ$.

Figure 16.- Concluded.



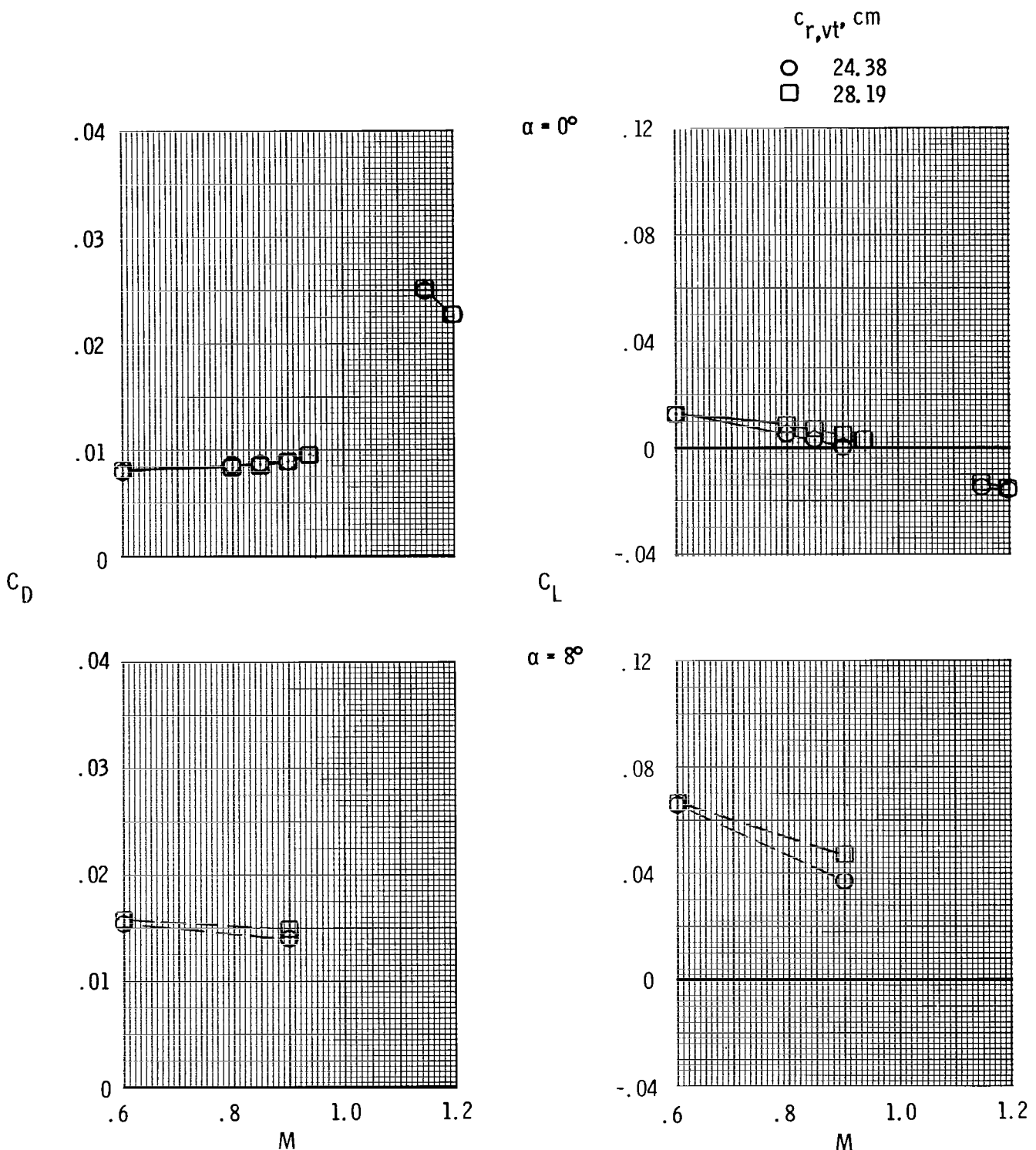
(a) Total aft-end lift and drag coefficients.

Figure 17.- Effect of twin-vertical-tail root-chord length on aft-end characteristics for scheduled NPR. Horizontal tails aft; vertical tails fwd; symmetrical vertical-tail airfoil; $\phi_t = 0^\circ$; $\phi_{t\perp} = 0^\circ$; basic interfairing.



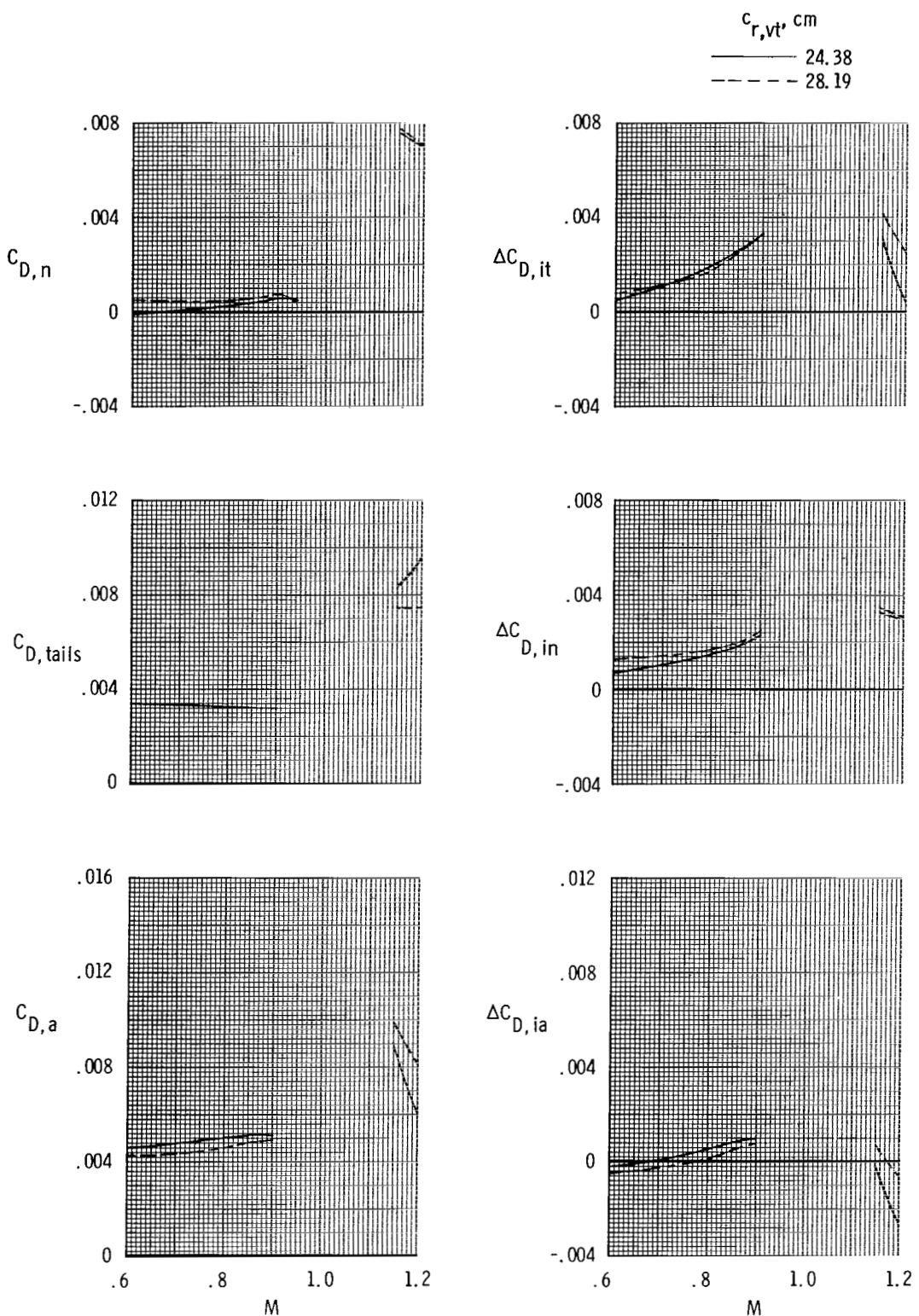
(b) Aft-end drag-coefficient components and tail interference-drag-coefficient increments; $\alpha = 0^\circ$.

Figure 17.- Concluded.



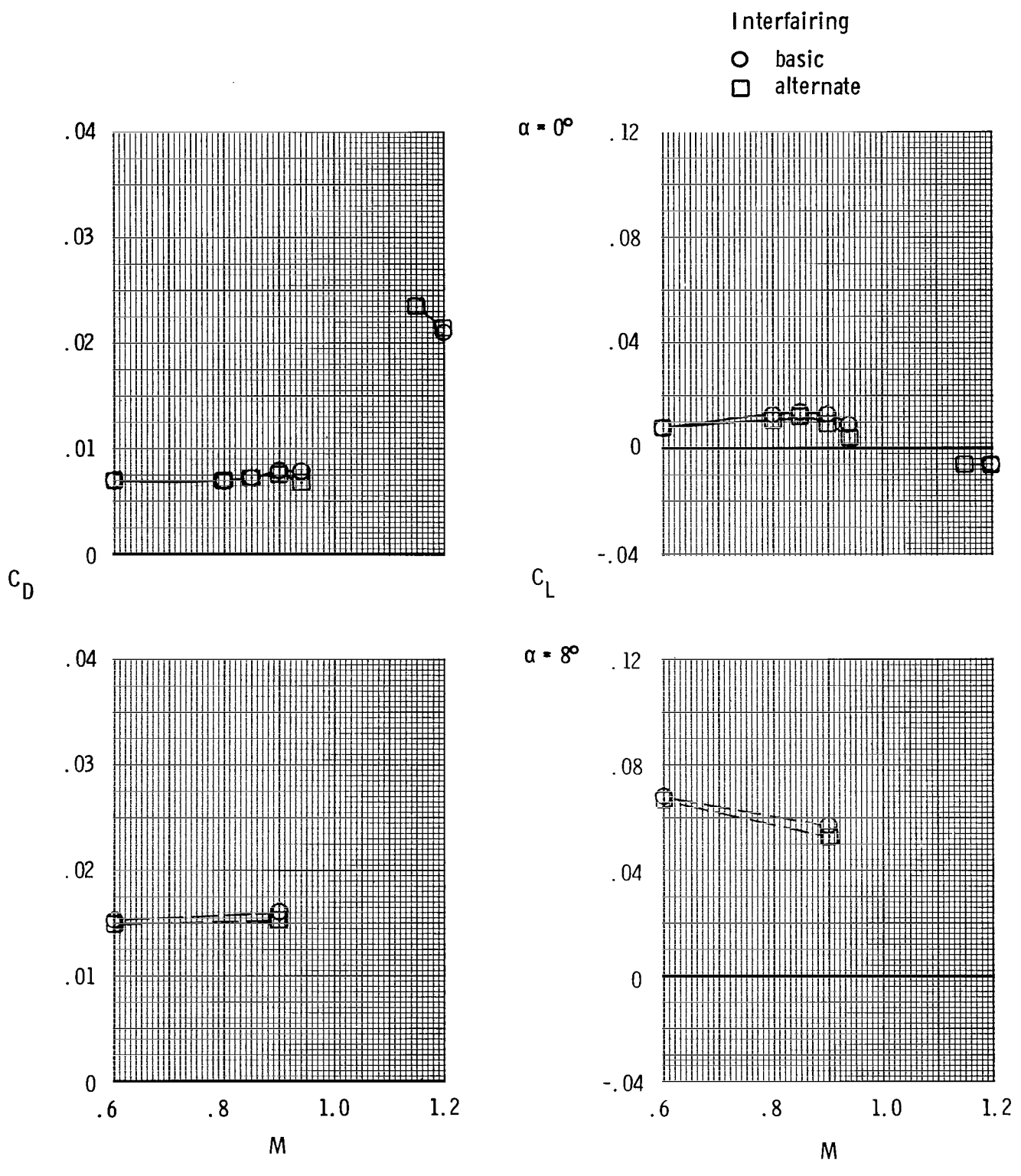
(a) Total aft-end lift and drag coefficients.

Figure 18.- Effect of twin-vertical-tail root-chord length on aft-end characteristics for scheduled NPR. Horizontal tails aft; vertical tails aft; symmetrical vertical-tail airfoil; $\psi_t = 0^\circ$; $\phi_t = 0^\circ$; basic interfairing.



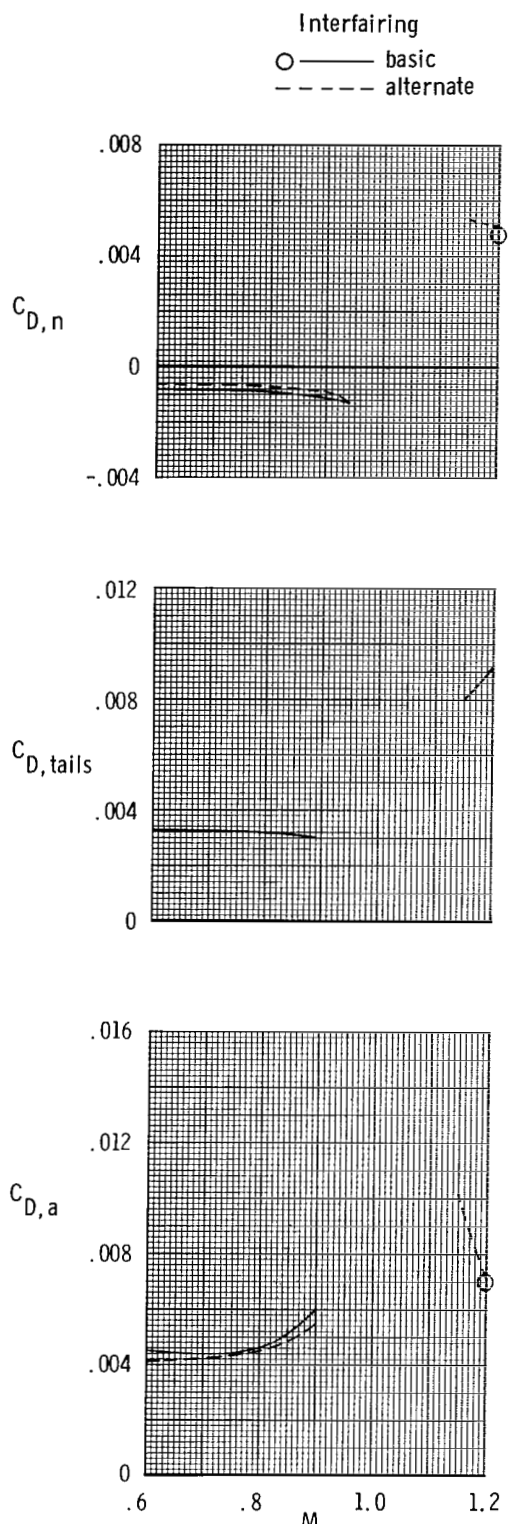
(b) Aft-end drag-coefficient components and tail interference-drag-coefficient increments; $\alpha = 0^\circ$.

Figure 18.- Concluded.



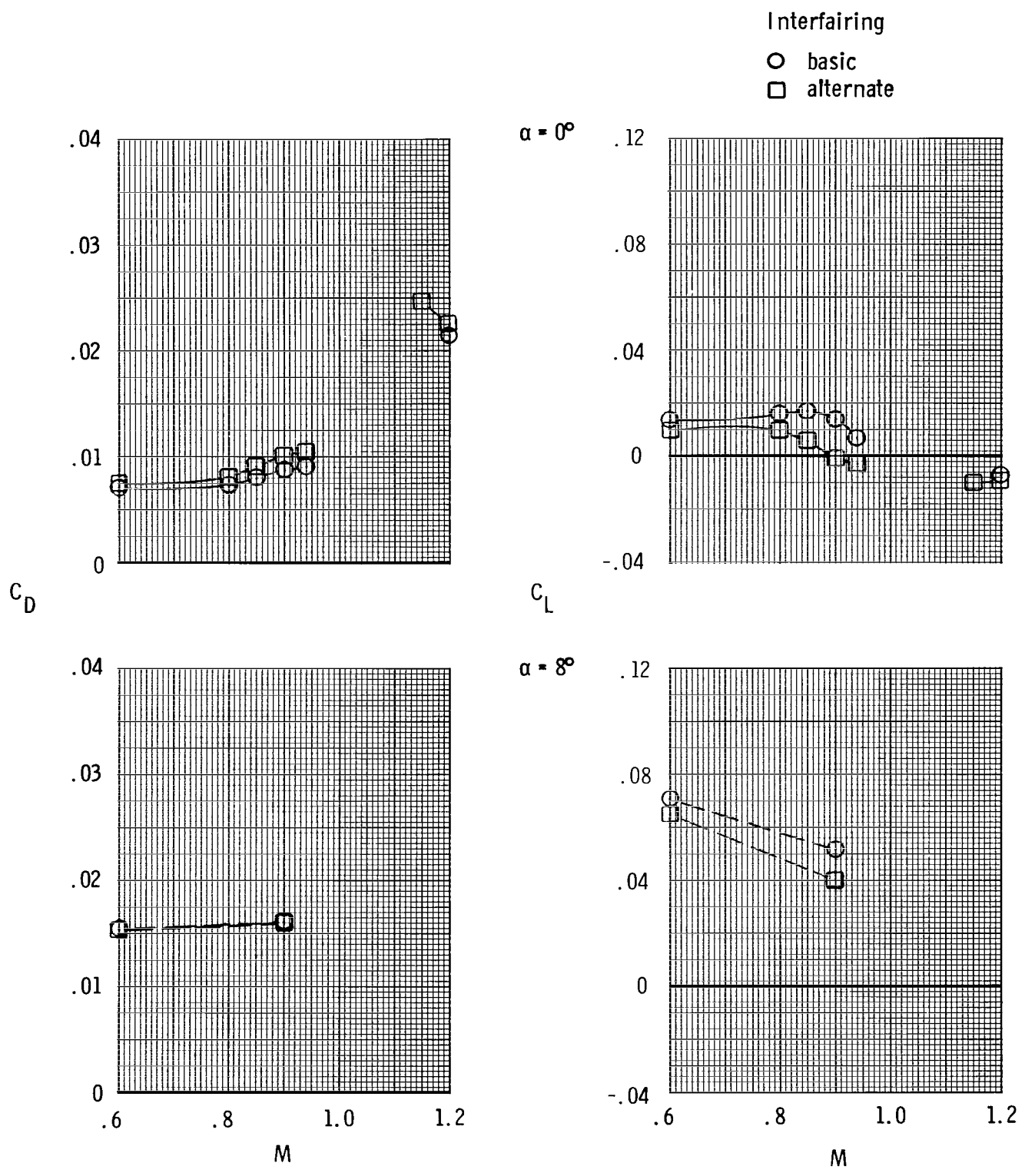
(a) Total aft-end lift and drag coefficients.

Figure 19.- Effect of engine interfairing on aft-end characteristics for scheduled NPR. Horizontal tails aft; short-root-chord vertical tails fwd; symmetrical vertical-tail airfoil; $\phi_t = 0^\circ$; $\psi_t = 0^\circ$.



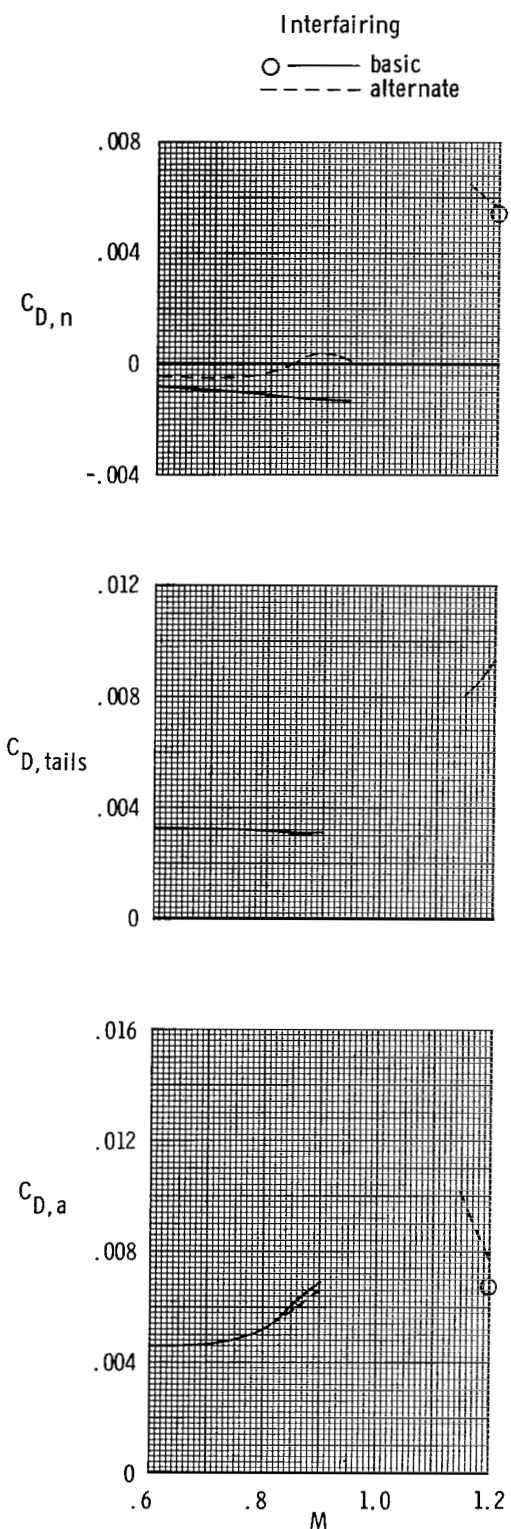
(b) Aft-end drag-coefficient components; $\alpha = 0^\circ$.

Figure 19.- Concluded.



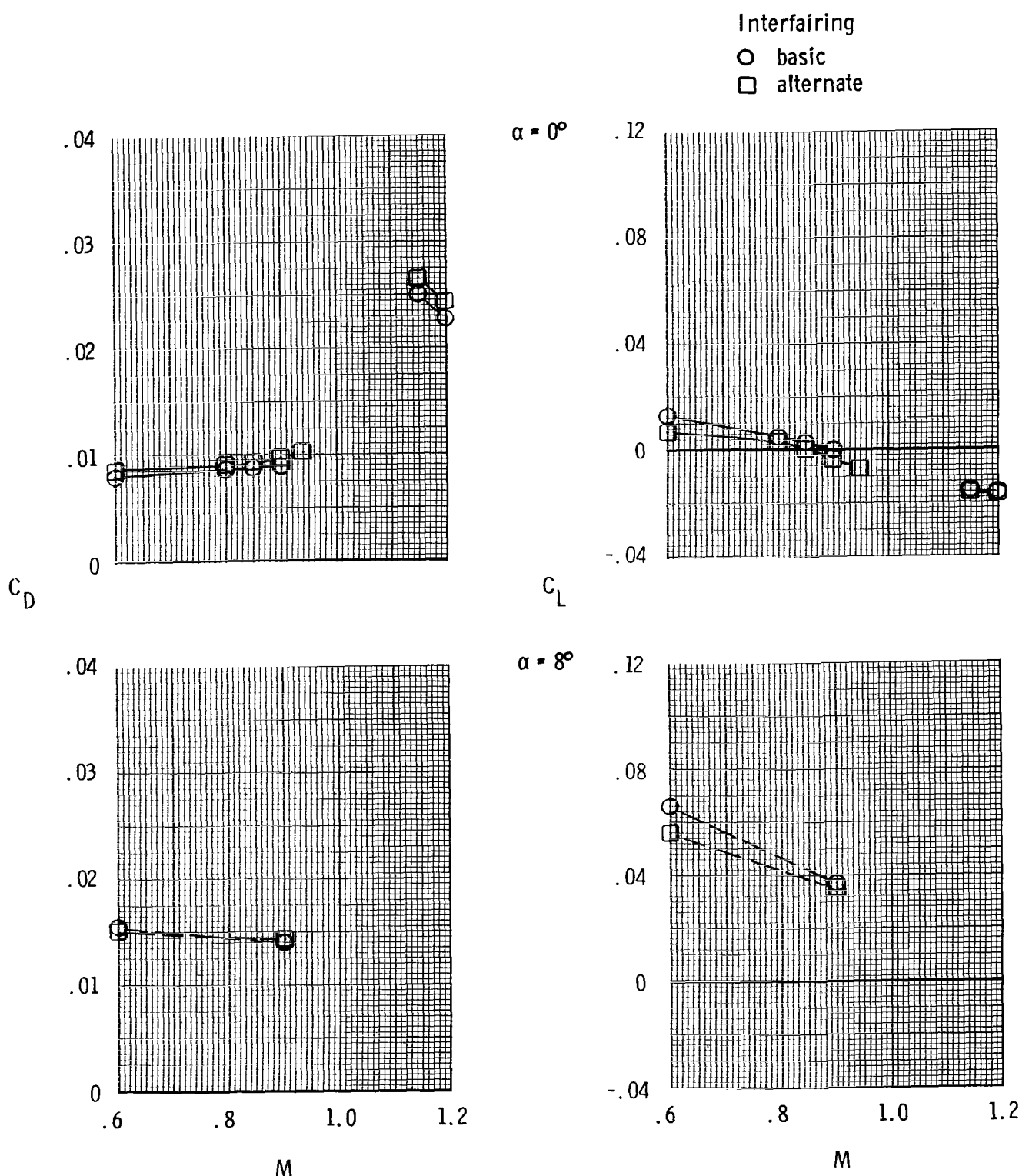
(a) Total aft-end lift and drag coefficients.

Figure 20.- Effect of engine interfairing on aft-end characteristics for scheduled NPR. Horizontal tails aft; short-root-chord vertical tails mid; symmetrical vertical-tail airfoil; $\phi_t = 0^\circ$; $\phi_t = 0^\circ$.



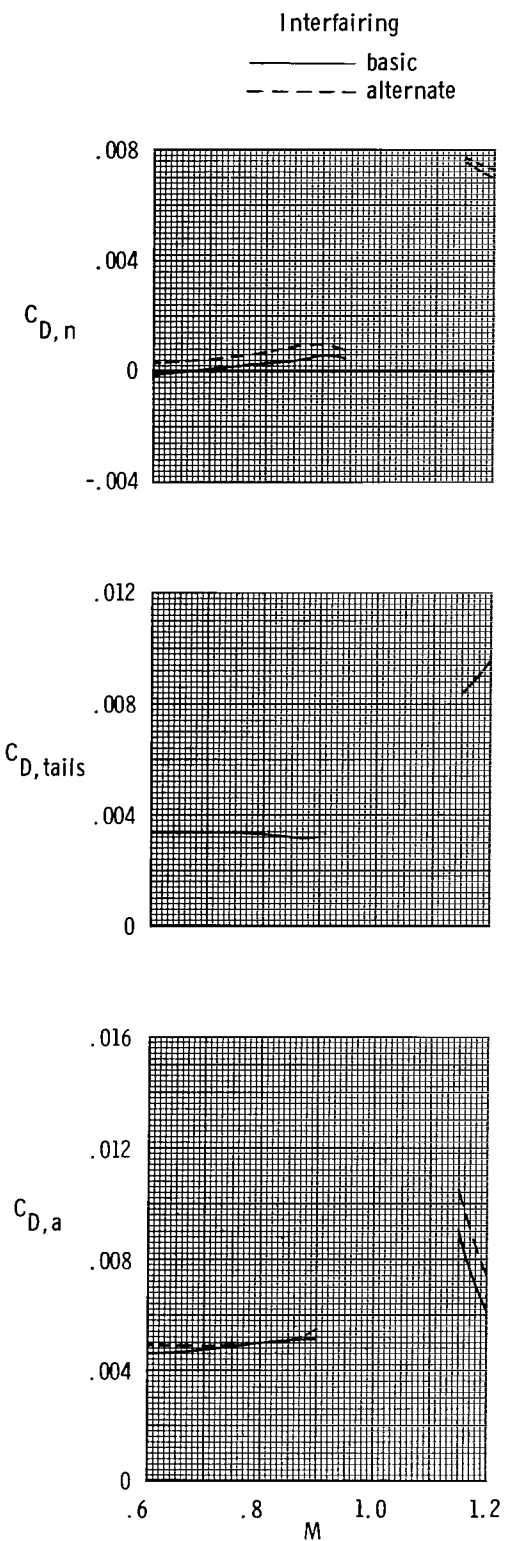
(b) Aft-end drag-coefficient components; $\alpha = 0^\circ$.

Figure 20.- Concluded.



(a) Total aft-end lift and drag coefficients.

Figure 21.- Effect of engine interfairing on aft-end characteristics for scheduled NPR. Horizontal tails aft; short-root-chord vertical tails aft; symmetrical vertical-tail airfoil; $\phi_t = 0^\circ$; $\phi_{t\bar{t}} = 0^\circ$.



(b) Aft-end drag-coefficient components; $\alpha = 0^\circ$.

Figure 21.- Concluded.

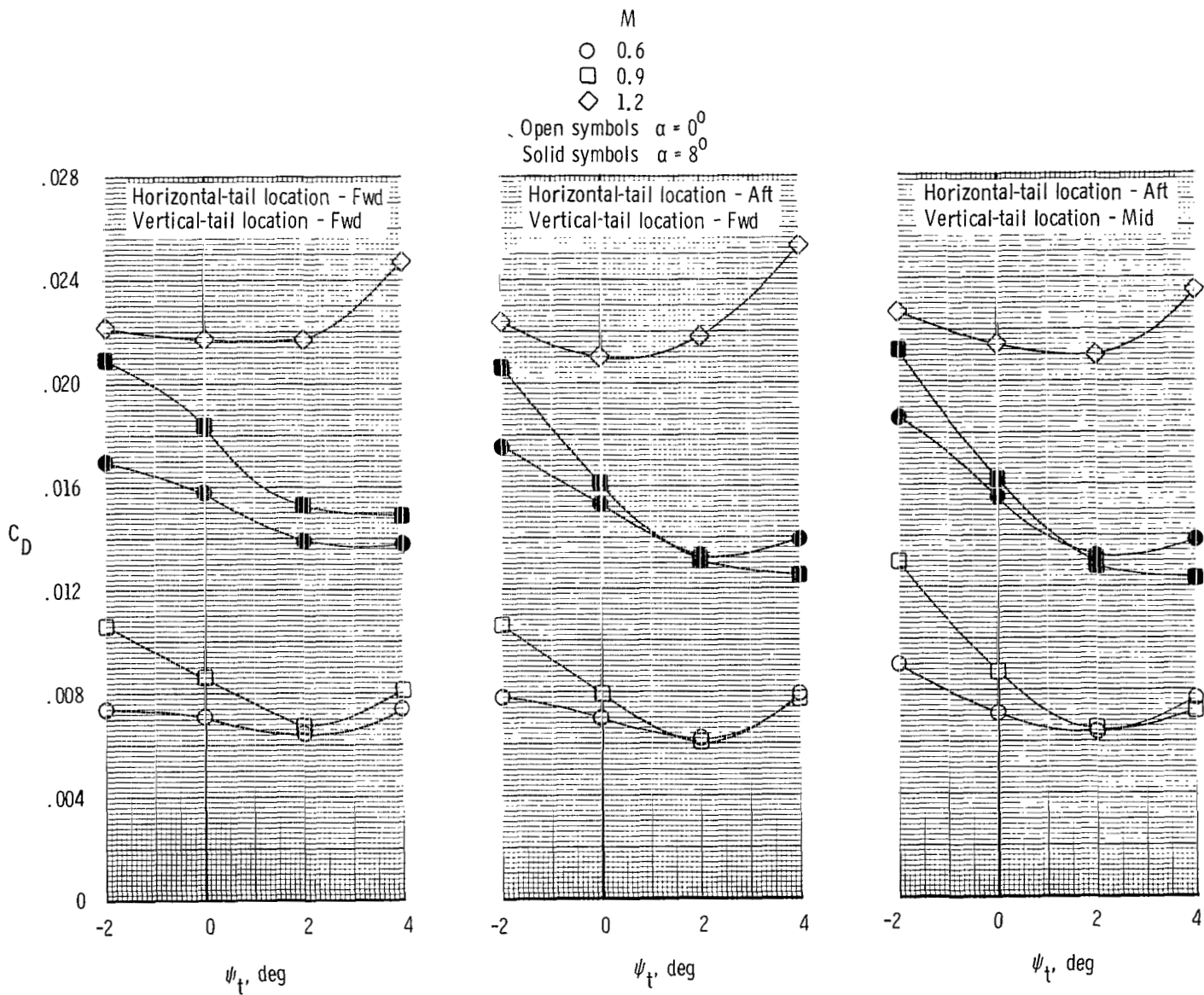


Figure 22-- Summary of the effects of twin-vertical-tail toe angle on total aft-end drag characteristics for scheduled NPR. Short-root-chord vertical tails; symmetrical vertical-tail airfoil; $\phi_t = 0^0$; basic interfairing.

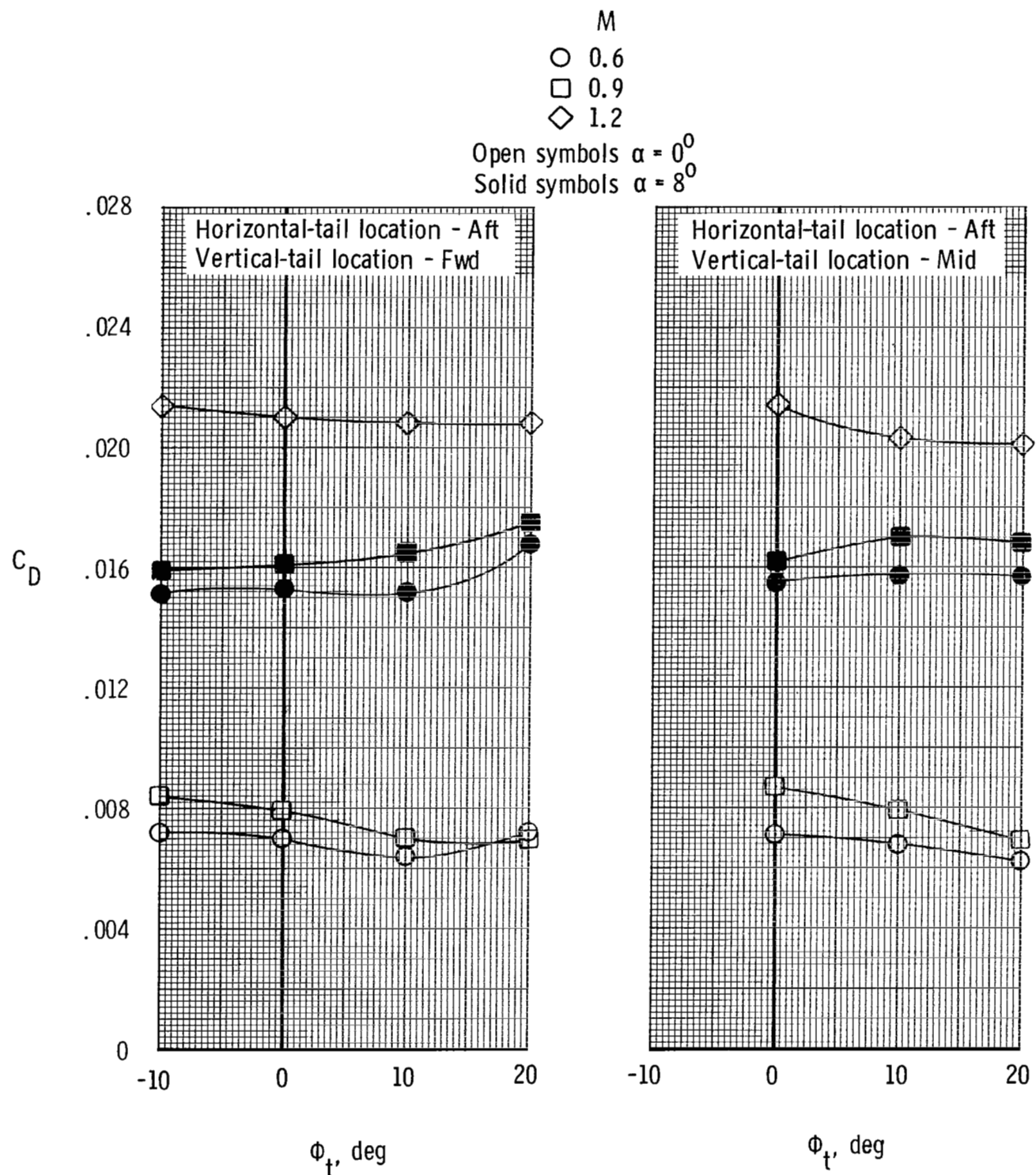


Figure 23.- Summary of the effects of twin-vertical-tail cant angle on total aft-end drag characteristics for scheduled NPR. Short-root-chord vertical tails; symmetrical vertical-tail airfoil; $\phi_t = 0^\circ$; basic interfairing.

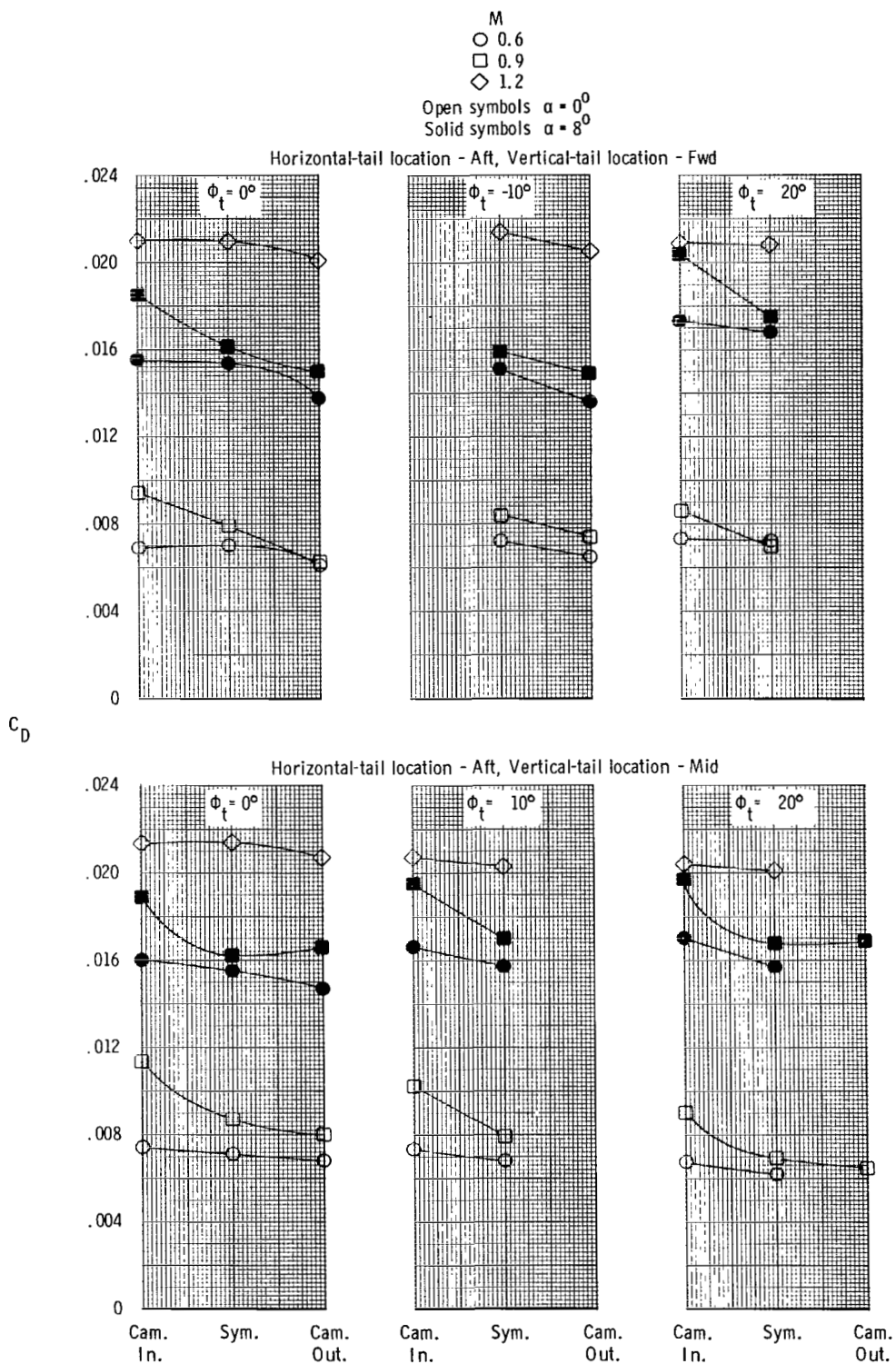


Figure 24.- Summary of the effects of twin-vertical-tail camber on total aft-end drag characteristics for scheduled NPR. Short-root-chord vertical tails; $\phi_t = 0^\circ$; basic interfairing.

1. Report No. NASA TP-2158	2. Government Accession No.	3. Recipient's Catalog No.	
4. Title and Subtitle EFFECTS OF TWIN-VERTICAL-TAIL PARAMETERS ON TWIN-ENGINE AFTERBODY/NOZZLE AERODYNAMIC CHARACTERISTICS		5. Report Date May 1983	
7. Author(s) Laurence D. Leavitt and E. Ann Bare		6. Performing Organization Code 505-43-23-01	
9. Performing Organization Name and Address NASA Langley Research Center Hampton, VA 23665		8. Performing Organization Report No. L-15570	
12. Sponsoring Agency Name and Address National Aeronautics and Space Administration Washington, DC 20546		10. Work Unit No.	
15. Supplementary Notes		11. Contract or Grant No.	
		13. Type of Report and Period Covered Technical Paper	
		14. Sponsoring Agency Code	
16. Abstract An experimental investigation has been conducted in the Langley 16-Foot Transonic Tunnel to determine the effects of several empennage and afterbody parameters on twin-engine aft-end aerodynamic characteristics. Model variables included twin-vertical-tail cant angle, toe angle, airfoil camber, and root-chord length and afterbody/engine interfairing shape. Tests were conducted over a Mach number range from 0.6 to 1.2 and over an angle-of-attack range from -2° to 10°. Nozzle pressure ratio was varied from 1.0 (jet off) to approximately 10.0.			
17. Key Words (Suggested by Author(s)) Tail interference Twin vertical tails Twin-engine afterbody Toe angle Cant angle Camber		18. Distribution Statement Unclassified - Unlimited	
19. Security Classif. (of this report) Unclassified		20. Security Classif. (of this page) Unclassified	
		21. No. of Pages 104	22. Price A06
Subject Category 02			

For sale by the National Technical Information Service, Springfield, Virginia 22161

NASA-Langley, 1983

National Aeronautics and
Space Administration

Washington, D.C.
20546

Official Business
Penalty for Private Use, \$300

THIRD-CLASS BULK RATE

Postage and Fees Paid
National Aeronautics and
Space Administration
NASA-451



3 110,A, 830509 S00903DS
DEPT OF THE AIR FORCE
AF WEAPONS LABORATORY
ATTN: TECHNICAL LIBRARY (SUL)
KIRTLAND AFB NM 87117

NASA

POSTMASTER: If Undeliverable (Section 158
Postal Manual) Do Not Return

S